

Northumbria Research Link

Citation: Gray, Kathryn (2018) T cell responses to ursodeoxycholic acid and antibody profiles in primary biliary cholangitis. Doctoral thesis, Northumbria University.

This version was downloaded from Northumbria Research Link:
<http://nrl.northumbria.ac.uk/id/eprint/36282/>

Northumbria University has developed Northumbria Research Link (NRL) to enable users to access the University's research output. Copyright © and moral rights for items on NRL are retained by the individual author(s) and/or other copyright owners. Single copies of full items can be reproduced, displayed or performed, and given to third parties in any format or medium for personal research or study, educational, or not-for-profit purposes without prior permission or charge, provided the authors, title and full bibliographic details are given, as well as a hyperlink and/or URL to the original metadata page. The content must not be changed in any way. Full items must not be sold commercially in any format or medium without formal permission of the copyright holder. The full policy is available online: <http://nrl.northumbria.ac.uk/policies.html>



**Northumbria
University**
NEWCASTLE



UniversityLibrary

**T CELL RESPONSES TO
URSODEOXYCHOLIC ACID AND
ANTIBODY PROFILES IN PRIMARY
BILIARY CHOLANGITIS**

KJ GRAY

2018

**T cell responses to ursodeoxycholic
acid and antibody profiles in Primary
Biliary Cholangitis**

Kathryn Jane Gray

Department of Applied Sciences

Faculty of Health and Life Sciences

This thesis is submitted for the degree
of
Doctor Of Philosophy

January 2018

Abstract

Primary Biliary Cholangitis (PBC), formerly 'Primary Biliary Cirrhosis', is an autoimmune disease of the interhepatic bile ducts. Their damage leads to bile retention in the liver and subsequent damage to hepatocytes, leading to perpetuating injury and tissue damage, causing destruction of the normal liver architecture and eventual cirrhosis.

The current therapy given to PBC patients, ursodeoxycholic acid (UDCA), is insufficient to prevent disease progression, and appears to only slow the natural history of the disease. Additionally, the drug is only effective in around 80% of patients with the remaining 20% showing no apparent benefit after a year of use. Breakthrough studies appear to suggest that there may be differences in clinical biochemical parameters between these patient groups which may explain their marked differences in response to the drug. These findings are leading to PBC being considered as an umbrella term encompassing two- or more separate disease subsets, broadly 'responders' and 'non-responders' referring to response to UDCA, with 'non-responder' categorisation requiring the inability of the drug to significantly lower a patient's blood AST, ALP and bilirubin levels during the given time frame. Further elucidation of these subsets is crucial to identify patients and potentially allow the development of differential therapies which may benefit these "non-responders".

The mechanism of action of UDCA has been investigated in this thesis with the aim to use this data to highlight key pathways of interest differentiating the responder/non-responder subgroups. This involved flow cytometric analysis and ELISpot analysis of the effect of UDCA on T cells and also xCELLigence and supernatant transfer assays to investigate an impact on the cholangiocytes.

Further elucidation of the responder/non-responder subgroups came from comparing antibody profiles of these groups. Multiple indirect enzyme-linked immunosorbent assays (ELISAs) were carried out to measure antibody titre and therefore detect patterns of auto-antibody isotypes in serum from PBC patients known to be "responders" (62) or "non-responders" (15) to UDCA. Recombinant human PBC autoantigens E2, E2 inner lipoyl domain (E2ILD) and E3 binding protein (E3BP) were used to uncover statistically significant differences in antibody responses. Using cross-sectional analysis, it was found that results from patient data were able to replicate the proposed responder and non-responder grouping based on age and liver function criteria. It was found that compared to responders,

non-responders have higher levels of anti-E2 IgE ($p=0.025$), anti-E2ILD IgA ($p=0.047$) and anti-E2ILD IgG₃ ($p=0.01$). The study also found that men with PBC, generally considered non-responders, have significantly lower levels of some antibodies, which are higher in non-responders, anti-E2IgE ($p=0.003$) and anti-E2ILD IgG₃ ($p=0.05$). This is further evidence that men with PBC may constitute their own sub group of non-responders.

These findings provide further evidence that the disease includes biologically different subsets which should be treated differently. Differences in antibody isotype to dominant autoantigens suggests that there may be significant functional differences in T helper cell subsets in each patient group. Further investigation into the differences between these subsets could provide a diagnostic tool which could be used early on in diagnosis to categorise patients for stratified treatment.

Table of contents

Abstract	3
Table of contents	5
Acknowledgments	11
Author's declaration	12
Abbreviations	13
1 Chapter 1 - Introduction	15
1.1 Introduction to Immunity	15
1.2: The adaptive immune system	16
1.2.1: T cells	16
1.2.2: B cells and antibody production	21
1.3: Cytokine induced cell signalling	24
1.3.1: T and B cell interaction	25
1.4: Concept of autoimmunity	27
1.4.1: Tolerance and loss of tolerance	27
1.5: The function and structure of the liver	28
1.5.1: Structure	28
1.5.2: Functions	29
1.6: Primary Biliary Cholangitis (PBC) background	30
1.6.1: Environmental factors, clustering, infection and xenobiotics	32
1.6.2: Dominant autoantigens	32
1.6.3: Subsets of PBC	33
1.6.4: UDCA & its mechanism of action	34
1.6.5: Other drugs: Farnesoid x receptor agonists	37
1.6.6: Genetics	37
1.7: Conclusion	40
1.8: The future	41
1.9: Aims of this thesis	42
Chapter 2 – General Methods	43
2.1: Laboratory procedure	43
2.2: Common reagents	43
2.3: Isolation and culture of PBMCs and cell lines	43
2.3.1: Phlebotomy	43
2.3.2: PBMC isolation	44
2.3.3: Culture of PBMCs	44
2.3.4: Culture and splitting of adherent cell lines	44
2.3.5: Freezing and thawing of cells	45
2.4: Flow Cytometry	45
2.4.1: Background	45
2.4.2: Washing cells	45
2.4.3: Staining	46
2.5: Enzyme-linked immunospot (ELISpot)	47
2.6: xCELLigence	47
2.7: Enzyme-linked immunosorbent assay (ELISA)	48
2.7.1: Background	48
2.7.2: Reagents	48
Chapter 3 – Design of an assay which can distinguish between different subsets of T cell for use in categorising patient subgroup T cell populations and to investigate any skewing ability of UDCA on T cell populations.	49

3.1: Introduction.....	49
3.1.1: Flow Cytometry	51
3.1.2: Jurkat cell line	55
3.1.3: Aims of the chapter	55
3.2: Methods.....	56
3.2.1: Enrichment of T cells for the determination of the best T cell enrichment kit assay	56
3.2.2: Fresh and frozen cell comparison.....	58
3.2.3: Jurkat cells	58
3.2.4: Priliminary proliferaton experiment	59
3.2.5: T cell proliferation methods	59
3.2.6: Flow Cytometry preparation	62
3.3: Results.....	63
3.3.1: Method of T cell isolation.....	63
3.3.2: Fresh and frozen primary T cell comparison.....	65
3.3.3: Jurkat cells	67
3.3.4: Flow cytometry preliminary data	70
3.3.5: Flow Cytometry Optimisation.....	72
3.3.6: Determination of method of proliferation to be used	78
3.3.7: Finalisation of flow cytometric assay	84
3.4: Discussion	89
3.4.1: Aims.....	89
3.4.2: Method of T cell isolation.....	89
3.4.3: T cell proliferation fresh and frozen comparison	89
3.4.6: Optimising the proliferation method	91
3.4.7: T cell subset identification panel.....	91
3.4.8: Limitations.....	92
Chapter 4: Further elucidating the mechanism of action of UDCA in PBC: investigating a direct effect on T cells in the cholangiocytes.....	93
4.1: Introduction.....	93
4.1.1: UDCA Background.....	93
4.1.2: Contextualising UDCA and its conjugates	94
4.1.3: Mechanism of action of UDCA	95
4.1.4: Aims and Introduction Summary.....	96
4.2: Methods.....	97
4.2.1: Apoptosis assay	97
4.2.2: ELISpot method	97
4.2.3: ELISpot cell viability Flow Cytometry Experiment.....	100
4.2.4: Flow cytometry proliferation experiments	101
4.2.5: H69 Cholangiocyte cell line experiments	102
4.2.6: Large Flow Cytometry assay	104
4.3: Results.....	104
4.3.1: Trypan Blue apoptosis assay on isolated T cells	104
4.3.2: ELISpot Results	111
4.3.4: H69 cholangiocyte experiments	127
4.4: Discussion	134
4.4.1: Aims.....	134
4.4.2: Investigating a toxic effect of UDCA	134
4.4.3: Investigating an antiproliferative effect of UDCA on T cells.....	135
4.4.4: Investigating an impact of UDCA on the reactivity of T cells in the ELISpot assay	137
4.4.5: Investigating an anti-proliferative effect of UDCA on a cholangiocyte cell line	139
4.4.6: Investigating an indirect effect of UDCA on the proliferation of T cells.....	140
4.4.7: Conclusion	141
4.4.8: Further work.....	141
4.4.9: Limitations.....	142

Chapter 5: The development of an ELISA assay using End Point Titre to compare serum levels of anti-PDC autoantibodies in UDCA responder and non-responder PBC patients.	143
5.1: Introduction	144
5.1.1: Common autoantigens in PBC	144
5.1.2: Isotypes and class switching	145
5.1.3: Potential for genetic differences between groups	147
5.1.4 The ELISA assay	148
5.1.5: Aims of this chapter.....	152
5.2: Methods	152
5.2.1: Isolation of bE2/E3BP and recombinant human proteins	152
5.2.2: Optimisation of the protein coating concentration	153
5.2.3: ELISA screen	154
5.2.4: Short dilutions	155
5.2.5: Statistics.....	155
5.3: Results	156
5.3.1: Optimisation of the protein coating	156
5.3.2: Initial screen results and end point titre tabularised results.....	157
5.3.3: Cut-offs	159
5.3.4: Outliers in patient data	161
5.3.5: End point titre graphs	161
5.3.6: Spearman's Rank Correlation Coefficient results	162
5.4: Discussion	163
5.4.1: Aims.....	163
5.4.2: Discussion of results	163
5.4.3: Discussion Summary.....	164
5.4.4: Limitations.....	164
Chapter 6: Investigating differences in immune responses between PBC patients that are responders and non-responders to UDCA	165
6.1: Introduction	166
6.1.1: Background.....	166
6.1.2: Clinical liver evaluation.....	168
6.1.3: The use of liver damage enzymes in diagnosis of PBC	171
6.1.4: Chapter Aims	172
6.2: Methods	172
6.2.1: Methods introduction	172
6.2.2: Statistical Analyses	175
6.2.3: Methods Implementation	177
6.3: Results	178
6.3.1: Normal Distribution.....	178
6.3.2: Spearman's Rank Correlation Coefficient.....	182
6.3.3: Mann Whitney	186
6.3.4: Power of the study	193
6.3.5: Kruskal-Wallis	196
6.3.6: Multinomial analysis	198
6.4: Discussion	201
6.4.3 ELISA results	204
6.4.4: Multinomial regression	209
6.4.5: Future work and limitations of this chapter	210
6.4.6: Concluding remarks: The future for PBC diagnosis?	211
7: General Discussions	213
7.1: Results Summary	213
7.1.1: Chapter 3: Design of an assay which can distinguish between different subsets of T cell for use in categorising patient subgroup T cell populations and to investigate any skewing ability of UDCA on T cell populations.	213
7.1.2: Chapter 4: Further elucidating the mechanism of action of UDCA in PBC: investigating a direct effect on T cells in the cholangiocytes.....	215

7.1.3: Chapter 5: The development of an ELISA assay using End Point Titre to compare serum levels of anti-PDC autoantibodies in UDCA responder and non-responder PBC patients.	217
7.1.4: Chapter 6: Investigating differences in immune responses between PBC patients that are responders and non-responders to UDCA	218
7.2: Further work	219
7.3: General remarks	221
Chapter 8: Appendix	223
References	261

Acknowledgments

Reasons for undertaking this project are my own passion for medical science and desire to work as a researcher pushing forward the current knowledge in order to widen the understanding of diseases and how they could be treated to further human health.

There are several individuals who deserve my utmost thanks. Without their teaching, guidance and patience, this award would not be possible. My primary thanks are of course reserved for Dr Hannah Walden who has provided endless support both relating to the project and also in my personal life as well. I am extremely grateful to have had such a caring primary supervisor and I wish her all the best with future students who will go on to achieve great successes with her support.

Secondly, I must thank Prof Stephen Todryk who has provided much support in the laboratory and helped me to obtain the diverse repertoire of skills I boast today. Additionally, I cannot thank him enough for stepping in and taking on the load of a fourth PhD student when my primary supervisor was on maternity leave.

I must also thank Dr Sharon Cookson, who has been invaluable in assisting my lab work, particularly in flow cytometry, and has also metaphorically and literally provided a shoulder to cry on and at times acted as an unofficial third supervisor.

I truly believe I have made lifelong friends in the three above-mentioned and am forever grateful for their help and support.

Further thanks go to Prof Dave Jones of Newcastle University and Dr Vinod Hegade for providing patient samples which were essential to keep this project a patient-based study with potential real clinical applications. Additional thanks go to Dr Jeremy Palmer and Dr Ben Millar for providing recombinant autoantigen proteins and cell lines respectively, which were extremely beneficial to my experiments. To Prof Ngianga-Bakwin Kandala, I am grateful for the expert advice towards my statistical analyses.

Paul Agnew I must thank extensively for his endless patience, guidance and support. He has been an invaluable help.

I am also grateful to staff at University of Glasgow, where I hold my current position, including Prof Simon Milling and Prof Alan Mowat, who have provided advice and encouragement for the final stages of my thesis writing.

Lastly, I must thank those who although uninvolved in my PhD project, provided endless emotional support and guidance through the stresses which come alongside undertaking a PhD programme. My parents and sister; Marian Sandison, David Sandison, Peter Gray, Suzie Morrison and Heather Gray; have provided me with essential escapes from my studies and always believed I could achieve whatever I set my mind on, even at times when I struggled to believe it myself. I must thank my Uncle David Gray, who has provided hours of phone calls providing emotional support and guidance. I am also grateful to my best friends who have provided endless support and picked me up when I needed them the most.

Author's declaration

Declaration

This thesis is submitted for the degree of Doctor of Philosophy at Northumbria University. Research was conducted in the Department of Applied Sciences, Faculty of Health and Life Sciences, Northumbria University, under the supervision of primary supervisor Dr Hannah Walden, senior lecturer, and secondary supervisor, Professor Stephen Todryk, Professor of Immunology and Head of Mammalian cell biology. Work was conducted between September 2013 and January 2018. All work contained herein is my own, unless otherwise stated. The research was funded by Northumbria University.

The word count for this thesis excluding bibliography, footnotes and appendix, is 63089.

I declare that all new research contained within this thesis is my own and has not been submitted previously at this university or any other.

Kathryn Jane Gray

January 2018

Abbreviations

2-OGDC – 2-oxoglutarate dehydrogenase complex
AMA – Anti-mitochondrial antibodies
ANA – Antinuclear antibodies
APC – Antigen presenting cell
BEC – Biliary epithelial cell
BCOADC – branched chain 2-oxo-acid dehydrogenase complex
CD – Cluster of differentiation
CDCA – Chenodeoxycholic acid
CMV - Cytomegalovirus
DAPI - 4',6-diamidino-2-phenylindole
DMEM – Dulbecco's modified eagle medium
DMSO – Dimethyl sulphoxide
EBV – Epstein Barr Virus
ELISA – Enzyme-linked immunosorbent assay
FACS – Fluorescence activated cell sorting
FCS – Foetal calf serum
FMO – Fluorescence minus one
FXR – Farnesoid X Receptor
GUDCA – Glycoursodeoxycholic acid
GWAS – Genome-wide association study
IFN- γ – Interferon gamma
Ig – Immunoglobulin
IL – Interleukin
ILD – Inner lipoyl domain
ITAM – Immuno-tyrosine activating motif
MHC – Major histocompatibility complex
NFAT – Nuclear factor of activated T cells
NF κ B – Nuclear factor κ B
PBC – Primary biliary cholangitis
PBMC -Peripheral blood mononuclear cell
PBS – Phosphate buffered saline
PDC – Pyruvate dehydrogenase complex
PHA – Phytohaemagglutinin
PMA – Phorbol 12-myristate 13-acetate
PSA – Pseudomonas antigen
PWM – Pokeweed mitogen
RPMI – Rosewell Park Memorial Institute (name of culture medium)

RXR – Retanoic X receptor

SD – Standard deviation

SI – Staining index

SA-ALP – Alkaline phosphatase conjugated streptavidin

TCR – T cell receptor

TGF β – Transforming growth factor β

TNF α – Tumour necrosis factor α

TUDCA – Tauroursodeoxycholic acid

UDCA – Ursodeoxycholic acid

1 Chapter 1 - Introduction

1.1 Introduction to Immunity

At its core, the immune system is a mechanism within the host to protect from pathogens and toxins. An essential requirement of this system is the ability to differentiate between self-molecules and foreign, potentially harmful antigens.

The immune system has evolved over many millions of years to protect the body from pathogenic invasion. There is a pathway which has been in existence since before plants and animals diverged from each other in evolutionary history (Belvin and Anderson, 1996). This pathway, the Toll pathway, involves the release of the protein complex nuclear factor kappa-light-chain-enhancer of activated B cells, NF κ B, by degradation of inhibitor κ B, allowing NF κ B to carry out its functions such as: DNA transcription; causing release of cytokines; protection from toxic, bacterial or viral compounds (Ruben et al. 1991). Genes for this pathway are conserved over millions of years of evolution and are found in organisms of invertebrates, vertebrates and plants (Belvin and Anderson, 1996). For millions of years, it has been crucial for an organism's survival to have the ability to fight harmful pathogens and throughout human evolution the immune system has become the complex and intricate network that humans possess today.

The understanding of the immune system has also evolved, with the first recorded acknowledgement of immunity dating back to 430 BC, when Athenian historian Thucydides wrote of the ability of those who had previously contracted the plague to be able to care for others infected during the plague of Athens without the risk of infection (Kousoulis *et al.*, 2012). By 1549, there was some acknowledgement of inoculation: in China, people would insert pus from the sores of smallpox sufferers into their nostrils in the knowledge that they could then only suffer a less severe form of the disease (Boylston 2012). 1796 saw the first vaccination against smallpox (Boylston 2012); 1890 saw the identification of substances in the blood, transferable between organisms, which could render some pathogens harmless (von Bhering, 1991); in the early 1900s came understanding of the nature by which antibodies bind to antigens (Marrack, 1976). Today exists the extensive and vast and expanding knowledge of the pathways, cells and proteins which make up the complex mechanism of the immune system.

1.2: The adaptive immune system

There are several important cells important in the immune system, called the leucocytes, all of which differentiate from the common haematopoietic stem cells. The first differentiation from haematopoietic stem cells is to lymphoid and myeloid progenitor cells. Myeloid progenitor cells then differentiate into granulocytes, erythrocytes, monocytes or platelets whereas lymphoid progenitor cells differentiate to T cells, B cells and natural killer (NK) cells (Chaplin 2003).

There are two strands to the immune system: the innate immune system and the adaptive immune system. The innate immune system acts as a crucial first line defence from pathogens with no memory or long-term immunity offered. The adaptive immune response is a second line, more specialised system which offers memory whereby the body is pre-prepared on subsequent experiences of the antigen (Chaplin 2003).

1.2.1: T cells

T cells are lymphocytes which control cell mediated immune responses. They mature in the thymus where they acquire a T cell receptor (TCR) and other surface molecules, helping to define the T cell subsets.

The T cell receptor is the most defining characteristic of the T cell. Made up of subunits α and β , or in much smaller abundances γ and δ , this is the molecule which recognises specific antigen as presented by MHC molecules on antigen presenting cells (APCs) (Attaf *et al*, 2015). Cellular development of TCR specificity is outlined in section 1.2.1.1.

Importantly, T cells also require a CD4 or a CD8 molecule which determines the type of major histocompatibility complex molecule (MHC) it can recognise and therefore helping to determine its immune function. Antigens are processed by cells and expressed on the surface within an MHC molecule, which the T cells can recognise and respond to, if they encounter the antigen to which they respond as expressed by an MHC molecule. MHC I is expressed on all nucleated cells and usually presents intracellular proteins whereas MHC II is present usually only on professional antigen presenting cells (APCs), and presents extracellular antigens where an extracellular molecule has been phagocytosed by the APC, digested and processed then expressed on the surface within the MHC II molecule (Sadegh-Nasseri, 2016).

As all haematopoietic stem cells originate in the bone marrow, progenitor T cells must migrate from the bone marrow into the blood to reach the thymus, the site of T cell maturation. VDJ recombination, or somatic recombination, allows the progenitor T cell to obtain its own T cell receptor and become a naïve T cell. The naïve T cell will then leave the thymus and migrate to the lymph node. Here, it is determined whether the T cell should be allowed to

proliferate based on the antigen it recognises and how beneficial or possibly harmful proliferation of this T cell would be to the organism. Some are positively selected, if they are able to bind to the MHC molecule, ensuring it will only respond to antigen that is MHC-bound. Some T cells are found to react when presented with a self-antigen, and so are selected for killing: they are negatively selected. The T cell will then undergo a permissive interaction with the APC causing it to proliferate and differentiate into either a CD8+ cytotoxic T cell or a CD4+ helper T cell (Takaba and Takayanagi, 2017). The development of these different types of T cells is outlined below.

1.2.1.1: The generation of pre-T cells from Hematopoietic stem cells

Well before its commitment down a T cell lineage, the cell begins as a haematopoietic precursor or haematopoietic stem cell (HSC), generated in the bone marrow.

Haematopoietic stem cells are able to self-renew, or differentiate into one of the many different leucocytes, shown in figure 1.2.1.1, (Luc *et al.*, 2012). The early T cell precursor migrates from the bone marrow to the thymus.

The lineage potential of cells at the point where they become thymic immigrants remains unclear. Some studies have shown that highly purified recent thymic immigrants maintain only T cell or granulocyte monocyte-restricted potential (Wada *et al.*, 2008), whereas others have suggested that they may also maintain B cell lineage potential (Luc *et al.*, 2012). The latter would imply that thymic immigrants show a lymphoid progenitor phenotype, as shown in figure 1.2.1.1. Importantly, it is in the thymus where the T cell passes further lineage determining stages, rendering it committed to becoming a T cell, discussed in section 1.2.1.2.

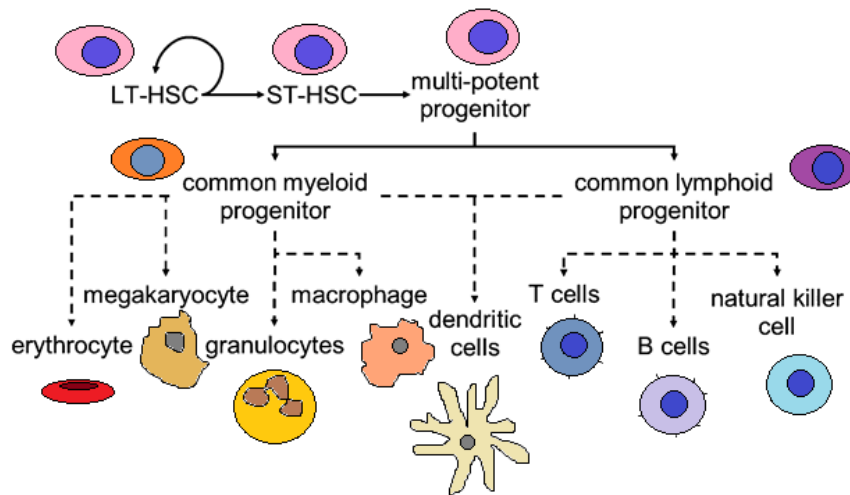


Figure 1.2.1.1: Differentiation of haematopoietic stem cells.

Adapted from Nelson and Roy 2015, this figure illustrates how haematopoietic stem cell can self renew or differentiate into the different leucocytes. Likely, new thymic immigrants exhibit a common lymphocyte progenitor phenotype (Luc *et al.*, 2012).

LT-HSC – long term haematopoietic stem cell; ST-HSC – short term haematopoietic stem cell.

1.2.1.2: The T cell receptor; CD4+ T cells and CD8+ T cells.

While a T cell is still developing in the thymus, it lacks both CD4 and CD8 surface receptors: it is 'double negative' (DN). The DN population of T cells can be further subdivided based on expression and/or lack thereof of 2 further surface receptors, CD44 and CD25, which is determined by its developmental stage. Importantly, at the DN3 stage, the cell is committed to becoming a T cell, when it is CD4⁻CD8⁻CD25⁺CD44⁻. This is when rearrangement of the T cell receptor β chain (TCR β) may occur, and will eventually lead to the T cell developing its own specificity to an antigen. This leads to a transient CD4⁺CD8⁺ stage, and eventual loss of either CD4 or CD8 and commitment to being cytotoxic (CD8⁺) or helper (CD4⁺) (Abbey and O'Neill, 2008). Figure 1.2.1.2.1 shows an overview of the stage of commitment of a T cell progenitor down the T cell differentiation route.

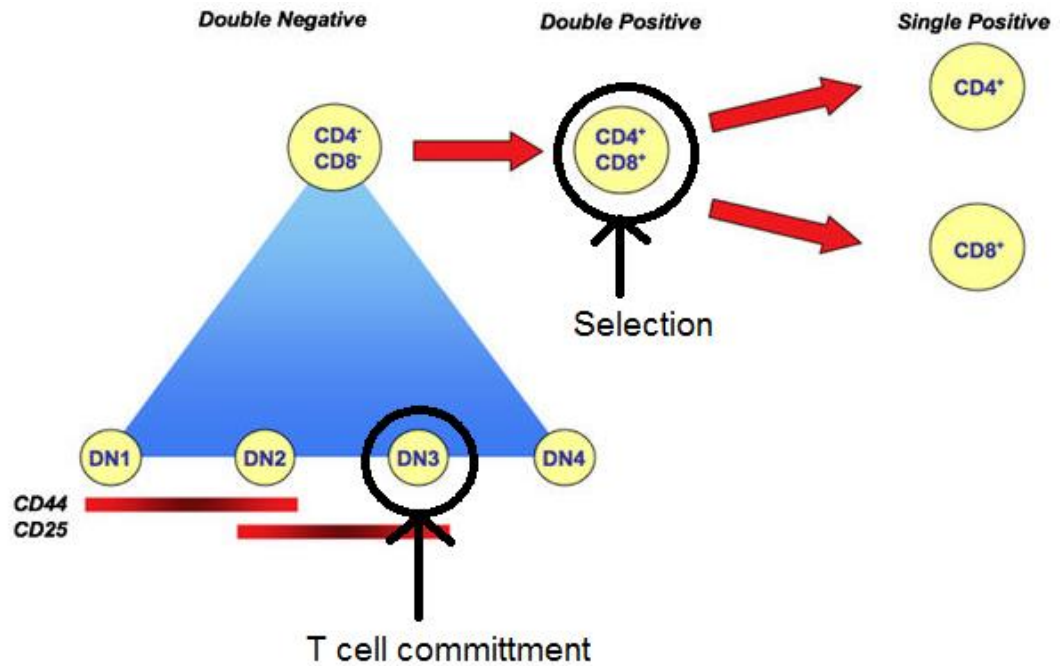


Figure 1.2.1.2.1 T cell commitment down the eventual CD4⁺/CD8⁺ differentiation pathway

Within the thymus lies a population of 'double negative' cells. These are at various stages down their commitment paths to become a mature lymphocyte. At stages DN1 and DN2, the cell has the potential to become a cell other than a T cell, but by stage DN3, when the cell expresses CD25 and CD44 expression has been downregulated, its path to become a T cell is confirmed. Selection of useful but non-self harming T cells occurs at the CD4⁺CD8⁺ stage. This figure is adapted from Abbey and O'Neill, 2008.

The specificity of the T cell is reliant on recombination of genetic material directing the amino acid sequence which will eventually make up the variable region of the TCR. The diverse repertoire of antigens T cells will encounter demands a system for a diverse range of TCRs. The process is similar to recombination events involved in isotype switching, outlined in section 1.2.2. A series of irreversible genetic rearrangements occur, firstly to join a diversity (D) fragment to a joining (J) fragment within the β chain, then with a variable (V) region joined in front of the diverse fragment, and finally a constant, C, region added on the end, depicted in figure 1.2.1.2.2. Splicing of mRNA removes intervening sequences, leaving the completed protein transcript for the β chain. A chain genetic rearrangements follow from β rearrangements and α and β chains combine to give the completed $\alpha\beta$ TCR. A $\gamma\delta$ TCR also exists but is of less importance for this thesis and these cells are in far less abundance than $\alpha\beta$ TCR expressing T cells (Boyd *et al.* 2009).

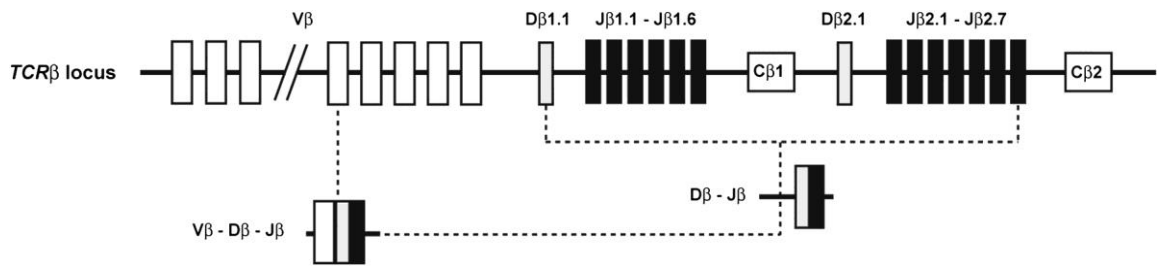


Figure 1.2.1.2.2: Outline of beta-chain genetic recombination events.

This diagram shows a schematic depiction of the pre-recombined TCR locus including joining of D to J and subsequent V joining which leads to eventual TCRβ construction after transcription, mRNA splicing and translation. This figure is taken from Murray *et al.* 2012.

1.2.1.2: CD4+ T cells

CD4+ T cells, through the CD4+ molecule, recognise extracellular antigen on MHCII on the surface of professional APCs. There are several subsets of CD4+ T cells, including helper T cell subsets and regulatory T cell subsets.

The CD4 molecule comprises IgG-like domains denoted D1, D2, D3 and D4. CD4 binds the antigen-presenting MHCII molecule of the APC, spatially distinct to TCR binding. CD4-MHCII interaction increases T cell antigen sensitivity by order of 10^2 -fold.

Helper T cells include Th1, Th2, Th17 and Th1/17. They are involved in many strands of the immune system including helping to activate B cells, cytotoxic T cells and macrophages (Sadegh-Nasseri 2016). They can be identified by their surface receptors, the cytokines they release and the transcription factors they use.

Th1

Th1 CD4+ T cells are important in cell-mediated immunity and secrete interferon γ (IFN- γ), interleukin-2 (IL-2) and tumour necrosis factor β (TNF- β) (Romagnani, 2000). IFN- γ activates macrophages, which engulf pathogens, and stimulates expression of MHCII (Gray and Goeddel, 1982). IL-2 has many functions, including promoting the differentiation of T cells to regulatory T cells. TNF- β is involved in regulation of cell proliferation, differentiation and apoptosis (Nedwin *et al.*, 1985). Their surface receptors include CD3, CD4, CXCR3. Th2 cells are primarily concerned with humoral immunity. They are essential in B cell class switching, described in section 1.2.2, but are also important for activation of cytotoxic T cells and phagocytic cells. Th2 cells release IL-4, IL-5, IL-6, IL-9 and IL-13, with individual functions including causing isotype switching in B cells; activation of B cells and secretion of immunoglobulins; cell proliferation and preventing of apoptosis (Sadegh-Nasseri, 2016). Extracellular markers include CD3, CD4, CXCR4, CCR3, CCR4. Th17 cells produce IL-17,

IL-21 and IL-22 and have functions which include maintenance of mucosal barriers and inhibition of Treg differentiation. Th17 cells have been known to interact with B cells and may be involved in antibody production and/or isotype switching (Takagi *et al.*, 2008). Extracellular markers include CD3, CD4, CCR4, CCR6. Regulatory T cells have the primary function of suppressing the immune response such that excessive damage from excessive inflammation does not occur. Regulatory T cells can also have an important function in preventing autoimmune diseases by suppressing the action of cells which could potentially recognise self-antigen (section 1.4.1) (Corthay 2009). Identifiers include intracellular FoxP3 and extracellular CD25, CD4, CD3. Follicular T cells are found in germinal centres at the outside of B cell follicles within secondary lymphoid organs and are important in determining survival of B cells (Linterman *et al.* 2009). Th9 cells mature in the presence of TGF- β , released by many different cell types, and IL-4, released by Th2 cells and they release IL-9. Only recently defined, they appear pleiotropic, functionally, but may help to ensure the survival of B cells (Linterman *et al.*, 2009).

1.2.1.3 : CD8+ T cells

Most CD8+ T cells are cytotoxic T cells. Cytotoxic T cells secrete IFN- γ and also granules with cell-killing properties. These granules contain the enzyme granzyme B which causes permeabilisation to the target cell and its eventual apoptosis (Catalfamo and Henkart 2003). Similarly to CD4+ T cells, cytotoxic T cells also have subset populations with similar cytokine-expressing profiles to their helper counterparts but are less well-defined. CD8+ T cells primarily target cells infected with intracellular pathogens such as bacteria and viruses (Gulzar and Copeland, 2004).

1.2.2: B cells and antibody production

B cells are lymphocytes which control the humoral immune responses. The humoral response protects the spaces in between cells which microorganisms use to transport from host cell to host cell. A B cell, upon activation which usually requires interaction with a CD4+ helper T cell, will become a plasma cell and secrete antibodies into these extracellular spaces to attach to these microorganisms, eventually rendering them unable to further infect host cells.

The progenitor B cell remains in the bone marrow where it undergoes VDJ (somatic) recombination to produce its own antibodies, usually initially of isotype IgM, and become an immature B cell. The immature B cell then migrates to the lymph node (Chaplin 2003). The mature B cell could then become activated upon interaction with a helper T cell which recognises the same antigen as it, or in some circumstances could be activated by the antigen directly. Upon activation, the B cell then enters the dark zone of the germinal centre where it undergoes somatic hypermutation, the process by which mutations in the DNA coding for the antibody undergoes mutations which can increase the affinity, diversity or specificity of the antibodies. The B cell then moves into the light zone of the germinal centre, where it becomes a centroblast and undergoes class switching and clonal expansion. The centroblast will differentiate into either a memory B cell or an antibody secreting plasma cell (Chaplin 2003).

1.2.2.1: Immunoglobulins and their isotypes

Often depicted as a Y-shape, the immunoglobulin contains four chains, two light and two heavy. Disulphide bonds link the heavy chains to the light chains. Each immunoglobulin has a variable region and a constant region. The variable region contains the paratope, which will bind its corresponding epitope of the antigen. The antigen is the protein to which the response is being made and the epitope is the specific region of this antigen to which the antibody binds. Immunoglobulins have different isotypes, covered more thoroughly further on. Figure 1.2.2.1 shows a detailed diagram of an immunoglobulin in monomeric form, the IgG isotype. The structure is divisible into 2 fragments. The crystallisable fragment is the region which interacts with surface receptors of cells and can also activate the compliment system, important in the innate immune system. The antigen-binding region binds to the target molecule: the antigen. (Flajnik 2002).

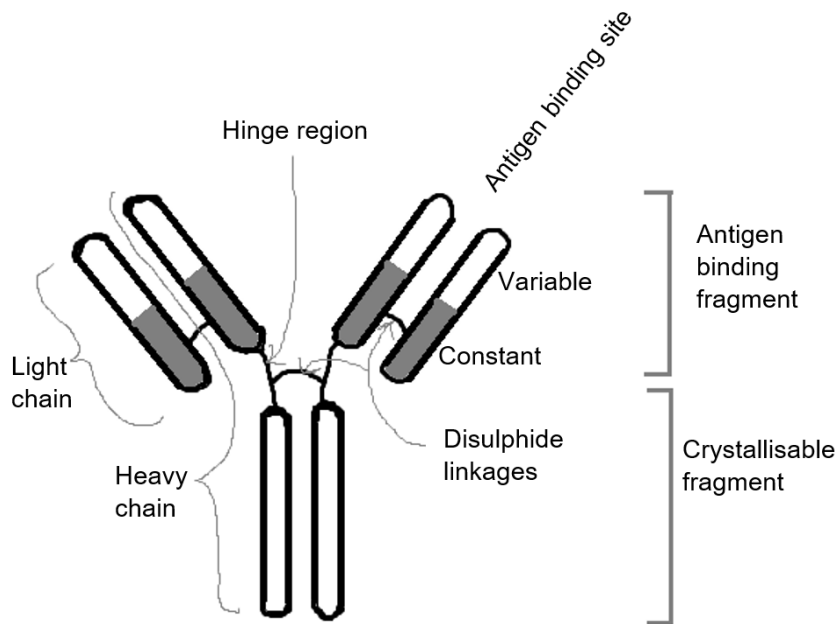


Figure 1.2.2.1: Diagram of the IgG immunoglobulin

This figure outlines the regions of particular interest of the immunoglobulin, often denoted by their abbreviations:

Antigen binding fragment - F_{AB}

Crystallisable fragment - F_C

Constant region - C

Variable region - V

B cells not only have the potential to produce antibodies against millions of antigens but also they can alter the type of antibody against the antigen to give a different response. There are five classes giving rise to nine types of antibody isotype: IgM, IgD, IgG(1-4), IgA(1, 2) and IgE, each of which having a different heavy chain, denoted μ , δ , γ , α , ϵ . The different isotypes of antibody are adapted to trigger different effector cell responses depending upon the antigen source (Flajnik 2002).

Multiple gene rearrangements occur which lead to unique codes for unique antibodies to be produced. In the genome there are 2 light chain loci, λ and κ , and one heavy chain locus. Each light chain locus contains several L, V, J and C regions and the heavy chain locus contains regions L, V, D, J and a C, where L encodes a leader peptide, V a variable region, J a joining segment, D a diversity section and C a constant region of the eventual whole polypeptide chain. Somatic recombination in the DNA of the cell leads to most of these segments being removed. The light chain gene then eventually only consists of: one L exon, one V and J encoding exon and a C region exon. The heavy chain, similarly becomes: a leader exon, the complete V_H exon (comprising V-D-J), then the C region exons including a hinge region. The order of heavy chain C region exclusion determines the isotype of the antibody. The first 2 are used initially, C_μ and C_δ , and differential splicing of the RNA transcript gives rise to IgM or IgD antibodies respectively. Subsequent C regions γ , α and ϵ lead to IgG, IgA and E. Further subsetting of isotypes occurs with there being 4 subsets of

IgG, labelled 1-4 corresponding to their relative abundance in the blood and IgA subtypes 1 and 2 denoting whether it is in monomeric or dimeric form. Different C regions leading to different isotypes of antibody allow for a range of different functions and also means that different antibodies can occupy different areas. Further diversity of immunoglobulins is established by somatic hypermutation in the V region genomic sequences which can also lead to more specific binding of an antibody to its target over a period of days after the primary response. (Nemazee 2006).

1.3: Cytokine induced cell signalling

Differential responses of immune cells rely heavily on the release and interpretation of signals of many different proteins such as cytokines. Cytokines are released by a variety of cells in the immune system such as T and B cells and have a large variety of potential responses, necessary when there is such a diverse repertoire of pathogens with the potential to invade the human body and cause harm. Cytokines come in many different forms and often require assembly of 2 heterodimer molecules and corresponding assembly of heterodimer receptor molecules. Figure 1.3 depicts IL-12 signalling pathway which eventually leads to downstream binding of STAT4 to the IL-12 response element (Newport, 2003).

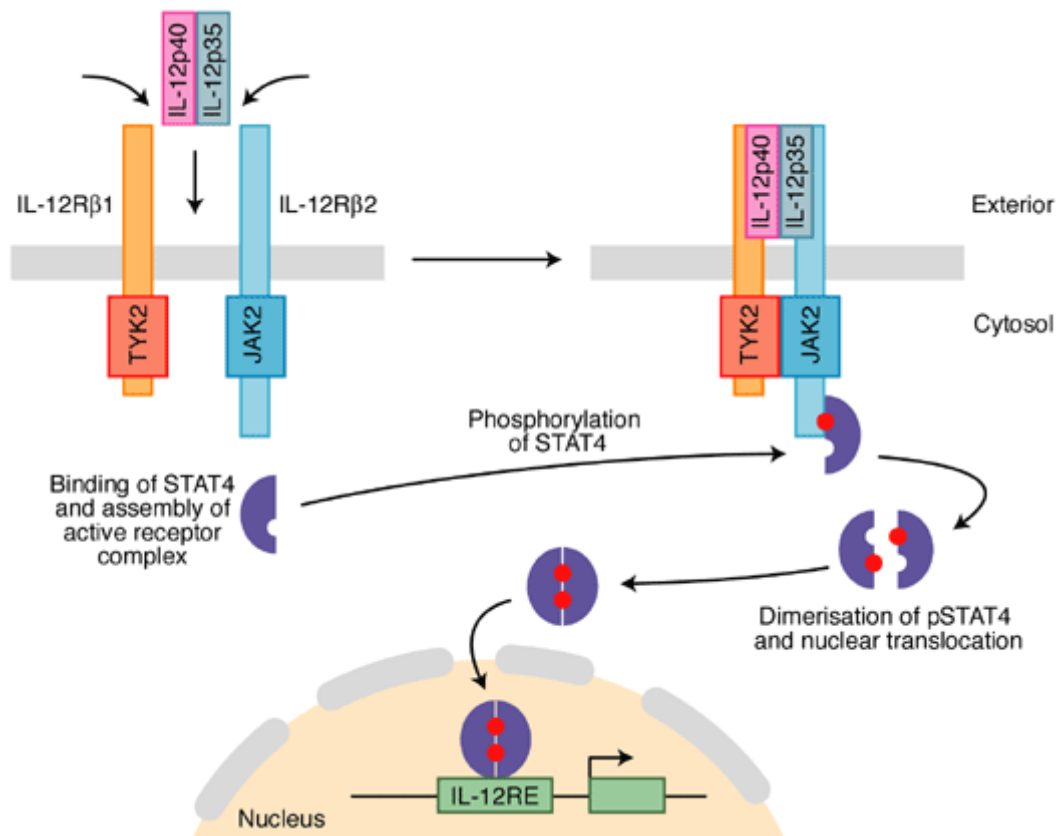


Figure 1.3: Depiction of IL-12 and downstream signalling pathway

This figure shows the combination of the sub-units of IL-12, p40 and p35, combining to form IL-12 and interacting with the heterodimer IL-12 receptor. The signalling pathway involves IL-12 binding to the dimerised receptor and subsequent phosphorylation of tyrosine kinase 2 (TYK2) and Janus kinase 2 (JAK2), causing docking of STAT4 which is then phosphorylated. STAT4 then forms a homodimer and translocates to the nucleus and binds with IL-12 response element (IL-12RE). This figure is taken from Newport, 2003.

Another layer of signal diversity can lie in that some cytokines share subunits with other cytokines, which may lead to competition of the most abundant combination winning out to confer a particular signal. This is further outlined in chapters 5 and 6.

1.3.1: T and B cell interaction

Some cytokines produced by T cells are B cell-acting and their binding to their receptor on the B cell activates downstream signalling pathways which have downstream effects of prompting isotype switching. Additionally, some cytokines, produced by cells such as T cells have the function of triggering regulatory networks which suppress isotype switching. In order for the B cell to receive these signals from the T cell, the CD40 on the surface of the B cell must interact with the CD40L on the T cell surface. Engagement of the T cell receptor (TCR) with the recognised-peptide-expressing MHCII on the surface of the B cell is the primary event, followed by binding of CD40 and CD40L and the secretion of cytokines by the T cell which will enhance, modify or skew the response (Elgueta *et al.*, 2009).

Many actions of T cell cytokines on B cell isotype switching have been well-documented for many years. IL-4, produced by Th2 cells, is known to induce switching to IgG₁ and IgE and inhibit switching to IgG₃. Th1-secreted IFN- γ has been shown to inhibit IL-4 mediated IgG₃ and IgE switching and enhance IgG₂ switching. TGF- β , secreted by many cell types, can induce an increase in IgA, for example. More detail is in chapters 5 and 6.

The type of antibody produced by a B cell also depends on whether it was activated in a T cell dependent or T cell independent manner. It has been shown *in vitro* that lipopolysaccharide (LPS), found in gram-negative bacterial membranes and commonly used *in vitro* to stimulate an inflammatory environment, stimulates IgG₃ isotype switching, and this action is inhibited by IL-4 and IFN- γ , therefore this T cell independent pathway is blocked by T cell activity to favour a T cell dependent mechanism. Often, such situations do occur where a B cell will experience multiple signals all at once and must be able to cope with often conflicting signals and, as isotype switching involves gene rearrangement, only one type of antibody can be produced by a B cell at once. Additionally, other factors specific to the environment can influence the resulting antibody isotype secretion such as B cell survival or proliferation and the concentrations of the individual incoming cytokines. Further studies in the LPS-induced inflammatory environment *in vitro* have shown that, although IFN- γ is able to inhibit IL-4 mediated isotype switching signals, neither TGF- β nor IL-4 is able to inhibit the effects of IFN- γ but IL-4 is able to inhibit TGF- β signals (Deenick *et al.*, 2005). This conflicted with previous studies which implied that TGF- β is able to inhibit IgG₁, IgG_{2a}, IgG₃ and IgE production (McIntyre *et al.*, 1993). These data together suggest that the antibody response produced to an antigen is dependent on many factors including the environment and direction from T cells.

The type of immune response, even down to type of Th cell response, elicited towards a pathogen can, then, be extremely important. How successful the host is at fighting infection can rely on the correct response being elicited. For example, when a patient is infected by tuberculosis-causing bacteria *Mycobacterium leprae*, the type of disease they exhibit is largely dependent on the type of response to the antigen. If Th1 cells are activated, the cytokines released are IL-2, IFN- γ and TNF- β which together enhance macrophage activity. The resultant disease is tuberculoid leprosy with cell mediated immunity, involving low infectivity, low levels of infective organism, normal T cell responses with *M. leprae* specificity and normal serum immunoglobulin levels. In contrast, the exact same organism can cause lepromatous leprosy, when there is a Th2 response rather than Th1, and there is release of IL-4, IL-5 and IL-10 which together B cell activity. The type of immune response is humoral immunity which is far less effective against this particular pathogen. There is significant organism growth, high infectivity, low T cell responsiveness and hypergammaglobulinaemia (Pinheiro *et al.*, 2011). Therefore, regulation of the correct type of immune response is extremely important and inappropriate or incorrect activation of the wrong pathway can have dire consequences for the host on infection.

Further studies have shown that other cytokines can influence B cell isotype switching, which is discussed in more detail in chapters 5 and 6.

1.4: Concept of autoimmunity

The immune system requires differentiation of self-molecules and foreign molecules in order to function effectively and without damage to the host. Pathogens have evolved with humans over millions of years and therefore have evolved to have molecules similar to those of humans, leading to the requirement for the immune system to adapt and become intricately capable of differentiating between these foreign molecules and those of its own body. There are several mechanisms in place to avoid an autoimmune attack despite remaining an effective system for killing invading pathogens.

1.4.1: Tolerance and loss of tolerance

There are tissues in the body which have a function of expressing self-molecules to T cells to determine if they will recognise these antigens and this will lead to their destruction. Developing T cells, in the thymus are challenged with self-peptide expressed by bone marrow-derived antigen-presenting cells, orchestrated by autoimmune regulator gene (AIRE). Those which respond to self-antigen with strong antigen binding will be sent This occurs while the cells are still CD4+CD8+, outlined in section 1.2.1.1 (Abbey and O'Neill, 2008).

Occasionally, a T cell recognising self-molecules will escape negative selection and become a circulating T cell with the potential to recognise a self-molecule, and therefore with the potential to perpetuate damage to self-tissues. This is not usually problematic because there are several peripheral tolerance-inducing mechanisms which will render the T cell unable to surmount an immune response even if it interacts with the antigen as presented by an MHC molecule: it will be 'tolerant' to the antigen it recognises. If this self-reactive T cell recognises antigen on any cell other than a professional antigen presenting cell (APC) then it will not receive the essential costimulatory signal in order to be activated. Without this costimulatory signal, the T cell will become anergic and be unable to propagate an immune response. (Fabbri, Smart *et al.*, 2003).

Antibodies are not necessarily completely specific to a target epitope.

Due to interactions between antibody and antigen being relatively weak and non-specific, an antibody may occasionally bind to, or cross react with, different antigens with different relative strengths. This promiscuity between peptide sequences and antibodies also gives rise to the theory of molecular mimicry, a process whereby pathogen-derived peptides can lead to the development of autoimmunity. If a pathogenic peptide shares structural

homology with a self-protein, antibody raised against this pathogenic epitope could also bind the self-protein leading to autoimmunity. (Elde and Malik, 2009).

1.5: The function and structure of the liver

1.5.1: Structure

The macrostructure of the liver contains four lobes: the right, left, caudate and quadrate. These are separated by ligaments composed of the same double membranes which engulf the entire structure of the liver. The hepatic portal vein and the hepatic artery provide the blood supply to the liver. The hepatic portal vein provides approximately three quarters of the blood volume but only half of the liver's oxygen supply, whereas around one quarter of blood volume and half of the oxygen supply come from the hepatic artery. Microscopically, the liver is composed of many lobules, roughly hexagonal in shape and through each corner of these is a triad of hepatic portal vein, hepatic artery and small bile duct and also lymphatic vessel and vagus nerve, shown in figure 1.5.1 (Ricken *et al.*, 2015). There is a central vein through each lobule and hepatocyte plates spread from these. Running through these plates are the sinusoids which are large capillaries through which blood from the hepatic portal vein and hepatic artery enters and where exchange of materials between the liver and the blood occurs. This blood then collects in the central, or hepatic, vein before leaving the liver. (Elias and Bengelsdorf, 1952).

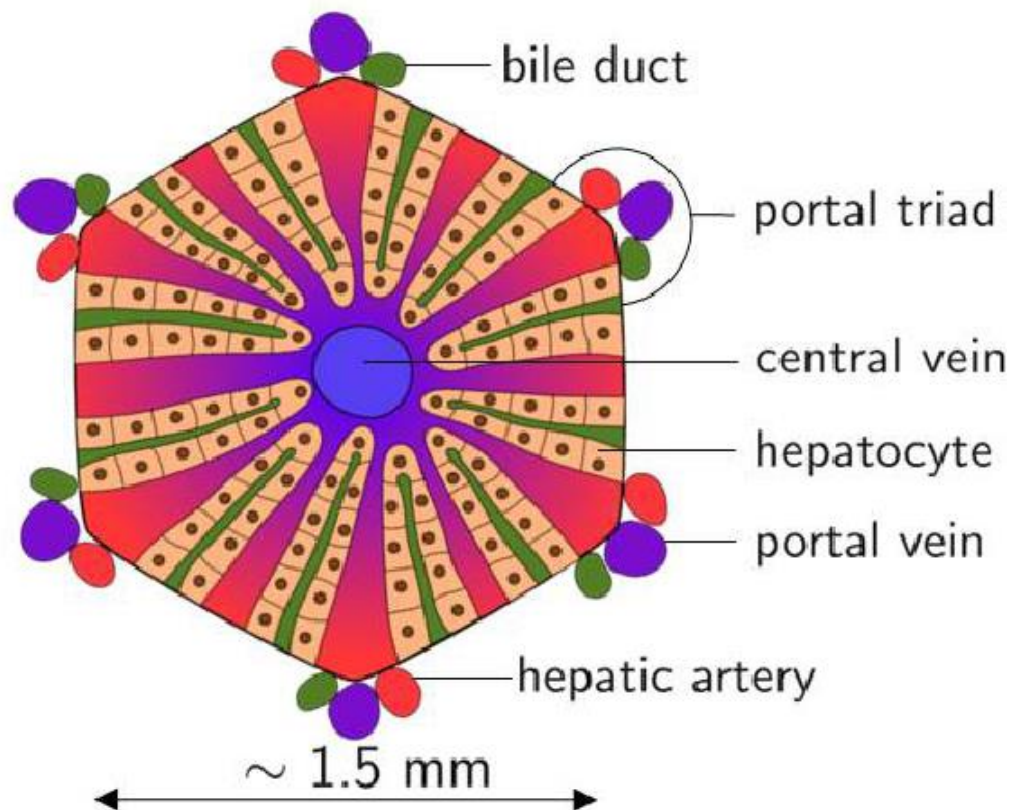


Figure 1.5.1: Diagram of liver lobule structure, taken from Ricken, *et al.*, 2015.

This figure shows the structure of a liver lobule as arranged around the central vein. The hepatic portal vein transports blood from the intestine. The hepatocytes are the main functional cells of the body of the liver.

1.5.2: Functions

As well as having major importance in the digestion of carbohydrates, fat and proteins, the liver also has many other functions such as detoxification of chemicals, metabolising drugs, breaking down red blood cells, producing proteins important in blood clotting, synthesising amino acids (Attili *et al.*, 1986). Most relevant in PBC, the liver is responsible for synthesising bile which is required for breakdown of lipids in the diet. Bile is toxic to hepatocytes and in some liver diseases, bile is unable to leave the liver, causing death of hepatocytes and scar tissue formation, which can propagate to fibrosis or cirrhosis of the liver (Xia *et al.*, 2006).

Liver fibrosis occurs in response to liver injury and involves accumulation of extracellular matrix molecules produced by hepatic stellate cells (HSC) in response to fibrogenic cytokines, including TGF- β 1, angiotensin II and leptin, released by activated hepatocytes and activated stellate cells. This accumulation of extracellular matrix molecules is scar tissue, which is a response to repeated liver injury. In large cases of repeated liver

damage and subsequent scar tissue formation, there can be serious disruption to the architecture and functional integrity of the liver (Batalla and Brenner, 2005).

1.6: Primary Biliary Cholangitis (PBC) background

The pathogenesis of PBC involves destruction of biliary epithelial cells which line intrahepatic bile ducts leading to bile retention. Hepatic portal inflammation exacerbates chronic liver fibrosis leading to eventual loss of liver function as the scar tissue interferes with bile duct activity (Jones, 2003a, Neuberger et al., 1997). This cycle eventually leads to liver failure and a liver transplant is required (Poupon et al., 1997). The series of events involved in the aetiology of PBC is outlined in figure 1.6. Left completely untreated, mean survival time after diagnosis can range from 1-20 years (Kim and Jeong, 2011). The current therapy for PBC is ursodeoxycholic acid, a secondary bile acid which is usually endogenously obtained from intestinal bacteria (Lepercq et al., 2005). Clinically this is thought to increase biliary flow and replace more toxic bile acids in the bile acid pool. It is prescribed in concentrated form to those with PBC and some other diseases (Poupon et al., 1991, Beuers et al., 1992). Although its exact mechanism of action in PBC is unknown, UDCA seems to attenuate the effects in most PBC patients and prolong the time before a transplant is required (Kim and Jeong, 2011).

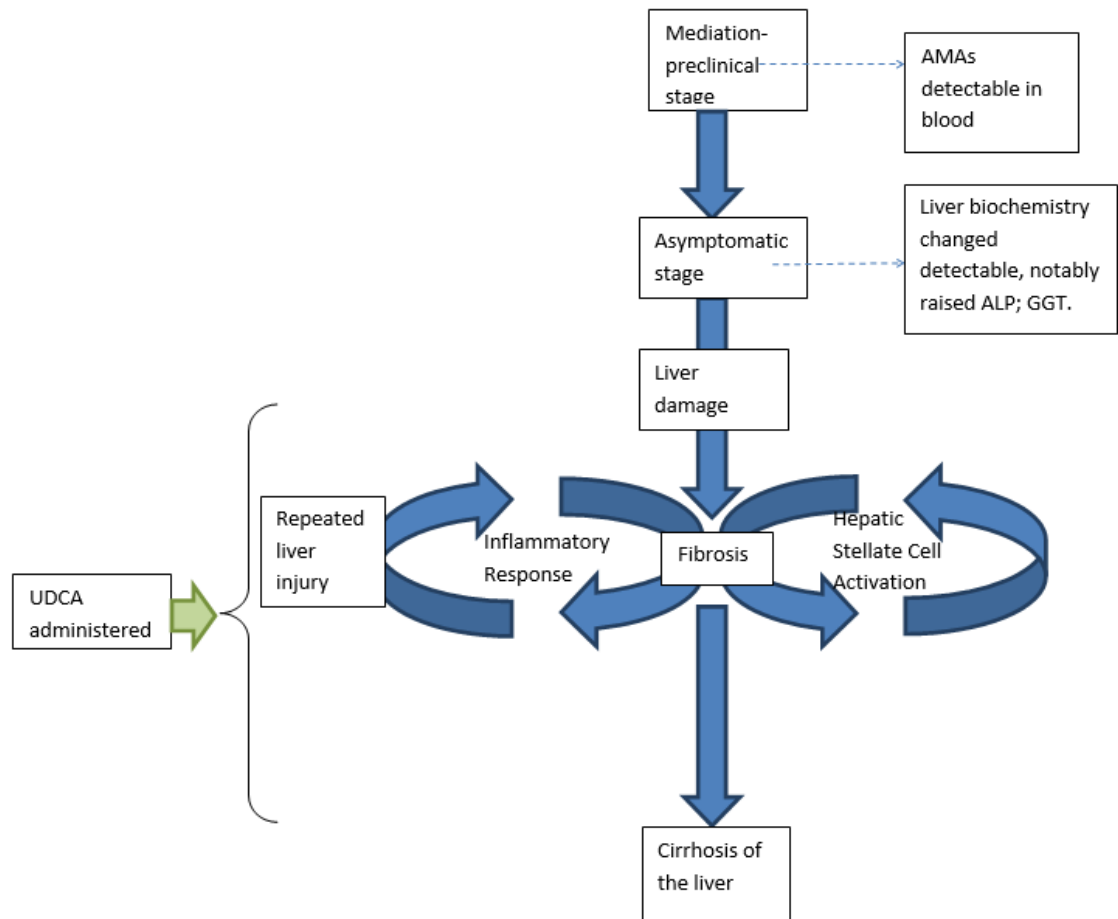


Figure 1.6: Flow diagram of progression of PBC

This flow chart illustrates the rough sequence of events involved in PBC. The disease is detectable before liver insufficiency and hence before the disease becomes symptomatic. Once liver fibrosis has begun, it is self-perpetuating by immune action through inflammation and hepatic stellate cell activation. At this stage, only UDCA may be of potential benefit, however does not prevent progression to cirrhosis of the liver and eventual liver failure. This is adapted from *Addison's other disease*, DE Jones, 2003 (Jones, 2003a).

Symptoms can include chronic fatigue, pruritus, dry eyes and mouth, abdominal pain and diagnosis is based on increased IgM, raised aspartate aminotransferase/alanine aminotransferase (AST/ALT) levels, with a ratio between 1.0 and 2.0; raised alkaline phosphatase; the presence of anti-mitochondrial antibodies (AMAs) in over 95% of patients, notably against the E2 or E1 α component of the pyruvate dehydrogenase (PDC) complex (Fussey et al., 1991a, Jones, 2000); Anti-nuclear antibodies (ANAs) are also seen in a significant proportion of PBC patients (Invernizzi et al., 2001). Although the pathogenesis involves a common series of events including bile duct loss, liver fibrosis, liver cirrhosis and eventual liver failure (Jones, 2003a), outlined in figure 1, the rate of decline and ultimate outcome can vary widely between patients (Carbone et al., 2013).

The presence of self-reactive antibodies and PDC specific infiltrating T cells are indicative of the failure of immune tolerance (Yeaman et al., 2000). One postulated mechanism for the

loss of tolerance to self-antigen is cross-reactivity between responses generated against pathogen-derived PDC peptides and host PDC (Jones et al., 2002). Bacterial PDC, although not pathogenic, is immunogenic: the structural similarity between many of these peptides and their human counterparts could potentially lead to endogenous PDC being recognised by antibody, a mechanism known as molecular mimicry (Zavala-Cerna et al., 2014). Although, there is little evidence of the presence of relevant pathogens in patients, as tolerance breakdown occurs a significant time prior to diagnosis, presence of any initiating microorganism would be unlikely. Also, this theory does not explain the geographical clustering of the disease (Smyk et al., 2010).

1.6.1: Environmental factors, clustering, infection and xenobiotics

It has been reported that those living in certain geographic areas, for example those with high pollution, and potentially a specific type of xenobiotic exposure, are at a greater risk of contracting PBC (Koulentaki et al., 2014, Prince et al., 2001, Ala et al., 2006). Studies have suggested that exposure to certain xenobiotics could increase the likelihood of PBC incidence. Xenobiotics could potentially modify self-PDC into a form against which there is no immune tolerance, antibodies produced against this modified form may then also bind non-modified PDC, leading to breakdown of self-tolerance. Several animal models have demonstrated that tolerance to PBC can be broken by sensitisation with non-self or chemically modified PDC. A mechanism for inclusion of xenobiotics into PDC has been demonstrated which shows that 6-bromohexanoic acid can be processed by human lipoylation enzymes in the place of lipoic acid and could modify self-PDC-E2. This altered PDC binds more avidly than native PDC with patient antibodies and is likely to be sufficiently different to break tolerance in susceptible individuals (Walden et al., 2008). Although this evidence is compelling, there is still only a relatively small incidence of the disease in these areas, therefore there are likely other factors, both environmental and genetic, in determining the likelihood of contracting the disease.

1.6.2: Dominant autoantigens

There are two main recognised disease-specific autoantigens in PBC: E2 and E3 binding protein (E3BP), both of which are subunits of pyruvate dehydrogenase complex (PDC). PDC is a multi-subunit enzyme complex located in the mitochondrial matrix and has the function in respiration of splitting pyruvate to generate Acetyl Coenzyme A (Acetyl CoA) which can then enter the citric acid cycle. Other subunits of PDC include E1 and E3 (Mooney *et al.*, 1999). A complex of E1, E2 and E3 are depicted in figure 1.6.2. Many repeats of this complex and also structural subunits such as E3BP, make up PDC.

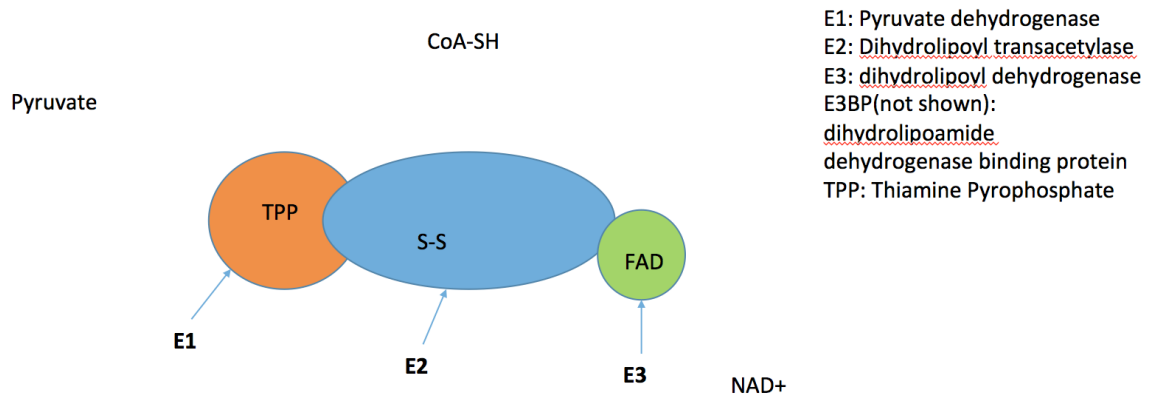


Figure 1.6.2: E1, E2 and E3 of PDC 1

This schematic diagram shows how the key functional subunits are bound for transfer of pyruvate and its metabolites are transferred to the system, eventually leading to Acetyl CoA entry into the citric acid cycle.

The initial and rate limiting stage involves binding of pyruvate to thiamine pyrophosphate (TPP) which is the cofactor of E1, a pyruvate dehydrogenase enzyme. TPP binds to pyruvate, removing CO₂ and generating hydroxyethyl TPP (Marobbio *et al.*, 2002). E2, a dihydrolipoyl transacetylase, contains the cofactor lipoic acid which contains a disulphide bond, to which the hydroxyethyl, or acetyl, group is then passed, creating a high energy thioester bond. This bond allows transfer of the acetyl group to CoA in solution, giving rise to acetyl CoA which can then enter the citric acid cycle (Chueh *et al.*, 2011). The removal of the acetyl group leaves two reduced sulphurs on the lipoic acid of E2. The E3, a dihydrolipoyl dehydrogenase, contains FAD, which removes the two hydrogens from these sulphurs, regenerating the disulphide bond. NAD⁺ in solution then oxidises the FADH₂ to FAD, forming NADH and H⁺. E3BP, a dihydrolipoyl dehydrogenase binding protein, binds E3 and maintains proximity of E3 to the core E2 subunit (Patel *et al.*, 2014).

The two disease specific autoantigens E2 and E3BP have a high similarity, with differences being that E3BP is without the outer lipoyl binding domain and a key discrepancy in the amino acid sequence of the inner lipoyl domain (Palmer *et al.*, 1999).

Despite antibodies against E3BP having been isolated from the blood of some PBC patients, it is not considered a dominant autoepitope. It has been suggested that these antibodies are a result of cross reactivity with E2 or epitope spreading.

1.6.3: Subsets of PBC

Until recently, studies into PBC have used only small study sizes due to relatively few patients treated at each centre. PBC was classed as one single disease with varying

degrees of severity. A UK-PBC cohort study was recently carried out which encompassed 2353 patients and assessed and compared features such as: response to UDCA therapy, laboratory results and symptom impact as reported by the patient (Carbone et al., 2013). Relationships discovered between various characteristics suggest that there are different subtypes of the disease. Research into therapies for PBC should therefore accommodate each individual subtype. This would increase the overall capacity for patient response. This concept is explored more thoroughly in chapters 5 and 6.

1.6.4: UDCA & its mechanism of action

Ursodeoxycholic acid (UDCA) is the only current PDA approved therapy for PBC and its administration has long preceded research into its possible mechanisms of action (Bachrach and Hofmann, 1982).

The discovery of the relevant mechanisms of action of UDCA in PBC could give insight into why some patients respond and others do not with the highlighting of key proteins and pathways affected by UDCA. This discovery would be unlikely to lead to the discovery of a cause of PBC, as UDCA cannot completely prevent disease progression, however may give insight into the differing phenotypes of the different disease subsets.

Primary bile acids are generated in the liver and are transported into interhepatic bile ducts, drained into the left and right hepatic ducts and then collected in the common hepatic duct where it can be diverted to the cystic duct for storage in the gallbladder for later release into the duodenum of the intestine following food entry into the duodenum (Griffin et al., 2017). On release into the intestine, primary bile acids are metabolised to form secondary bile acids by intestinal bacteria to form secondary bile acids such as UDCA. UDCA is then reabsorbed into the bloodstream and then is drained directly to the liver through the hepatic portal vein (Griffin et al., 2017).

UDCA is not itself generated in the liver although it does form tertiary bile acids tauroursodeoxycholic acid and glyoursodeoxycholic acids by conjugating with taurine and glycine respectively by gut bacterial enzyme activity.

Bile duct loss in PBC can lead to bile retention in the hepatocyte which damages the tissue, preceding fibrosis. UDCA has been shown to stimulate bile flow by increasing the number of bile salt export pumps (Bsep) and conjugate export pumps (Mrp2) on the canalicular, or apical, membrane (Paumgartner and Beuers, 2002). This appears to be due to the hydrophilic UDCA conjugate Tauroursodeoxycholic acid (TUDCA) mediated increase in Bsep and Mrp2 insertion into the apical membrane (Beuers et al., 2001). The function of Bsep is to eliminate bile acids and salts into bile ducts from hepatocytes *via* cholangiocytes and Mrp2 is a multidrug resistance associated protein also involved in biliary transport (Nezasa et al., 2006). In this way, UDCA administration may increase bile

drainage, decreasing the damage caused by bile retention and increasing the time until significant bile duct damage shortly preceding liver failure. Additionally, if xenobiotics are having an effect in the pathology of the disease, UDCA may also help to excrete these reducing the potential of further self-antigen modification which may play a minor role in the further exacerbation of disease.

It has been shown that UDCA can indirectly stimulate HCO_3^- secretion, likely by increasing intracellular Ca^{2+} in cholangiocytes (Beuers et al., 1993) causing stimulation of Ca^{2+} -dependent Cl^- channels. The resultant increase in Cl^- concentration in the bile duct causes an increased $\text{Cl}^-/\text{HCO}_3^-$ exchange *via* the exchanger protein anion exchanger 2, as shown in figure 1.6.4. HCO_3^- is a component in bile and so its stimulated release by UDCA may help bile formation thus reducing bile build up in hepatocytes. HCO_3^- release has been implicated in PBC due to attenuated anion exchanger 2 expression (Melero et al., 2002), therefore this is likely a mechanism in which UDCA helps responders to eliminate bile and anion exchanger 2 expression could be an example of a pathway implicated in only responders.

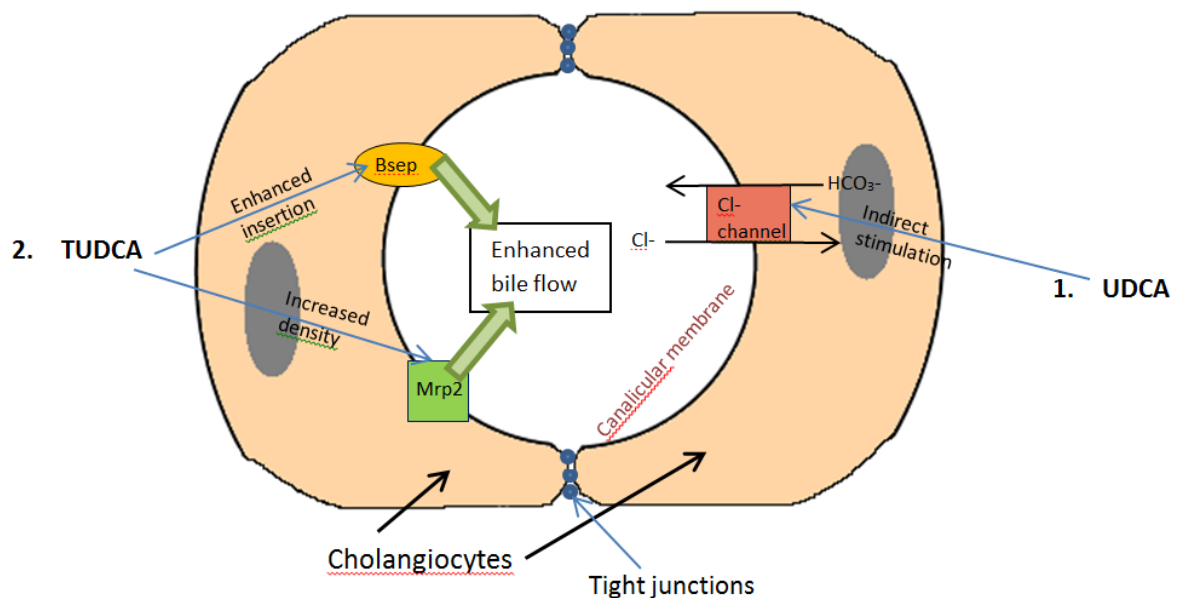


Figure 1.6.4: This diagram of cholangiocytes forming a small bile duct illustrates some of the potential mechanisms by which UDCA may illicit a therapeutic response in PBC.

1. UDCA has been shown to increase intracellular Ca^{2+} which can increase Cl^- transport out of the cholangiocyte via the Ca^{2+} dependent Cl^- channel. The increased extracellular Cl^- concentration causes an increase in $\text{Cl}^-/\text{HCO}_3^-$ exchange via this exchanger. As HCO_3^- is a bile constituent, this process can help increase bile drainage from the liver.

UDCA conjugate, tauroursodeoxycholic acid, has been shown to increase the insertion of transport proteins Mrp2 and Bsep into the canalicular membrane of cholangiocytes, which is believed to help increase bile drainage from the liver.

1.6.4.1: Protection against bile acid induced apoptosis

Build-up of bile acid in hepatocytes can lead to their apoptosis. UDCA may send a survival signal to hepatocytes that would otherwise apoptose.

Bile build up in the hepatocyte can damage the mitochondria and cause mitochondrial swelling (Rodrigues et al., 1998a). Additionally, studies in rats have shown that increased hepatocyte exposure to glycochenodeoxycholic acid, a bile duct constituent, resulted in significantly increased enzyme cytolysis, indicating a large increase in cell apoptosis (Benz et al., 1998). This increased cytolysis was then significantly lowered with the co-incubation with TUDCA, at certain concentrations. The mechanism of action is thought to be an apparent decrease in the uptake of toxic bile acid constituents into the mitochondrial membranes, caused by UDCA (Rodrigues et al., 1998b, Benz et al., 1998). This may reduce ATP depletion associated with mitochondrial damage (Krähenbühl et al., 1994).

1.6.4.2: The immunosuppressant effect

Many studies have shown that UDCA could have an immunosuppressive effect which could help slow disease progression in responding patients (Zhang et al., 2009).

It has been investigated if UDCA can be used to help prevent graft rejection due to its potential anti-inflammatory effects (Zhang et al., 2009, Pageaux et al., 1995). There are conflicting studies: Zhang and colleagues found that mice given one intravenous 25mg/kg dose of UDCA on the day of transplant could survive indefinitely with a fully mismatched cardiac allograft (Zhang et al., 2009). However, Pageaux and colleagues report a failure of UDCA to prevent liver transplant rejection in humans given an oral dose of 600mg UDCA every day for 2 months commencing 3-5 days after surgery (Pageaux et al., 1995). There could be many reasons for this disparity, including: different organisms, different time transplant of administration, different method of drug delivery, different dose concentration. Further research into this area could investigate whether the success in mice could be made applicable to humans by experimenting with the delivery conditions, for example intravenous delivery the day after transplantation.

These findings, coupled with the finding that UDCA only attenuates the symptoms in a certain range of patients, raise the question of what the difference in phenotype between responders and non-responders is which potentially allows UDCA to protect mitochondrial membranes in only some patients, which is an area for potential further study.

1.6.5: Other drugs: Farnesoid x receptor agonists

Just as UDCA has been shown to increase the expression of transporter proteins such as Bsep on the canalicular membrane of the bile ducts, other bile acids can indirectly stimulate the expression of the same transporter by acting as ligands for Farnesoid X receptor (FXR). FXR, in a heterodimer with Retinoic X receptor α (RXR α), can bind hexamer response element targets to induce expression of bile export protein Bsep. Bsep is then transported to the canalicular membrane where it can increase clearance of bile acids into the small bile duct lumen. The endogenous bile acid chenodeoxycholic acid (CDCA) functions as an endogenous FXR agonist, however this action can be inhibited by lithocholic acid (LCA), another bile acid. Synthetic ligands for FXR have been identified. (Neuschwander-Tetri *et al.*, 2014)

1.6.6: Genetics

1.6.6.1: GWAS

Incidence of PBC increases from 0.002-0.04% to 1.33-9% when there is an affected first degree relative (Mells *et al.*, 2013). Previous studies show that the class II MHC loci DR8, DQA1*0102 and DQ*_1*0402 appear to be associated with PBC (Zhang *et al.*, 1994). Additionally, the incidence increases from 0.002-0.04% to 1.33-9% when there is an affected first degree relative, suggesting a genetic basis (Mells *et al.*, 2013). Genome-wide association studies have characterised some coding and non-coding at risk loci which could predispose to PBC.

Many genes relating to immune function were discovered to be significantly linked to PBC (Liu *et al.*, 2012), displayed in table 1.6.6.1. These include: IRF5, with immune system activity (Krausgruber *et al.*, 2011); ORMDL3, cytokine and chemokine inducible (Ha *et al.*, 2013); DENND1B, can be associated with asthma (Sleiman *et al.*, 2010); NFKB1, activated by cytokines. Arguably, a more significant find in the GWAS study is a number of significant differences in genes important in T cell function being a relatively regular find. These are: STAT4 and IL-12, involved in Th1 development and controlling the Th17:Treg ratio (Xu *et al.*, 2011); CD80, necessary for T cell T cell activation and survival; IL7R, essential for T cell development and also is involved in immunoglobulin class switching in B cells (Taniuchi *et al.*, 2013). This evidence implies that PBC may be largely a T cell disease. Research into the differing phenotypes of self-reactive T cells from UDCA responders and non-responders could give insight into the difference between UDCA responders and non-responders and also early and late onset patients. Given that not all patients respond and that disease progression continues, albeit at a slower pace in responders, drugs which target earlier

stages must be investigated and then administered early enough to have an effect, i.e. before irreversible liver damage.

Gene	SNP	At-risk Allele	Chromosome position	P-value
MMEL1	rs10752747	T	1p36	2.65×10^{-3}
IL12RB2	rs17129789	C	1p31	9.48×10^{-20}
IL12A	rs485499	T	3q25	2.29×10^{-16}
(MHCs)	rs7774434	C	6p21	3.86×10^{-34}
IRF5	rs12531711	G	7q32	8.90×10^{-17}
ORMDL3	rs7208487	T	17q12	7.89×10^{-7}
SPIB	rs3745516	A	19q13	1.63×10^{-13}
DENND1B	rs12134279	T	1q31	1.07×10^{-9}
STAT4	rs10931468	A	2q32	2.55×10^{-12}
CD80	rs2293370	G	3q13	7.70×10^{-11}
NFKB1	rs7665090	C	4q24	5.33×10^{-7}
IL7R	rs860413	A	5p13	3.09×10^{-10}
-	rs6974491	A	7p14	3.39×10^{-6}
CXCR5	rs6421571	C	11q23	3.53×10^{-10}
TNFRSF1A	rs1800693	C	12p13	5.51×10^{-8}
RAD51L1	rs911263	T	14q24	1.68×10^{-9}
CLEC16A	rs12924729	G	16p13	7.68×10^{-11}
-	rs11117432	G	16q24	1.20×10^{-6}
MAP3K7IP1	rs968451	T	22q13	4.31×10^{-7}

Table 1.6.6.1: GWAS genes of interest in PBC

This figure shows the potential susceptible genes in PBC, as discovered in a whole genome analysis study. SNPs described in the table, in these genes, appear linked with an increased risk of PBC. The genes of particular interest are, arguably, STAT-4, IL-12, CD80 and IL7R as they implicate a T cell function, as prior studies also suggest. Much further study is required to elucidate the potential impact of each of these SNPs. Additional immune response genes of interest include: IRF5, ORMDL3, DENND1B, NFKB1. Adapted from Mells *et al.*, 2013.

1.6.6.2: X chromosome loss

Enhanced X monosomy in PMBCs, especially T and B cells, is commonly found in women with PBC and also two other autoimmune diseases (Miozzo *et al.*, 2007). X monosomy is also linked with older age (Russell *et al.*, 2007). Haploinsufficiency of genes involved in tolerance maintenance and immune function due to loss of an X chromosome could play a role in autoimmune diseases such as PBC. Two such genes are CSF2RA and CD40. The CSF2RA protein is involved in control, differentiation and production of macrophages and granulocytes (Goldstein *et al.*, 2011) and CD40 is involved in T cell dependent immunoglobulin class switching (Mohammadinejad *et al.*, 2014). Notably, defects in CD40 have been linked to hyper IgM syndrome (Hirbod-Mobarakeh *et al.*, 2014). It is possible that insufficient CD40 due to X chromosome loss could lead to raised IgM in PBC. As this is more common in those of older age (Miozzo *et al.*, 2007), it potentially could be a contributing factor for those with the later onset, less aggressive form of the disease. To validate this, an investigation into the extent of raised IgM and age of patient, or the extent of X chromosome loss, could be carried out. It is important to note, however, that the

mechanisms of the disease may be due to other genes on the X chromosome inactivation and not necessarily CD40.

The possible involvement of X monosomy in PBC should be further investigated because X monosomy is related to age, which also seems to be related to the subset of disease a patient is presenting (Carbone et al., 2013), therefore could potentially be one key factor differentiating between aggressive and non-aggressive disease. X chromosome loss must, then, also be investigated in younger patients, to determine whether it could be impacting PBC as a whole or just the older patients. Additionally, the possible involvement of other genes escaping X inactivation must also be studied, such as CSF2RA, which, if involved, indicates a granulocyte or macrophage involvement in the disease as well as the established T cell involvement, thus potentially further helping to elucidate the cause of disease.

1.7: Conclusion

Typically, removal of the stimulus is important for reversal of fibrosis (Pellicoro et al., 2012), an impossibility in PBC where the antigenic stimulus is endogenous. The chronic inflammatory response leads to further tissue damage and a cascade of fibrosis eventually precluding correct tissue function (Pellicoro et al., 2012), illustrated in figure 1. Ideally, therapies which target T cells must be administered at the earliest possible stage in order to give maximum effect, before the cycle of chronic inflammation is fully established. Therefore, once fibrosis has begun, the stage has passed whereby T cell therapies could give maximum effect.

Given the variable effects of UDCA treatment, considerable recent research has been focussed on the development of novel treatments (Jones et al. 2011, Levy et al. 2011). However, positive results from the latest trials have yet to be presented, and several trials have been halted due to insufficient efficacy at phase II. Given the potential spectrum of pathogenicities involved, it may be that not all recruited patients were likely to respond to specific immunotherapy, a factor which may have contributed to the failure of recent clinical trials.

If the differing underlying pathologies were better understood it may be possible to identify which patients will not respond to standard treatment early following diagnosis, rather than when fibrosis is established, as displayed in figure 1. This would give the potential to stratify both clinical trials and anti-inflammatory treatment and therefore lead to promising novel

drugs being assessed more appropriately and potentially more effective treatment in patient subsets.

The study carried out by Carbone and colleagues which identified the sub-classification of PBC was statistical and symptomatic, based on phenotype alone. It has been well established in the literature that the dominant autoantigen in PBC is the E2 component, particularly the inner lipoyl domain, however other regions of the E2 protein and also the E3BP have also been shown to be autoreactive in PBC (Palmer *et al.*, 1999). It could be that there are different levels of diseased severity relating to different autoantigens in the disease. As the key determining factors in the Carbone study were age, response and sex, this would, then, imply that there could be a link between the particular autoantigen against which the patient develops an immune response and their age, likelihood to respond and blood biochemistry. It is unlikely that the autoantigen alone could determine these factors, however differences in antibody isotype could help explain these differences.

This example highlights the importance of the type of immune response. PBC could involve a crossroads whereby the type of immunological response could determine the severity of the disease. This could be related to responsiveness to the drug because it is well known that UDCA does not completely halt disease progression, only slows it down. The effectiveness of UDCA could be less important than type of response, such that if a patient is giving the ineffective immune response then any effect by UDCA will be negligible.

1.8: The future

All types of PBC lead to a similar phenotype (Carbone *et al.*, 2013). However the journey towards this outcome may be significantly different in terms of the affected pathways (Carbone *et al.*, 2013). There may be differing triggers of the disease in individuals, be they genetic, xenobiotic, biological or a combination of these (Jones, 2003b). Their effects on the general population and how they correspond to disease incidence are unknown. We believe a paradigm shift in the understanding of the pathogenicity of PBC is taking place, and that by fully elucidating mechanisms of disease within different patient groups we can devise more effective treatments.

1.9: Aims of this thesis

This thesis aims to further clarify the subgroups of PBC patients to help bring the disease into the era of stratified medicine whereby patients can receive a therapy which is tailored to their type of disease. This thesis aims to bring new evidence to light to characterise these subgroups biologically such that in the future there may be a diagnostic tool which can distinguish patients in the different subgroups at diagnosis to avoid ineffective therapy from being given inappropriately and unnecessarily to the non-responders. In attempt to achieve this, the impact of UDCA was investigated including both its impact on immune cells and on cholangiocytes. The subgrouping was discovered in its most broad sense in the light of UDCA response, therefore further elucidating the mechanisms of action of this drug may highlight key pathways of interest which may differ from responder to non-responder. Furthermore, biological differences were investigated between the subgroups of PBC patients. This was done by quantifying the autoantibody titres in patients and comparing the different groups of patients. Together these data begin to underpin biological reasoning behind the discovered phenotypic discrepancies between different patients all currently denoted 'PBC patients' under what is likely an umbrella term.

Chapter 2 – General Methods

2.1: Laboratory procedure

All work was conducted under the safety policy of Northumbria University with relevant risk assessments having been undertaken by the PhD student and signed off by one of the supervisory team and checked by technical staff. All work was in compliance with Control Of Substances Hazardous to Health (COSHH) and Control Of Biological Substances Hazardous to Health (BioCOSHH) records, written by the PhD student using relevant chemical information sheets and other product guidance from the supplier, and which were then checked by a member of the supervision team and checked by technical staff. All potentially harmful biological material, such as unscreened healthy volunteer blood, was treated as potentially infected and category II+ containment facilities were used.

2.2: Common reagents

Non-sterile phosphate buffered saline (PBS) was used for all work not carried out under the containment hood or not for flow cytometric analysis. To make 10x working concentration of non-sterile PBS: 80g NaCl, 2.0g KCl, 14.4g Na₂HPO₄, 2.4g KH₂PO₄ were dissolved in 800ml distilled water in a 1l Duran. pH was then adjusted to 7.4 and the volume adjusted to 1l, then the PBS was autoclaved. PBS was diluted in distilled water 1 in 10 for working concentration use. Sterile PBS was purchased from Sigma Aldrich.

Rosewell Park Memorial Institute culture medium (RPMI) was used for cell culture of non-adherent cell lines. Unsubstituted RPMI (R0) was used where specified but for all culturing purposes RPMI was substituted with 10% FBS, 1% L-Glutathione and 1% Penicillin and streptomycin antibiotic cocktail to make complete RPMI media (R10).

2.3: Isolation and culture of PBMCs and cell lines

2.3.1: Phlebotomy

Blood was taken from consenting healthy volunteers who had read and signed full consent forms. Phlebotomy was carried out by a fully trained phlebotomist with certificate and signed off as per Northumbria University procedures. 5 x 10ml lithium heparin-containing vacutainers were used per patient at one time and blood was taken using a 21-gauge butterfly needle. The lithium heparin inactivates thrombin and thromboplastin to prevent blood clotting within the glass container.

2.3.2: PBMC isolation

15ml of lymphoprep was first added to each filter-containing Falcon tube and then pulse centrifuged. Up to 30ml of whole blood was then added on top of each filter within the tube and the tubes were spun at 2100rpm for 12 minutes with brake set to 0. The blood would then be separated into a large serum fraction containing the buffy PBMC-containing fraction. Serum would then be removed and frozen at -20°C. The PBMC-containing buffy layer would then be carefully removed, washed in R10 and resuspended and counted for use.

2.3.3: Culture of PBMCs

PBMCs are cultured at 1×10^6 /ml in R10 unless otherwise stated in individual methods. This same method was applied to the Jurkat cell line.

2.3.4: Culture and splitting of adherent cell lines

Adherent cell line H69 was cultured and allowed to grow until 70-80% confluent, then split 1:5 or otherwise stated. Culture medium used was Dulbecco's Modified Eagle Medium (DMEM) low glucose and F12 Ham (2:1), supplemented with FBS (10% of total media volume), penicillin and streptomycin antibiotic mixture (1% of total media volume), L-glutamate (1% total media volume), Adenine (120µl per l media of 0.2mg/ml working solution), Triiodothyronine (135µl per l total media volume of 10ng/ml working solution), epinephrine (20µl per l total media volume of 50mg/ml stock solution made up in 0.5N HCl), ITS-X (10ml per l total media volume), Hydrocortisone (20ml per l total media volume). The H69 cell line is an immortalised cell line originally isolated from intrahepatic bile ducts (Tabibian *et al.*, 2014). Cells were obtained from Dr Ben Millar, Institute for Cellular and Molecular Biosciences, Newcastle University, in culture form in 10ml of full media in a cell culture flask. Cells had been checked and confirmed negative for mycoplasma contamination immediately before their release to Northumbria University for this study. Splitting of these cells was carried out by checking cell health microscopically, decanting culture medium, washing with PBS 3 times then adding pre-warmed trypsin solution and incubating at 37°C for ten minutes or as long as it took for cells to be visibly dissociated by microscopic visualisation, then collected, centrifuged at 400 x g for 5 minutes and resuspended in their culture medium for counting. Cells were then plated either by 1:5 or to the required number of cells/ml.

2.3.5: Freezing and thawing of cells

Cells were frozen by centrifuging and resuspending at 1×10^7 /ml in 50% culture medium, 40% FCS and 10% dimethyl sulphoxide (DMSO) in 1ml vials and quickly placed in the 'Mr Frosty' freezing container (ThermoFisher) which contained a sponge and isopropanol layer for slow freezing. This was then placed at -80°C overnight, then vials were transferred to liquid nitrogen for long term storage. Cells needed to be quickly transferred into the 'Mr Frosty' as DMSO is potentially toxic to cells at above 0.3% volume of culture media, outlined in chapter 3. The 'Mr Frosty' ensures that cells are frozen at 1°C per minute. Slow freezing helps prevent cells from bursting due to rapidly expanding liquids and DMSO renders the cells porous to allow diffusion of large quantities of liquid, again to prevent bursting (Angel *et al.*, 2016).

Cells were thawed rapidly at 37°C and diluted drop-wise to avoid both DMSO toxicity and osmotic shock. Once diluted 15-fold, cells were rested in media for 30mins then centrifuged to remove DMSO and resuspended to required cell concentration.

2.4: Flow Cytometry

2.4.1: Background

4',6-diamidino-2-phenylindole (DAPI) is a fluorescent dye which strongly binds A-T regions. Live cells are impermeable to DAPI whereas porous dead cells are not. Therefore, live cells can be differentiated from dead cells by the presence of DAPI in only dead cells. DAPI is read in the BV421 channel (Gomes *et al.*, 2013).

Carboxyfluorescein succinimidyl ester (CFSE) is a cell permeable molecule which covalently binds to intracellular molecules, particularly the lysine residues of proteins. Due to the covalent nature of the binding, CFSE can stably remain inside the cell for a long period of time. When the stained cell divides, the dye is divided between the two daughter cells and so is diluted down each generation. Because of this effect, the proliferation of the cells can be studied using flow cytometry over time based on the relative intensity of the dye within each generation of cells (Banks *et al.*, 2012).

2.4.2: Washing cells

Unless otherwise stated, washing of cells entailed adding 2ml of FACS buffer and spinning at $400 \times g$ for 5 minutes and then removing the supernatant and resuspending in FACS buffer for the subsequent wash.

2.4.3: Staining

For staining for flow cytometry, cells were first washed 3 times in FACS buffer, made up of sterile 1 x phosphate-buffered saline solution (PBS) containing 5mM ethylenediaminetetraacetic acid (EDTA) and 2% fetal bovine serum (FCS). Cells were then, if applicable to the panel tube, stained with 4',6-diamidino-2-phenylindole which involved first washing with sterile PBS 3 times and then incubating in the dark on ice in sterile PBS containing 3 μ M DAPI at 1 x 10⁶ cells/ml for 30mins. Cells were then washed and resuspended in FACS buffer. Extracellular identifiers such as surface receptors were then stained for by resuspending cells at 1 x 10⁷/ml in FACS buffer and the titrated concentration for each antibody based on stain index (usually equivalent to 1/200 dilution of raw antibody). Staining took place over an incubation of 30mins at room temperature in the dark then washed 3 times and resuspended in FACS buffer.

The Treg tube required intracellular staining which was performed after extracellular staining. The kit used for intracellular staining of Foxp3 was the eBiosciences FoxP3/Transcription factor staining buffer set. Solutions were firstly made up as per manufacturing guidelines: fixation/permeabilisation concentrate was diluted 1 in 4 with fixation/permeabilisation diluent and permeabilisation buffer concentrate was diluted 1 in 10 in distilled water. 1 x 10⁶ cells were spun at 400 x g and then supernatants discarded. Cells were then resuspended and then 1ml of fixation/permeabilisation working solution was added and the tube was vortexed. Cells were incubated for 30-60 minutes at room temperature in the dark. 2ml permeabilisation buffer was then added per tube and spun at 400 x g for 5 minutes and the pellet resuspended in residual permeabilisation buffer after decanting the supernatant. Cells were then blocked with 2 μ l of FCS added directly to the residual solution and mixed, then incubated for 15 minutes at room temperature. The titrated volume of FoxP3 antibody is then added and cells are incubated for 30minutes at room temperature. Cells were then washed in working concentration permeabilisation buffer and spun at 400 x g for 5 minutes before being resuspended in FACS buffer for flow cytometric analysis.

For proliferation experiments, cells were stained with CFSE prior to culture where specified to measure numbers of proliferation cycles. For CFSE staining, 2 μ l of the 5mM CFSE stock solution was diluted 1/100 in PBS to give 200 μ l 0.05mM CFSE solution, 2ml of which was then diluted 1/25 in PBS to give a 2 μ M CFSE solution. 10% FBS RPMI was kept on ice. Cells to be stained were counted, then washed twice in 0.1% FBS PBS then resuspended in 0.1% FBS PBS at 1X10⁷/ml. This was mixed with an equal volume of 2 μ M CFSE solution and incubated at 37°C for 5 minutes. Cold 10%FBS RPMI was then added to terminate the reaction at a volume equal to the cell solution and CFSE solution mixture. The sample was then placed on ice for five minutes. The tube was then topped up with 10% FBS RPMI and centrifuged at 800 g for ten minutes and resuspended in 10% FBS RPMI, then rewashed

before final resuspension in 10% FBS RPMI. Antibodies and clones used for staining are listed in the appendix, table 8.6.

2.5: Enzyme-linked immunospot (ELISpot)

The ELISpot uses enzymes with cleavage properties such that the cleaved product is visible, so that the release of a cytokine by a cell in response to antigenic encounter can be visualised in the form of a spot. The number of spots visible relates to the number of antigenic encounters in the well. The ELISpot was carried out to determine if UDCA was having an effect on T cells to recognise antigen (Todryk *et al.*, 2009). 50µl of diluted capture antibody, diluted in bicarbonate buffer, at the pre-determined best concentration for that antibody was added to each well, ensuring thorough covering of the bottom of every well. This was incubated at 4°C overnight (8-48 hours is acceptable). Excess capture antibody was removed and the plates washed 3 times with PBS. The plates were then blocked with RPMI containing 10% FCS for 1-8 hours at room temperature to minimise non-specific binding. Blocking solution was then removed to virkon solution.

2.6: xCELLigence

The xCELLigence assay was used to determine if UDCA was having an impact on cholangiocyte cell line proliferation. The proliferation of cells is proportional to the electrical impedance detected on the gold plate, transferred to the software. As a cell makes contact with the golden plate at the bottom of the well, there is increased electrical impedance whereby the greater cell density causes current opposition, which is used as a measure for proliferation.

Microelectrodes cover 80% of the well surface and throughout the duration of the experiment, there is a voltage applied across these electrodes and impedance is measured every 15 minutes throughout the experiment. Impedance is the overall opposition to current flow, given resistance, reactance and capacitance of the elements in the circuit. As cells proliferate, they provide additional impedance to the circuit as the microelectrodes are positioned such that their presence obstructs the flow of electrons. Therefore, the impedance relates to the number of cells present in the well and so gives a representation of proliferation (Martinez-Serra *et al.*, 2014).

2.7: Enzyme-linked immunosorbent assay (ELISA)

2.7.1: Background

The ELISA assay was used to quantify the titres of autoantibody found in patient and volunteer serum. Each well was coated with the protein of interest to allow adherence of the antibody. A secondary antibody conjugated to an enzyme attached. The enzyme had cleavage properties such that the substrate produced has a colour which has a measurable intensity, proportional to the titre of antibody in the serum sample (Engvall and Perlmann, 1971).

2.7.2: Reagents

Tween 20-substituted PBS (PBST) was used in ELISA assays to wash plates between stages. This was made up of 0.05% tween 20 mixed slowly in PBS, slowly to avoid bubbling. ELISA blocking solution was made up of 5% skimmed milk powder dissolved in PBST.

Diluent solution used as the blank and to dilute patient and volunteer samples was made up of blocking solution diluted 1 in 10 in PBST.

Patient serum samples were kindly donated by Prof Dave EJ Jones and Dr Vinod Hegade, Freeman Hospital, provided in raw serum form and immediately transferred to -20°C storage until use.

Citrate phosphate buffer was made by adding 9.149g dibasic sodium phosphate and 4.668g citric acid to 800ml of distilled water then adjusting the pH to 5.0 before adjusting the volume to 1l with distilled water.

Chapter 3 – Design of an assay which can distinguish between different subsets of T cell for use in categorising patient subgroup T cell populations and to investigate any skewing ability of UDCA on T cell populations.

Abstract

There is convincing evidence in the literature that PBC may be a T cell mediated disease with many autoantigen specific T cells, in particular CD4+ T cells, detected around the damaged sites in PBC. Increasing evidence suggests the importance of many signalling pathways in PBC, including IL-12/IL-23 p40, IL-17A and IL-22, IFN- γ and others which does not satisfy the cytokine release profile of just one subset of CD4+ T cells, indicating that there may be several different T cell subsets involved in the pathogenesis of PBC. This chapter describes the design of a flow cytometric assay which can distinguish between cells of different T cell subsets within a population. This involves design of a panel of antigens, establishing the ideal voltage for each channel, titration of each dye, establishing of the negative gate and compensation of all dyes together. This assay was designed to investigate skewing of the normal ratios of T cell subsets by action of UDCA, and to investigate any proliferation inhibition activity that may be specific to one or more types of T cell. Healthy controls were used, with the aim to also use patient cells in the future to determine if responder and non-responder patients have similar responses.

3.1: Introduction

CD4+ T cells recognise extracellular antigen displayed by MHCII molecules which are usually only present on professional antigen presenting cells (APCs) (Mosmann *et al.* 1986). Some types of APCs are macrophages, B cells, dendritic cells and biliary epithelial cells (BEC). BEC are the cholangiocytes that make up the small bile ducts. Their primary role is not thought to be as APCs but they do possess the ability to regulate T cell activation. Although they do highly express MHCII for antigen presentation, BEC do not express essential costimulatory molecules CD80 or CD86, however T cell activation can occur in an alternative way using programmed death ligand 1 (PD-L1) and prostaglandin E2 production (Kamihira *et al.* 2005). APCs take up extracellular antigen, process it internally, then present it on the cell surface within an MHCII molecule which can then be recognised by a CD4+ T cell (Trinchieri and Sher, 2007). CD8+ T cells recognise processed antigen displayed on MHCI, which is present on all nucleated cells in the body. Another mechanism by which antigen can be presented is by APCs using MHCI to CD8+ T cells, a process called cross-presentation. The common autoantigens in PBC are those from oxo-acid dehydrogenase

complexes, predominantly PDC, and are known to be intracellular antigens, however both autoreactive CD4⁺ and CD8⁺ T cells have been isolated from PBC patient blood and also shown to be enriched in the liver of PBC patients (Palmer *et al.*, 1999). This suggests that the autoantigens are being recognised and processed as both intracellular and extracellular antigen.

Aberrant surface expression of PDC-E2 has been shown in BECs of PBC patients, however studies have shown that this is insufficient to cause disease on its own (Inamura *et al.*, 2006), therefore BECs are unlikely to be the primary APC in PBC. Additionally, presence of AMAs alone does not seem to be pathogenic, as some post-liver transplant patients have been shown to have high AMA levels for years post-transplantation without disease recurrence (Neuberger and Thompson, 1999). Additionally, AMA level is not predictive of disease progression (Van Norstrand *et al.*, 1997). Another mechanism must exist for the recognition of PDC subunits as extracellular antigen. Some studies have suggested a B cell origin for CD4⁺ T cell recognition, whereby the B cells take up and express PDC subunits on the surface which are then recognised by autoreactive CD4⁺ T cells (Zhang *et al.*, 2014), more of which is discussed in Chapter 1: Introduction. A recent study has brought to light the possible importance of CD4⁺ Th1 and Th17 cells in PBC (Kawata *et al.* 2013), outlined below.

In response to some antigens and also the inflammatory environment, APCs can release IL-12, which causes differentiation of naïve T cells to Th1. Additionally, macrophages and dendritic cells may release IL-23, which causes differentiation of naïve T cells to Th17. IL-12 and IL-23 share a subunit of IL-12B, also known as p40. When p40 is bound with p19, this forms IL-23 and when p40 is bound with p35, this forms IL-12. Therefore, the relative ratio of IL-12 and IL-23, and therefore possibly also the relative levels of Th1 and Th17 cells, could be being governed by the relative levels of p35 and p19 (Kawata *et al.*, 2013). Similarly, the IL-12 receptor subunit IL-12R β 1 forms a heterodimer with both IL-23R and IL-12R β 2 to form the IL-23 and IL-12 receptors, respectively. A recent study used mice with a deletion of p40, p35 or p19 with 2-octynoic acid conjugated to bovine serum albumin (2OA-BSA) immunisation-induced cholangitis, to investigate the potential role of these subunits in PBC. They found that there was less portal inflammation and cholangiocyte damage in the p35 and p19-deleted mice than wild type mice, when there were downregulated levels of either Th1 or Th17, however the p40 deleted mice showed no detectable lymphocytic infiltration (Kawata *et al.*, 2013). They concluded that when there is no IL-12 or IL-23 to cause differentiation to Th1 or Th17 respectively, there is less overall portal inflammation than without any deletion, however when there is no IL-12 and no IL-23 together, there is no detectable portal inflammation (Kawata *et al.* 2013). This data is suggestive that Th1 and Th17 cells are important in the initiation of inflammation in PBC, giving some evidence to suggest an early importance of CD4⁺ Th1 and Th17 cells.

Regulatory T cells (Tregs, CD4+CD25+FoxP3+) are also of interest in PBC because their levels are lower in PBC patients than in the healthy population (Lan *et al.* 2006). Tregs are known to be of importance in preventing breakdown of self-tolerance and are implicated in many autoimmune diseases (explained in detail in the main introduction). Specifically to PBC, it has been found that there are significantly fewer circulating CD4+CD25+Tregs in PBC patients compared to the healthy population (Lan *et al.*, 2006). It has not been investigated if Tregs could play a role in determining whether a patient is a 'responder' or 'non-responder' to UDCA (response and non-response are discussed more in chapters 5 and 6).

One study indicated an early abundance of Th2 cells, followed by an eventual decline in Th2 levels, and the prevalence of Th1 cells into late stage disease (Sekiya *et al.*, 1999). The group stained T cells isolated from patient blood for intracellular cytokines, using patients at different disease stages and determined that there was a prevalence of Th1 cells into late stage disease and a decline of Th2 cells (Sekiya *et al.*, 1999). The study was not carried out in the context of PBC responders and non-responders, however does indicate a potential early importance of Th2 cells and a potential importance of Th1 cells for disease progression.

These data together suggest that there is evidence to suggest importance of CD4+ T cell subsets but how, why and when the differences in T cell differentiation are orchestrated is poorly understood.

Chapter 1, section 1.6.6, outlines how there could be different genetic variants within different groups of PBC patients, and this may have a consequential impact on the levels and ratios of different T cell subsets. This chapter aims to develop an assay which can take a population of patient PBMCs and analyse the relevant quantities of Tregs, Th1 cells, Th2 cells and Th17 cells. This can be used to provide further evidence on the peripheral T cell population in PBC. This assay can furthermore be used to distinguish any differences in T cell populations between patient sub groups which have been shown to be phenotypically different (Carbone *et al.*, 2013). The subgrouping of PBC patients identified in this study is further explained in chapters 1, 5 and 6.

3.1.1: Flow Cytometry

The flow cytometer can be used to analyse a solution of cells based on their physical properties and the light properties of antibodies attached to them based on the biomarker profiles of the cells in question. Cells are placed into the machine which draws them up and they undergo pressure from sheath fluid which forces the cells into single file so that they can be analysed individually (Bandura *et al.*, 2009). The cell is subject to a laser to measure forward scatter and side scatter of the laser beam based on properties of the cell. For cells in the size range of lymphocytes, forward scatter can be used to predict the approximate

size of the cell and also side scatter can indicate internal complexity or density of organelles. When the initial laser comes into contact with the cell, some of the laser's signal is scattered due to the change in relative refractive index (Bandura *et al.* 2009). Some scatter is determined by the cell as a whole and the size of the cell governs the degree of this scatter whereas some light enters the cell and is scattered by organelles. The scatter caused by the cell, forward scatter, is measured as is that caused by organelles, side scatter, and this data is represented in a forward/side scatter scatter graph (Cossarizza *et al.* 2017).

Based on prior knowledge or a reference graph, it can be estimated where the lymphocytes are on a graph of forward scatter against side scatter, which will later be checked based on other identification markers. Cells are usually stained with fluorescent antibodies targeting surface markers, intracellular markers and/or other dyes. Further lasers challenge these markers and electrons in the fluorescent conjugates can be excited to higher energy states, and then energy of a discrete wavelength is emitted when electrons fall back to a lower energy state, allowing determination of which colours are present (Nicholas *et al.* 2016). Antibodies are chosen based on their fluorochrome and also the epitope to which they bind, therefore presence of a pulse of light in a particular channel is indicative of presence of that particular epitope. Other fluorescent dyes attach other proteins, for example CFSE binds to cytoplasmic proteins and its concentration indicates the number of divisions carried out by that cell (Banks *et al.* 2011) as explained in General Methods. The presence of DAPI indicates that a cell is dead because its presence inside a cell indicates a porous membrane which has allowed the dye to enter the cell, which is characteristic of a dead cell. Manipulation of biomarkers and properties of cells in this way allows cells to be examined so that conclusions can be drawn about the cell population (Zhao *et al.*, 2010).

3.1.1.1: Distinguishing between different types of T cell based on extra- and intra-cellular markers

The population of T cells in a given sample can be determined by examining the specific surface markers or intracellular markers of the cells within the sample. CD3, CD4, CD8, CD25, CXCR3, CCR6, CD45RO and FoxP3 can be used to identify the relative numbers of T cells, divided T cells, CD4+ helper1 or helper 2 T cells, CD8+ cytotoxic T cells and memory or naïve memory T cells (Okado *et al.* 2008). All T cells have the CD3 marker, therefore will stain positively for CD3, and within the T cell population: helper T cells stain CD4+CD8-, cytotoxic T cells stain CD4-CD8+ and regulatory T cells stain positively for FoxP3 and CD25 (Owen *et al.* 2003).

3.1.1.1.1: CD3

Cluster of differentiation 3 (CD3) functions as the T cell receptor co-receptor. Chains within this complex bind the TCR when it recognises antigen to help in T cell activation upon recognition of an antigen by the TCR, as presented by the MHC molecule on the presenting cell. CD3 contains extracellular regions made up of heterodimers of polypeptide chains γ , δ and ϵ in the conformation of $\epsilon\gamma$ and $\epsilon\delta$ (Saito *et al.*, 1987). CD3 also contains an intracellular homodimer $\zeta\zeta$. The γ , δ and ϵ each contain an intracellular region the ζ subunits are fully intracellular. The intracellular regions of these subunits contain the intracellular signal transducing immunoreceptor tyrosine activation motifs (ITAMs), with each of γ , δ and ϵ having one ITAM and each ζ having 3 ITAMs, totalling ten ITAMs per CD3 molecule (Neumeister *et al.*, 1995).

3.1.1.1.2: CD4

CD4 is on the surface of helper T cells and functions as a co-receptor of the T cell receptor (TCR). The TCR binds to the MHCII of the antigen presenting cell (APC) during interaction with the APC and functions to amplify downstream signalling eventually leading to activation of NF- κ B transcription factors and activation of the T cell (Voll *et al.*, 2000). CD4 is also found on the surface of monocytes, macrophages and dendritic cells. It has subunits which include extracellular immunoglobulin domains. These include D1 and D3 which are similar to IgV domains, and D2 and D4 which are similar to IgC domains. It is the D1, which is not present in CD8, which binds MHCII (Silva *et al.*, 2007).

3.1.1.1.3: CD8

CD8, present on the surface of cytotoxic T cells, is a co-receptor for the TCR which binds the MHCI of the APC and causes downstream signalling eventually leading to the activation of transcription factors such as NF- κ B, NFAT and AP-1 (Masuda *et al.*, 1993). CD8 contains subunits CD8- α and CD8- β which each contain an extracellular domain similar to IgV. It is the CD8- α , not present in CD4, which binds the α 3 subunit of MHCI, leading to the specificity of cytotoxic T cells binding MHCI, not MHCII (Willemsen *et al.*, 2006).

3.1.1.1.4: FoxP3

FoxP3 is a nuclear receptor known as the master regulator of T cells. It is a protein in a large family of transcription factors called the forkhead transcription factor family. Expressed in CD4+ regulatory T cells, it acts to suppress NFAT and NF κ B which are transcription factors for many inflammation-generating and immune-response genes such as IL-2 and effector cytokines in T cells. Along with CD25 and CD4, it can be used to identify CD4+ regulatory T cells by flow cytometry (Tzang *et al.*, 2017).

3.1.1.1.5: CD25

CD25, or IL2RA, functions as the α chain for receptor for interleukin 2 (IL2), which is a heterotrimer made up of an α , β and a γ chain, $\alpha\beta\gamma$. Other combinations include $\alpha\alpha\gamma$ and $\beta\beta\gamma$, which give lower affinity receptors with the lowest affinity receptor being $\alpha\alpha\gamma$. The β and γ chains span the cellular membrane and include intracellular tyrosine kinase- bound domains which are involved in signal transduction. CD25 is associated with CD4+ Tregs and is one marker which can be used to identify these cells, alongside CD4+ and FoxP3 (Tzang et al., 2017).

3.1.1.1.6: CXCR3

CXCR3 is a $G\alpha_i$ protein coupled receptor which acts as a chemokine receptor which regulates leucocyte trafficking. CXCR3 is expressed on Th1 cells and promotes Th1 maturation. CXCR3 is involved in T cell migration. In activated T cells, it binds chemokines CXCL9, CXCL10 and CXCL11, related to migration. Where Th1 T cells express CXCR3, it is not expressed in Th2 and Th17 cells (Groom and Luster, 2011a).

3.1.1.1.7: CCR6

An important Th17 cell marker, CCR6, is a G protein coupled receptor important for B cell lineage maturation, specifically antigen driven B cell differentiation. Its ligand is MIP-3, an inflammatory protein released by macrophages. Th1 cells are CXCR3+CCR6-, Th17 cells are CXCR3-CCR6+ and Th2 cells are CXCR3-CCR6-, allowing flow cytometric distinguishing of Th1, Th17 and Th2 cells (Gosselin et al.).

3.1.1.1.8: CD45RO

CD45RO is one of many isotypes of CD45. Also known as Protein Tyrosine Phosphatase Receptor Type C, PTPRTC, CD45 is involved in cell growth and differentiation but negatively impacts cytokine production. If a cell expresses CD45RA, this is indicative of a naïve T cell, whereas a memory T cell will express CD45RO, therefore CD45RO and CD45RA can be used to differentiate memory from naïve T cells. CD45RO presence, alongside CD4, CD25 and FoxP3 can indicate memory T cells where CD4+CD25+FoxP3+CD45RO- Tregs are likely naïve (Thiel et al., 2015). CD45RO has had exons RA, RB and RC removed and so can essentially be thought of as 'CD45 R naught'.

3.1.2: Jurkat cell line

The Jurkat cell line is an immortalised T lymphocyte cell line originally isolated from a 14-year old leukaemia patient. This is a potentially suitable cell line for proliferation studies because it expresses the CD3 antigen therefore addition of an anti-CD3 mitogen can stimulate proliferation of this cell line just as with primary human T cells. The Jurkat cell line will be tested for use in the assay being developed in this chapter. If these cells are suitable for flow cytometric, including proliferation, experiments, this will be far more convenient than using primary cells because Jurkat cells have the capacity to grow to 20 passages for reliable use in experiments whereas primary T cells cannot be passaged and require a healthy volunteer for each new experiment (Schneider *et al.*, 1977).

3.1.3: Aims of the chapter

The primary aim of this chapter was to design of an assay which can distinguish between different subsets of T cell for use in categorising patient subgroup T cell populations and to investigate any skewing ability of UDCA on T cell populations.

There are many stages involved with designing a multicolour flow cytometry assay. These include: design of a panel of antigens, establishing the ideal voltage for each channel, titration of each dye, establishing of the negative gate and compensation of all dyes together.

The development of a robust protocol to categorise the populations of T cell subsets in PBC patients is important as it may allow further categorisation of the responder/non-responder subgroups and possibly may eventually lead to directed therapeutic intervention (Hardie *et al.*, 2016). Initially this assay will be used on healthy volunteer cells having been incubated with different concentrations of UDCA to investigate any skewing of T cell ratios by UDCA or any proliferation inhibition activity that may be specific to one or more types of T cell.

3.2: Methods

3.2.1: Enrichment of T cells for the determination of the best T cell enrichment kit assay

PBMCs were isolated from whole blood as described in Chapter 2: General Methods, and counted using a haemocytometer. They were then separated into 5 groups: PBMCs, Easysep, Rosettesep, Miltenyi and plastic. All groups of cells except for the PBMC group were subject to one of the T cell isolation methods, described below, and stained with antibodies APC-anti-CD4, FITC-anti-CD8 and PerCP-anti-CD3 antibodies as per the flow cytometry preparation staining protocol in Chapter 2: General methods. DAPI staining and CFSE staining are also described in General Methods. Cells were then run through the flow cytometer as described in General methods and data analysed using FACSDiva software to determine the most effective T cell proliferation kit.

3.2.1.1: Easysep:

The STEMCELL technologies Easysep negative selection kit contains a cocktail of antibodies which attach to all cells other than the desired cells and then attaches those unwanted cells to magnetic particles which can be separated by magnetism with a large magnet and pouring the desired cells away from those bound to the beads.

A negative selection kit was chosen rather than a positive selection kit which would include a cocktail and bead combination that would cause the T cells to be bound to the magnetic beads and leaving the rest of the PBMCs in solution. Although the positive selection method would be effective, the negative selection kit was selected in order to leave the cells of interest as undisturbed as possible. These T cells were then used in proliferation experiments, in which it is important to activate T cells only at the desired time, therefore the negative selection kit was most appropriate.

PBMCs were isolated from whole blood as per the method in chapter 2, General Methods. Cells were counted, then transferred to a sterile 5ml polystyrene round bottom tube with cap and centrifuged at 1400rpm for 5mins then resuspended in PBS with 2% FCS and 1mM EDTA to a concentration of 5×10^7 cells/ml with a maximum of 2ml in each tube. Easysep Human T cell Enrichment cocktail was then added at 50 μ l per ml volume of cell suspension, mixed thoroughly and incubated at room temperature for 10 mins. Easysep D Magnetic Particles were then vortexed for 30 seconds and then added at 50 μ l per ml cell suspension volume. The solution was mixed well then incubated at room temperature for 5 minutes. PBS with 2% FCS and 1mM EDTA was then added to bring the total volume to 5ml and gently mixed. The cap was removed from the tube and placed into the magnet and left for 5min. Without disturbing the nature of the beads, the magnet and tube were picked up

together and inverted, pouring the remaining solution fraction which contains the purified T cells into a fresh collecting tube.

3.2.1.2: Rosettesep:

The STEMCELL technologies Rosettesep assay used is a negative selection kit similar to Easysep but is designed to eliminate the need for a second stage with magnetic beads and instead incorporates isolating the T cells with removing the red blood cells from the whole blood. The Rosettesep kit includes a cocktail which cross links PBMCs not of interest to the red blood cells so that they are pelleted with red blood cells in a density gradient centrifugation.

Rosettesep Human T cell Enrichment cocktail was added to the whole blood at 50 μ l per ml of blood and then the blood was mixed well. The blood was incubated at room temperature for 20 mins and then diluted 1:1 with PBS containing 2% FCS and 1mM EDTA. Blood was then layered carefully to prevent mixing over a density medium such as lymphoprep in a 50ml falcon tube and the sample was spun as per blood separation method, general methods. The lymphocyte fraction contained only T cells. This fraction was collected and the rest discarded.

3.2.1.3: Miltenyi

The Miltenyi T cell isolation kit, like the Easysep kit, utilises magnetic beads although, rather than having to tip off the cells of interest, the Miltenyi kit passes the bead-containing mixture through a column of similar magnetic beads which allowing only unbound cells to pass through.

Cells were counted and prepared such that there were 10^7 cells in 40 μ l PBS with 2% FCS and 1mM EDTA. 10 μ l Pan T cell Biotin-Antibody Cocktail was added per 10^7 cells and mixed well then the mixture was refrigerated at 2-8 $^{\circ}$ C for 5 min. 30 μ l of PBS with 2% FCS and 1mM EDTA and 20 μ l Pan T cell MicroBead Cocktail were then added per 10^7 cells. The mixture was incubated for 10mins at 2-8 $^{\circ}$ C. The MACS magnetic column was then assembled and washed with 3ml of PBS containing 2% FCS and 1mM EDTA. A suitable collecting tube was placed underneath the column and the cell suspension was added to the column. Another 3ml of PBS containing 2% FCS and 1mM EDTA was then added to the column and the run-off was added to the initial collection. This stage is in place to collect any T cells stuck in the column.

3.2.1.4: Plastic:

Incubating the PBMCs in a culture flask overnight takes advantage of the nature of some PBMCs to adhere to the plastic surface, for example monocytes, such that a more enriched T cell suspension can be poured off.

PBMCs were suspended at 1×10^6 in their culture medium and incubated overnight at 37°C in a culture flask. All remaining PBMCs in solution were then poured into a suitable collecting container and kept as this was the T cell-containing fraction.

3.2.2: Fresh and frozen cell comparison

As the main aim of this study was to establish a flow cytometry panel assay which could be used to determine differences in patient cells, it needed to be established if patient cells may be frozen prior to their use in the assay or if they must be used fresh. Logistically, using frozen cells would be far more feasible as many samples could then be collected and processed at the same time.

Blood was collected from 3 healthy volunteers and PBMCs were isolated as per the protocol outlined in Chapter 2: General methods. T cells were then isolated from the blood using the Easysep T cell enrichment kit, protocol described in section 3.2.1.1. Half of these cells from each volunteer were then frozen using the cell freezing method outlined in Chapter 2: General methods. The other half were stained with CFSE dye and incubated in their media their substituted RPMI containing $10\mu\text{l}$ Dynabeads and 50U/ml IL-2 to induce proliferation. Cells were extracted each day including day 0, the day the experiment was set up, until media discolouration occurred, which implied that the cells had depleted their media nutrients and begun to die, and also until proliferation peaks could be seen on analysis with the flow cytometer. For flow cytometer analysis, cells were stained with APC-anti-CD3 to allow gating round all T cells.

3.2.3: Jurkat cells

Jurkat cells (ATCC[®] TIB-152[™]) were kindly provided by Dr K. Padgett, Faculty of Health and Life Sciences, Northumbria University.

It was initially intended to use Jurkat cells in T cell proliferation experiments to monitor the effects of proliferation in different conditions and to optimise assays. This would theoretically be more convenient than using primary T cells which would involve the need for a healthy volunteer and isolation of the PBMCs every time. Jurkat cells survive in culture for a number of passages, giving an advantage over using primary cells.

3.2.3.1: Jurkat growth curve

Firstly, the optimal conditions and concentrations for optimal growth were established. Cells were allowed to grow to 80% confluency in a flask then plated in triplicate in a 24-well plate at 1×10^5 cells/ml. Every 24 hours, cells were counted using a haemocytometer and trypan blue staining. These are displayed on a graph so that the optimal growth period can be established from the steepest positive gradient straight line portion of the graph and the number of days until cells die off without a media change or splitting can also be established, and the concentration of cells at which this happens.

3.2.3.2: Jurkat healthy cells bead titration

To establish the concentration of Dynabeads which is most appropriate for proliferation of Jurkat cells, a titration experiment was carried out to compare the effect of different concentrations of Dynabeads on Jurkat cells with the same concentration on healthy control cells. Cells were stained with CFSE dye and incubated for 3 days in the presence of 50U/ml IL-2 and every 24 hours including the set up day, day 0, cell samples were harvested for staining with APC-anti-CD3 for analysis by flow cytometry.

3.2.4: Priliminary proliferaton experiment

T cells were isolated from whole blood of 3 volunteers by first using the PBMC isolation method and then purifying the T cells using the easysep method described in section 3.2.1.1. T cells were then CFSE-stained and set up for proliferation in the presence of $10 \mu\text{l}$ Dynabeads T cell proliferation beads and 50U/ml at different concentrations of UDCA in a 24-well tissue culture plate for 3 days. Samples were extracted from culture every 24 hours and prepared for flow cytometric analysis by method and stained with anti-CD3APC. CD3+ T cells are gated around and then analysed on a FITC-channel histogram to view proliferation peaks and compared to $0 \mu\text{M}$ UDCA. The zero-UDCA contains the ethanol carrier at 0.3%, the same volume of ethanol as in all other wells.

3.2.5: T cell proliferation methods

Several proliferation methods were trialled, (anti-CD3 mitogen; IL-2; IL-2 plus Dynabead T cell proliferation beads; phytohaemagglutinin (PHA); phorbol 12-myristate 13-acetate (PMA) at different concentrations with ionomycin) to establish the most suitable for future assays.

Factors considered included: if the number of divisions could easily be counted based on the peak patterning and which cytokines are likely to be produced on activation by each method. If the cytokines give too much of a skew towards a particular T cell sub-type, then it may be difficult to observe a pattern in different T cells produced by different PBC populations.

Section 2.2.5 of this chapter details optimising strategy in detail. Briefly, PBMCs were isolated from whole blood by the method in Chapter 2: General Methods and stained with CFSE. Each of the assays for testing was set up with PBMCs at 1×10^6 /ml across 5 x sterile 5ml flow cytometry tubes and incubated for up to 7 days, with a tube used at days 3, 4, 5, 6 and 7 and stained with dead/alive comparison dye DAPI for flow cytometric analysis for proliferation.

3.2.5.1: Anti-CD3 mitogen

The α CD3 mitogen is a monoclonal antibody that binds to the ϵ -chain of CD3. CD3 is the T cell antigen receptor and the ϵ -chain is non-antigen related. The α CD3 mitogen binds and crosslinks the TCR, mimicking the effect of binding an antigen and related MHC. Although unable to cause a response in the T cell due to lack of a surface the T cell can be cross-linked to, α CD3 is sufficient to cause proliferation of the T cell in the presence of IL-2, which is provided by other PBMCs when it is a PBMC cell suspension (Jason and Inge, 1996). The α CD3 is diluted 1/200 from 1mg/ml to 5 μ g/ml in complete RPMI for working concentration use.

3.2.5.2: IL-2+beads

Dynabeads Human T-Activator beads can be used to stimulate proliferation of T cells. They consist of metal beads bound with anti-CD3, anti-CD28 and anti-CD137 (glossary ref here). IL-2 is also added to the culture to induce proliferation at a concentration of 50 U/ml.

The beads are magnetic so that they can be removed prior to flow cytometry if necessary. The required volume of Dynabeads is first calculated using the guide provided in the information pack with the kit and these are placed in a vial and mixed 1:1 with PBS containing 2% FCS and 1mM EDTA. The vial is placed in the magnet and left for 5min. All liquid is poured into waste and then the beads are resuspended in their initial volume, of PBS with 2% FCS and 1mM EDTA. Beads are required to be added at a ratio of 1:1 beads to cells, therefore, according to the manufacturer guidelines, a final cell concentration of 1×10^6 will require 25 μ l per ml of cells. However, in this study a titration was carried out which showed adequate T cell proliferation using only 10 μ l of beads, as shown in the results section of this chapter, figure 3.3.3.2, therefore 10 μ l of beads would be used in further experiments.

3.2.5.3: IL-2 alone

IL-2 is added to the cells at a concentration of 50 U/ml to see compare with IL-2 and Dynabeads to see what difference adding the beads makes compared with just IL-2.

IL-2 is a cytokine which targets T cells, B cells, NK cells, monocytes and macrophages. Downstream mechanisms of IL-2 include inducing proliferation in and inducing expression of more IL-2 and IL-2R in CD3⁺ T cells. In theory, IL-2 is insufficient to induce proliferation alone in the absence of antigenic response, however some groups have recorded increased T cell proliferation in vitro even without adding antigen (Kennell et al., 2014). Therefore, IL-2 will be tested for its ability to proliferate T cells in the PBMC population and compared to other T cell proliferating methods.

3.2.5.4: Phytohaemagglutinin (PHA)

The poorly-defined mechanism by which PHA causes T cell expansion is thought to involve the alternative activation pathway of CD2. CD2 offers an alternative proliferation pathway for T cells to CD3, and potentially gives a larger response with more IL-2 released and stronger Th cell responses. A lectin, PHA binds to glycoproteins on the cell surface, including the TCR, and cross links them, inducing metabolic activity and cell division (O'Flynn et al., 1986). It can be predicted that this method will not give reliable proliferation results by way of a predictable peak patterning on CFSE staining as the alternative pathway can induce apoptosis and is generally a more sporadic pathway (Wesselborg et al., 1993).

3.2.5.5: Phorbol 12-myristate 13-acetate (PMA) + ionomycin

PMA, a small organic compound, diffuses through the cell membrane and into the cell, directly activating protein kinase C, thus bypassing the need for cell surface glycoprotein cross linking.

Ionomycin is used in conjunction to raise intracellular IL-2, IL-4, IFN- γ and perforin and the intracellular Ca²⁺ level, which is required for intracellular signal transduction (Heit et al., 2006).

The concentration of PMA to use depends on the cell type, therefore it is necessary to titrate the concentration to obtain optimal concentration of PMA to proliferate T cells. The standard 1 μ g/ml of ionomycin is used along with 0.5, 5.0 or 50ng/ml PMA, depending on the result of the titration, therefore all of these concentrations are used in this assay.

3.2.6: Flow Cytometry preparation

3.2.6.1: Antibody titration

It is necessary to find the optimal staining concentration for antibodies before their use in a major flow cytometry experiment. The antibody is diluted 1 in 10 with PBS such that very small volumes of antibody can be added accurately, avoiding pipetting tiny volumes of undiluted antibody. Cells are stained as per flow cytometry staining method outlined in Chapter 2: General methods, but taking into account the different volumes and the dilution of the antibody, and run on the flow cytometer. The ideal stain concentration range is taken from a graph of concentration of antibody in cell suspension during staining against the standard index, calculated by the below formula:

$$\text{Standard Index, SI} = (\text{median}_{\text{pos}} - \text{median}_{\text{neg}}) / 2\text{xSD}_{\text{neg}}$$

The ideal range of antibody concentrations is the upper-most portion of the curve, as shown in figure 3.3.5.2.

3.2.6.2: Voltages

Voltages for each antibody need to be adjusted to ensure that both the negative and positive peaks are visible in the displayed range. There is a method to determining the optimal voltage range for each dye (Maecker and Trotter, 2006), however in practise the most important aspect is that the positive and negative peak are clearly visible and fully between 0 and 10^5 on the x axis such that no extremely low or high values are cut off by the limitations of the graph. Voltage adjustment is carried out for every dye to ensure they satisfy this criterion using the voltage menu in the FACSDiva software. Figure 3.3.5.2 shows the maximum range of voltages permissible. In this dye, anti-CD8 PE-Cy7, ideally the voltage would be decreased to move the positive peak below the 10^5 mark on the x axis, however doing this would move the negative peak to below the zero. Adjusting the voltage for each dye is important for before compensating the dyes.

3.2.6.3: Fluorescence Minus One, FMO

Fluorescence Minus One, FMO, analyses must be carried out for each antibody to ensure that the gates for positive and negatives are in fact in the correct places. The FMO uses every dye except the dye in question to help place the negative gate for that dye. The negative gate cannot be placed based on unstained cells because this is not indicative of how the other dyes interact with that channel, which for the demonstrative figure is the BV510 channel. Figure 3.3.5.4 shows the difference between unstained cells and the FMO. The FMO gives a more accurate negative because it allows ruling out of spill-over fluorescence from other dyes.

3.2.6.4: Isotype negatives

Using an isotype negative for an antibody is a way of determining how inclined the cell is to randomly bind antibodies of this isotype despite non-specificity, or how inadequate the blocking stage of the staining protocol is. The isotype negative is used in place of the antibody to test how many positives there are. The isotype negative is an antibody of the same isotype as that in question and with the same conjugate but is raised against a random antigen, not present on the cell. Therefore, any positive readings in the channel in question are likely due to not all non-specific binding sites being blocked effectively (Baksh *et al.* 2007).

3.2.6.5: Doublet and clump discrimination

When 2 or more cells stick together, then 2 cells may be unintentionally read as one cell, therefore a dye can appear twice as bright as it actually is. To ensure only singlet cells are examined, a graph of forward scatter height against forward scatter area. Forward scatter can be indicative of cell size. 'Height' describes a cell's total maximum signal, 'Width' describes the time the cell spends passing through the laser beam and 'Area' is a total of all of the 'H' readings made during time 'W'. Cells that show a smaller 'Height' per unit 'Area' are likely clumps or doublets because they also then give more 'Area' per unit 'Height', so more readings per unit cell size, implying there are more scatter readings than expected for something which should only be one cell. These cells are gated out so that those cells analysed are likely only singlets. This is important because if analysing doublets, it may appear as though there are twice as many biomarkers in one cell than there actually are. Gating out the doublets and clumps is illustrated in figure 3.3.7.2.1.

3.3: Results

3.3.1: Method of T cell isolation

Four methods of T cell enrichment were compared for their efficiency at producing a pure enriched T cell population. Easysep was chosen based on giving a greater percentage of CD3+ cells and also more total CD4+ T cells plus CD8+ T cells.

Figure 3.1 shows the gating flow cytometric analysis for how these results were obtained and table 3.1 shows the tabularised results from the gating in figure 3.3.1, as counted using FACSDiva software. Table 3.3.1 shows that there are 95.51% T cells in culture isolated by the Easysep method when gated by CD4+ and CD8+ presence and 98.58% T cells in culture when gated by CD3+ presence, higher values in both criteria than any other method.

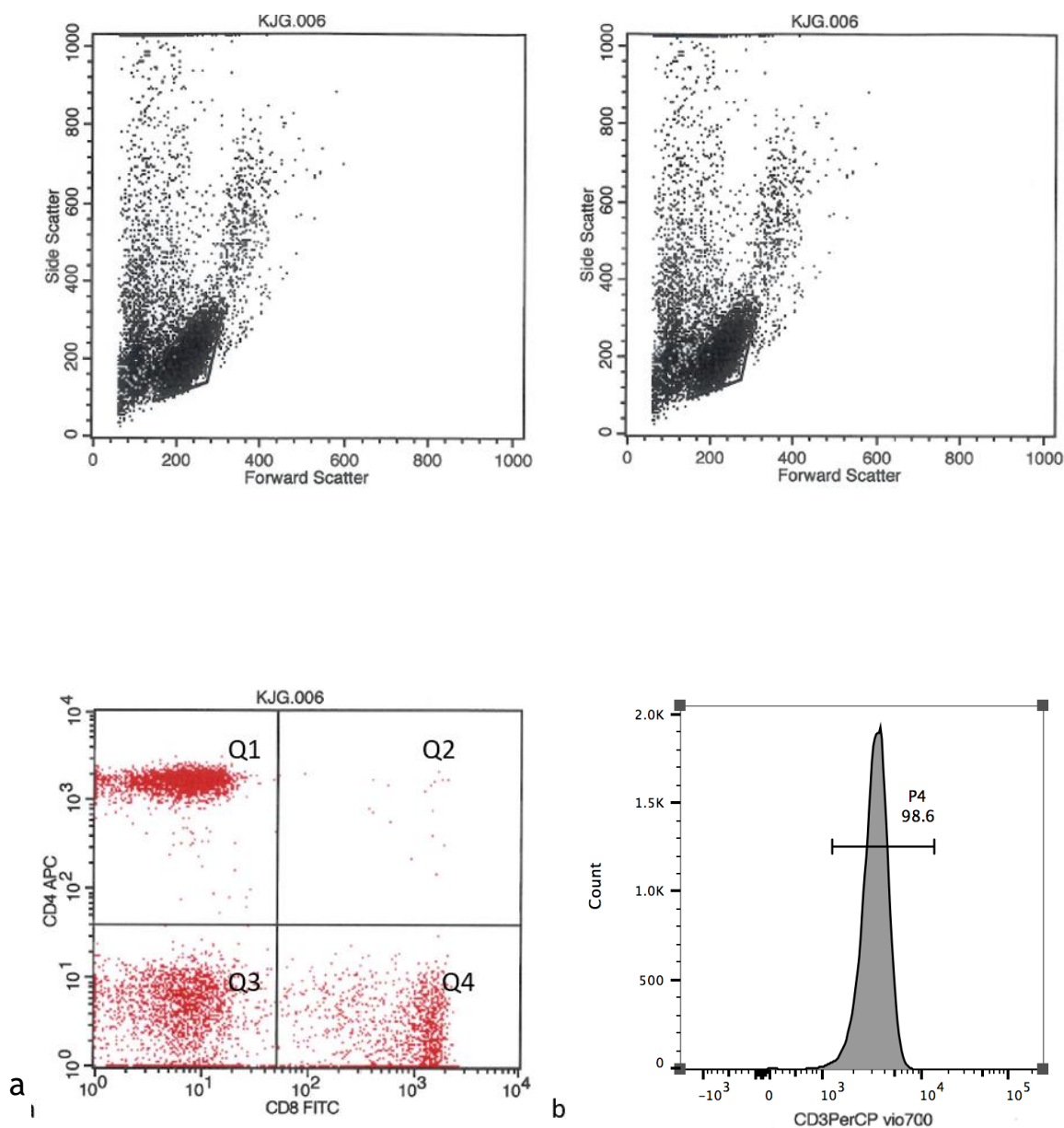


Figure 3.3.1: Flow Cytometry counting of T cell sub sets for isolation kit comparison

This figure shows how the cells are gated and analysed for their surface markers. The top graphs in black show gating around the lymphocyte fraction based on side scatter and forward scatter separation. The bottom graphs show gating to discriminate the different cell populations. The number of cells within a gate or quadrant are counted by the software.

a: The graph is separated into quadrants where Q1 gates around CD4+CD8- cells, Q2 gates around CD4+CD8+ cells, Q3 gates around CD4-CD8- cells and Q4 gates around CD4-CD8+ cells. Quadrants Q1, Q2 and Q4 are totalled.

b: The histogram feature is used to quantify all anti-CD3 PerCPvio700 positive cells (P4).

		Percentage within lymphocyte gate				
		CD4	CD8	CD4CD8	Total	CD3
T cell enrichment method	Easysep	66.34	29.09	0.08	95.51	98.58
	Rosettesep	66.46	24.27	0.06	90.79	93.61
	Miltenyi	65.49	25.69	0	91.18	92.64
	Plastic	58.1	23.2	0.19	81.49	84.6
	PBMCs	15.21	25.1	0.42	40.73	41.7

Table 3.3.1: Table to compare T cell isolation methods.

This table shows the percentages of CD4+, CD8+, CD4+CD8+ and CD3+ T cells within the lymphocyte gate shown in figure 3.3.1, isolated using each of the different methods outlined in section 3.2.1: Methods.

3.3.2: Fresh and frozen primary T cell comparison

T cells isolated from the whole blood of 3 healthy volunteers were proliferated using IL-2 and proliferation beads where one sample from each patient was frozen and reanimated and the other sample was freshly isolated and not frozen. Fresh and frozen proliferation results were compared by t testing by counting the populations of 1 and 2+ shown in figure 3.3.2 and no significant results were found, therefore it was determined that frozen cells could be used if inconvenient to use fresh cells, particularly in incidences of receiving large numbers of patient blood samples. However, in order to ensure experimental parity any experiment using patient cells would use frozen cells.

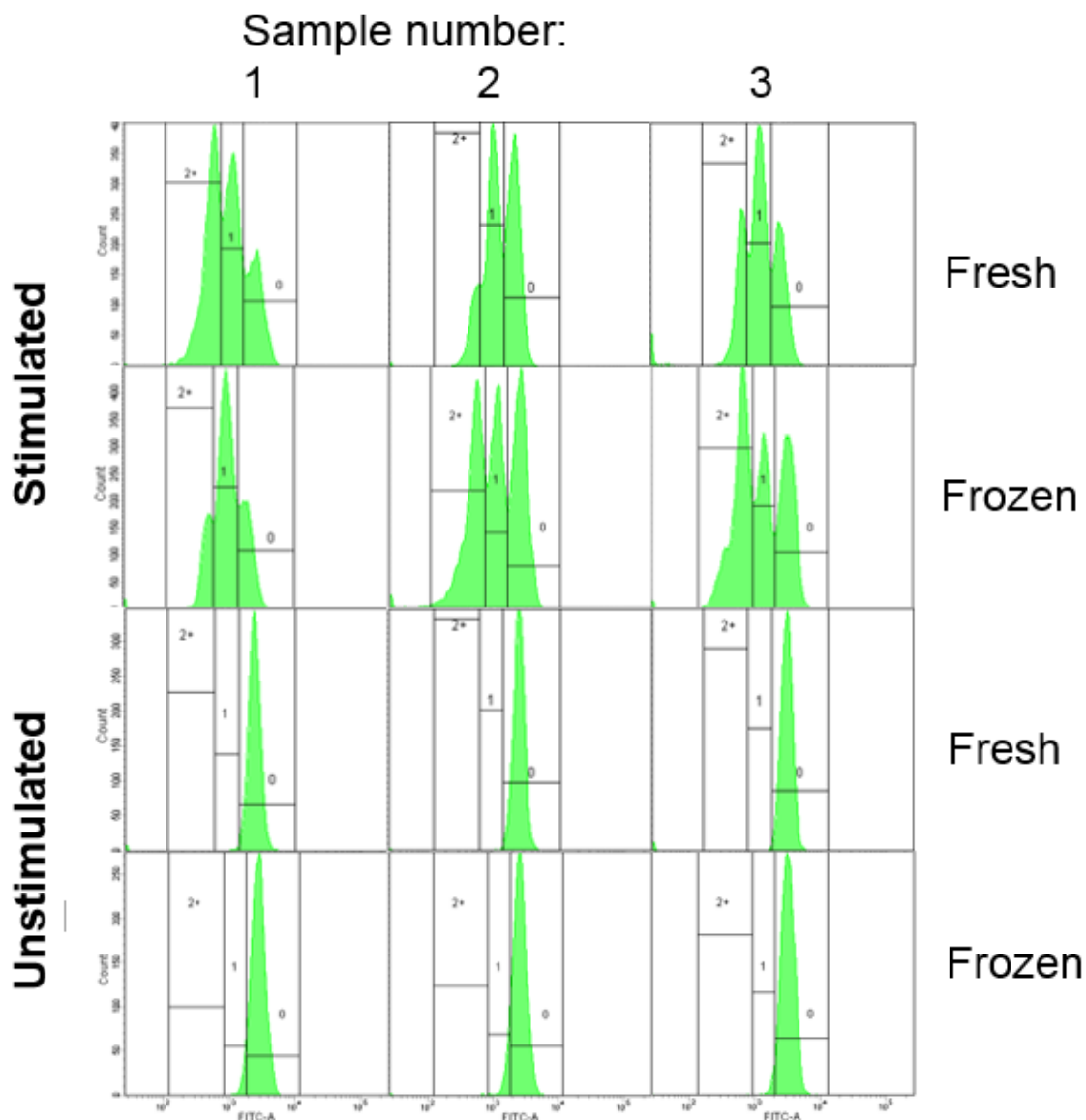


Figure 3.3.2: Fresh and frozen proliferation comparison

This is a comparison between cells frozen to -150°C then reanimated and cells isolated from fresh whole blood and used immediately. Stimulated samples have IL-2 and proliferation beads added to induce proliferation. There was no significant difference found between divided frozen cells and divided fresh cells. Unstimulated cells are included to illustrate that the right-most peak on proliferation graphs is likely representative of cell proliferation without any stimulant.

3.3.3: Jurkat cells

3.3.3.1: Jurkat cells growth curve

Figures 3.3.3.1 a and b show the growth of Jurkat cells and healthy volunteer cells over time. This graph suggests that Jurkat cells appear to proliferate uniformly until day 8 when they begin to die, as shown by the drop off in the lines. Healthy T cells proliferate more sporadically, not closely following the average line.

3.3.3.2: Jurkat cell proliferation assay

Figure 3.3.3.2 shows Jurkat cell proliferation using Dynabeads, mechanism of action outlined in section 3.2.2, compared with proliferation of healthy volunteer T cells using Dynabeads. With the healthy controls, there are clear fractions of T cells which have proliferated a discrete and measurable number of times relative to the right-most peak. The area under the curve of each peak is indicative of the number of cells in this fraction and can be counted using the software. Regarding the Jurkat cells, for all concentrations of Dynabeads there is only one peak from which no proliferation data can be inferred, suggesting that Jurkat cells are inappropriate for further cell proliferation experiments.

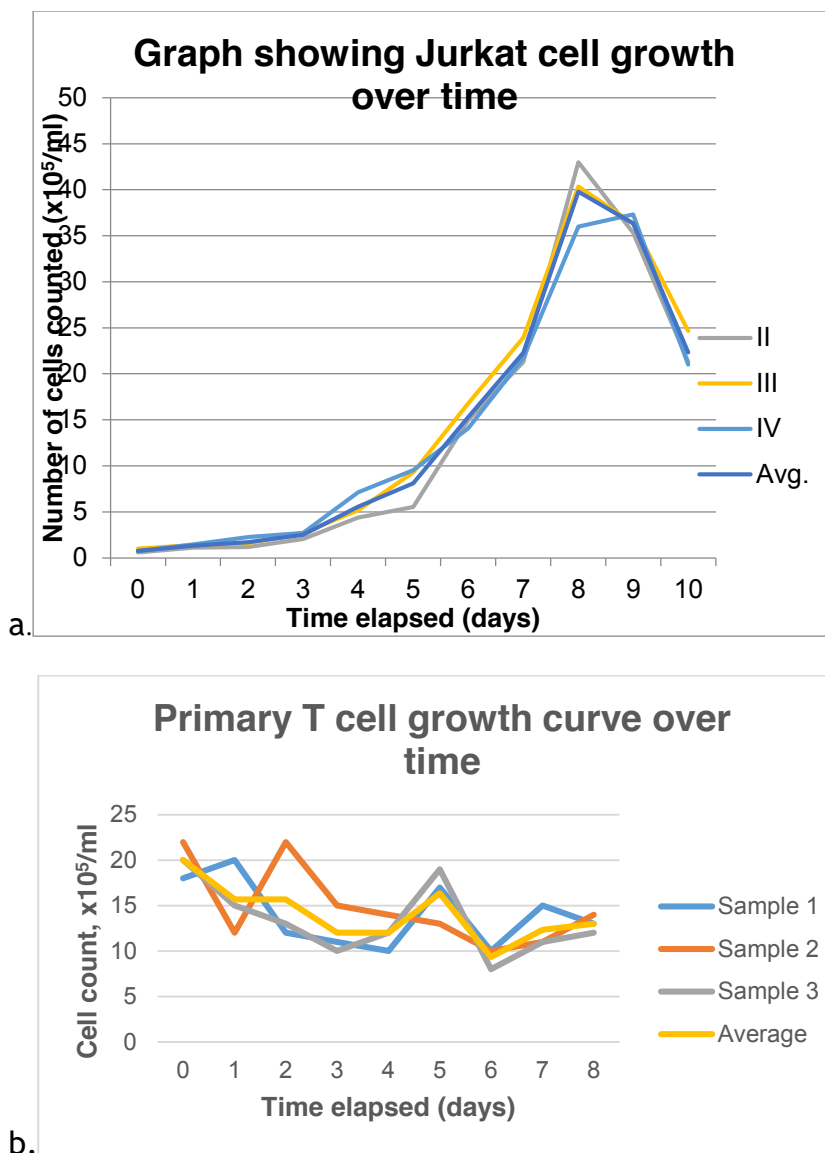


Figure 3.3.3.1: Growth curve of cells of the JURKAT cell line.

a: The graph shows the number of cells counted per ml over time, encompassing lag phase, exponential phase, plateau and death phase.

b: This graph shows a growth curve of healthy volunteer T cells isolated from PBMC culture, isolated from whole blood of a healthy volunteer.

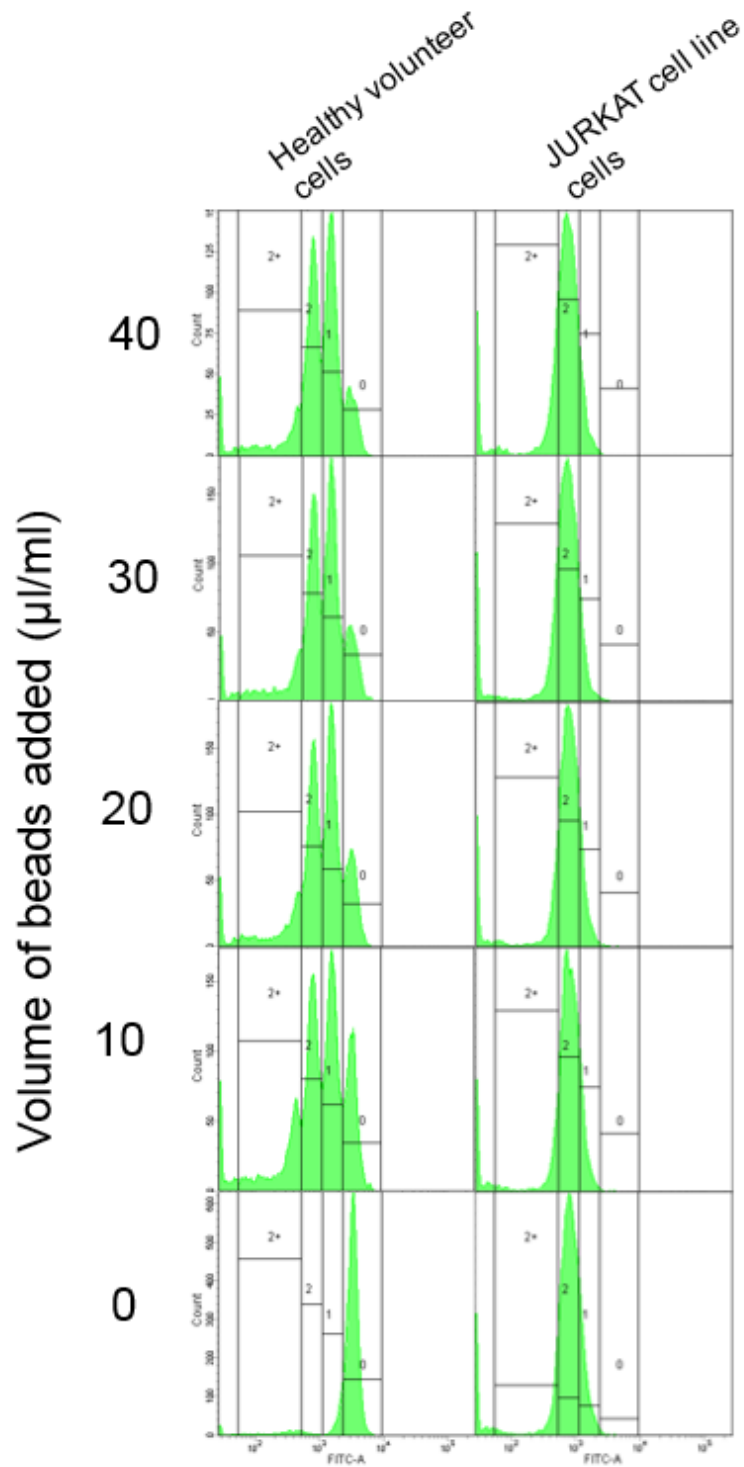
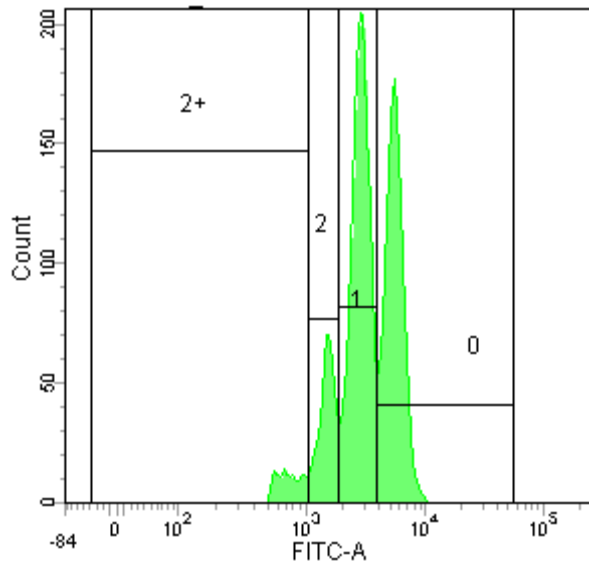


Figure 3.3.3.2: Proliferation bead titration for healthy T cells and JURKAT cells. JURKAT cells are compared by their proliferation pattern to healthy T cells isolated from a volunteer to assess their use as an adequate model cell line in T cell proliferation studies.

3.3.4: Flow cytometry preliminary data

A preliminary experiment was carried out to determine if there was an effect on T cell proliferation of isolated T cells by UDCA which could then direct further investigation into if different subtypes were affected differently. Figure 3.3.4.1 shows the pattern of proliferation peaks visible when cells have divided by different numbers of divisions within the population. The far-right and most CFSE-intense peak is representative of cells which have not proliferated or cells which have proliferated the minimum number of times among the population, and this peak is used as the 'undivided' reference, which is possible when the far-right peaks line up across different concentrations including zero, which was the case. It was found that there was a significant difference in divided cells between cells incubated with 300 μ M UDCA and 0 μ M UDCA, as shown in figure 3.3.4.2 where t-testing proliferation of T cells in 300 μ M UDCA with proliferation of T cells in 0 μ M UDCA gives a p value of 0.039, which is significantly different.



Tube: 0_1mM UDCA and beads

Population	#Events	%Parent	%Total
All Events	31,727	###	100.0
Lymphocytes	7,494	23.6	23.6
CD3+	4,912	65.5	15.5
⊗ 0	1,846	37.6	5.8
⊗ 1	2,181	44.4	6.9
⊗ 2	657	13.4	2.1
⊗ 2+	241	4.9	0.8

Figure 3.3.4.1: Flow cytometric acquisition of counts of cells at different proliferation numbers.

Individual peaks in the histogram indicate number of divisions past the far-right peak of either zero divisions or the minimum number of divisions observed across the experiment. The fewer divisions the less dilution of the dye has occurred and the higher the intensity of CFSE. The table shows counting of cells in each group with cells in peaks 1, 2 and 2+ added to give total proliferated.

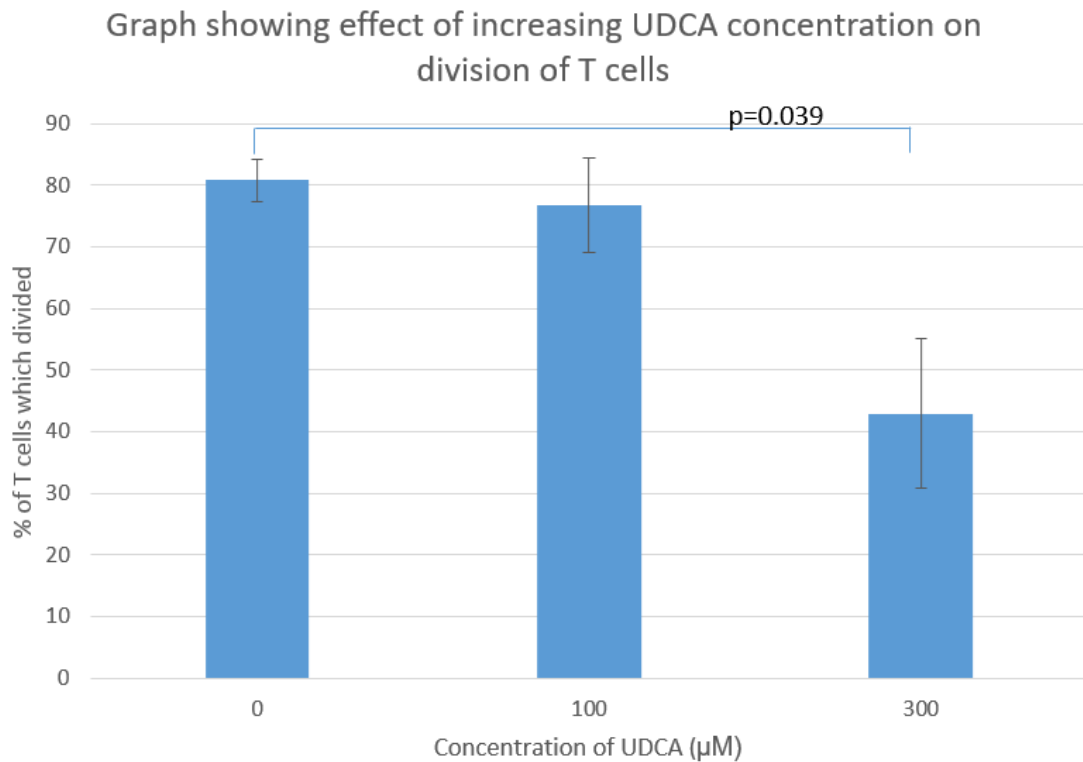


Figure 3.3.4.2: Graph displaying average percentages of proliferated T cells of the 3 volunteers.

The graph includes error bars as the standard error of the data. There is a significant difference between cells divided at 300 μM and 0 μM UDCA ($p=0.039$).

3.3.5: Flow Cytometry Optimisation

Antibodies for use in flow cytometry were titrated to optimise the ideal concentration for their use. Figure 3.5.1 shows how populations of positively stained and negatively stained dyes are gated using FACSDiva software. The software can be used to give mean values, median values and standard deviations from the mean for the points within a gate in terms of their x and y axis readings. Figure 3.3.5.2 shows the graph plotted to infer ideal concentration and table 3.5.1 shows the calculated values used to plot this graph. Figure 3.3.5.2 shows that 30ng/ml of antibody is within the ideal range and table 3.3.5.1 indicates that this is obtained by adding 2 μl of raw antibody.

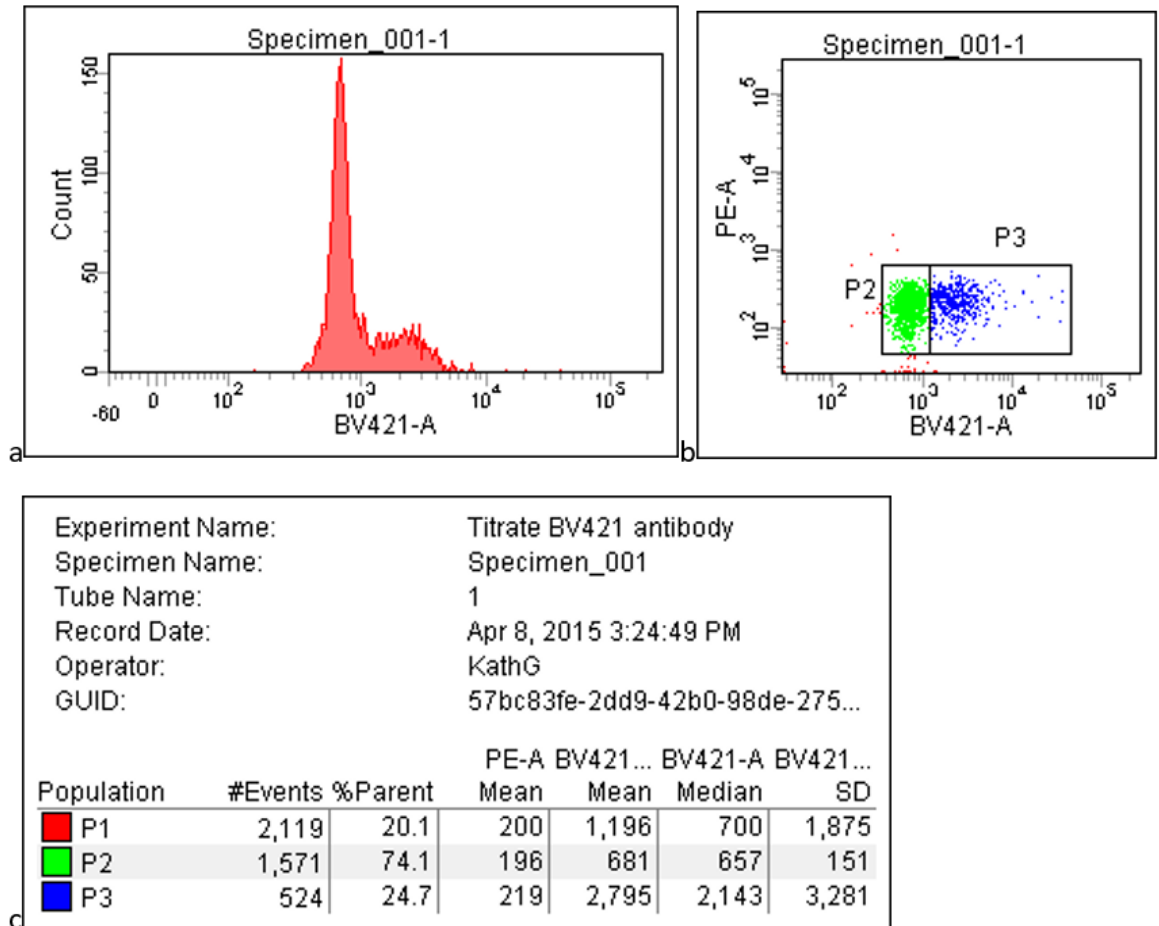
Optimisation of voltages is carried out using FACSDiva software. Figure 3.3.5.3 shows an example of optimised voltage peaks. The negative peak, labelled, needs to be readable above 0 intensity and the positive peak, labelled, must be ideally below 10^5 . This is so that both positively and negatively stained cells are comparable on the same graph. The voltages for each dye were adjusted using commands in the FACSDiva software to position the peaks for each dye to satisfy these criteria.

Negative gates for dyes are calculated using FMOs. Finding one FMO is depicted in figure 3.3.5.4. This is important because, as figure 3.3.5.4 shows, gating on the unstained alone does not accurately allow for negative gating in the context of all other dyes added together as there is an element of background into a channel from dyes for other channels.

Throughout this study, isotype negatives were used to assess the 'stickiness' of the cells in question. Use of isotype negatives was incorporated into the FMO experiment, where isotype negatives were used instead of unstained.

After gating out lymphocytes, singlets were discriminated from doublets or clusters using the criteria outlined in section 3.2.6.5. Figure 3.3.7.2.1 shows the lymphocytes selected, and then applied to a FSC-H vs FSC-A graph and the singlets gated around for further counting. The singlet gate determines cells examined in the following graph, which selects for live and dead cells.

In addition, all dyes were compensated for spectral overlap by adjusting the voltage parameters. This is carried out using scatter plots of all dyes against each other, selecting statistical view and then adjusting the voltage parameter for each dye such that for one particular dye, the positive mean and negative mean are the read at close to the same value on the other dye (not shown). This is important because it standardises positive and negative measures for each dye against the other, controlling for low level noise spilling into one channel from another.



P1 = total population
 P2 = negatively staining population
 P3 = positively staining population

Figure 3.3.5.1: Images copied directly from FACSDiva software showing the acquisition of numeric data for the antibody titration of anti-CD3 BV421.

a shows the histogram peaks where the positive and negative peaks are discernible.
 b shows the scatter plot and gating of the positive and negative populations.
 c shows the results from counting of the numbers of cells in each gate from b. The software can be manipulated to also calculate the mean, median and standard deviation within the populations.

Volume added (μ l)	Mass antibody (ng)	Final conc. (ng/ml)	Median _{pos}	Median _{neg}	SD _{neg}	2xSD _{neg}	SI
20	60	300	2143	657	151	302	4.92
10	30	150	2173	861	148	296	4.43
7.5	22.5	112.5	2073	786	154	308	4.18
5	15	75	1762	509	117	234	5.35
2	6	30	916	176	51	102	7.25
1	3	15	521	96	34	68	6.25
0.5	1.5	7.5	446	96	35	70	5

Table 3.3.5.1: Table of values used to plot the graph of 3.3.5.2.

This graph shows the values established as per figure 3.5.2 for all of the different concentrations of antibody used in the antibody titration for this particular dye. The Standard Index (SI) is calculated using the formula:

Standard Index, SI = $(\text{median}_{\text{pos}} - \text{median}_{\text{neg}}) / 2\text{xSD}_{\text{neg}}$

The volume added is from a dilution of 1 in 10 of the original antibody concentration in order to allow the antibody to be titrated to very small concentrations avoiding a high error from the pipette. The mass of antibody and final concentration are calculated from the manufacturer stated concentration of undiluted antibody.

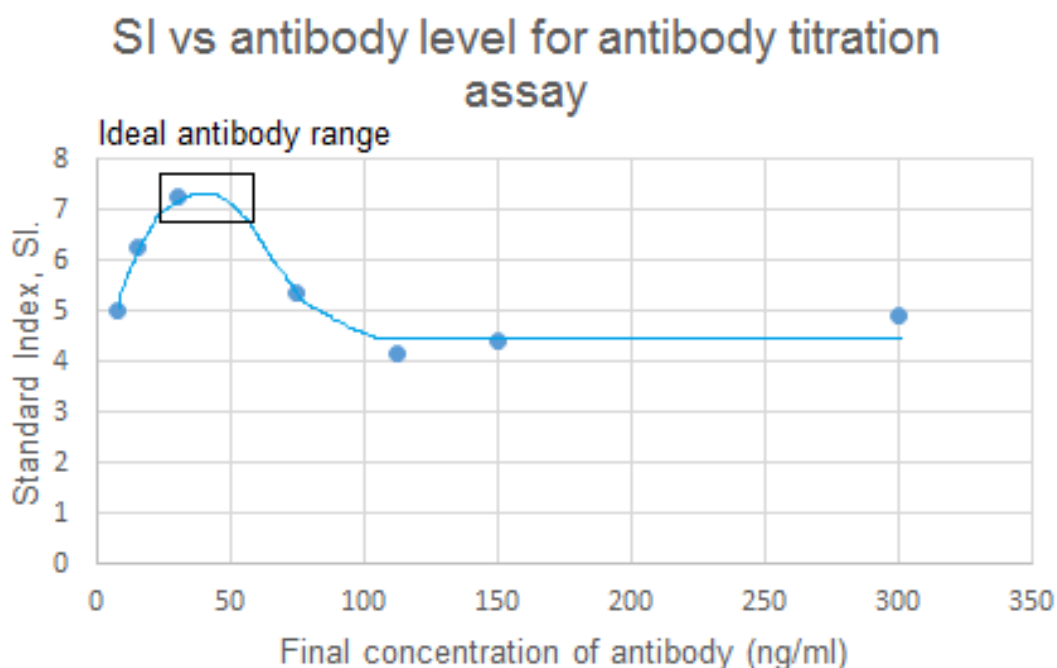


Figure 3.3.5.2: Graph of final concentration of antibody against standard index of dye for antibody titration assay.

Values in table 3.3.5.1 were plotted to give this graph to establish the ideal concentration, labelled here as 'Ideal antibody range'. Concentrations in this range, shown as giving the highest SI values, whereby the concentrations are readable on the x axis, give the largest distance between the positive and negative values per unit standard deviation, therefore the values are the best distance apart while including values with less variance which can make values difficult to distinguish.

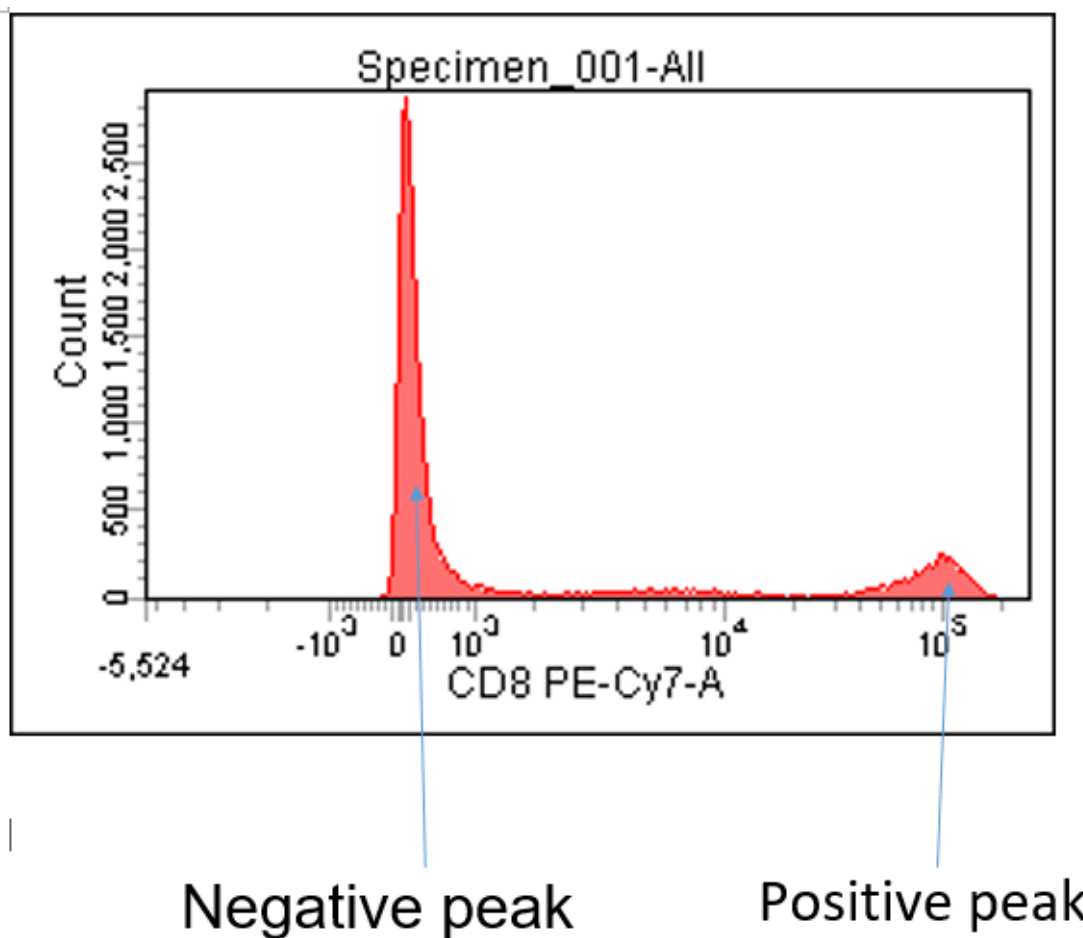


Figure 3.3.5.3: Voltage optimisation for anti-CD8 PECy7 dye.

This histogram shows the number of counts per unit intensity of fluorescence for voltage optimisation for the anti-CD8 PECy7 fluorescent antibody. The negative peak, labelled, needs to be readable above 0 intensity and the positive peak, labelled, must be ideally below 10^5 . This is so that both positively and negatively stained cells are comparable on the same graph.

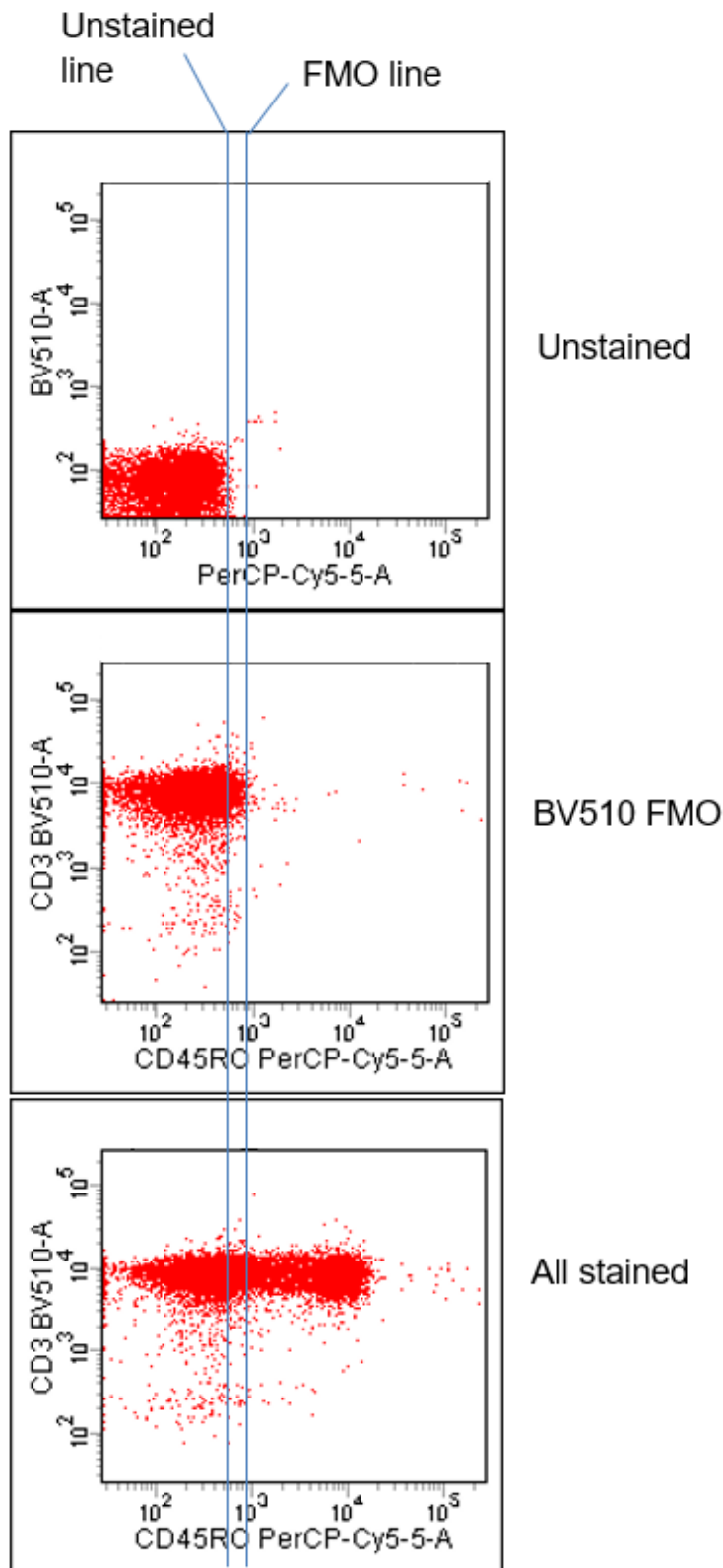


Figure 3.3.5.4: Figure illustrating the difference between using the unstained population for the negative gate and using the FMO

The unstained graph would suggest that the negative gate can be applied at around the 5×10^2 mark on the x axis, whereas the FMO, which takes into account spill-over from other channels and is more accurate, shows the truer negative to be gated at approximately 9×10^2 . This illustrates the discrepancy between the unstained and the FMO and highlights the importance of using the FMO, not the unstained, for reference when plotting the negative gate.

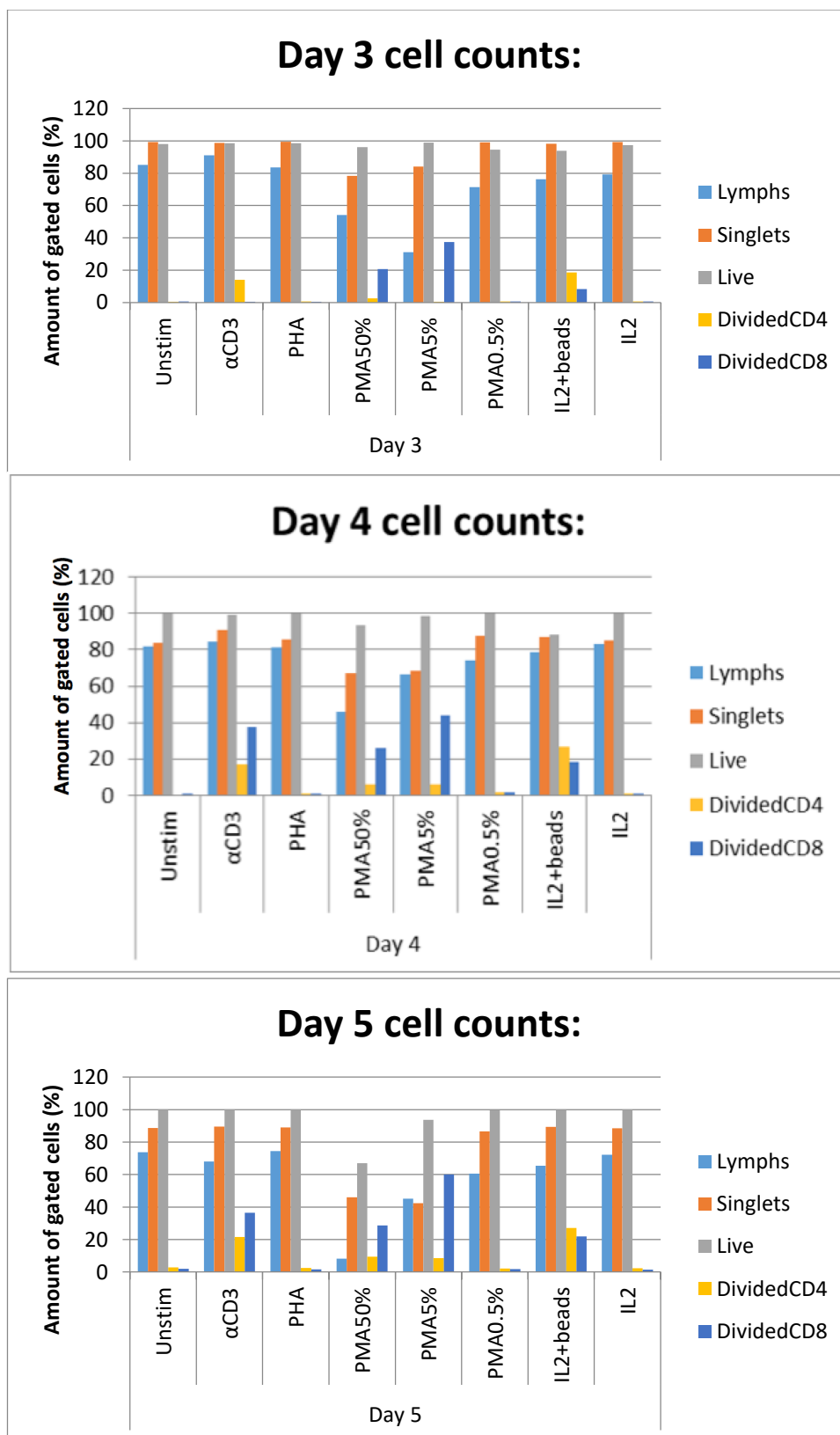
3.3.6: Determination of method of proliferation to be used

There are many different T cell proliferation methods accepted in the literature for use in T cell expansion studies, outlined in section 3.2.5.1. In order to decide which would be the most appropriate for further studies, examining and quantifying T cell subsets in the presence of different concentrations of UDCA, some available T cell proliferation methods were tested and compared by methods outlined in section 3.2.5.1. The normal ration of CD4/CD8 T cells is usually approximately 2.0 (Bogner *et al.*, 1989), so methods were examined for their ability to maintain this ratio and not give to much of a CD4 or CD8 bias. Also, proliferation needed to be approximately uniform across divisions such that divided cells could be discriminated from undivided cells for their accurate quantification. Figures 3.3.6.1 show bar charts depicting the relative levels of cells within gates at each gating stage and allows visual comparison of CD4+ and CD8+ divided cells between days and methods. For example, comparing IL-2 with IL-2 and beads can show that by adding Dynabeads there is much greater proliferation of T cells, but the ratio of CD4/CD8 looks like it is roughly maintained where the CD4 bar is larger than the CD8 bar throughout all days. Table 3.3.6.1 shows the quantified amounts of cells within each gate by percentage of parent gate, where lymphocyte number shows percentage of all input that are lymphocytes. 'Singlets' shows the estimated percentage of lymphocytes not in doublets or clumped due to sticking together which can happen during cytometry preparation as cells are centrifuged a number of times. 'Live' indicates the percentage of singlet cells which did not absorb the DAPI stain, therefore are likely alive. Cells within this live gate are examined on CFSE graphs to discriminate divided and undivided. All divided cells are counted and also CD4+ and CD8+, as shown by the CFSE scatter graphs coming from the live cell graph.

The quadrant graph shows all CD4+ cells as those right of the vertical division line and all CD8+ cells as all of those above the horizontal division line. The upper right quadrant shows that some cells are CD4+/CD8+, however these were a negligible percentage (<0.1% total divided cells) so were unlikely to interfere with the overall CD4/CD8 ratio.

Table 3.3.6.1 and figures 3.3.6.1 show that anti-CD3 gives a sudden increase in CD8 T cells dividing at day 5, with CD4:CD8 being 16.8:37.5 on day 5 after 14.1 to 0.5 on day 4. CD8 cells. This low CD4/CD8 ratio is maintained through to day 7 with 25.1:41.9. PHA gives relatively low CD4+ and CD8+ proliferation compared to the other methods, with the maximum proliferation occurring at day 7 with 9.6% and 2.6% of divided cells making up CD4+ and CD8+ T cells respectively. IL-2 alone gave similarly low results of 4.4% and 2.0% at day 7. PMA methods with 5.0 and 50ng/ml ionomycin giving a very low CD4/CD8 ratio referring to percentage of divided cells, most apparent with 5.0ng/ml ionomycin with 2.5% divided cells CD4 and 57.5% divided cells CD8 at day 7. Figure 3.3.6.1 displays the trend for CD8 to be higher than CD4 for PMA with 5.0 and 50ng/ml ionomycin throughout the experiment. PMA with 0.5ng/ml ionomycin gives relatively low levels of proliferated CD4+

and CD8+ T cells compared to other methods, with the day with the highest percentages of CD4+ and CD8+ T cells in the divided population being day 7, with 4.5% of divided cells CD4+ and 3.0% of divided cells CD8+.



Figures 3.3.6.1: Cell counts for various proliferation methods, days 3-5. These bar charts display the % of divided cells at days 3, 4 and 5, proliferated by the different methods. The series names indicate the criteria by which cells were gated, displayed in figure 3.6.2. 'Lymphs' refers to lymphocytes gated based on forward and side scatter criteria described in section 3.1.1.

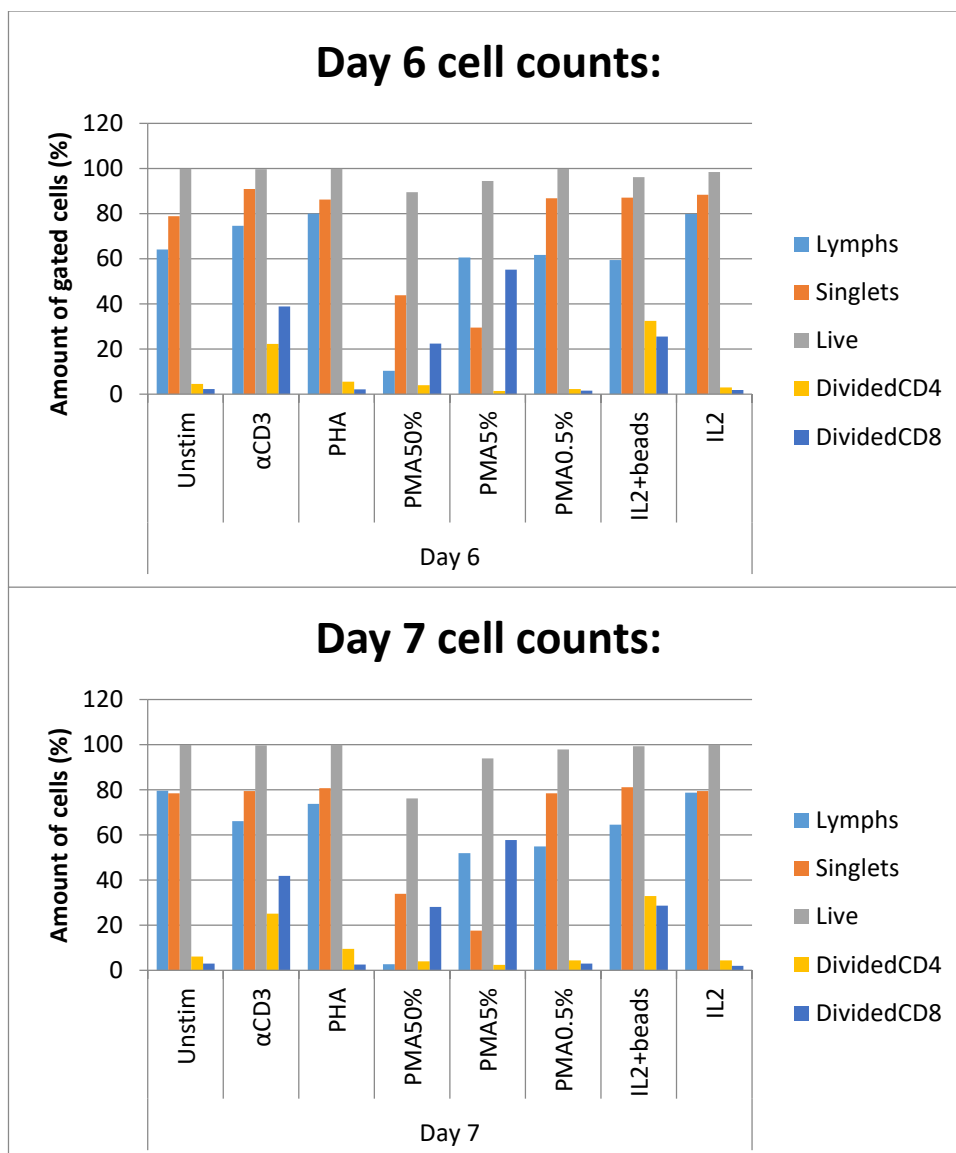


Figure 3.3.6.1 cont.:

Cell counts for various proliferation methods, days 3-5.

These bar charts display the % of divided cells at days 3, 4 and 5, proliferated by the different methods. The series names indicate the criteria by which cells were gated, displayed in figure 3.6.2. 'Lymphs' refers to lymphocytes gated based on forward and side scatter criteria described in section 3.1.1.

Percentages of cells:

	Method	Lymphs	Singlets	Live	DividedCD4	DividedCD8
Day 3	Unstim	85.1	99.3	98.0	0.5	0.7
	α CD3	91.1	98.7	98.5	14.1	0.5
	PHA	83.6	99.5	98.6	0.7	0.5
	PMA50%	54.1	78.3	96.2	2.6	20.7
	PMA5%	31.2	84.1	98.9	0.5	37.5
	PMA0.5%	71.4	99.1	94.5	0.7	0.6
	IL2+beads	76.3	98.3	93.9	18.7	8.3
IL2	79.3	99.2	97.3	0.7	0.6	
Day 4	Unstim	81.9	84.0	99.7	0	0.7
	α CD3	84.6	90.7	99.4	16.8	37.5
	PHA	81.0	85.7	99.7	0.6	0.8
	PMA50%	46.1	66.8	93.4	5.9	26.1
	PMA5%	66.7	68.4	98.6	6.3	44.1
	PMA0.5%	74.4	87.5	100	1.4	1.3
	IL2+beads	78.6	87.0	88.6	26.7	18.5
IL2	83.3	85.3	99.9	0.7	0.7	
Day 5	Unstim	73.8	88.6	99.9	2.8	1.9
	α CD3	68.0	89.5	100	21.5	36.4
	PHA	74.5	89.0	99.9	2.5	1.6
	PMA50%	8.2	46.0	66.9	9.4	28.7
	PMA5%	45.1	42.4	93.6	8.6	60.0
	PMA0.5%	60.5	86.5	99.5	2.2	1.8
	IL2+beads	65.4	89.4	99.8	27.1	21.9
IL2	72.2	88.4	99.9	2.3	1.5	
Day 6	Unstim	64.2	78.9	99.9	4.6	2.3
	α CD3	74.6	90.9	99.8	22.3	38.9
	PHA	80.0	86.3	99.9	5.6	2.2
	PMA50%	10.4	43.9	89.5	4.1	22.4
	PMA5%	60.6	29.6	94.5	1.5	55.2
	PMA0.5%	61.8	86.8	99.9	2.3	1.6
	IL2+beads	59.4	87.1	96.2	32.5	25.6
IL2	79.9	88.4	98.4	3.0	1.9	
Day 7	Unstim	79.6	78.5	99.9	6.1	3.0
	α CD3	66.1	79.4	99.8	25.1	41.9
	PHA	73.8	80.7	100	9.6	2.6
	PMA50%	2.7	34	76.2	4.1	28.2
	PMA5%	51.9	17.7	93.9	2.5	57.7
	PMA0.5%	54.9	78.4	97.9	4.5	3.0
	IL2+beads	64.6	81.2	99.3	33.0	28.7
IL2	78.7	79.5	100	4.4	2.0	

Table 3.3.6.1: Percentages of cells within the gating criteria for the proliferation method comparison experiment.

The table shows percentages of cells within a gate of the whole parent population, for example 'Lymphs' (referring to lymphocytes) shows the percentages of cells within the lymphocyte gate of all cells registering on the forward/side scatter graph; 'Singlets' readings indicate the percentage of cells that are considered singlets from the lymphocyte population. Gating of populations is depicted in figure 3.3.6.2.

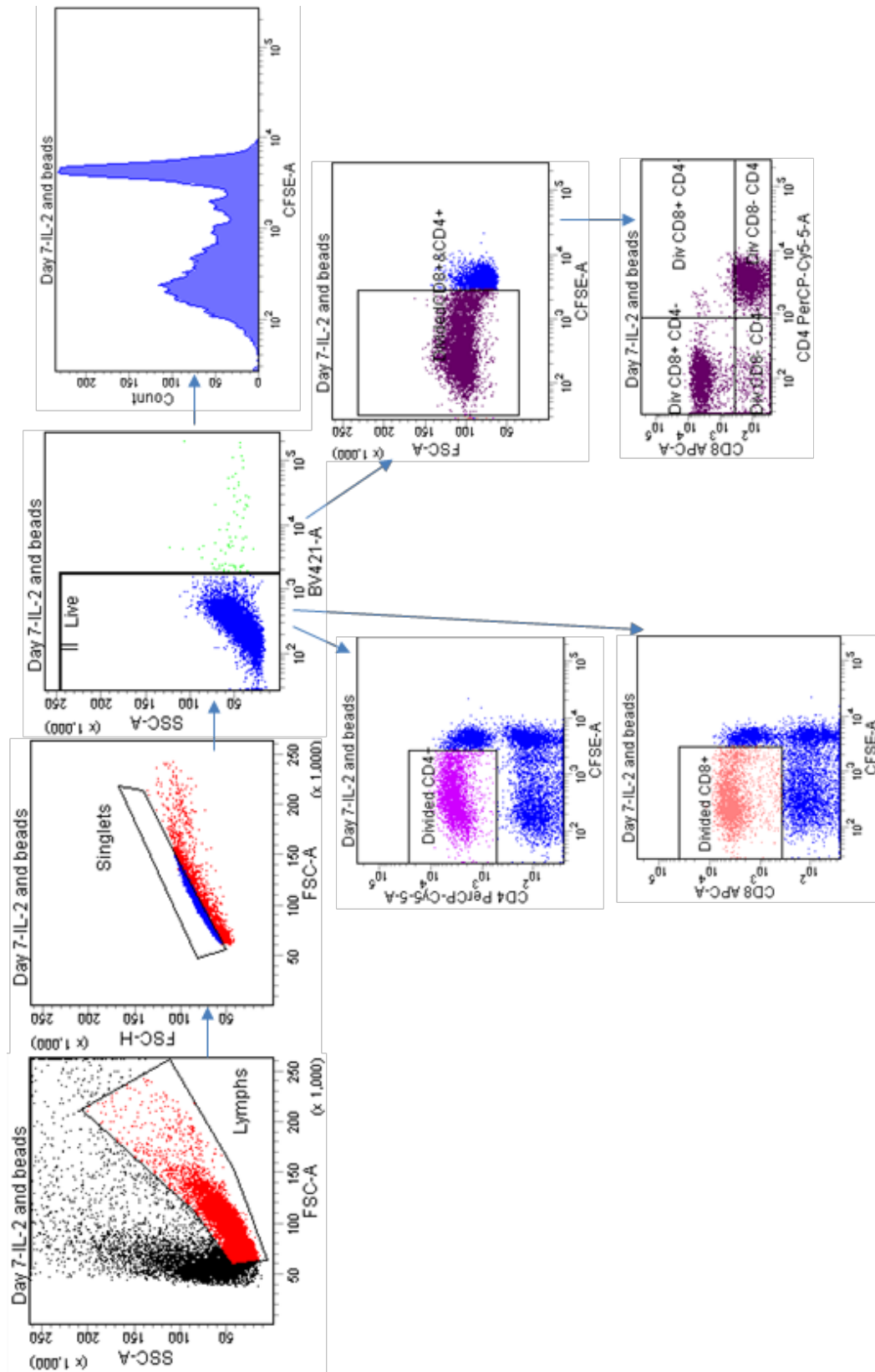


Figure 3.3.6.2: Gating of populations from their parent populations using FACS-Diva software

This figure shows the gates used in communicating with the FACS-Diva software which groups of cells to count, based on decided parameters. From a population, the sub-population of interest is isolated and gated around. The lymphocyte population is selected based on known side and forward scatter criteria; the singlets are gated based on height-area forward scatter proportionality, explained more in section 1.1; live cells are selected based on being DAPI-stain negative; divided cells are selected based on being less CFSE positive than the most CFSE-rich (least divided) population; CD4+ and CD8+ are selected based on presence of the relevant dye. Gating criteria is outlined in further detail in section 2.6.

3.3.7: Finalisation of flow cytometric assay

There were 2 fluorescent antibody panels for consideration. One, shown in figure 3.3.7a, uses only one tube, whereas the other, shown in figure 3.3.7b and c (used in conjunction) uses 2 tubes.

Figure 3.3.7a shows a panel, Panel 1, with the potential of differentiating Tregs, Th1, Th2 and Th17 T cells: CFSE identifies and allows quantification of number of proliferation cycles of cells; CD3+ identifies T cells; CD4 discriminates CD4+ T cells such as helper T cells from other T cell subsets (such as cytotoxic T cells); CD4, CD25 and FoxP3 in conjunction identify Tregs and further along with CD45RO identify memory Tregs; CD4+ and presence of CXCR3 but absence of CCR6 identifies Th1 cells; CD4 and presence of CCR6 but absence of CXCR3 identifies Th17 cells and CD4 and absence of CXCR3 and CCR6 identifies Th2 cells, as explained in section 3.1.1.1

Figure 3.3.7b and c shows a panel, Panel 2, of 2 tubes used in conjunction where the above parameters apply over 2 tubes with the addition of CD8 to identify cytotoxic T cells in conjunction with CD3 and DAPI to allow discrimination of live cells from dead cells.

Panel 1 is advantageous over Panel 2 whereby more data can be obtained from fewer cells, whereas Panel 2 has the potential to obtain more data overall, but more cells are required.

a:

Channel:	FITC	PE	PerCP-Cy5.5	PE-Cy7	APC	APC-CY7	BV421	BV510
Dye:	CFSE	CD25	CD45RO	FoxP3	CCR6	CD4	CXCR3	CD3

b:

Channel:	FITC	BV510	PE-Cy7	APC	PerCP-Cy5.5	BV421
Dye:	CFSE	CD4	CD8	CCR6	CXCR3	DAPI

c:

Channel:	FITC	APC	PE	PE-Cy7	PerCP-Cy5.5
Dye:	CFSE	CD4	CD25	FoxP3	CD45RO

Figure 3.3.7: Tables showing fluorescent antibody panels for identifying different subsets of T cells.

These tables depict different antibody panels for flow cytometry use to analyse the quantities of different T cells of different patterns. 'a' was the initial designed panel which could envision Treg and T cell subsets using just one tube where 'b' and 'c' would separately investigate helper/cytotoxic T cells and Tregs, to be used in conjunction with each other.

Figures 3.3.7.1.1 and 3.3.7.2.1 show Panel 2 cell gating which leads to data gathering shown in figures 3.3.7.1.2 and 3.3.7.2.2. Lymphocytes are gated based on known forward and side scatter criteria and, from those, the further sub-populations are gated. The actual cell counts and percentage parent populations are displayed by the software in table form, shown in figures 3.3.7.1.2 and 3.3.7.2.2. This data was then tabularised and analysed in chapter 4.

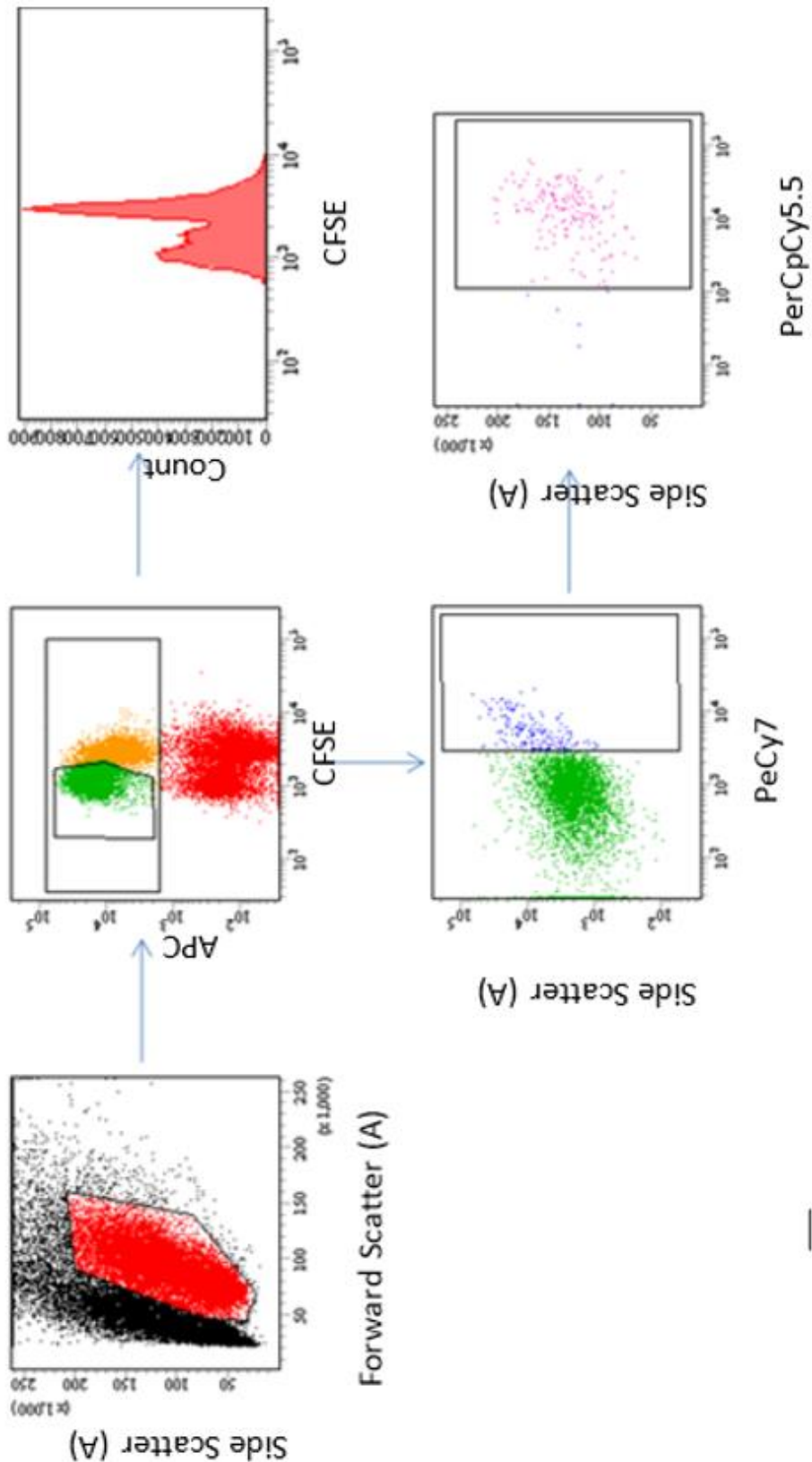


Figure 3.3.7.1.1: Gating criteria for Treg results

This figure shows how each population is gated from its 'parent'. Lymphocytes are gated based on known side and forward scatter properties; CD4+(APC+) cells are then gated and divided CD4+(CFSE^{low}) cells are gated from these; Treg cells are then gated based on FoxP3+ and CD45RO-/+ are then discriminated (where PercpCy5.5+ is CD45RO+)

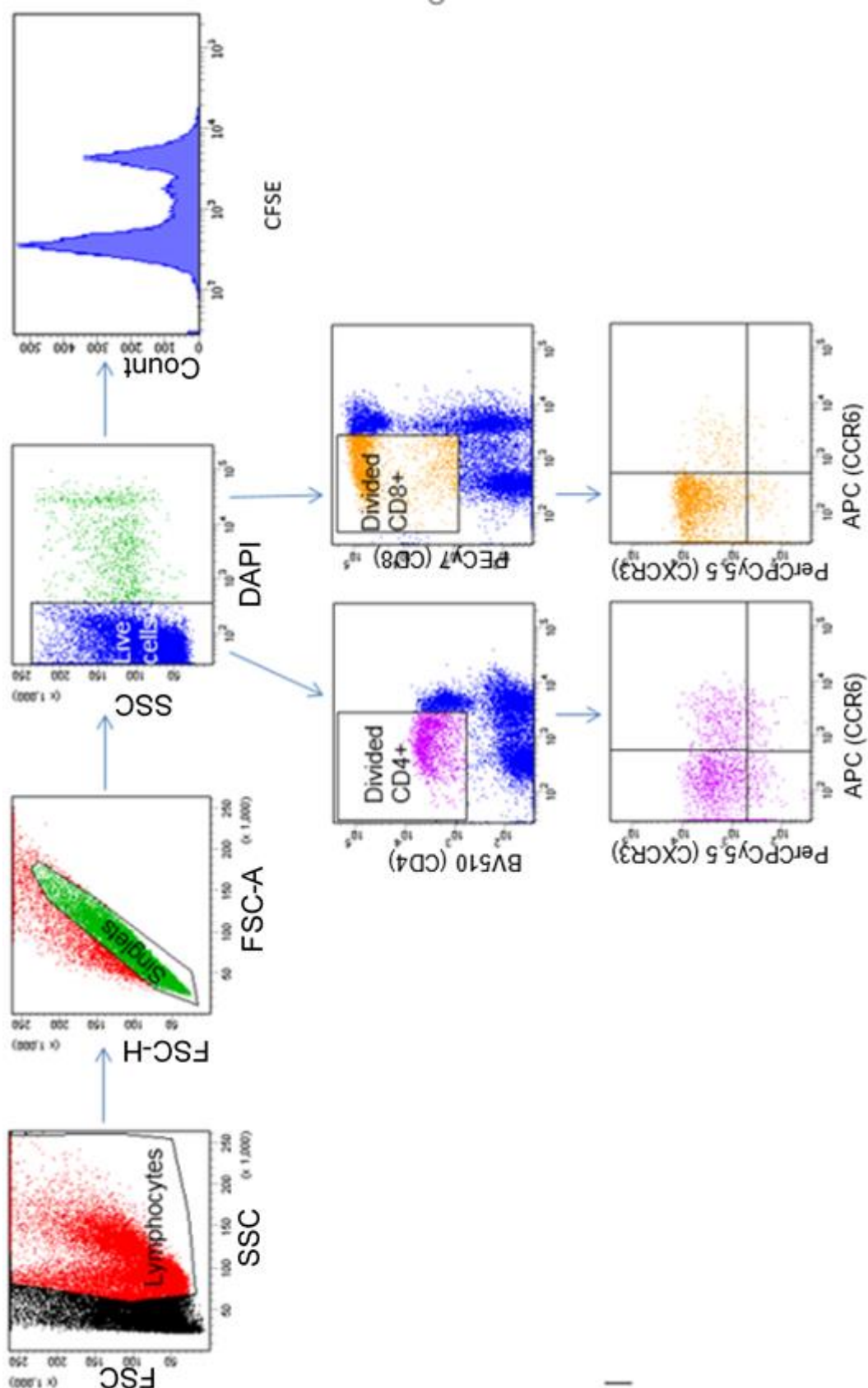


Figure 3.3.7.2.1: Gating criteria for typing helper and cytotoxic T cells

This figure shows how each population is gated from its 'parent' population. Lymphocytes are gated based on side/forward properties, singlets are gated based on proportionality between proportionality between forward scatter 'height' and 'area'; live cells are gated by those that are DAPI-negative; divided CD4⁺ and 8⁺ cells are then gated (CFSE^{low}) and then subsets are gated based on their CXCR3⁺/⁻ and CCR6⁺/⁻ criteria.

Tube: 0_25 mM urso

Population	#Events	%Parent	%Total
All Events	40,798	####	100.0
Lymphs	21,142	51.8	51.8
CD4+	10,702	50.6	26.2
Divided CD4+	5,168	48.3	12.7
Tregs	179	3.5	0.4
CD45RO+	170	95.0	0.4

Figure 3.3.7.1.2: Quantification of numbers of cells within the gates depicted in figure 3.3.7.1.1 for proliferation of different types of CD4+ T cell analysis.

All events indicates the total number of particles examined within the parameters of the set forward and side scatter voltages. Percentage parent indicates the percentage of cells within the previous population that satisfy the gating criteria of this population. The parent population is the population of cells shown in a scatter graph that were used to select this population from.

Tube: 0_1 mM urso

Population	#Events	%Parent	%Total
All Events	43,076	####	100.0
Lymphs	24,204	56.2	56.2
Singlets	21,271	87.9	49.4
Live	20,242	95.2	47.0
Divided CD4+	1,906	9.4	4.4
Th1	1,301	68.3	3.0
Th1/Th17	333	17.5	0.8
Th2	174	9.1	0.4
Th17	98	5.1	0.2
Divided CD8+	2,711	13.4	6.3
Tc1	2,436	89.9	5.7
Tc1/Tc17	137	5.1	0.3
Tc2	119	4.4	0.3
Tc17	19	0.7	0.0
Live all	30,799	71.5	71.5

Figure 3.3.7.2.2: Quantification of numbers of cells within the gates depicted in figure 3.3.7.2.1 for proliferation of Treg analysis.

All events indicates the total number of particles examined within the parameters of the set forward and side scatter voltages. Percentage parent indicates the percentage of cells within the previous population that satisfy the gating criteria of this population. The parent population is the population of cells shown in a scatter graph that were used to select this population from.

3.4: Discussion

3.4.1: Aims

The primary aim for this chapter was designing a flow cytometry assay with the ability of differentiating T cell sub sets. This assay would be able to detect an effect of UDCA on proliferation of T cells but also differentiate the T cell subsets to see if UDCA is causing a particular skew toward a certain subtype of T cell. The most impactful use of this assay would be in comparing the T cell profiles of UDCA responders and UDCA non-responders to assess if there is the potential for a more aggressive disease state to be related to a different T cell response to the relevant autoantigen.

3.4.2: Method of T cell isolation

Four T cell isolation methods were tested for their ability to produce a pure sample of isolated T cells. Easysep was chosen as the method for further experimental analysis of purified T cells as it gave the most pure culture compared with other methods, so culture is likely less influenced by remaining PBMCs than in any other. Table 3.3.1 and section 3.3.1 show and outline that Easysep gives 95.51% or 98.58% T cell purity depending on quantification criteria.

3.4.3: T cell proliferation fresh and frozen comparison

It was determined that frozen cells were acceptable for use as they did not show significantly different proliferation to fresh T cells and the proliferation peaks looked similar across fresh and frozen groups. Figure 3.3.2 shows that sample 1 appeared to show decreased proliferation into the 2+ division from fresh to frozen, whereas sample 2 shows the opposite. Sample 3 shows similar-looking proliferation peaks from fresh to frozen. Also, there was no statistically significant difference in average numbers of divided cells comparing fresh and frozen groups.

3.4.5.1: Jurkat growth curve

A Jurkat growth curve was plotted after a counting assay to display how Jurkat cells grow in terms of their proliferation and eventual death. This growth curve is shown in figure 3.3.1 and can be compared with the growth curve of healthy volunteers in figure 3.3.3.1. The Jurkat cells show a more predictable and traditional growth pattern than the healthy cells. The Jurkat cells appear to proliferate in uniform until day 8, then plateau in number and then enter death phase in day 9, as per the pattern shown in figure 3.3.3.1. Primary T cells, growth curve depicted in figure 3.3.3.1, have a less uniform growth, roughly following a

pattern of number decline until day 4, then rising in number into day 5 before declining again. Unlike the Jurkat growth curve, cells do not closely follow the average line. This data is not T tested because it was intended only to gain an idea of the growth of Jurkat cells compared with primary T cells to decide if it would be worth testing their proliferation with proliferation beads. As their growth appears predictable and uniform, it was decided to test them with proliferation beads to see if they can be used in proliferation experiments.

3.4.5.2: Jurkat bead titration

The recommended volume of proliferation beads (Dynabeads™) to add for healthy cells is 20µl per ml of cells at 1×10^6 /ml. This is for primary human T cells, not Jurkat cells, therefore it is important to titrate the volume of proliferation beads to be added to Jurkat cells to give adequate proliferation.

As shown in figure 3.3.2, the Jurkat cells do not proliferate in a distinct pattern as the healthy volunteer purified T cells do. The healthy T cells, when stained with CFSE, divide giving a distinct pattern when analysed by flow cytometry as the dye is diluted 50:50 between daughter cells and is therefore visible as a peak closer to the y axis with every subsequent division, as explained in section 3.2.3.2. The Jurkat cells proliferate in a manner that is not trackable. There are no series of distinct peaks, therefore, it is not possible to compare proliferated cells with unproliferated cells. As the pattern of proliferation appeared to be different from that seen when using primary T cells it was decided to use only primary cells from healthy volunteers to develop the assay as these are expected to more closely resemble primary patient cells.

In addition, it was decided to use only 10µl of proliferation beads despite the manufacturing guidelines suggesting twice this volume. Data in this chapter shows better proliferation with 10µl where more cells enter each division fraction, including the 2+ divisions fraction where the peak is higher in comparison with other peaks in within the same graph in this band than with more beads, as apparent in figure 3.3.2.

In figure 3.3.2, if the graph for 0 beads is compared to all other Jurkat graphs, there appears to be no difference. Figure 3.3.1, showing the growth curve for Jurkat cells, would indicate some growth after day 3, if the day 3 point is read at the y axis. It may be that the Jurkat cells need more time in culture before they begin dividing, or that they do not absorb the CFSE dye as readily as healthy T cells.

The literature suggests that it is possible to obtain trackable proliferation with Jurkat cells and CFSE (Begum *et al.*, 2013), however proliferation is slower than that shown in healthy volunteers in this study. Future experiments could incubate Jurkat cells for 3+ days before proliferation, however if healthy volunteers are available they should be prioritised over Jurkat cells as they do show fast proliferation by the methods in this study. Another limitation of using Jurkat cells is that using Jurkat cells cannot mimic T cell sub set variance within

the population and only faux t tests can be carried out, that is several measurements of essentially the same sample.

3.4.6: Optimising the proliferation method

Further to titrating the volume of proliferation beads to be added to cell culture, it was decided to experiment with other proliferation methods and determine the most effective that would not skew the T cell subsets too much from that expected in accordance with the literature. These methods were using an anti-CD3 mitogen; IL-2 and proliferation beads; IL-2 alone; PHA; PMA at various concentrations with ionomycin.

It was decided to use Dynabeads with IL-2 for further experiments using proliferation of T cells as the peaks were clearly discernible, such that it was easy to distinguish divided cells from undivided cells. Proliferation was consistently high, with some of the highest percentages of divided cells being CD4+ and CD8+, with 1.87% divided being CD4+ and 8.3% divided being CD8+ on day 3 to 33.0% and 28.7% on day 7; conservative of the CD4/CD8 ratio, maintaining higher CD4+ than CD8+.

Anti-CD3 giving a high CD8+ T cell percentage may be congruent with the literature in that one of the mechanisms is in causing increased IL-10, which, in some tumour environments, has been shown to cause expansion of tumour-resistant CD8+ T cells (Emmerich et al., 2012). In addition, using anti-CD3 would come with the limitation of being unable to stain for cell surface CD3, as this may lead to competition for CD3 between the anti-CD3 mitogen and the anti-CD3 fluorescent antibody and therefore may produce a weaker signal for the fluorescent marker (Green, 2014).

3.4.7: T cell subset identification panel

As panel 2 has the potential to provide more information about the cell population than panel 1 as outlined in section 3.3.7, this panel was chosen over panel 1 despite the need for an extra tube of cells. It was noted that should cell abundance be inadequate, then panel 1 would instead be used. For each experiment, the number of available cells will be counted and the number of cells required for planned experiments will be calculated to assess if there are sufficient available cells for panel 2, otherwise panel 1 will be used at the cost of additional information available in using panel 2. The number of available cells becomes important in patient blood studies where samples available are controlled by the Freeman hospital.

One limitation using Panel 2 is in that cells are different shapes across panels under acquisition so voltages must be altered for side and forward scatter between tubes. The reason for this is because to stain for intracellular marker FoxP3 in the Treg tube, cells must be made permeable with an intracellular stain kit to allow the antibody against FoxP3 to

enter the cell causing the cells to be smaller in size. In addition, staining for FoxP3 is incompatible with DAPI staining because DAPI staining relies on live cells being impermeable to dyes, but the stain kit for FoxP3 renders cells permeable to DAPI as well as fluorescent antibodies, meaning all cells would stain positively with DAPI and appear dead.

3.4.8: Limitations

One limitation of the flow cytometric assay for analysis of helper T cell subsets is that there is no positive identifier specifically for Th2 cells: they are identified by being CD4+CXCR3-CCR6-. This is acceptable in the literature as a Th2 identifying combination (Lubberts, 2015), a more accurate Th2 identifying combination would be CD4+CCR6-CXCR3-CCR4+, as this eliminates the risk of falsely identifying a Th2 when either CCR6 or CXCR3 has been lost (De Jager *et al.*, 2008). Due to there being a limited number of channels on the flow cytometric equipment used, this panel was designed to be a tester panel for if there were any measurable differences in T cell subsets, which could then be more further investigated with a more thorough panel which would include CCR4.

Chapter 4: Further elucidating the mechanism of action of UDCA in PBC: investigating a direct effect on T cells in the cholangiocytes

Abstract

Although heavily studied, the precise mechanism of action of Ursodeoxycholic acid, UDCA, in PBC patients has not been fully elucidated. Most research into the mechanism of action of UDCA has thus far focussed on protection of the cholangiocytes and aiding movement of bile out of the liver but little research has been carried out to determine if the drug is having a direct effect on the damage-causing cells in the disease, particularly the T cells. Recent studies have suggested that there is more than one different type of disease under an apparent umbrella term of PBC and these differences have been discovered under the context of response or lack thereof to the drug UDCA. There is likely to be an underlying cause to this large disparity, possibly immunological. In this chapter, apoptosis assays, ELISpot assays, flow cytometric analyses and xCELLigence are used to investigate a direct mechanism of action of UDCA on immunological cells, in particular the T cells, which have been shown to be present in abundance around the cholangiocytes, at the site of inflammation in PBC. It was found that increasing concentrations of UDCA can have a negative impact on T cell proliferation and ability to react to antigens and may also have an indirect effect on T cell proliferation by cholangiocyte action. Elucidating a function of UDCA which impacts the T cells could direct future research into the underlying differences causing PBC patients to fit the newly-discovered grouping system and could direct further research into therapies for PBC.

4.1: Introduction

4.1.1: UDCA Background

4.1.1.1: A history of UDCA usage

Oral use of Ursodeoxycholic acid, UDCA, for the treatment of liver ailments was initiated as far back as 618-907AD because it was thought to help flush out toxic bile acids from the liver but also it was thought to replace toxic endogenous bile acids with non-toxic bile acids (Al-Harthy *et al*, 2012). Its value has long been appreciated, however it has only been in the past 30 years that its mechanism of action in such ailments have been able to be explored (Trauner *et al.*, 1998). The majority of studies have focussed on its mechanical properties or its potential ability to protect the damaged cholangiocytes.

4.1.1.2: UDCA formation and conjugation

UDCA is a secondary bile acid. Bile acids aid digestion of hydrophobic lipids by causing a decrease in liquid surface tension which causes the compounds to more readily form micelles (Trauner *et al.*, 1998). UDCA is formed endogenously by action of bacteria in the gut microbiome. It is thought that certain bile acids are harmful to bacteria in the gut in that they prevent bacterial proliferation, therefore these bacteria have evolved mechanisms to transform these bile acids into less harmful forms: secondary and tertiary bile acids such as UDCA, a secondary bile acid, then TUDCA and GUDCA, tertiary bile acids (Invernizzi *et al.*, 1999).

4.1.2: Contextualising UDCA and its conjugates

An estimate for the concentration of UDCA in the blood can be calculated to be a maximum of 250 μ M. The dose given to a patient is 13-15mg/kg/day (mg drug/kg their weight/day) given over 2-4 doses per day, therefore a maximum dose is 7.5mg drug per kg their weight. Average human blood volume is 77ml/kg which would be 0.097mg/ml or 97 μ g/ml (Lindor *et al.*, 2009). The molecular weight of UDCA is 392.57 therefore the highest possible concentration given 100% bioavailability of the drug is approximately 250 μ M. 100% bioavailability is unlikely, therefore circulating blood levels are likely to be lower than this estimated maximum. However, it is likely and widely reported that there is enrichment of bile acids in the liver (Beuers, 2006) therefore cells in the liver and bile duct regions may realistically experience concentrations much higher than this of bile acids including UDCA. Unfortunately, it is difficult to accurately estimate the concentration of UDCA and other bile acids experienced by immunological cells and cholangiocytes in patients. A study was carried out which measured the levels of bile acids in the interhepatic region of the liver which studied the concentration of UDCA in duodenal biopsy before UDCA administration and after 15mg/kg/day was taken for 3 weeks in 11 PBC patients and 11 healthy matched controls. Although levels of UDCA remained virtually unchanged in patients and volunteers (0 \pm 0 μ M pre-treatment and 3 \pm 3 μ M post-treatment in both groups), there were raised levels of other tertiary bile acids, GUDCA (patients 95 \pm 143 μ M to 3902 \pm 4545 μ M; healthy controls 208 \pm 274 μ M to 3461 \pm 6814 μ M) and TUDCA in both patients and healthy controls in post-treatment samples compared with pre-treatment samples. This is highly suggestive of liver enrichment of tertiary bile acids, as the bile leaves the liver and directly enters the duodenum with no other likely potential source of these bile acids (Dilger *et al.*, 2012). For the purpose of experiments in this study, UDCA is used because it is the therapy prescribed to PBC patients, not TUDCA or GUDCA, and it is not certain the impact of the conjugation with glycine or taurine. It is entirely likely that the UDCA is having the impact of interest in the liver and then when passed into the duodenum is conjugated to glycine or taurine,

rendering TUDCA and GUDCA clinically less interesting than UDCA (Wahlstrom *et al.*, 2016). Some studies have attempted to compare TUDCA with UDCA to determine if TUDCA is therapeutically similar to UDCA. One study has shown that UDCA may preferentially conjugate with glycine over taurine *in vivo* (Rudolph G *et al.* 2002) and another compared bile secretion of patients given TUDCA with those given UDCA, and found similar levels of bile secretion (Ma *et al.*, 2016) but so far it remains unclear if TUDCA can replace UDCA as a therapy or precisely when and where UDCA is conjugated with UDCA *in vivo*. One study examined the bile acid content of the liver and blood of normal rats compared with germ-free rats, who lacked the gut microbiome required to convert primary bile acids to secondary bile acids including UDCA (Swann *et al.*, 2011). They found that in the germ-free rat, rendered 'germ-free' by administration of antibiotics, there was little difference to the bile acid levels in blood serum compared with the microbiome containing rat in terms of bile acid content (Swann *et al.*, 2011). This suggests that the drug, rather than remaining in the blood serum, is quickly absorbed into tissues and therefore is heavily enriched in organs and tissues, for example the liver. Therefore, the estimation of UDCA concentration in human blood in the previous paragraph should not necessarily be used as a limiting factor for usable concentrations of UDCA in *in vitro* experiments in this study.

4.1.3: Mechanism of action of UDCA

UDCA has been the primary therapy for PBC for many years although only recently has research begun to elucidate its mechanism of action. It was long believed that UDCA served only to mechanically aid flushing of bile and other toxic compounds out of the liver. Recent and current studies are discovering more and more biochemical functions of UDCA, suggesting it serves many more purposes than as a physical aid.

One such mechanism of action of UDCA is its potential to increase export pumps on the canalicular membrane of the small bile ducts. Studies in mice have shown post-transcriptional effects of UDCA on the amount of Bsep, a cholate conjugate transporter, in cholangiocytes isolated from mice. Those fed UDCA had significantly more positive staining for Bsep on the canalicular membrane of tissue stained by immunohistochemistry than that of those fed no UDCA and a similar trend was also reported for Mrp2, a multidrug resistance protein (Fickert *et al.*, 2001). The impact of more Bsep and Mrp2 at the canalicular surface is an increase in transport of bile constituents and other toxic compounds from the hepatocytes, through the cholangiocytes and into the bile duct lumen. In PBC, cholangiocytes are broken down, therefore more of these export pump proteins in the remaining functional cells could attenuate the impact of cholangiocyte damage by rendering those surviving cholangiocytes as more efficient at bile transport.

Cholangiocytes, in the past thought of as passive cells, have been shown to secrete HCO_3^- into the small bile duct lumen to contribute towards bile secretion. This HCO_3^- secretion is

Cl⁻ dependent. HCO₃⁻ is formed from CO₂ from the interstitial fluid diffusing into the cholangiocyte and H₂O in the plasma, producing HCO₃⁻ and H⁺, catalysed by carbonic anhydrase. Cl⁻ passively diffuses out of the cell through the CFTR ATP binding ion channel and the Cl⁻ is then moved back into the cell by secondary active transport for the exchange of an HCO₃⁻ by the anion exchanger 2 protein (Hwang and Kirk, 2013). It is thought that UDCA may raise cellular Ca²⁺ levels which can enhance Cl⁻ movement back into the cell, increasing HCO₃⁻ output (Shimokura et al., 1995).

There are many other potential mechanisms of action of UDCA, however, there is very little being carried out to investigate a direct impact of UDCA on lymphocytes such as T cells. One study in mice has shown that UDCA may cause preferential differentiation to the Treg phenotype by suppression of CD4⁺ T cell cytokines IL-2, IL-6 and IFN- γ and an increase in IL-10 which can suppress Th1 and Th17 differentiation and favour Treg differentiation (Zhang et al., 2009). The study was carried out to investigate an effective of UDCA to help prevent allograft rejection. As the study used mice not humans, it is currently unknown if UDCA could be affecting T cell differentiation or proliferation in humans.

It is well documented in the literature there is much evidence to indicate T cell importance in PBC (Hiromi *et al.*, 2003). One key mechanism of action of UDCA could be in decreasing proliferation of T cells. Investigating this could also offer some explanation as to why there are different subtypes of PBC. Differences in T cell subset patterns between these PBC subgroups and an added preferential effect of UDCA on some T cell subtypes over others could lead to different overall effects on the immune cell population and its effectiveness between different PBC populations. This idea is covered in more detail in chapters 5 and 6.

4.1.4: Aims and Introduction Summary

The effect of UDCA is potentially of key importance because of recent research which suggests there are divisions of patients with PBC based on phenotypic data (Carbone et al., 2013). One large area for research is into whether there is an immunological basis for the differences in disease subtypes. If UDCA is having an effect on certain immune cells and not others then differential immune responses in patient groups could be the reason why a subset of patients do not respond to UDCA. Therefore, this chapter will aim to examine any effects on immunological cells of UDCA, with a particular focus on T cells and their proliferation.

4.2: Methods

4.2.1: Apoptosis assay

PBMCs isolated from whole blood, method described in Chapter 2: General Methods, were then purified using the Easysep T cell enrichment kit, method described in chapter 3.

Enriched T cells were then plated in a 24 well plate, 1ml per well of cells at a concentration of 1×10^6 cells/ml. Cells were incubated at different concentrations of UDCA in triplicate, and in 2 separate assays whereby one used the carrier ethanol as the UDCA solvent and the other used DMSO. Concentrations of UDCA, obtained from Sigma Aldrich, catalogue number U5127, were used in triplicate for each carrier: carrier only (no UDCA), 10 μ M, 100 μ M and 300 μ M. Because ethanol and DMSO can be toxic to cells at certain concentrations, the carrier solvent was kept to 0.3% total volume. UDCA was initially dissolved at 333.3x the final concentration in the carrier, then 3 μ l was added to the well. The cells were incubated at 37°C for 4 days. Every 24 hours the cells were resuspended and a 10 μ l sample taken. Each sample was mixed 1:1 with trypan blue dye which allows discrimination of live and dead cells as it is excluded by non-porous healthy cell membranes. The cells were counted using a haemocytometer and the number of live and dead cells/ml of the cultures were calculated.

Once the carrier least damaging to cells was established and chosen, the experiment was repeated using only this carrier but without the T cell enrichment stage, to give apoptosis assay results for non-purified PBMCs.

Further experiments were then carried out on enriched T cells exploring greater UDCA concentrations and at different increments and for a longer period of time: extending to 8 days.

4.2.2: ELISpot method

The plate required for ELISpot is the Millipore multiscreen flat-bottomed 96-well assay plate for ELISpot.

The ELISpot sandwich assay is illustrated in figure 2.2.1. 50 μ l of diluted capture antibody, diluted in bicarbonate buffer, at the pre-determined best concentration for that antibody was added to each well, ensuring thorough covering of the bottom of every well. This was incubated at 4°C overnight (8-48 hours is acceptable). Excess capture antibody was removed and the plates washed 3 times with PBS. The plates were then blocked with RPMI containing 10% FCS for 1-8 hours at room temperature to minimise non-specific binding. Blocking solution was then removed to virkon solution. PBMCs isolated from blood by the

method described in General Methods, were then diluted to the optimised concentration for the cytokine of interest (usually 8×10^6 or a dilution of 1 in 5, 1 in 10 or 1 in 20 of this) and added to each well at 50 μ l per well and 50 μ l of stimulus then also added. The plates were then incubated at 37°C (in a 5% CO₂ incubator) for 18-20h. Cell suspension was then removed to virkon solution and the plates washed 6 times with PBS. The biotinylated antibody was then diluted in PBS to the required concentration of 1 μ g/ml and 50 μ l added to each well. The plates were then incubated at room temperature for 2-4h. The detector antibody was then removed to waste and the plate washed 6 times in PBS. Alkaline phosphatase conjugated streptavidin (SA-ALP) was then added at a 1 in 1000 dilution in PBS at 50 μ l per well and incubated for 1-2h at room temperature. SA-ALP was then flicked off and the plate washed 6 times with PBS. 50 μ l of substrate, assembled per manufacturer's guidelines (Bio-Rad AP conjugate kit, 170-6432), was then added to each well. The plate was then allowed to develop at room temperature for 5 minutes and then tap water was added to terminate the reaction and wash off excess substrate. The plate was allowed to dry for 1-2 days at room temperature and then read using the ELISpot reader. The number of spots read from a given well is directly related to the number of reactive cells per million total cells. The number of reactive cells per million (10^6) was calculated as outlined below. 50 μ l, the volume of cell suspension added per well = 0.05ml. The initial concentration of cells in cells/ml can be multiplied by 0.05ml to find number of cells added. The concentration of cells initially was, for e.g., 8×10^6 cells/ml, therefore $8 \times 10^6 \times 0.05\text{ml} = 0.4 \times 10^6$ cells. This is 0.4×1 million cells, therefore this was multiplied by 2.5 in order to make 1 million cells. Therefore to find the number of reactive cells per million total cells, if the concentration initially was 8×10^6 cells/ml then the number of reactive cells per million is the spot count multiplied by 2.5. If the concentration of cells added was further diluted from 8×10^6 cells/ml, the multiplication factor was adjusted accordingly so that it reflected what the concentration of cells would need to be multiplied by to make 10^6 . Control wells were also included containing medium and cells but no stimulus to account for any background response, for example any response to anything which may have been in the media alone causing a response.

A panel of common antigens were run on 4 volunteers for an idea of the antigens they respond to so that the effect of UDCA on their response to a true antigen, rather than a mitogen, could be investigated. Once a particular antigen was established for each individual which gave a high response, ELISpots were carried out which investigated different concentrations of UDCA on the reactivity against the chosen antigen for each individual patient under different concentrations of UDCA. The cells at different patient were plated in triplicate in a series of UDCA concentrations. The same assay was carried out using the α CD3 mitogen in parallel.

The α CD3 mitogen is a monoclonal antibody that binds to a non-antigen related region of CD3, which is the T cell antigen receptor. Although unable to cause a response in the T cell

due to lack of a surface the T cell can be cross-linked to, α CD3 is sufficient to cause proliferation of the T cell in the presence of IL-2, which is provided by other PBMCs when it is a PBMC cell suspension (Jason and Inge, 1996).

Stimuli used were either an anti-CD3 mitogen or an antigen of interest. Antigens of interest used included those test common antigens used in the initial screen, described below, and PBC antigens, which were named PDC 1-4, or respectively: rhE2, rhE2ILD, rhE3BP and rhE3BPILD, all of which are described in chapter 1: Introduction, and with sequences in table 4.2.2.1.

Healthy volunteers were all screened with a panel of antigens to determine an antigen that they respond highly to, which could be used to stimulate their cells in later experiments assessing the effect of UDCA on their reactivity to an antigen. The screening panel contained the following antigens: pokeweed mitogen (PWM), cancer cell line (K), Adenovirus (Adeno), Salmonella, cytomegalovirus (CMV), Epstein-Barr virus (EBV), Haemophilus influenza (Hib), pseudomonas antigen (PSA). The pokeweed mitogen is a positive control to ensure that cells will react and are alive and undamaged. Derived from the *Phytolacca americana* plant, the pokeweed mitogen binds to sugar residues on surface glycoproteins and causes their cross linking. This includes molecules associated with cell expansion (De Vries et al. 1980). Therefore, this mitogen has large proliferative properties and is an ideal positive control.

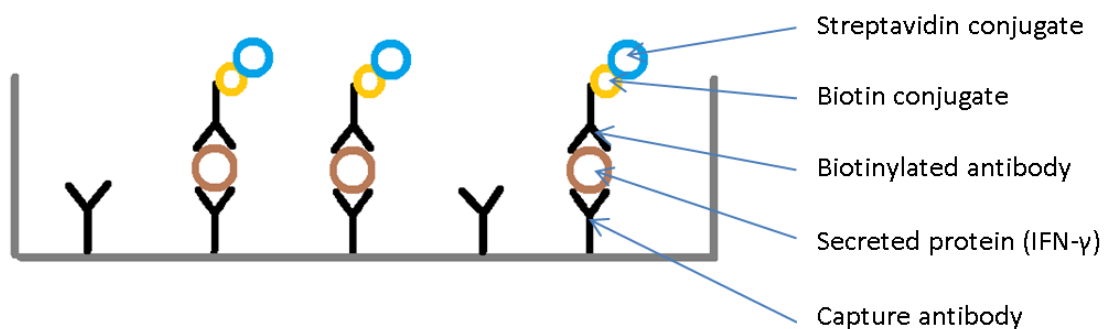


Figure 4.2.2.1: Diagram of the ELISpot sandwich assay whereby the secreted cytokine is sandwiched between antibodies.

This diagram illustrates the arrangement of the added components of the ELISpot assay. The secreted protein becomes sandwiched between a capture and a detector antibody. The detector antibody is the biotinylated antibody. The biotin conjugate mediates spot formation when it reacts with the streptavidin conjugate and forms a visible precipitate.

Pep.No.	Name of polypeptide	Sequence	Length of sequence (no. amino acids)
1	E2pdh163	GDLLAEIETDKATI	14
2	E3BP34	GDALCEIETDKAVV	14
4	E2ogdc	EQSLITVEGDKASM	14
5	E2pdh159	KLSEGDLLA	9
6	Psaer1	ALAEGDLLA	9
12	SciTop586	AKVFRTYNASITLQQQL	17

Table 4.2.2.1: Table of PBC antigen peptides

This table shows a selection of peptides used which are thought to be of interest in PBC, used to screen healthy volunteer blood for reactivity so that these results can be compared to results from patient blood.

4.2.3: ELISpot cell viability Flow Cytometry Experiment

In order to test that the cells were still viable within the assay the ELISpot was carried out as per the method in section 4.2.2, but cells were then extracted after completion of the experiment, stained with DAPI and other cell surface markers and put through the flow cytometer to analyse the alive/dead status and subtypes of T cells.

This ELISpot was carried out to test if UDCA was having a direct effect on the immune cells such that if by increasing the effect of the drug there is a decrease in number of spots formed, which would be a direct indicator of number of cells which have responded to the test antigen. However, if there were a toxic effect of UDCA on these immune cells, then a toxic effect could be masquerading as a direct effect on the immune activity of these cells. There have been assays carried out in this study which have shown that UDCA is likely not toxic at concentrations up to 300µM for up to 72h and longer, the apoptosis assay studies cells at rest likely undergoing no significant activity. The context of the ELISpot, although occupying under 24h of time, is entirely different in that cells are being stimulated and may begin to prepare for proliferation in response to the antigen. This test was carried out to monitor if cells were apoptosing in response to the raised drug concentration in the ELISpot context.

The ELISpot was set up as per the panel in figure 4.2.3.1. Purified protein derivative, ppd, is an antigen which mimics tuberculosis, specifically *Mycobacterium tuberculosis*. It is diagnostically used to test for tuberculosis reaction to determine if a patient needs the vaccination or not, but can be used scientifically to cause a reaction in T cells in assays such as the ELISpot assay (Stavri *et al.*, 2012) if the individual has encountered this antigen before and responds strongly, as is determined beforehand in a screen assay like that

described in section 2.2. The individual used for this assay gave a strong response to the ppd antigen as determined by a screen (data not shown). For the ELISpot mitogen, the anti-CD3 mitogen used was the Purified NA/LE Mouse Anti-Human CD3 Clone HIT3a from BD Biosciences. This is diluted 1/200 from 1mg/ml to 5µg/ml. αCD3 is normally used at cell concentrations of 4×10^5 for spot counting, however this does not give sufficient total cells per well to use for flow cytometry, therefore this same set up was repeated for an additional 3 columns with a higher cell count, 8×10^6 , these wells contain too many cells to give readable spots: the well shows a 'blackout'. The different concentrations were required to give countable spots but also enough cells for a flow cytometry analysis. Medium alone (no stimulus) was used alone so that the death of cells when there is the stimulus and without could be assessed.

		ELISpot:						Flow Cytometry:					
Stimulus->		αCD3			ppd			αCD3			medium alone		
Cell concentration ->		4×10^5 /ml			4×10^6 /ml			8×10^6 /ml			8×10^6 /ml		
Sample no.->		1	2	3	1	2	3	1	2	3	1	2	3
Concentration of UDCA (mM)	medium												
	carrier												
	0.01												
	0.05												
	0.1												
	0.25												
	0.5												
	1												

Figure 4.2.3.1: Diagram of layout of ELISpot plate for the ELISpot alive/dead assay

The above shows the layout of the ELISpot designed to assess whether UDCA may be having a toxic effect in the context of the ELISpot at certain concentrations. Samples are plated in triplicate. Concentration of UDCA for a given row is shown to the far left and the stimulus for a given column along with cell concentration is shown above.

4.2.4: Flow cytometry proliferation experiments

4.2.4.1: Preliminary experiment

In order to detect any effect on proliferation of T cells of UDCA, a preliminary experiment was carried out which used the method outlined in chapter 3, and involved isolated T cells from 3 healthy volunteers. They were stained with CFSE as per the protocol in Chapter 2: General Methods, and separated into 3 different wells, each with different concentrations of UDCA in 0.3% ethanol carrier, including a control with 0µM UDCA but still including the ethanol carrier. Concentrations of UDCA used were 100µM UDCA and 300µM UDCA. Cells were proliferated with 10µl CD3/CD28 T cell proliferation Dynabeads and IL-2 (method outlined in chapter 3), incubated for 4 days and then samples taken for flow cytometric analysis after staining with anti-CD3-APC conjugated antibody, as per flow cytometric preparation and staining protocol. Cell samples were analysed by flow cytometry, using

FACSDiva software to count cells based on their proliferation and presence of CD3+, further explained in chapter 3.

4.2.4.2: T cell proliferation assay analysing different T cell subsets and the effect on proliferation of UDCA

An assay was also designed that could investigate an effect on proliferation on individual T cell subsets. The design of this assay is described in chapter 3. PBMCs of 3 volunteers were incubated by criteria outlined in chapter 3, in different conditions: unstimulated and no UDCA, no UDCA or carrier, 0.25mM UDCA in carrier, 0.1mM UDCA in carrier, 0.3% carrier alone and 1% carrier alone. Cells were processed for flow cytometric analysis, following Panel 2 criteria, outlined in chapter 3, including DAPI stain for CD4+ helper T cell subsets and analysed using FACS-Diva software.

4.2.5: H69 Cholangiocyte cell line experiments

4.2.5.1: H69 cholangiocyte media

H69 cells were cultured in media which is 2:1 DMEM low glucose and F12 Ham, supplemented with FBS (10% of total media volume), penicillin and streptomycin antibiotic mixture (1% of total media volume), L-glutamate (1% total media volume), Adenine (120 μ l per l media of 0.2mg/ml working solution), Triiodothyronine (135 μ l per l total media volume of 10ng/ml working solution), epinephrine (20 μ l per l total media volume of 50mg/ml stock solution made up in 0.5N HCl), ITS-X (10ml per l total media volume), Hydrocortisone (20ml per l total media volume). The H69 cell line is an immortalised cell line originally isolated from intrahepatic bile ducts. Cells were obtained from Dr Ben Millar, Institute for Cellular and Molecular Biosciences, Newcastle University, in culture form in 10ml of full media in a cell culture flask. Cells had been checked and confirmed negative for mycoplasma contamination immediately before their release to Northumbria University for this study. All media and additives were obtained from Sigma Aldrich.

4.2.5.2: Supernatant transfer assay

H69 cells were incubated in their medium until approximately 60-80% confluent. Some medium of H69 was harvested and frozen prior to its use on cells and frozen, alongside some media harvested from the cell culture at 60-80% confluent. UDCA was added to the H69 cells to a final concentration of 250 μ M in an ethanol carrier not allowing ethanol concentration to exceed 0.3%. H69 culture was then incubated for a further 24 hours to allow the cells to respond to the drug, then some more media was harvested from the H69 culture and frozen. Cells were then washed 3x by centrifugation and resuspension in their

media to ensure that all UDCA had been washed from the H69 cells. The H69 cells were then re-suspended in media and incubated for 24h and another sample of media was then harvested. Cells were cultured for a further 4 days with media harvested at days 2, 3 and 5 from addition of UDCA. A lysate of H69 was prepared by rapid freeze/thaw cycles followed by manual disruption and topped up to a concentration of 10% cells in their media.

PBMCs from the blood of 3 healthy controls are extracted as per method in General Methods. Cells were stained with CFSE dye as per the method in chapter 3, then cultured at 1×10^6 per ml in a 24 well plate with 50% their own media with 1 in 200 α CD3 mitogen to stimulate proliferation and 50% one of 8 additive preparations as per table 4.2.5.2.

Tube number:	Additive making up 50% total culture media:
1	Unused H69 media
2	Harvested media from confluent H69 cells Harvested media from H69 cells after 1 day of incubation with
3	UDCA.
4	Media from 3x washed H69 cells, 24h after UDCA addition.
5	Media from 2 days after wash.
6	Media from 3 days after wash.
7	Media from 5 days after wash.
8	Media containing H69 cell lysate.

Table 4.2.5.2: Table of additives used in supernatant transfer assay

The above figure shows the additives used in the supernatant transfer assay which would make up 50% of the total media in this sample. This experiment investigates the effect of any substance released by H69 cells in response to UDCA on the T cells.

4.2.5.3: xCELLigence

Prior to an xCELLigence, is it usually a requirement to carry out a prior experiment which involves plating cells at different numbers per well and running the experiment to determine the ideal number of cells to use per well. This would require 2 E-plates in total to use, one for the cell number titration experiment and another for the proliferation experiment itself. Acquisition of 2 plates was unfeasible due to budget constraints, therefore only one E-plate was available. Therefore, cells were seeded at 2000 per well as this is the number generally used in the literature and has been shown to give ideal results with the H69 cholangiocyte cell line (Chaiyadet et al., 2015a).

Cells were seeded into each well at 2000 cells per well, with each well containing a total volume of 100 μ l of cells and their normal media, made up as per section 2.2.4.1. Cells had been kept at 0.05% FCS overnight to serum-synchronise them prior to the experiment. This arrests the cells in the same stage of proliferation so that they proliferate in synchronisation with each other once FCS levels resume to normal. The experiment was run for 97 hours, with readings taken every 15 minutes to test for their adherence and proliferation. UDCA

was added 24 hours into the recorded experiment. As a cell makes contact with the golden plate at the bottom of the well, there is increased electrical impedance detected in the gold plate and transmitted to the computer. Every 15 minutes readings of electrical impedance were measured and the results plotted in a graph by the software provided. This provides a graph of electrical impedance, which is proportional to cell number, against time. The resulting curve gives an indication of the proliferation of the cells, comparable to each other. The area under each curve gives a numerical value which can be directly compared to the others.

4.2.6: Large Flow Cytometry assay

Methodology for this section is not outlined in this chapter as the previous chapter is concerned with design of the assay used for this section. Methodology can be found in chapter 3.

4.3: Results

4.3.1: Trypan Blue apoptosis assay on isolated T cells

Numbers of cells counted, corrected to $\times 10^5/\text{ml}$, are represented graphically in figure 4.3.1 for the ethanol carrier and 4.3.1.2 for the DMSO carrier. Relevant p values are tabularised in table 4.3.1.1 for ethanol carrier; 4.3.1.2 for DMSO carrier. P values refer to comparison with carrier only at the stated concentration. Significantly different results when ethanol is used occur at 0h, 100 μM ($p=0.037$) UDCA but at all other counts there is no significant difference from the carrier only. Significantly different results when DMSO is used occur at 24h, 100 μM ($p=0.042$); 120h, 100 μM ($p=0.004$).

A further apoptosis assay was then carried out using smaller increments of UDCA and also comparing the ethanol carrier to no carrier, to see if there is a toxic effect of the carrier alone compared to no carrier. All other comparisons were made to the carrier control. There are no significantly different results between the carrier (Control 1 or no carrier, figure 4.3.1.3 and table 4.3.1.3).

A further apoptosis assay was carried out to see if higher concentrations of UDCA could be used and also if the cells could be incubated in UDCA for longer periods of time with no significant decrease in alive cells. This used concentrations of UDCA up to 3mM and was carried out for 8 days of counting. The graph showing live counts is shown in figure 4.3.1.4 with relevant p values in table 4.3.1.4. As can be seen in table 4.3.1.4, there appears to be significantly fewer live cells for concentrations of 0.5mM and above, at day 4 onward. The

p values are consistently significant above these values of time and concentration (shown in bold in table 4.3.1.4).

A further apoptosis assay was carried out to see if the effect of live cell number on T cells also applies to PBMCs, as some further experiments were planned to use the PBMC population. This was a direct replication of the assays for figure 4.3.1.1 only used PBMCs. The only significantly different results, shown in bold in table 4.3.1.5, were for 0h, possibly due to non-uniformity of cells due to their possible stickiness from culture which led to cell plating.

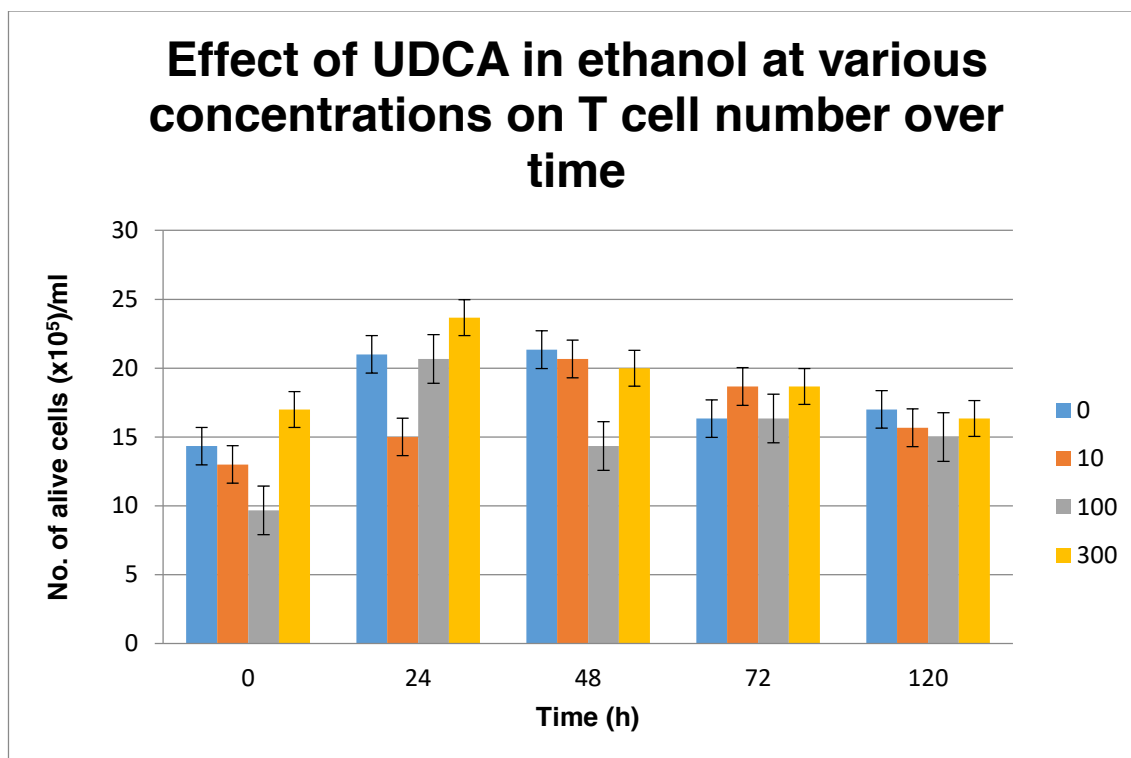


Figure 4.3.1.1: Graph of alive T cells against time using ethanol as carrier

This graph shows the counts of alive cells using trypan blue staining and the haemocytometer. Cells were counted at 24hour intervals. Different concentrations, shown in μM , were used in order to assess a toxic effect of UDCA.

		p values for ethanol		
		UDCA conc. (μM)		
		10	100	300
Time elapsed (h)	0	0.717	0.037	0.254
	24	0.594	0.999	0.373
	48	0.998	0.470	0.958
	72	0.933	0.999	0.963
	120	0.966	0.548	0.994

Table 4.3.1.1: p values for data from live cell count against time at different UDCA concentrations using an ethanol carrier

P values are from one way ANOVA with Dunnett's correction for multiple comparison.

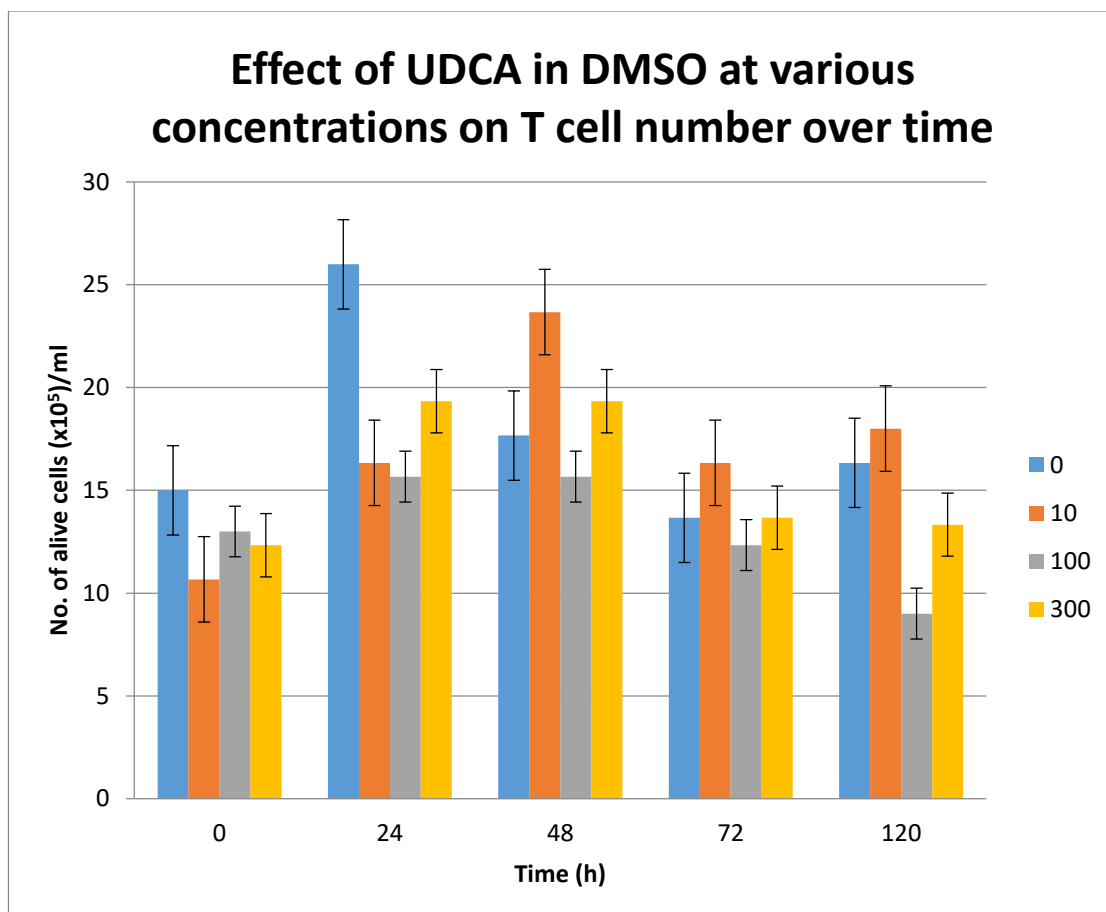


Figure 4.3.1.2: Graph of alive cells against time using DMSO as carrier
 This graph shows the counts of alive cells using trypan blue staining and the haemocytometer. Cells were counted at 24hour intervals. Different concentrations, shown in μM , were used in order to asses a toxic effect of UDCA.

		p values for DMSO		
		UDCA conc. (μM)		
		10	100	300
Time elapsed (h)	0	0.543	0.332	0.176
	24	0.129	0.042	0.113
	48	0.408	0.946	0.977
	72	0.498	0.634	0.999
	120	0.910	0.004	0.401

Table 4.3.1.2: p values for data from live cell count against time at different UDCA concentrations using an DMSO carrier

P values are from one way ANOVA with Dunnett's correction for multiple comparison.

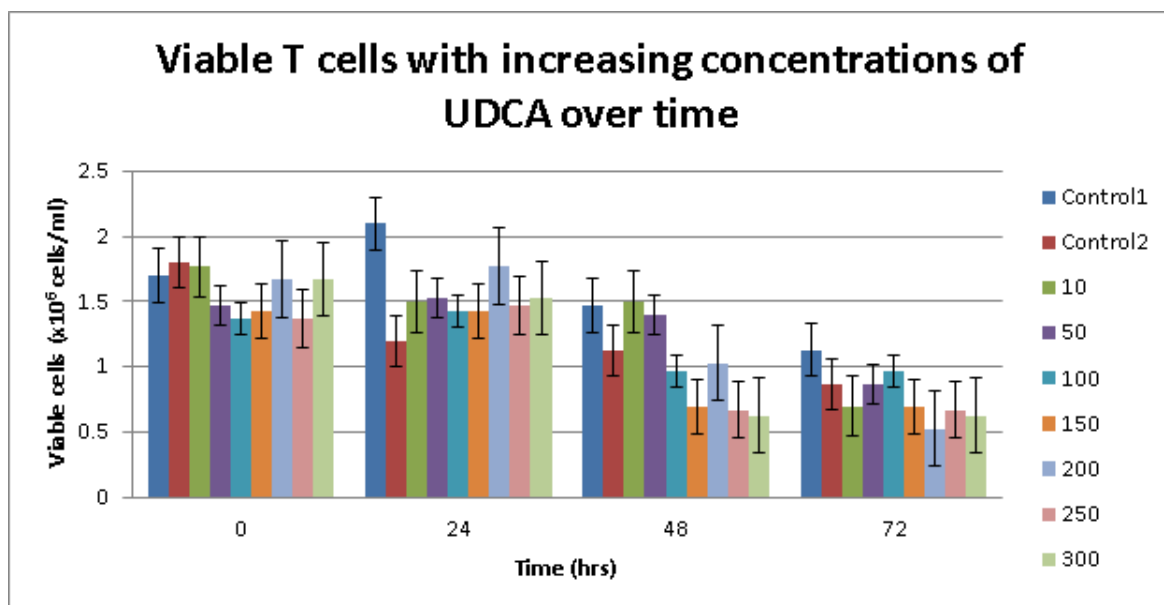


Figure 4.3.1.3: Graph of live T cell counts over time

This graph shows the counts of alive cells using trypan blue staining and the haemocytometer. Cells were counted at 24hour intervals. Different concentrations, shown in μM , were used in order to assess a toxic effect of UDCA. Ethanol was used as the carrier. Control 1 is where no carrier is used and control 2 is where the ethanol carrier alone is used at 0.3% total volume, as per previous experiments and as per wells with UDCA.

Carrier:		10	50	100	150	200	250	300
0h	0.423	0.999	0.284	0.185	0.144	0.451	0.560	0.451
24h	0.189	0.245	0.171	0.581	0.806	0.430	0.394	0.171
48h	0.230	0.602	0.986	0.999	0.869	0.999	0.828	0.783
72h	0.264	0.398	0.999	0.995	0.939	0.466	0.872	0.781

Table 4.3.1.3: p values for data from live cell count against time at different UDCA concentrations (μM) using an ethanol carrier

P values for carrier vs media from 2 tailed students' t tests; p values for concentrations vs carrier from ANOVA corrected with Dunnett's correction.

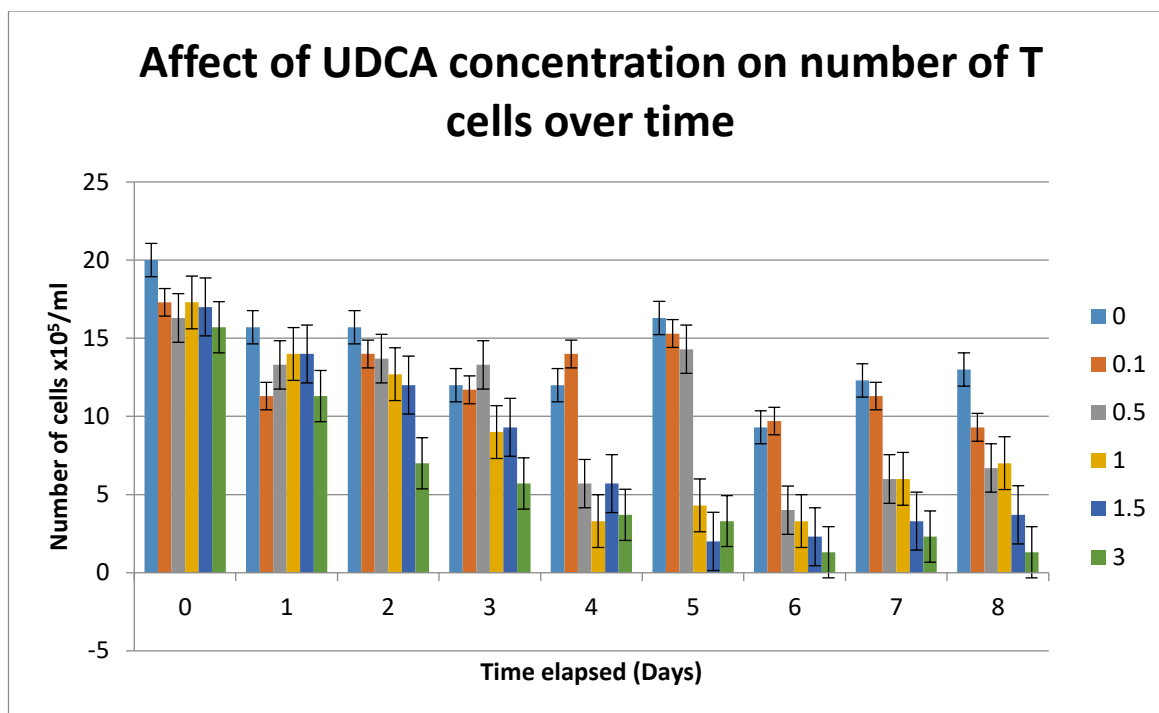


Figure 4.3.1.4: Graph of live T cell counts over time

This graph shows the counts of alive cells using trypan blue staining and the haemocytometer. Cells were counted at 24hour intervals. Different concentrations, shown in mM, were used in order to assess a toxic effect of UDCA. Ethanol was used as the carrier. Control 1 is where no carrier is used and control 2 is where the ethanol carrier alone is used at 0.3% total volume, as per previous experiments and as per wells with UDCA. This assay is a repeat of previous assays however extends the concentrations of UDCA used and also the number of days.

Table of P values

	UDCA concentration (mM)				
	0.1	0.5	1.0	1.5	3.0
0	0.514	0.249	0.514	0.412	0.143
1	0.328	0.810	0.937	0.937	0.328
2	0.988	0.975	0.887	0.791	0.14
3	0.999	0.986	0.703	0.789	0.083
4	0.411	0.001	<0.0001	0.0013	<0.0001
5	0.941	0.001	<0.0001	0.0013	<0.0001
6	0.999	0.014	0.0065	0.0020	0.0007
7	0.874	0.0010	0.0010	<0.0001	<0.0001
8	0.068	0.002	0.003	<0.0001	<0.0001

Table 4.3.1.4: p values for data from live cell count against time at different UDCA concentrations using an ethanol carrier

P values are from ANOVA with Drummert's correction assuming unequal variances comparing the corrected number of cells/ml for each UDCA concentration stated to carrier only for the stated time point.

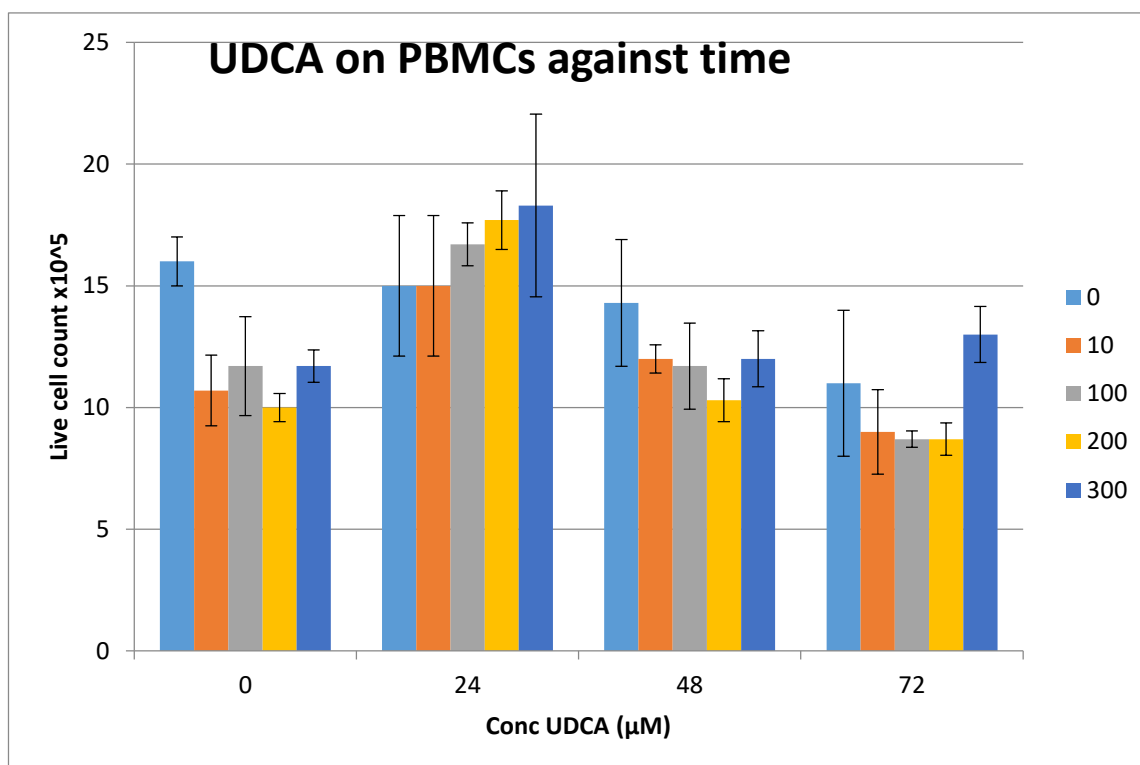


Figure 4.3.1.5: Graph of alive cells against time using ethanol as carrier

This graph shows the counts of alive PBMCs using trypan blue staining and the haemocytometer. Cells were counted at 24-hour intervals. Different concentrations, shown in μM , were used in order to assess a toxic effect of UDCA.

		Concentration UDCA (μM)			
		10	100	200	300
Time (h)	0	0.043	0.107	0.024	0.107
	24	>0.999	0.971	0.872	0.770
	48	0.687	0.591	0.275	0.687
	72	0.811	0.725	0.725	0.811

Table 4.3.1.5: p values for data from live cell count against time at different UDCA concentrations using an ethanol carrier

P values are from ANOVA with Drummatt's correction assuming unequal variances comparing the corrected number of cells/ml for each UDCA concentration stated to carrier only for the stated time point.

4.3.2: ELISpot Results

4.3.2.1: ELISpot cell viability Flow Cytometry assay

The results described here refer to the experiment outlined in section 4.2.3.

Figure 4.3.2.1 shows how the cells for flow cytometry, set-up of wells depicted in figure 4.2.3.1, were gated and counted by the software. Results for the ELISpot portion are shown in figure 4.3.2.1.2. This is the number of corrected spot forming cells per million established from the ELISpot portion of this assay, depicted in figure 4.2.3.1. Results for the Flow Cytometry portion are shown in 4.3.2.1.3. This is the number of dead cells, or the number of cells positively stained for the DAPI dye, counted by the FACSDiva software and depicted in figure 4.2.3.1.

Figure 4.2.3.1 shows that everything was carried out in triplicate. 'm' shows medium alone without carrier. T tests were carried out to compare values at all concentrations including no carrier to carrier alone. P values for the number of spot forming cells are shown in table 4.3.2.1.2 and p values for numbers of dead cells from flow cytometric analysis are tabularised and shown in table 4.3.2.1.3. Cells unstimulated appear to only have significantly more death at 1mM UDCA, $p=0.012$. Cells stimulated with a realistic antigen but weaker than the α CD3 mitogen have significantly fewer cells reacting to the stimulus only when UDCA concentration reaches approximately 1mM, $p=0.027$.

When cells are stimulated with the α CD3 mitogen, there appears to be, according to the data in this study, no significant increased cell death even at UDCA concentration of 1mM but decreased response to stimulus at concentrations 0.5mM and 1mM (p values = 0.007 and 0.0002 respectively).

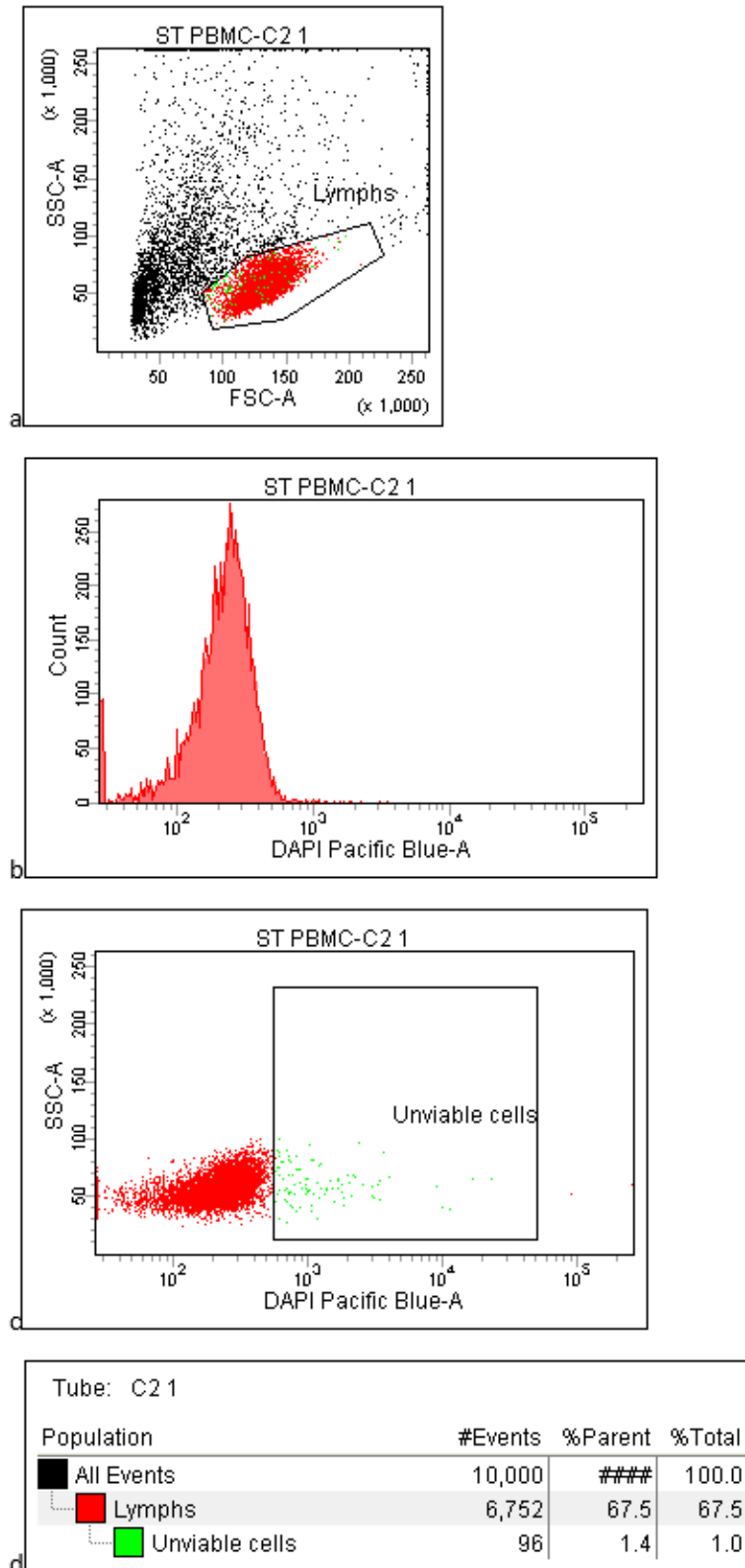


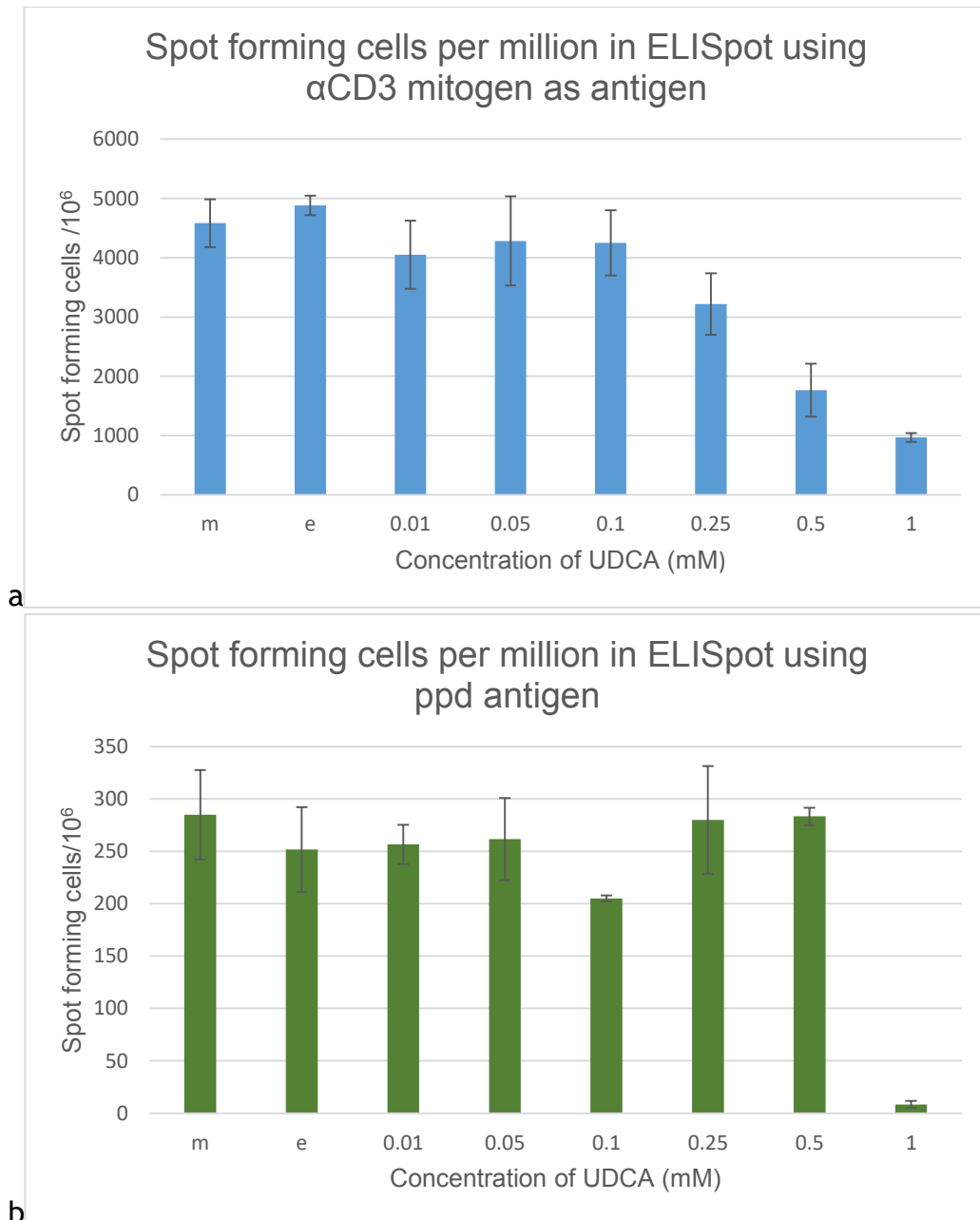
Figure 4.3.2.1.1: Gating of lymphocytes and graphs to show DAPI staining for dead and alive cells.

a – Lymphocytes are gated based on their known estimated forward and side scatter properties.

b – This histogram illustrates the relative proportions of DAPI + and – cells from the lymphocyte gate.

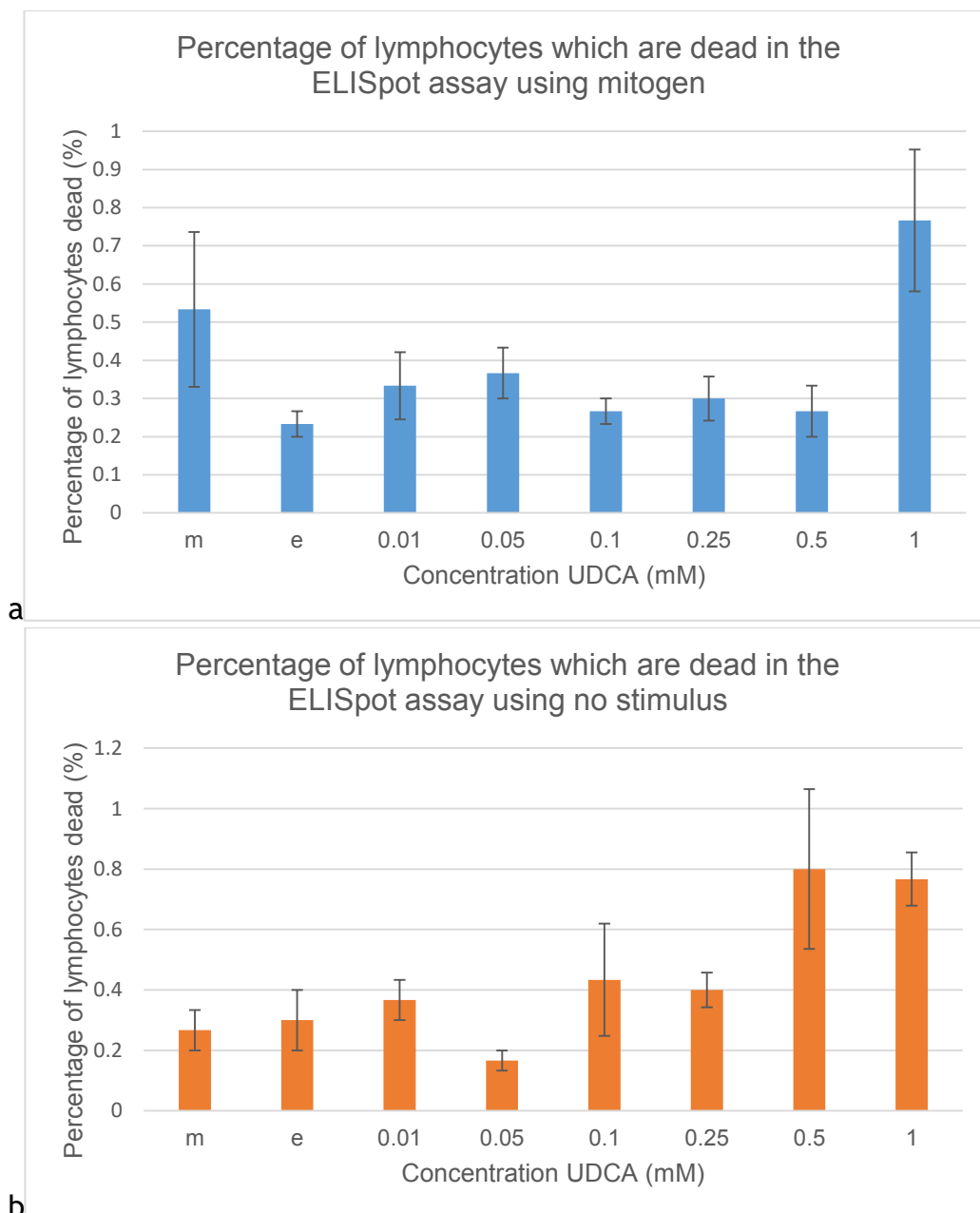
c – Unviable cells are gated based on established DAPI negative gate, using Flow Cytometry optimisation criteria in chapter [FACS set up].

d – Software counts the cells within set gates and displays the values in a tabularised format.



Figures 4.3.2.1.2 a and b: Graphs of spot forming cells per million at different concentrations of UDCA in ELISpot assays using the α CD3 mitogen and the ppd antigen.

The graph shows the effect of UDCA on the average number of spot forming cells per million at different concentrations of UDCA using the α CD3 mitogen and also a ppd antigen.



Figures 4.3.2.1.3 a and b: Graphs showing percentages of dead cells from flow cytometric analysis of cells from the ELISpot assay, a - using α CD3 mitogen and b – using no stimulus, at different concentrations of UDCA.

The graphs show the effect of UDCA on the average percentage of cells that are dead at different concentrations of UDCA using the α CD3 mitogen and also no stimulus.

ELISpot p values

Conc. UDCA (mM)	Antigen	
	α CD3	ppd
m	0.541	0.602
0.01	0.299	0.918
0.05	0.518	0.868
0.1	0.385	0.37
0.25	0.092	0.687
0.5	0.007	0.524
1	0.0002	0.027

Table 4.3.2.1.2: p values corresponding to figure 3.2.1.2.

Significant values include comparison of 0.5mM UDCA against carrier alone ($p=0.007$) and 1mM and carrier alone ($p=0.0002$) for α CD3; 1mM against carrier alone ($p=0.027$) for ppd.

Flow cytometry p values

Conc. UDCA (mM)	Antigen	
	α CD3	Medium
m	0.141	0.4
0.01	0.183	0.309
0.05	0.086	0.167
0.1	0.259	0.286
0.25	0.196	0.225
0.5	0.343	0.088
1	0.053	0.012

Table 4.3.2.1.3: p values corresponding to figure 4.3.2.1.3.

Significant values are for comparison between 1mM UDCA and carrier alone, $p=0.012$, in the unstimulated lane.

4.3.2.2: ELISpot results

Figures 4.3.2.2.1 a and b show the spot forming cells per 10^6 when 4 healthy non-PBC volunteers are challenged in the ELISpot context with a panel of common antigens to establish an antigen for each volunteer which produces a strong response for future experiments. The strongest response antigens for each individual are: EBV for 1 and 2, CMV for 3 and Salmonella for 4.

Figures 4.3.2.2.2 show similar data to 4.3.2.2.1 only using 7 volunteers and PBC antigens rather than common antigens. This was intended for comparison with PBC patients.

Figures 4.3.2.2.3 and 4.3.2.2.5 show results from ELISpot assays where serum from 4 volunteers is challenged for response to a stimulus where in 4.3.2.2.3, the stimulus is an α CD3 mitogen and in 4.3.2.2.5, the stimulus is the antigen established to be that which each individual responds strongly from figure 4.3.2.2.1. Figures 4.3.2.2.4 and 4.3.2.2.6 show the averages, respectively, of these, and tables 4.3.2.2.4 and 4.3.2.2.6 show the

relevant p values. These figures show a significant difference in spot forming cells per 10^6 when an α CD3 mitogen is used at concentrations 0.5mM and 1mM, p values 0.0027 and 0.00064 respectively, but no significant difference in spot forming cells per 10^6 when a common antigen each individual is known to respond strongly to is used.

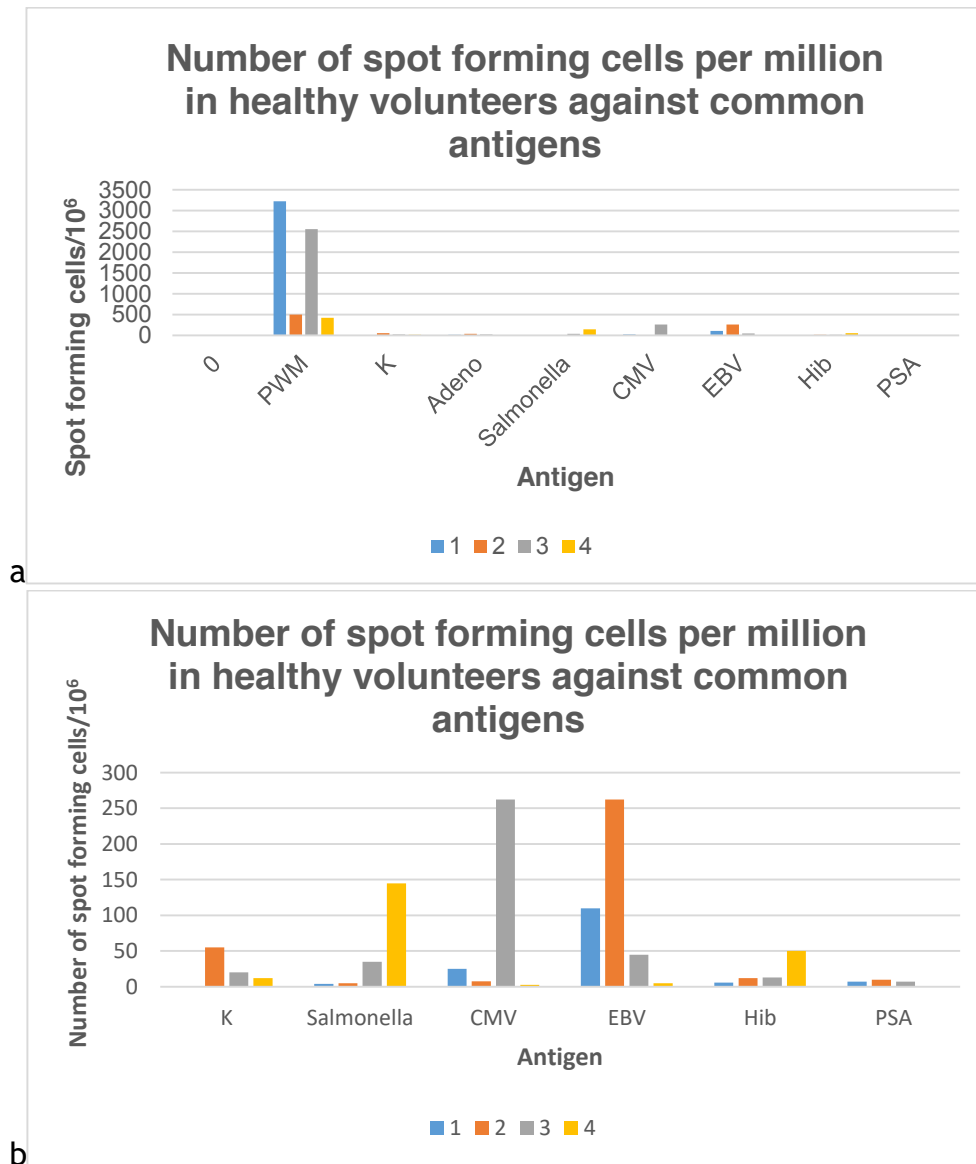


Figure 4.3.2.2.1 a and b: Graphs of number of spot forming cells per million when the PBMCs of 4 volunteers are challenged with a panel of common antigens. a shows a panel of antigens that 4 healthy volunteers were challenged with to determine one antigen each individual will respond to strongly for use in further experiments. b shows the same data as a but with the controls removed in order to better visualise the antigen counts, as they are small relative to the positive control. Numbers 1-4 refer to the assigned numbers of the different healthy volunteers.

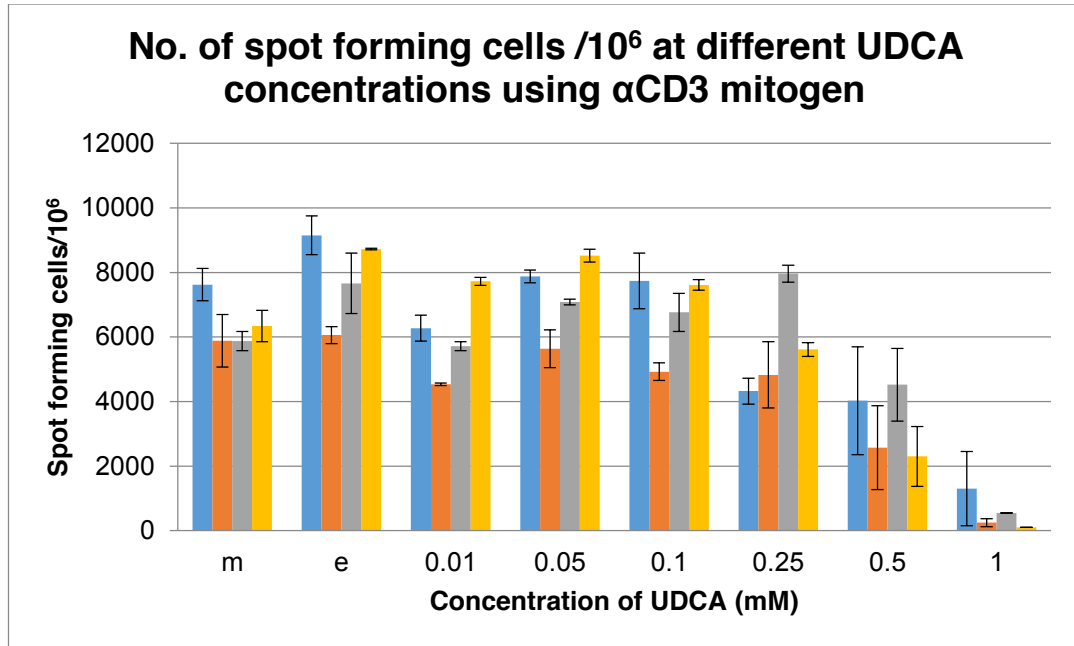


Figure 4.3.2.2.3: Graph of number of spot forming cells per million at different UDCA concentrations with α CD3 mitogen.

The above figure shows data for 4 healthy individuals. The graph shows the effect of UDCA on the average number of spot forming cells per million at different concentrations of UDCA where m denotes medium alone used instead of UDCA and e denotes where the carrier, ethanol, alone is used with no UDCA. Comparing e to m shows any response from the carrier alone, not attributable to UDCA. The stimulus used is the α CD3 mitogen. Different colours of bars are used for different volunteers, with one colour assigned to each volunteer.

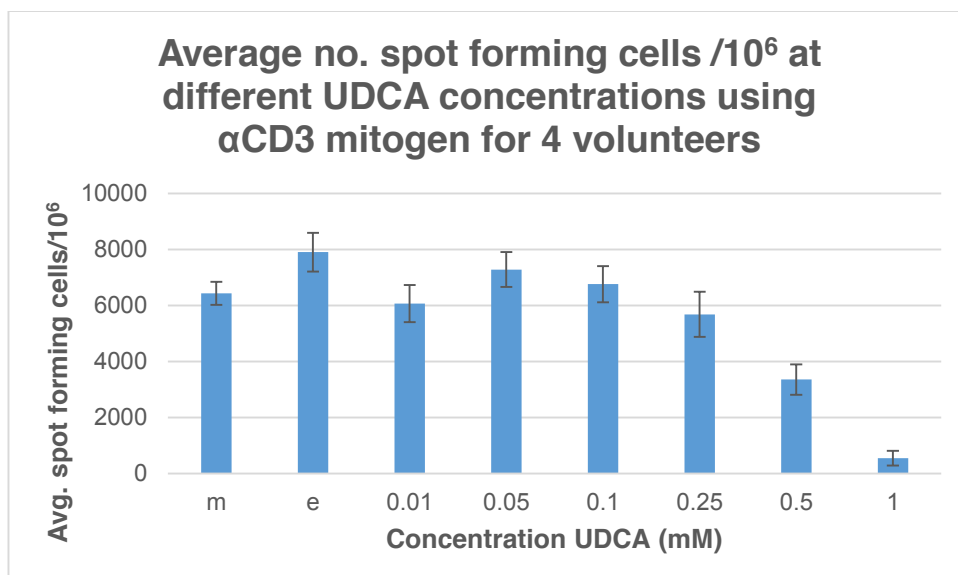


Figure 4.3.2.4: Graph of Average number of spot forming cells per million at different UDCA concentrations with α CD3 mitogen.

The above figure shows pooled data, averaged for 4 healthy individuals. The graph shows the effect of UDCA on the average number of spot forming cells per million at different concentrations of UDCA where m denotes medium alone used instead of UDCA and e denotes where the carrier, ethanol, alone is used with no UDCA. Comparing e to m shows any response from the carrier alone, not attributable to UDCA.

UDCA concentration (mM)	p	
	0	0.106
0.01	0.136	
0.05	0.537	
0.1	0.282	
0.25	0.081	
0.5	0.002	
1	0.0006	

Table 4.3.2.4: p values for Graph of Average number of spot forming cells per million at different UDCA concentrations with α CD3 mitogen, figure 3.2.2.4.

Significant comparisons are between carrier alone and: 0.5mM ($p=0.002$) and 1mM ($p=0.0006$).

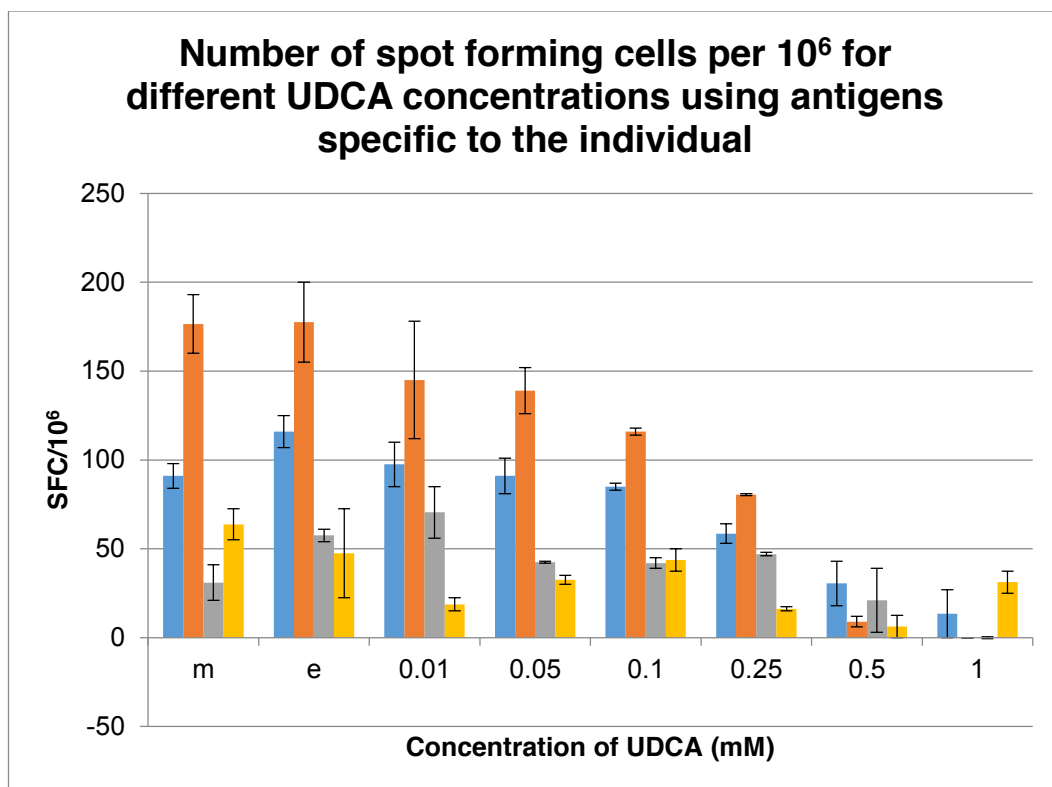


Figure 4.3.2.2.5: Graph of number of spot forming cells per million at different UDCA concentrations using antigen specific to the individual.

The above figure shows data for 4 healthy individuals. The graph shows the effect of UDCA on the average number of spot forming cells per million at different concentrations of UDCA where m denotes medium alone used instead of UDCA and e denotes where the carrier, ethanol, alone is used with no UDCA. Comparing e to m shows any response from the carrier alone, not attributable to UDCA. Antigens used vary between the individuals and were decided on by use of a panel of antigens to determine an antigen each individual will respond highly to. Different colours of bars are used for different volunteers, with one colour assigned to each volunteer.

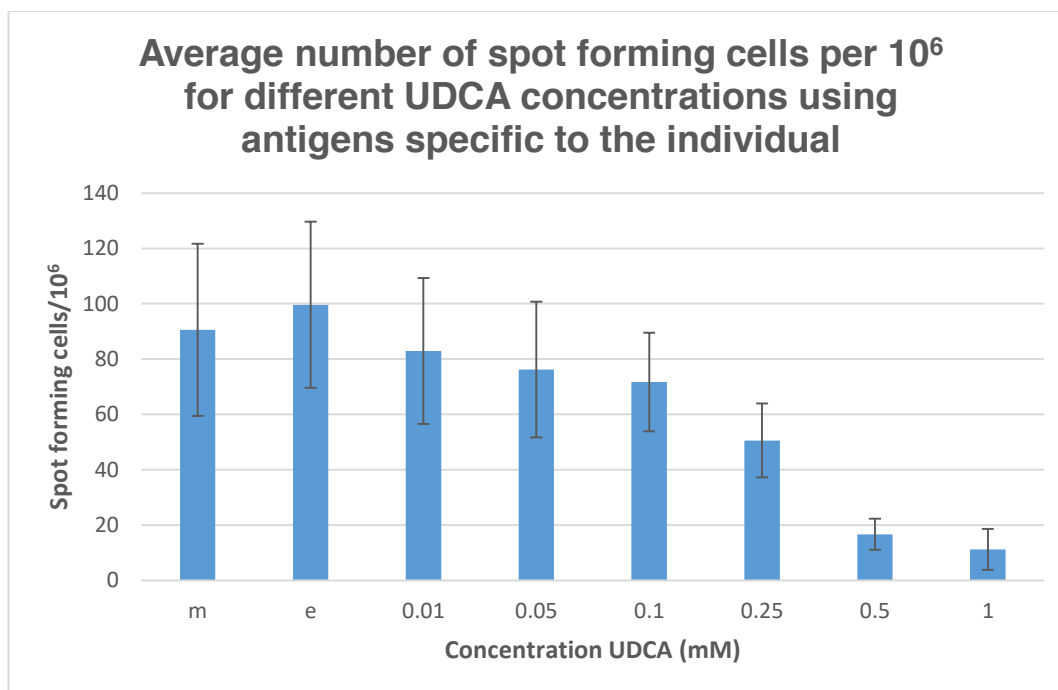


Figure 4.3.2.2.6: Graph of average number of spot forming cells per million at different UDCA concentrations using antigen specific to the individual.

The above figure shows pooled average data for 4 healthy individuals. The graph shows the effect of UDCA on the average number of spot forming cells per million at different concentrations of UDCA where m denotes medium alone used instead of UDCA and e denotes where the carrier, ethanol, alone is used with no UDCA. Comparing e to m shows any response from the carrier alone, not attributable to UDCA. Antigens used vary between the individuals and were decided on by use of a panel of antigens to determine an antigen each individual will respond highly to.

UDCA concentration (mM)	p	
	m	e
0.01	0.838	0.684
0.05	0.56	0.45
0.1	0.45	0.201
0.25	0.201	0.07
0.5	0.07	0.063
1	0.063	

Table 4.3.2.2.6: p values for Graph of average number of spot forming cells per million at different UDCA concentrations using antigen specific to the individual, figure 4.3.2.2.6.

These p values are from t tests comparing spot forming cells per million at different UDCA concentrations (or no UDCA and no carrier – m) to the carrier alone (e, ethanol).

4.3.3: Flow Cytometry results

4.3.3.1: Preliminary data

Figure 4.3.3.1.1 is a graphical depiction of preliminary data which shows that proliferation of T cells becomes ever more restricted as the concentration of UDCA rises. Each histogram is from cells gated for α CD3-APC staining, having been incubated for 3 days with IL-2 and Dynabeads T cell proliferation beads. At 300 μ M, the peak for cells having entered a third extra division relative to the highest staining peak, labelled 3+, looks visibly smaller than that for no UDCA. Visibly, there appears to be more of a skew towards the 0 relative divisions peak for 300 μ M compared to 0 UDCA. At 100 μ M, the peaks appear similar to those for 0 UDCA. As it cannot be discerned whether those cells in the right-most peak have divided or not, those cells counted in peaks representing further divisions are discussed in terms of how many more divisions they have incurred relative to the right-most peak.

Figure 4.3.3.1.2 is a bar chart displaying the average proliferation of T cells at different concentrations of UDCA. Proliferated cells are counted as those whose CFSE intensity has decreased to less than those cells making up the right most and most CFSE-intense peak. At 300 μ M UDCA, there is significantly less proliferation than with ethanol alone (0 μ M UDCA – contains 0.3% ethanol, used as the UDCA carrier), $p=0.039$.

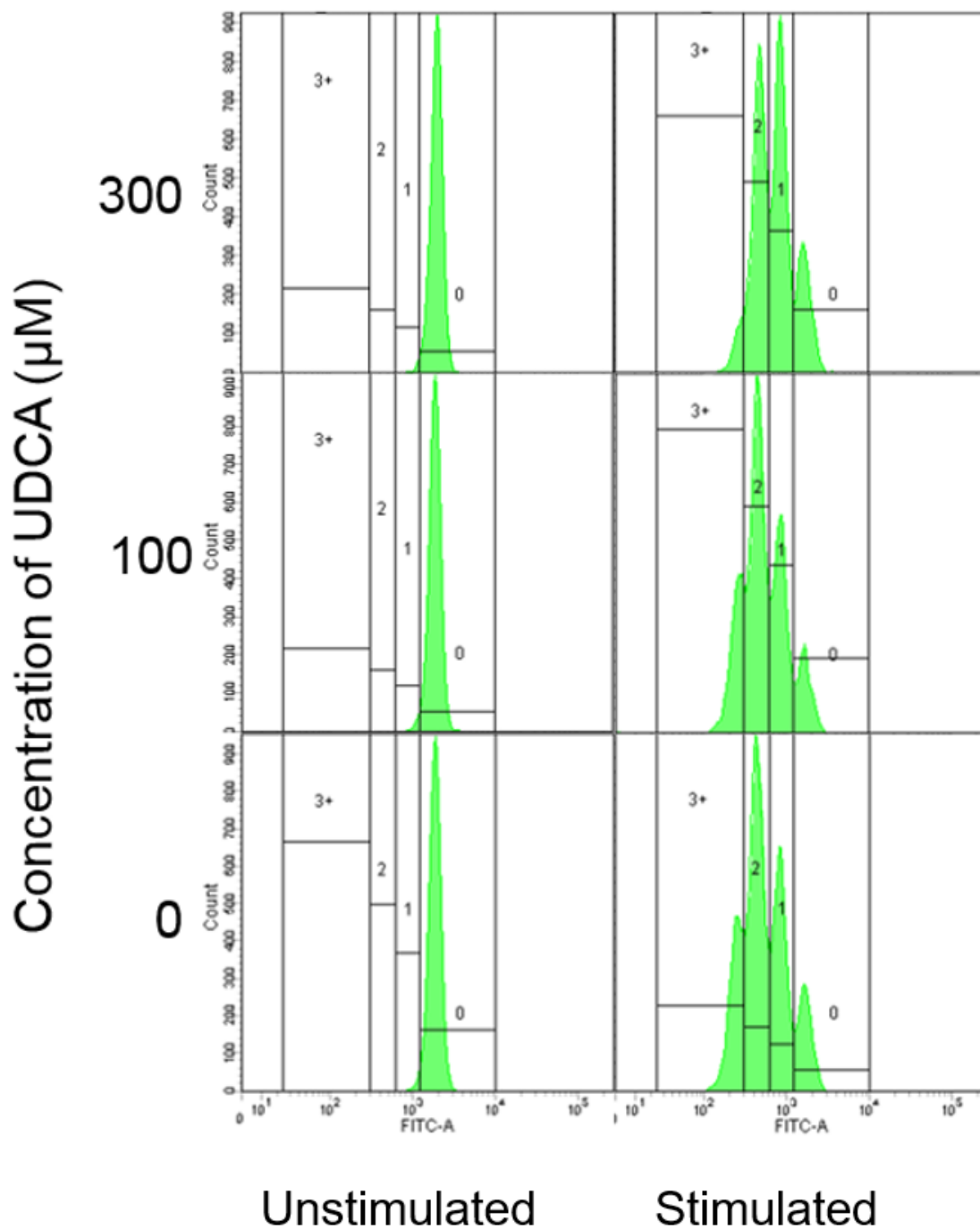


Figure 4.3.3.1: Graph to show the effect of increase in drug concentration on T cell proliferation

The graph shows proliferation, visualised by CFSE dye in cell cytoplasm, which is diluted down the daughter cells. The peaks are smaller in the 2 and 3+ columns the more UDCA is present. Unstimulated cells are shown to illustrate the effect of the proliferation beads and IL-2. This result is obtained after 3 days of incubation at 37°C.

Graph showing effect of increasing UDCA concentration on division of T cells

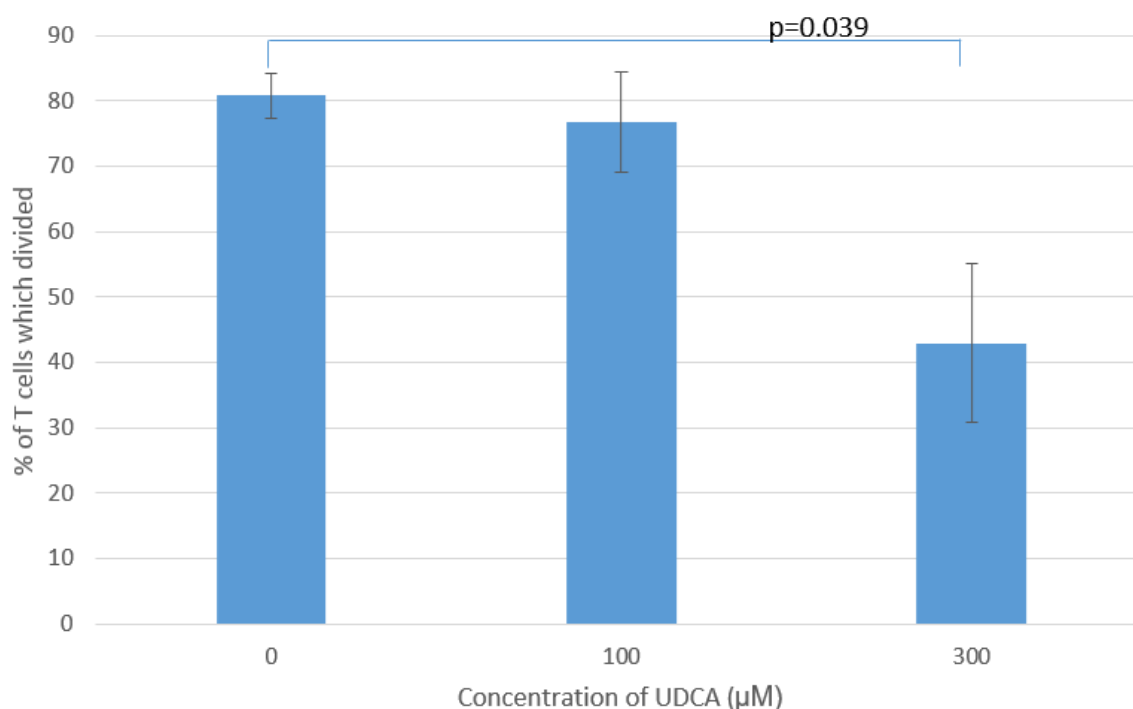


Table 4.3.3.1.2: Graph of quantified proliferation of T cells at different concentrations of UDCA.

This graph shows the average proliferation of T cells across 3 samples from different volunteers along with 'standard error' error bars and showing the significant difference between 300 μM UDCA and carrier alone.

4.3.3.2: The effect of UDCA on T cell subset proliferation

Cells were set up in the assay described in chapter 3 and gated as per figures 3.3.7.1.1 and 3.3.7.1.2. Figures 4.3.3.2.1-4.3.3.2.3 show graphical representation of average numbers across 3 volunteers of proliferated cells of Th1, Th1/Th17, Th2 and Th17 subsets and also the corresponding Tc subsets and CD4⁺ Tregs and CD45RO⁺ Tregs. Percentages of T cells are based on percentage of the parent population, which is why 'Divided CD4⁺' T cell bars are smaller than other bars. Gating criteria are outlined in chapter 3, figures 3.3.7.1.1 and 3.3.7.1.2.

Table 4.3.3.2 shows the p values where proportions of T cell subsets within the T cell population were compared with the 0.3% carrier (vehicle). Significant results are at 0.25mM UDCA, CD4⁺ T cells in the Treg tube ($p=0.008$) and CD8⁺ T cells (all $p=0.02$; Tc2 $p=0.03$).

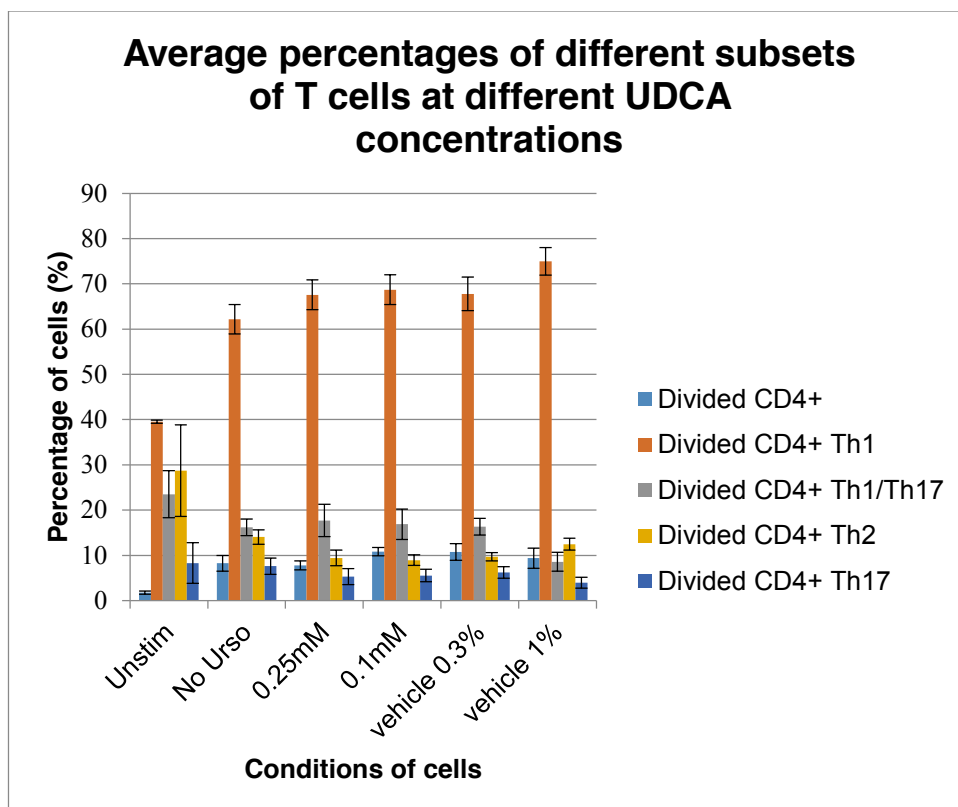


Figure 4.3.3.2.1: CD4+ T cell proliferation under different conditions, after incubation for 4 days with IL-2 and CD3/CD28 Dynabeads.

This figure depicts the different levels of divided CD4+ T cells and CD4+ T cell subsets based on percentage of parent gate or quadrant count, outlined in chapter 3. 'Standard error' error bars are also included.

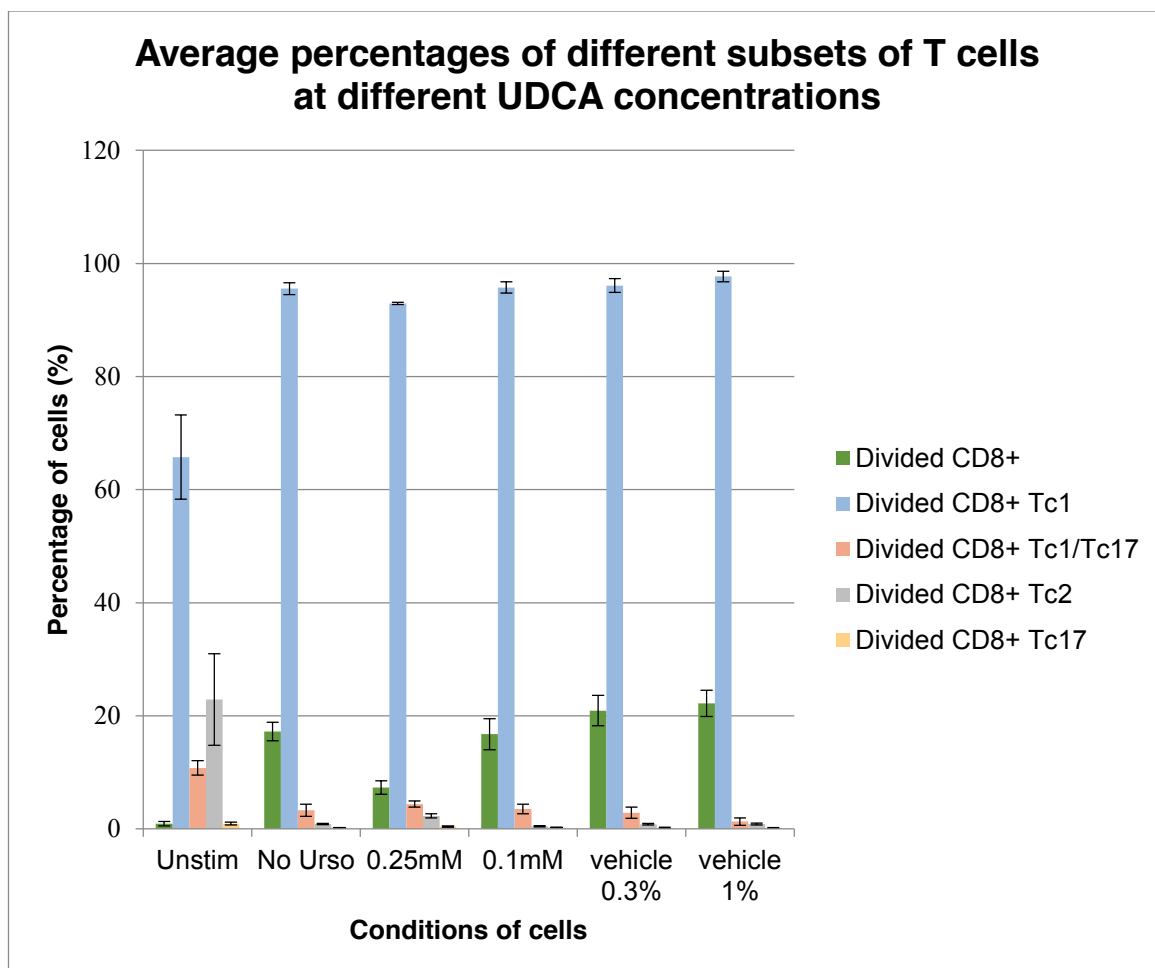


Figure 4.3.3.2.2: CD8+ T cell proliferation under different conditions, after incubation for 4 days with IL-2 and CD3/CD28 Dynabeads.

This figure depicts the different levels of divided CD8+ T cells and CD8+ T cell subsets based on percentage of parent gate or quadrant count, outlined in chapter 3. 'Standard error' error bars are also included.

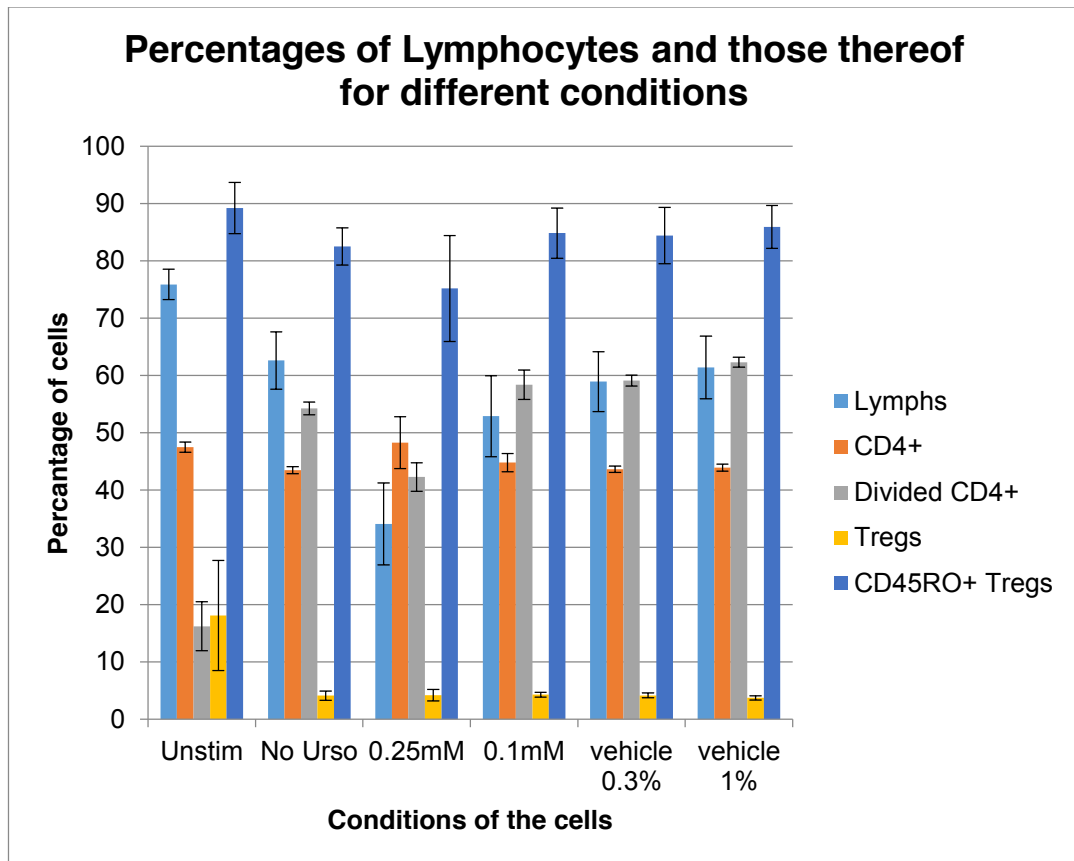


Figure 4.3.3.2.3: Treg cell proliferation under different conditions, after incubation for 4 days with IL-2 and CD3/CD28 Dynabeads.

This figure depicts the different levels of divided regulatory T cells and regulatory T cell subsets based on percentage of parent gate, depicted in chapter 3. 'Standard error' error bars are also included.

			UDCA concentration	
			0.1mM	0.25mM
CD4+ panel - Divided cells		CD4+ all	0.98	0.24
		Th1	0.86	0.97
		Th1/Th17	0.9	0.76
		Th2	0.64	0.9
		Th17	0.74	0.69
CD8+ panel - Divided cells		CD8+ all	0.34	0.02
		Tc1	0.84	0.12
		Tc1/Tc17	0.64	0.27
		Tc2	0.11	0.03
		Tc17	0.63	0.29
Treg panel Divided cells		CD4+	0.575	0.008
		Tregs	0.83	0.96
		CD45RO+	0.95	0.44

Table 4.3.3.2: p values for comparisons of populations of divided T cell subsets compared to carrier only

T tests were carried out to compare numbers of divided T cells, within gated subsets, incubated with UDCA to those of the corresponding subsets but without UDCA. This table shows the p values of these t tests. Significant results are for 0.25mM UDCA, CD4+ cells in the Treg tube ($p=0.008$) and CD8+ T cells (all CD8+, $p=0.02$; Tc2, $p=0.03$).

4.3.4: H69 cholangiocyte experiments

4.3.4.1: xCELLigence results

UDCA is added at the 24h point. Figure 4.3.4.1.1 shows the plotted results of average cell density over time. After addition of UDCA, the lines appear to indicate that the more UDCA there is in the culture medium, the less the cell density. 0.5mM UDCA and 1mM UDCA results appear to show a decrease in cell density with 0.25mM failing to increase and at 0.1mM, cell density appears to continue to increase but at a lower rate than at 0.01mM UDCA and under. 0.01mM UDCA appears to give no effect on cell density. Figure 4.3.4.1.2 shows the quantified area under curve values for the areas mapped out by the lines in figure 4.3.4.1.1. Visually, UDCA concentration shows a negative effect on cell density.

This is confirmed by the p values, shown in table 4.3.4.1, where 0.25mM, 0.5mM and 1mM all show a significant difference from E ($p=0.031$, $p=0.004$, $p=0.026$ respectively).

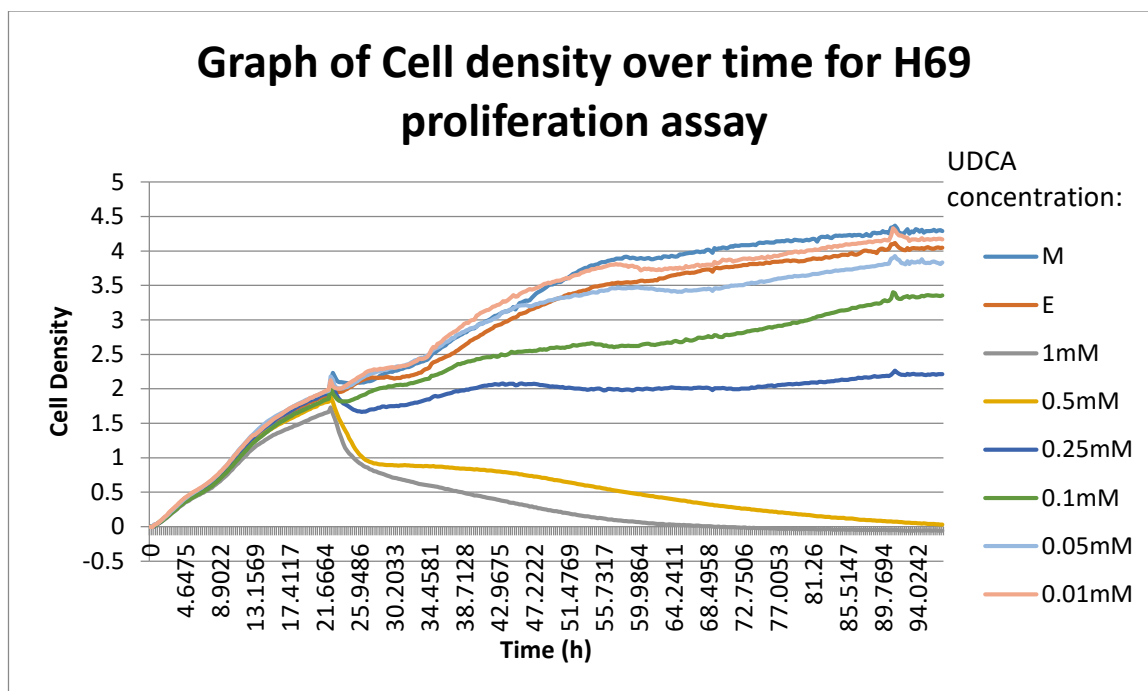


Figure 4.3.4.1.1: Graph of cell density of H69 cell line cells at different concentrations of UDCA over 96 hours

This graph shows cell density of H69 cells at different UDCA concentrations including carrier alone (E) and no carrier (M). Each concentration was plated in duplicate and cell densities were averaged, then lines plotted based on these averages. These results can be quantified and compared by calculating the area under curve of each individual line.

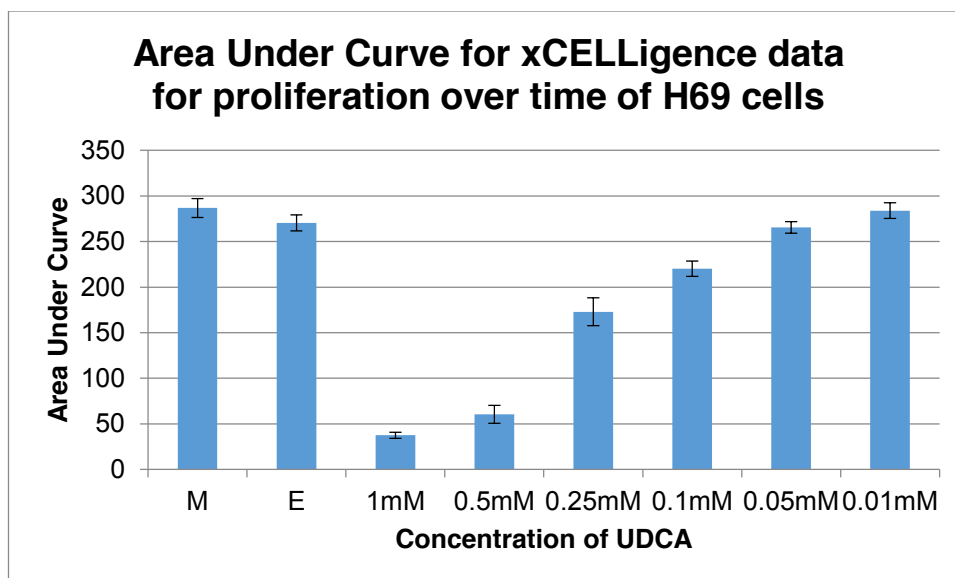


Figure 4.3.4.1.2: Graph showing the area under curve values for each concentration of UDCA used on H69 cells

This graph shows the area under curve for the average cell density at each concentration of UDCA used. Concentrations of 0.1mM and above appear to visibly show less cell density than the carrier.

P values for area under curve

Concentration UDCA	p
m	0.348
1mM	0.026
0.5mM	0.004
0.25mM	0.031
0.1mM	0.054
0.05mM	0.7
0.01mM	0.385

Table 4.3.4.1: p values for area under curve data

P values are from t tests of area under curve data comparing to the ethanol carrier, E. 0.25mM, 0.5mM and 1mM all show a significant difference from E (p=0.031, p=0.004, p=0.026).

4.3.4.2: Supernatant transfer assay

Cells analysed by flow cytometry were analysed by gating criteria shown in figure 4.3.4.2.1 where lymphocytes were gated from forward and side scatter, singlets were gated from lymphocytes, live cells were gated from lymphocytes, proliferated cells were gated from live cells and CD4+ and CD8+ is established by presence of anti-CD8+ PeCy7 antibody and/or anti-CD4+ APC-Cy7 antibody. Table 4.3.4.2 shows the proportions (in terms of percentage) of the divided cells that are each of the CD4/CD8 combination subsets, and the proportion of live lymphocytes which divided, for each volunteer and each condition of the experiment. As the values under the CD4/CD8 criteria headings are proportions of the live lymphocyte population, they do not indicate increases or decreases of these particular subtypes but instead analyse the whole population of divided cells and essentially the ratios of these different subsets within this population. Figure 4.3.4.2.2 is a bar chart showing comparable levels of the total divided T cell population average across the different criteria of cells cultured with: DMEM F12, Supernatant from confluent H69 cell culture, Supernatant from confluent H69 culture after addition of UDCA, Supernatant from H69 cells 1 day after their wash and media-change, Supernatant from H69 cells 2 day after their wash and media-change, Supernatant from H69 cells 3 day after their wash and media-change, Supernatant from H69 cells 5 day after their wash and media-change and H69 cell lysate. Significant results from t-test comparison are shown with dashed lines and the denotation of significance by: * - $0.05 > p > 0.01$, ** - $0.01 > p > 0.001$, *** - $0.001 > p > 0.0001$. The confluent media was found to give significantly less proliferation of T cells than DMEM alone ($p < 0.05$). Therefore, other results were also compared with confluent H69 supernatant and those found to show less T cell proliferation were supernatant from H69 cells 1 and 2 days after having been washed of all UDCA ($p < 0.05$; $p < 0.001$). The T cell subtype composition of the divided cells was then analysed to determine if there is a difference in ratios of CD4+ and/or CD8+ of the divided cells in the presence of the different supernatants being investigated. Figure 4.3.4.2.3 shows the relevant proportions of CD4+CD8+, CD4+CD8-, CD4-CD8+ and CD4-CD8- T cells within the divided T cell population to determine if the CD4+/CD8+ T cell ratios are changing in response to a molecule released by H69 cells but there were no significant differences detected for these T cell subsets.

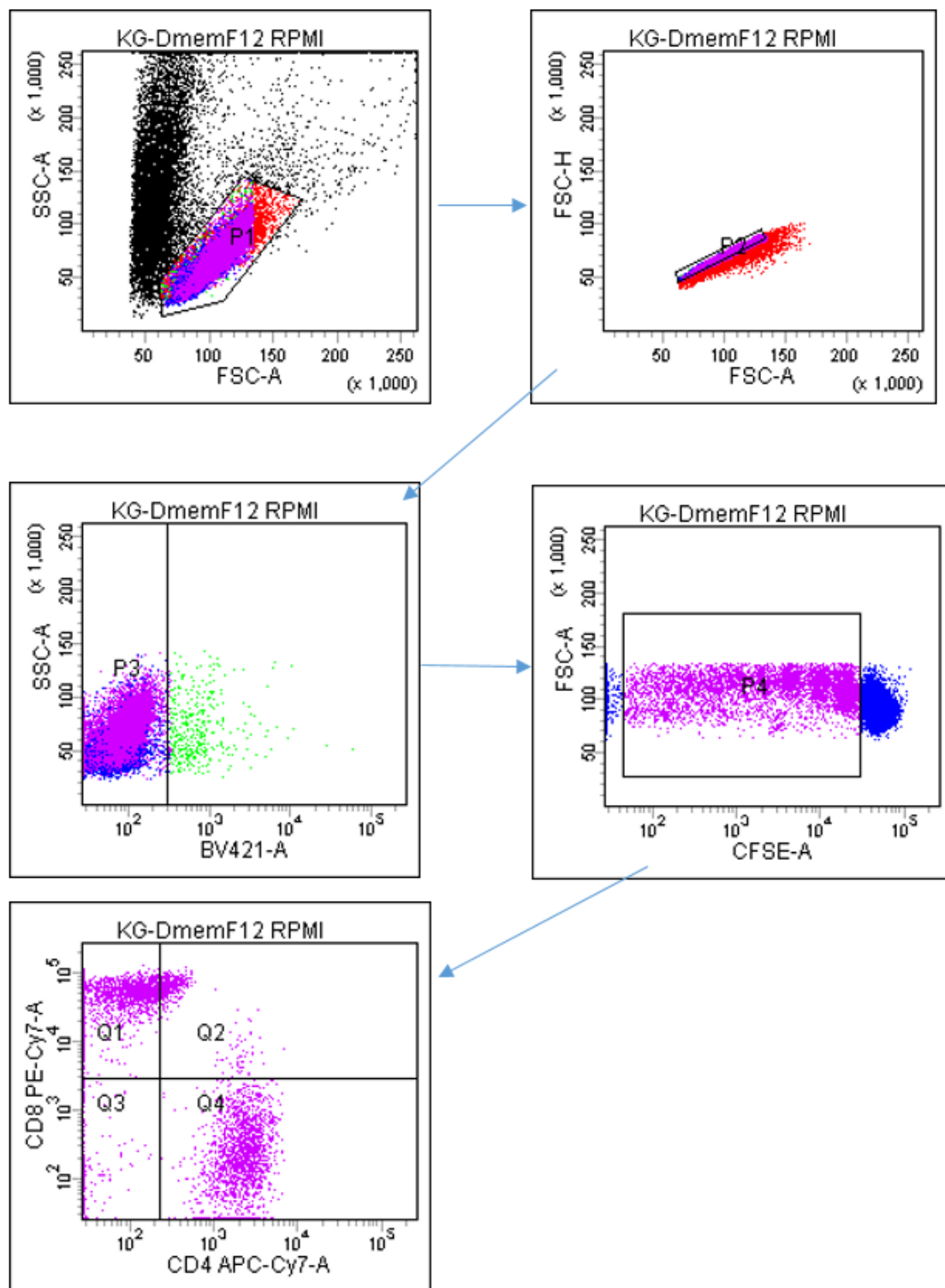


Figure 4.3.4.2.1: Gating of supernatant transfer assay

The image shows how lymphocytes were gated based on their dye retention and antibody staining. Firstly, the lymphocytes are gated based on their known forward and side scatter properties which allows their visual distinction on the forward scatter/side scatter graph. Then singlets are selected which are those that have a proportional forward scatter height and area (reasoning explained in chapter 3). Alive cells are then selected based on their negative DAPI staining, detected in the BV421 channel. Divided cells are then gated round, which are those that do not fully stain with CFSE and have undergone at least one division. Cells are stained with anti-CD4 APC-Cy7 and anti-CD8 PE-Cy7. A graph of anti-CD4 APC-Cy7 against anti-CD8 PE-Cy7 allows data collection on single-stained, double stained and unstained of these populations. Quadrant gates are based on single stained cells, FMOs and isotype negatives as per the methods outlined in chapter 3.

Volunteer	Tube	% divided	Of divided population:			CD4- CD8-
			CD4+CD8+	CD4+CD8-	CD8+CD4-	
1	a	37.6	4.1	36.2	55.5	4.2
	b	19.6	2.9	36.5	52.9	7.7
	c	14.8	1.2	40.8	41.0	17.1
	d	9.5	3.2	39.0	44.3	13.5
	e	7.0	2.9	36.0	43.7	17.3
	f	9.9	4.3	34.8	43.7	17.2
	g	19.8	7.9	32.9	50.6	8.7
	h	40.4	8.3	34.7	50.3	6.7
2	a	58.9	4.2	50.5	30.1	15.2
	b	33.6	2.8	55.5	25.4	16.3
	c	26.5	2.9	54.1	28.9	14.1
	d	2.5	0.0	22.5	16.1	61.5
	e	4.6	1.2	28.5	12.9	57.3
	f	23.2	2.1	61.4	22.5	14.0
	g	40.8	2.7	62.7	27.1	7.6
	h	43.1	3.6	49.8	26.1	20.4
3	a	55.0	1.5	44.3	45.7	8.5
	b	30.4	0.3	25.7	55.7	18.3
	c	20.9	0.1	25.5	51.1	23.4
	d	6.5	0.0	12.1	20.4	67.5
	e	7.6	0.0	19.3	23.2	57.5
	f	20.7	0.2	28.9	47.9	23.0
	g	40.3	0.4	31.9	56.0	11.7
	h	55.2	7.4	40.0	46.7	5.9

Table 4.3.4.2: Table to show amounts of each cell type as a percentage of the parent group.

This table shows the percentage of cells within a parent gate of the subgroup listed at the top of each column. The tube letter indicates the additive used, where:

a – DMEMF12

b – Supernatant from confluent H69 cell culture

c – Supernatant from confluent H69 culture after addition of UDCA

d – Supernatant from H69 cells 1 day after their wash and media-change

e - Supernatant from H69 cells 2 day after their wash and media-change

f - Supernatant from H69 cells 3 day after their wash and media-change

g - Supernatant from H69 cells 5 day after their wash and media-change

h – H69 cell lysate.

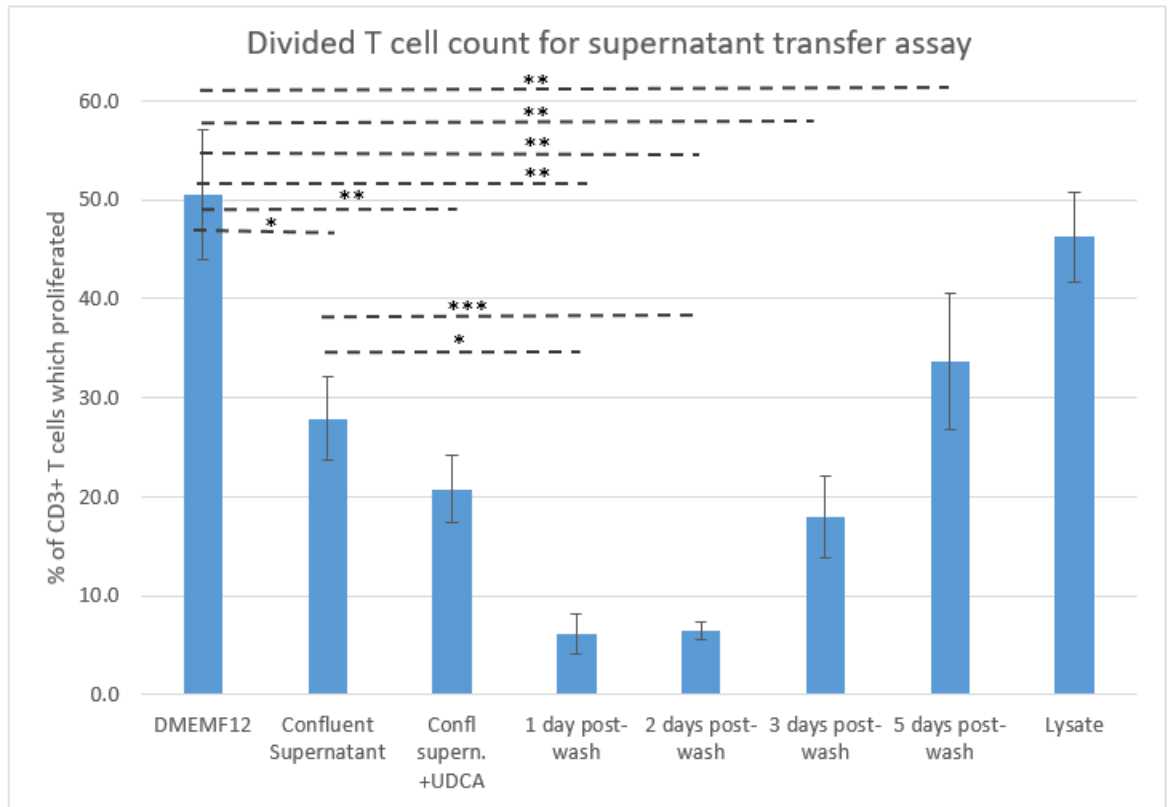


Figure 4.3.4.2.2: Chart to show significantly different results when comparing all conditions to DMEM only and with confluent supernatant
 Bar heights indicate the percentage of CD3+ T cells which proliferated, with different additives shown in the x axis. Significant results from are shown with dashed lines and the denotation of significance by: * - $0.05 > p > 0.01$, ** - $0.01 > p > 0.001$, *** - $0.001 > p > 0.0001$.

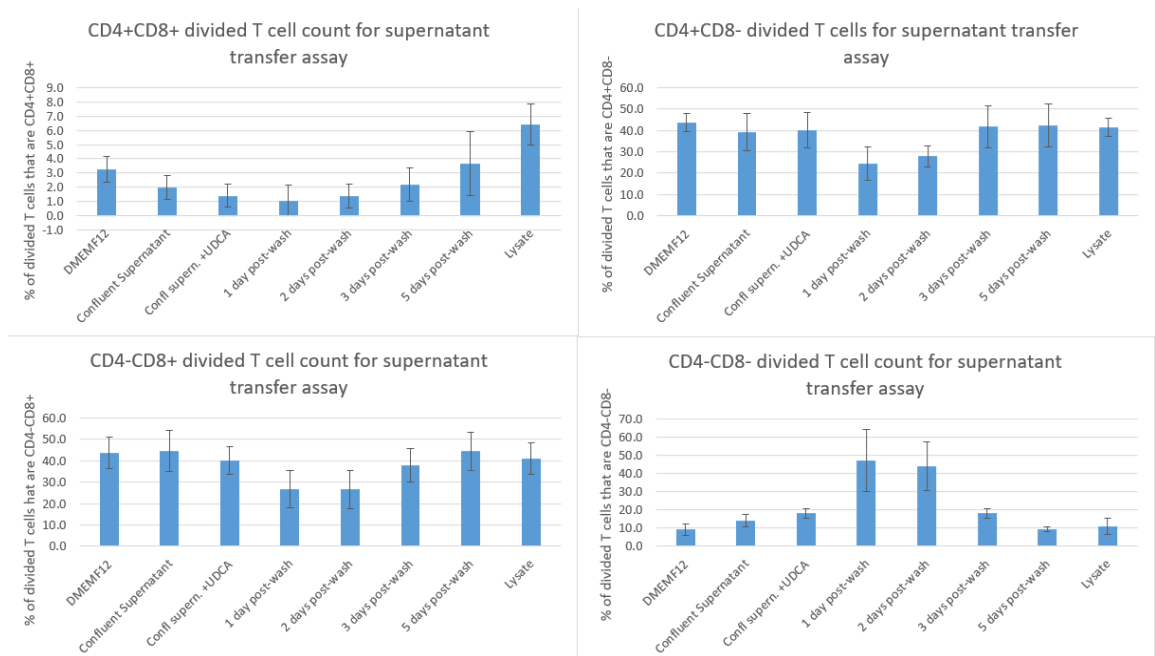


Figure 4.3.4.2.3: Chart to show percentages of divided cells of each of the different T cells investigated.

Bar heights indicate the percentage of each cell type which had proliferated, with different additives shown in the x axis. There were no significant results when comparing to DMDMF12 alone or confluent supernatant.

4.4: Discussion

4.4.1: Aims

The primary aim of this chapter was to investigate if UDCA could be having a direct effect on lymphocytes important in PBC, particularly the T cells. An effect on both proliferation of T cells and also their reactivity to antigen was investigated. The possibility of an indirect effect was also investigated by utilising the supernatant from a cholangiocyte cell line which had been treated with UDCA.

Furthermore, it was hypothesised that UDCA may be having a selective effect on certain subsets of T cells, which may alter the profile of cytokines released which have an influence on isotype switching in the plasma cells. Therefore, a flow cytometry experiment was developed to investigate if UDCA was having a selective effect on different T cell subsets. This data would then be compared with antibody data in chapter 6, which investigates the levels of antibodies of different isotypes, against the common autoantigens in PBC, in the serum of PBC patients.

This chapter also used the cholangiocyte cell line to determine if any effect on proliferation was specific to T cells.

4.4.2: Investigating a toxic effect of UDCA

Apoptosis assays were carried out to investigate a toxic effect of UDCA. The initial apoptosis assay used concentrations up to 300 μ M over 3 days. This assay used carriers of ethanol and DMSO. This was to compare the solubility of UDCA in ethanol and DMSO to decide which carrier to use. The UDCA used is not soluble in water or media.

None of the data in this study suggest that DMSO or ethanol are particularly harmful to cells at the concentrations used and there was no significant difference between apoptosis assay results when comparing DMSO to ethanol (p values not shown). Significantly different results when ethanol is used occur at 0h, 100 μ M (p=0.026) UDCA and 300 μ M (p=0.029), shown in figure 3.1.1. The significant p values at 0h in the ethanol experiment could be attributed to cells having not been mixed thoroughly or some being stuck together from the cell culture practise so that cells are not uniformly distributed in the culture, because after 24h the cell numbers are no longer significantly different regardless of UDCA concentration, so this is more likely a discrepancy relating to the culture of cells rather than toxicity of the drug. However, with DMSO, there is a less explainable pattern of significantly different

results, comparing to carrier alone. The results significantly different from carrier alone include for example at 24h, 100 μ M ($p=0.016$) and 120h, 100 μ M ($p=0.029$), which does not seem sensible given that there was no significant difference at any other time point for 100 μ M UDCA or for higher UDCA concentrations. One explanation could be that DMSO may be less soluble in cell culture medium than ethanol so that there may be pockets of higher concentration of DMSO, having a local toxic effect on the cells in some cases which is affecting the results and giving the significantly different counts. Because of this possibility, ethanol was used as the UDCA carrier for all further experiments involving the dissolving of UDCA.

4.4.3: Investigating an antiproliferative effect of UDCA on T cells

Although there is some data in the literature which suggests that cholangiocyte proliferation may be attenuated in the presence of UDCA (Munoz-Garrido *et al.*, 2015), no such study has been carried out on lymphocytes thought to be of importance in PBC, such as the T cells.

Figure 4.3.3.1 shows that at increasing concentrations of UDCA, there are fewer cells proliferating into beyond the second division and figure 4.3.3.2 indicates significantly less proliferation between 300 μ M UDCA and carrier alone. This is novel preliminary evidence to suggest that UDCA may be having a direct effect on the proliferation of T cells. Section 1, Introduction, of this chapter outlines potential clinical relevance of an antiproliferative effect of UDCA on T cells.

Following on from this, an assay was devised which would be able to differentiate the T cell sub-sets, such that CD4⁺ T cells, Th1, Th17, Th2, Th1/Th17, CD8⁺ T cells, Tc1, Tc2, Tc17, Tc1/Tc17, Treg cells and CD45RO⁺ Tregs could be counted as populations and compared. The generation of this assay is described in chapter 3. Notable findings include significantly less proliferation in CD8⁺ T cells in response to UDCA, but also some data suggests that CD4⁺ may also be relevant. The experiment uses 2 tubes per volunteer, one for examining an effect on CD4⁺ and CD8⁺ T cells and another for examining Tregs, using a CD4⁺ marker. In the CD4⁺/CD8⁺ tube, there did not appear to be an impact on the proliferation of CD4⁺ T cells ($p=0.24$), however in the Treg tube a significant attenuation of proliferation of CD4⁺ T cells was detected ($p=0.008$). Therefore, in this study there is evidence to suggest an antiproliferative effect of CD4⁺ T cells by UDCA but it is only sometimes detected. There are differences between the 2 tubes which could account for the discrepancy. The Treg tube uses a fixation technique not applied to

the other tube; the Treg tube does not make use of the DAPI dye; the Treg tube does not use a CD8+ identifier. The fact that no CD8+ identifier was used in the Treg tube means that the effect identified could apply to all T cells, not just CD4+. The DAPI dye is not used in the Treg tube, meaning cells are gated on the lymphocyte population, not the live lymphocyte population, so it cannot be known if this effect would be detectable within the live population. However, no significant effect of increased UDCA on live cell percentage was found in the other tube. The discrepancy could be where examining the live and dead cell population, there will be less recorded proliferation of all cells as the dead cells will not proliferate, so any effect on proliferation of a population caused by UDCA may seem exaggerated due to the inclusion of dead cells. To surmount this, a dead/live cell identifier which is compatible with the fixation/permeabilisation could be used instead of DAPI, and in both tubes. Some examples of these are Thermofisher Fixable Violet stain and Fixable Aqua stain, which use the BV421 and BV510 channels respectively, so this should not involve re-compensation of all dyes, none of which are in these channels. CD8+ T cells showed significantly less division in the presence of higher concentration of UDCA compared with the carrier of 0.3% ethanol alone. There was also a significantly larger proportion of CD8+ Tc2 T cells within the divided CD8+ population at 0.25mM UDCA compared with carrier alone ($p=0.03$). This could be suggested to indicate that this sub-population of CD8+ T cells is more resistant to the anti-proliferative effects of UDCA than other sub-types. Tc2 cells, or type 2 cytotoxic T cells, are involved in activation of dendritic cells. Like Th2 cells, Tc2 cells secrete IL-4 and IL-5 and so may be involved in related functions such as stimulating B cell immunoglobulin isotype switching to IgE and recruiting eosinophils, which combat infections such as multicellular parasites (Kemp *et al.*, 2005).

However, the Tc2 population is extremely small with the difference only increasing in terms of percentage of live lymphocytes from 0.148% to 0.176% (averages) or 0.87% of divided CD8+ T cells to 2.3% (averages). Therefore, any effect on these cells by UDCA is unlikely to show a large phenotypic difference compared with the action of other cells.

There was no difference seen in proliferation of any of the Th subsets in the presence of UDCA compared to vehicle alone. Although unlikely, it is possible that with a more highly powered study small differences may become significant. The volunteers available happened to be male and female and of vastly different ages, therefore their T cell subset blood levels could be influenced by age or gender, therefore a future study should involve sufficient volunteers to determine if there are

any fundamental differences between these groups. One study has shown a positive correlation between CD4+/CD8+ ratio and age and also a greater normal CD4+/CD8+ ratio range in males than females (Jentsch-Ullrich *et al.*, 2005), therefore a further study should be powerful enough to account for these differences.

Overall, the study investigated an effect on proliferation of T cells by UDCA and found a differential proliferation effect on T cell subsets, this data is interesting although not completely conclusive. This study is the first to investigate an antiproliferative effect of UDCA directly on T cells and shows promising evidence. A more thorough study is required to further underpin the types of T cell affected by UDCA in this way. The assay should involve different groups of individuals such as males of a young age group, males of an older age group, females of a younger age group, females of an older age group. This would mean that an age effect on the normal T cell profiles could be investigated while also investigating a differential effect on the proliferation of T cell subsets in an age and gender controlled manner. The groups should contain more individuals for a more highly powered study. Furthermore, any findings from this experiment should be confirmed by a Western blot staining for the extracellular proteins which identify these T cell sub sets or by RTqPCR of the T cells, to investigate proteins produced which would imply their subsets.

4.4.4: Investigating an impact of UDCA on the reactivity of T cells in the ELISpot assay

The ELISpot assay aims to mimic the environment in which lymphocytes release cytokines in response to a stimulus in a way that allows detection and quantification of the release of cytokines. This assay can be manipulated to provide different conditions to determine if the ability or inclination of a cell to respond to a stimulus is different depending on these conditions. In order to investigate if UDCA has an effect on a T cell's ability to respond to antigen, a series of ELISpot assays were carried out on PBMCs from healthy volunteer blood and these were manipulated by using the absence or presence of various antigens, and different UDCA concentrations were investigated.

Furthermore, to determine if any effect of the drug is due to toxicity or possibly a direct inhibition effect, a flow cytometry experiment was carried out on cells collected from the ELISpot assay and stained with DAPI to investigate the percentages of

alive and dead cells. It was found that there was no more death in cells at higher UDCA concentrations in the context of the ELISpot, when using the anti-CD3 mitogen therefore any difference in response to antigen at difference concentrations of UDCA is likely to be due to an inhibition effect of UDCA on the ability of the T cell to react to antigen. However, at 1mM UDCA, when cells are not stimulated, there were significantly more dead cells identified ($p=0.012$). In light of this discrepancy between stimulated and unstimulated cells in the ELISpot assay, it could be suggested that UDCA is more toxic to cells at rest than it is to active cells. One possible explanation for this may be an increased accumulation of the drug inside the resting cell and not the fast-dividing cell, however for this study it may be assumed that 0.5mM is the highest concentration investigated at which UDCA is not toxic to cells in the context of the ELISpot.

The PBMCs only remain in the assay for 18-20h. A rapidly dividing human cell may take approximately 24h to divide (Yoon *et al.*, 2010) therefore the ELISpot likely is not concerned with the division of T cells and only the reaction to antigen.

All ELISpots were carried out using the capture antibody for IFN- γ , therefore all results obtained are analysed with respect to cells which release IFN- γ in response to the antigen in question. Therefore, this study is concerned with helper T cells, with a particular interest in Th1, and also cytotoxic T cells.

When the ELISpot was carried out using an anti-CD3 mitogen to induce response in the T cells, it was found that there were significantly fewer cells reacting when the UDCA concentration was 0.5mM ($p=0.002$, table 4.3.2.2.4). However, when common antigens likely encountered by most healthy individuals were used to stimulate the T cells in a more realistic way, this significance was not apparent (table 4.3.2.2.6). Those common antigens used were cytomegalovirus (CMV), Epstein Barr Virus (EBV) and salmonella. Although use of a common antigen is a more realistic way to stimulate T cells, different test antigens were used on each individual. In this study, there were a small number of individuals available and a small panel of test antigens, therefore a best antigen for each individual had to be established. Response to different antigens is always different, particularly between different individuals, therefore this may explain why there was no significance with the realistic antigen when the result was apparent with the anti-CD3 mitogen. A future study should use more volunteers and a larger panel of antigens in order to establish one common antigen to which all of the volunteers respond in a similar way and this ELISpot should be repeated. This is more likely to give an accurate

result. The fact that a significant difference was apparent with the anti-CD3 mitogen is evidence to suggest that there is an inhibition effect of UDCA on the ability of the T cells to react to antigen and therefore it should be further investigated. Given that this is the highest dose which did not indicate a significantly toxic effect on T cells, it may otherwise be that UDCA places T cells under stress and leaves them less able to respond to stimulus.

4.4.5: Investigating an anti-proliferative effect of UDCA on a cholangiocyte cell line

An xCELLigence assay was carried out to investigate an effect on proliferation of the cholangiocytes by UDCA. The cholangiocyte cell line H69 was used. The H69 cell line is an immortalised cell line originally isolated from a liver harvested for transplantation, which has been transformed with simian vacuolating virus 40 to allow for continuous replication by suppression of cell death regulator p53 (Grubman *et al.*, 1994).

Flow cytometric analysis is not usually carried out to measure proliferation of adherent cells, but the xCELLigence assay can be used instead. The xCELLigence assay uses a gold plate with a voltage applied across it. A change in the ion concentration, which occurs when there is cellular proliferation, is detected by electrical impedance in the electrodes and this change is measured by the software (Ucran *et al.*, 2010).

Some evidence in the literature suggests that there may be an anti-proliferative effect on cholangiocytes by UDCA (Alpini *et al.*, 2002). This group compared the numbers of cells expressing proliferating cell nuclear antigen (PCNA) which is an intracellular DNA scaffold protein and its presence is indicative of DNA replication, therefore cell proliferation. They found significantly less PCNA in the cholangiocytes of rats fed with UDCA or TUDCA than those of the control rats. Additionally, apoptosis was not found to be increased in those rats fed UDCA or TUDCA (Alpini *et al.*, 2002). In accordance with this literature, the study in this chapter which investigates an antiproliferative effect using xCELLigence shows significantly less cholangiocyte proliferation at UDCA concentrations above 0.25mM as shown by the low index line in figure 4.3.4.1.1, low area under curve value in figure 4.3.4.1.2 and significant p values of 0.031 for 0.25mM, 0.004 for 0.5mM and 0.026 for 1mM. This data, although produced from only a single experiment, is useful as it not only supports that seen in the literature (Alpini *et al.*, 2002) but also reflects that seen

from our own T cell proliferation experiments, indicating that UDCA may have an anti-proliferative effect on a number of different cell types. To further confirm this, other unrelated cell types could also be investigated for an antiproliferative effect due to UDCA presence and potential mechanisms of this effect could be investigated.

4.4.6: Investigating an indirect effect of UDCA on the proliferation of T cells

To further investigate the effect of UDCA on the cholangiocytes and the role of T cells, a supernatant transfer assay was carried out to examine if metabolites or other compounds released by cholangiocytes in response to UDCA presence, could then itself affect proliferation of T cells. T cells were cultured in 50% H69 media for the control and H69 supernatant from various cultured of H69 cells and the proliferation was compared by flow cytometry, gated shown in figure 4.3.4.2.1. Figure 4.3.4.2.2 shows a significant difference between proliferation in DMEMF12 alone and 1, 2, 3 and 5 days after H69 wash post-UDCA treatment ($0.01 > p > 0.001$), however there also appears to be significantly less proliferation when just confluent H69 media is used without any UDCA treatment ($p < 0.05$), indicating that H69 cells may normally release a molecule which attenuates T cell proliferation. This is not completely surprising: although there is little in the literature to confirm this, one study has shown that healthy biliary epithelial cells BECs can regulate T cell proliferation both in a contact-dependent and contact-independent manner (Kamihira *et al.*, 2004). The study also suggested that BECs release prostaglandin E2 (PG-E2), controlled by IL-1 β and TNF- α and known to suppress T cell signalling, which is the factor responsible for the attenuation in T cell proliferation (Kamihira *et al.*, 2004). In order to investigate if there is an additional effect on T cell proliferation to do with UDCA treatment, the effects of supernatants post-wash on T cell proliferation were then compared with the confluent H69 media-containing cultures. Figure 4.3.4.2.2 shows that using H69 supernatant from culture from 1 and 2 days after wash post-UDCA treatment, there is less T cell proliferation than using confluent H69 culture (1 day – $p < 0.05$; 2 days – $0.001 > p > 0.0001$). Data from this experiment suggests that H69 cells, which can be used as a model for BECs (Grubman *et al.*, 1994), release a component, possibly PG-E2 based on the Kamihira study, which causes a decrease in T cell proliferation but also then if the H69 cells have been treated with UDCA, then there is an even greater effect. Furthermore, this effect can last for up to 2 days

post-UDCA exposure. This is evidence to suggest a new mechanism of action for UDCA.

4.4.7: Conclusion

This study has produced interesting data which suggests that UDCA may have an effect on cellular proliferation of a different cell types and activation of CD4⁺ T cells. Further experiments are required to confirm these finding and to elucidate futher the differential effect on different T cell subtypes. If any differences in the effect of UDCA on proliferation of T cell subtypes is found it may help to further our understanding of how UDCA elicits its effects in PBC patients. Further experiments which then investigated the mechanisms by which this effect is mediated, and if there is a difference in this effect between responders and non-responders, would help to elucidate phenotypic differences between these patient groups.

4.4.8: Further work

This chapter gave little to suggest a differential impact of UDCA on CD4+T cell subsets, however, as the data suggests a CD8+ importance, the panel could be redesigned to investigate CD8+ subsets rather than CD4. This could include focus on CCR7 and CD45RA to help identify naïve(CCR7+CD45RA+), central memory(CCR7+CD45RA-), effector(CCR7-CD45RA+), effector memory(CCR7-CD45RA-) CD8+ T cells to determine if there is a differential effect of UDCA on these subsets (Maecker *et al.*, 2012).

Additionally, the inclusion of a fixable live/dead stain such as ThermoFisher Live/Dead Fixible Aqua or Violet stain (using channels BV510 and BV421 respectively) would allow for live/dead analysis of cells in the Treg tube. Additionally, this panel could be applied for use on patient peripheral T cells before and after significant UDCA usage for a more accurate determination of if the drug usage has an effect on the population of T cells.

It has been suggested that prostaglandin-E2 is released by BECs which can cause a decrease in T cell proliferation by inhibiting the T cell receptors (Kamihira et al., 2004). Combined with the supernatant transfer assay data from this chapter, this raises the question of if it is this same substance which is causing the further decrease in proliferation apparent when H69 cells have been incubated with UDCA or if UDCA stimulates the release of another compound which could be causing the

further decrease in T cell proliferation. To answer this question, a metabolomics experiment could be carried out on the supernatants collected and frozen from the transfer assay in this chapter. This would involve gas chromatography-mass spectrometry on the supernatants where the analytes are separated and compared to a size standard of known metabolites. This could identify the compound of interest, or could confirm increased levels of prostaglandin-E2 in the samples from UDCA-treated H69 cells.

4.4.9: Limitations

ELISpot assays were carried out using capture antibodies against other cytokines, such as IL-17, IL-5, IL2, IL15 (data not shown as spots were not countable for their tabularisation). However, these led to blackouts as plate optimisation was not effectively carried out beforehand. When experimenting with a new capture antibody, the cell number must be carefully titrated beforehand to obtain a range of cell concentrations in which plenty spots are visible, which reduces error in the data, but also not so many that they merge together making them uncountable. In this instance it was not possible to optimised prior to the experiments being performed as due to cost constraints there were insufficient reagents available to both titrate the plates or carry out the experiments. Therefore, the risk was taken to carry out experiments using estimated values. Future experiments would repeat all successful ELISpots carried out in this study and carry out those highlighted for future work but using new capture antibodies as well, such as IL-17, IL-5, IL-2, IL-15. This would allow the assay to be carried out in the context of smaller populations of cells such that the effects in question on different T cell subtypes can be compared.

Prior to this study, many possibilities for the effect of UDCA have been investigated, such as protection of cholangiocytes against apoptosis (Benz *et al.*, 1998), an immunosuppressant effect in new tissue grafts (Zhang *et al.*, 2009), increased expression of ion exchange proteins and multidrug resistance proteins on the canalicular surface (Beuers *et al.*, 2001). However, this is the first study to investigate in such depth an effect of UDCA on the proliferation of T cells both direct and indirect.

This study has uncovered more than one potential effect of UDCA on not only on the isolated T cells but also the T cells within the PBMC population. A control substance for UDCA was, however, not established. A control substance is used to

compare the compound of interest to a similar exogenous substance. It is used to investigate if there is an element of the documented effect which may be due to toxicity, or a property which could be present in many substances and is not necessarily unique to the compound being used. As this is one of the first studies to explore a direct effect on T cells of UDCA, it is difficult to predict which property/properties of UDCA is/are causing the effects on T cells uncovered in this study and if there could be similar compounds which could have similar effects.

Chapter 5: The development of an ELISA assay using End Point Titre to compare serum levels of anti-PDC autoantibodies in UDCA responder and non-responder PBC patients.

Abstract

Evidence suggests that within the population of patients with Primary Biliary Cholangitis (PBC), there are subgroups of patients with different forms of the disease with different severities and showing different blood biochemistry, notably those who respond to UDCA, 'responders,' and those who do not, 'non-responders'. This chapter outlines optimising and testing the validity of autoantigen specific indirect end point titre enzyme-linked immunosorbent assays for their use in measuring antibody levels in PBC patients and healthy volunteers. End point titre ELISAs were used to investigate the magnitude of IgG antibodies against common autoantigens in PBC. These were then compared with values obtained by initial screening the serum for these antibodies to determine if by screening would be an adequate representation of the calculated end point titre. Results were compared by Spearman's Rank correlation. The results from this chapter will be brought forward into the next chapter for statistical analysis. Any differences found may further elucidate the mechanism behind the sub-grouping apparent in this disease and can help pave the way for more stratified treatment approaches.

5.1: Introduction

5.1.1: Common autoantigens in PBC

The common autoantigens in PBC are discussed in more detail in chapter 1 and further on in of this chapter. The most common autoantibodies in PBC are those against E2 and E3BP subunits of Pyruvate dehydrogenase complex (PDC) (Harriman *et al.*, 1998) (Jones, 2000) (Dedobbeleer *et al.*, 2017). Further studies have narrowed down the most commonly recognised epitope to be a region within the E2ILD binding region but also highlighted the importance of other less common autoepitopes within the E2 subunit of PDC (Suhr *et al.*, 1990). The subunits of E2 and E3BP are very similar in structure and sequence, with a further study characterising the similarity between the dominant PBC autoepitope from E2ILD with a region within E3BP which both contain a lipoyl domain (Todryk *et al.*, 2009). Therefore, it is possible that autoantigens could bind both epitopes due to epitope spreading. Figure 5.1.1 shows the similarity between the ILD autoepitope of E2 and the corresponding lipoyl domain of E3BP.

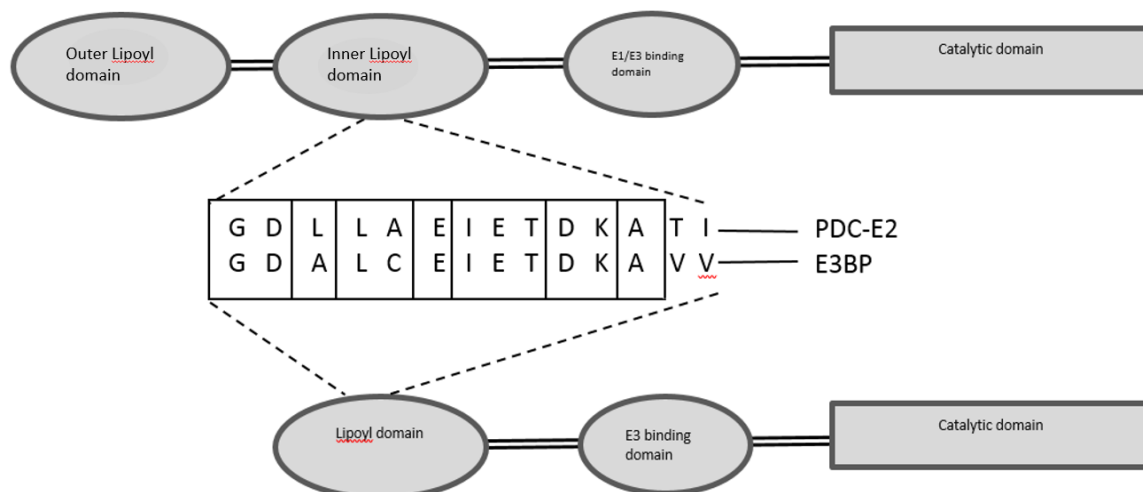


Figure 5.1.1: Domain diagram of PDCE2 and PDCE3BP to compare lipoyl domain autoepitope sequences.

Adapted from 'T cell responses to the putative dominant auto-epitope in primary biliary cirrhosis (PBC),' (Palmer *et al.*, 1999), this figure depicts a key region from within the ILD of E2 and the corresponding region of E3BP. The sequences are identical except for 2 residues: a Leucine/Alanine and an Alanine/Cysteine.

5.1.2: Isotypes and class switching

Briefly; to test for PBC, the AMA-M2 ELISA panel is used to detect anti-mitochondrial antibodies of the IgG isotype (Han et al., 2017) (section 5.1.3.5: AMA). In this study, the presence of various isotypes of patient antibody against the autoantigens is investigated. Cytokines released by CD4⁺ T cells can influence a plasma cell to undergo isotype switching, causing it to release a different isotype of antibody which still recognises the same antigen (Yu et al.). Chapter 4 postulates a selective effect of UDCA, the common therapy for PBC, on different subsets of T cell. Additionally, it has been heavily argued both within this work and also in the literature that PBC likely consists of different subsets, possibly with different biological underpinnings (Carbone et al., 2013). Some evidence from a genome-wide association study (GWAS) which may indicate a T cell influence to PBC is outlined below.

5.1.2.1: Known isotype switching influence by T cell subsets

It has been well-documented that some cytokines directly released by CD4⁺ T cells can directly affect isotype switching in B cells (Toellner et al., 1998). Furthermore, even very early on after differentiation, some T cells can be already influencing the antibody profile, therefore suggesting the T cell influence is of high importance to the antibody isotypes produced by B cells (Toellner et al., 1998). It is important to note, as outlined in the general introduction, that helper T cell CD40L binding to B cell CD40 is required to prime the B cell for T cell-dependent isotype switching. Although there is considerable variability within CD4⁺ T cell subsets, a general summary of the influence of each major subset is described below.

Th1

Th1 cells release IFN- γ favours an IgG3 isotype in terms of its influence on class switching, and can downregulate IgG1 and IgE (Abbey and O'Neill, 2008).

Th2

Th2 release cytokines IL-4, IL-5 and IL-13, known to affect isotype switching. IL-4 has been shown to predominantly cause switching to the IgE isotype but may also influence switching to IgG1 (Lebman and Coffman, 1988a). When there is IL-4 and IL-13 together, isotype switching can favour both IgG4 and IgE (Gascan et al., 1991). IL-5 has been shown not to cause isotype switching but to cause maturation of IgA-positive B cells into IgA-secreting B cells (Harriman *et al.*, 1998).

Th17

The effect on isotype switching by Th17 cells is not generally well-understood. However, a study which co-cultured Th17 cells with B cells and measured isotypes production in response to Th17 cytokines has suggested that IL-17 on its own favours IgG3, whereas together with Th17-released IL-21, favours IgG1 (Mitsdoerffera et al., 2010).

Treg

Treg cells release IL-10 and TGF- β . IL-10 is known to induce class switching to IgG1 and IgG3 (Fujieda et al., 1998) or together with TGF- β , IgA1 and IgA2 (Zan et al., 1998).

TFH

Follicular B cell helper T cells (T_{FH}) express IL-21 which has been shown to predominantly cause isotype switching to IgG1 (Mitsdoerffera et al., 2010).

IL-6, released by macrophages, dendritic cells and B cells but also some epithelial and endothelial and some other non-haematopoietic cells, has been shown to act antagonistically to IFN- γ in that it can prevent IFN- γ mediated reduction in IgG1, but also is mediated by IL-21 to enhance a Th2 response phenotype (Dienz *et al.*, 2009).

5.1.2.2: Functions of different antibody isotypes

The different antibody isotypes have different abundances, distributions and functions in the body. IgM is either used in monomeric form as part of the B cell receptor or is secreted in pentameric form. Membrane-bound IgM functions in combination with invariant proteins Ig α and Ig β to form the B cell receptor, with the IgM functioning as the detector of antigen and the accessory Ig portions associating with IgM heavy chains to transport it to the cell surface and transduce the signal intracellularly. Secreted IgM is pentameric, giving rise to multiple possible binding rendering it particularly useful for activating the complement system.

IgD forms the antigen recognition subunit of the BCR on naïve B but can also be secreted. IgD binds epitopes of low surface density on the target cell. IgD is able to bind basophils and mast cells to induce production of antimicrobial peptides.

IgG has 4 subtypes denoted 1-4 based on their abundance. IgG3 has the greatest functional potency, followed by IgG1 and then IgG2 and IgG4. IgG antibodies are particularly adapted for diffusion into extravascular sites. All IgG subtypes have the potential to neutralise pathogens. Particularly IgG1 and IgG3 are able to sensitise NK cells for killing of a pathogen and they are also able to sensitise mast cells (Lu *et al.*, 2017).

IgA is present in the serum in monomeric form and the mucosa in dimeric form. It is particularly effective for transport across epithelium and diffusion into extravascular sites (Lu *et al.*, 2017).

IgE is associated with a Th2 response and is able to sensitise mast cells. IgE is associated with allergies and parasite infection (Lu *et al.*, 2017).

5.1.3: Potential for genetic differences between groups

A genome-wide association study (GWAS) was carried out which identified key at-risk alleles in PBC and other autoimmune liver diseases. Many of the loci of interest in PBC were those within genes involved in T cell maturation and signalling, including STAT4, IL-12RB2, IL-12A, CD80, IL-7R, CXCR5 (Mells *et al.*, 2013). The natures of the mutations in terms of their effect on their protein function were not outlined in the study and in addition no study has yet been carried out to determine any possible categorisation of the mutations in the context of responder/non-responder sub grouping. However, they do highlight pathways which may be of interest in PBC pathogenesis and there could be responder/non-responder differences.

Of particular interest, IL-12RB2 and IL-12A are both also involved in the differentiation of naïve T cells to Th1 in response whereby IL-12RB2 is a subunit of the IL-12 receptor and IL-12A is p35, the subunit of IL-12 not shared with IL-23 (Lupardus and Garcia, 2008). STAT4 is the transcription factor involved in mediating the response of IL-12 in the Th1 cell (Varikuti *et al.*). Th17-directing IL-23 shares a subunit, p40, and also a receptor subunit, IL-12R β 1, with IL-12, therefore the ratio of Th1/Th17 cells there are in the environment depends in part on the ratio of p35/p19, the IL-12 and IL-23 specific subunits, associating with p40 (Lupardus and Garcia, 2008). Th17 cells have been associated with advanced PBC and are thought to be proinflammatory in autoimmune diseases (Tabarkiewicz *et al.*, 2015). Any loss of function mutation in STAT4, IL-12A or IL-12RB2, could then cause a Th17 skew, potentially leading to a more aggressive disease. If any of these hypothesised genotypes is specific to responders or non-responders, it would likely be the non-responding population, as the non-responders have an overall more progressive and fast-advancing disease (Carbone *et al.*, 2013). It is difficult to detect increased Th17 activity by isotype switching, as Th17 cells have not been shown to directly affect B cell isotype switching, however some studies in mice have shown that IL-17 and IL-21, released by Th17 cells, may cause isotype switching to IgG2 α and IgG3; IgG2 β and IgG1 respectively.

A Th1-dominant T cell population may be expected to show increased IgG2 α but possibly also IgG3, and possibly also lower levels of IgG1 and IgE (Mitsdoerffera et al., 2010). A Th17-dominant T cell population may be expected to show higher levels of IgG2 β and IgG1, or possibly increased IgG2 α and IgG3, depending on which cytokines are released (Mitsdoerffera et al., 2010).

IL-7R, a gene encoding a receptor subunit for IL-7, is important for B and T cell development, but is also involved in V(D)J recombination in both T and B cells (Hamel et al., 2014). A study has shown that IL-7 may, in the presence of T cells, cause isotype switching to IgE and IgG4, therefore increased IgE or IgG4 in one group compared with the other may suggest it is worth investigating the possibility of a gene variant in IL-7R which may genetically distinguish the groups (Jeannin et al., 1998).

CD80, although expressed on dendritic cells, activated B cells and monocytes, is important for T cell activation and survival as it provides a co-stimulatory signal for the TCR/CD3 interaction (Matsumoto et al.).

T_{FH} cells are an example of cell that expresses CXCR5. This cytokine is important for migration into B cell follicles in lymph nodes where the TFH cells induce maturation of B cells to antibody-secreting or memory B cells (Mitsdoerffera et al., 2010). T_{FH} predominantly secrete IL-21 which encourages isotype switching to IgG1 (Spolski and Leonard, 2010).

From all of the above information, it is possible that different patients present different isotypes of antibody against autoantigens within the PBC population potentially due to influence of cytokines produced by CD4⁺ T cells. Therefore, the presence of isotypes IgG (and its subtypes of IgG1, IgG2, IgG3 and IgG4), IgA, IgM and IgE will all be investigated in this study.

5.1.4 The ELISA assay

5.1.4.1: Indirect ELISA

ELISA is an assay which can measure levels of a biomarker such as a protein, peptide, hormone or antibody in a given substance. Detection and measuring of the response is facilitated by the detection antibody conjugated to an enzyme which, when the correct substrate is added, gives a coloured product, the intensity of which is read in a plate reader and displayed on relevant software. The detector antibody conjugate and necessary substrate can vary. In the case of this chapter, levels of antibody are being investigated in

patient serum. The indirect ELISA, depicted in figure 5.1.4.1, is most appropriate because it offers 2 levels of specificity: specific binding of the target molecule (serum antibodies) and their specific detection (Wang et al., 2017) whereas other methods such as the direct ELISA do not, and so are more prone to non-specific binding and background (Chughtai et al., 2017).

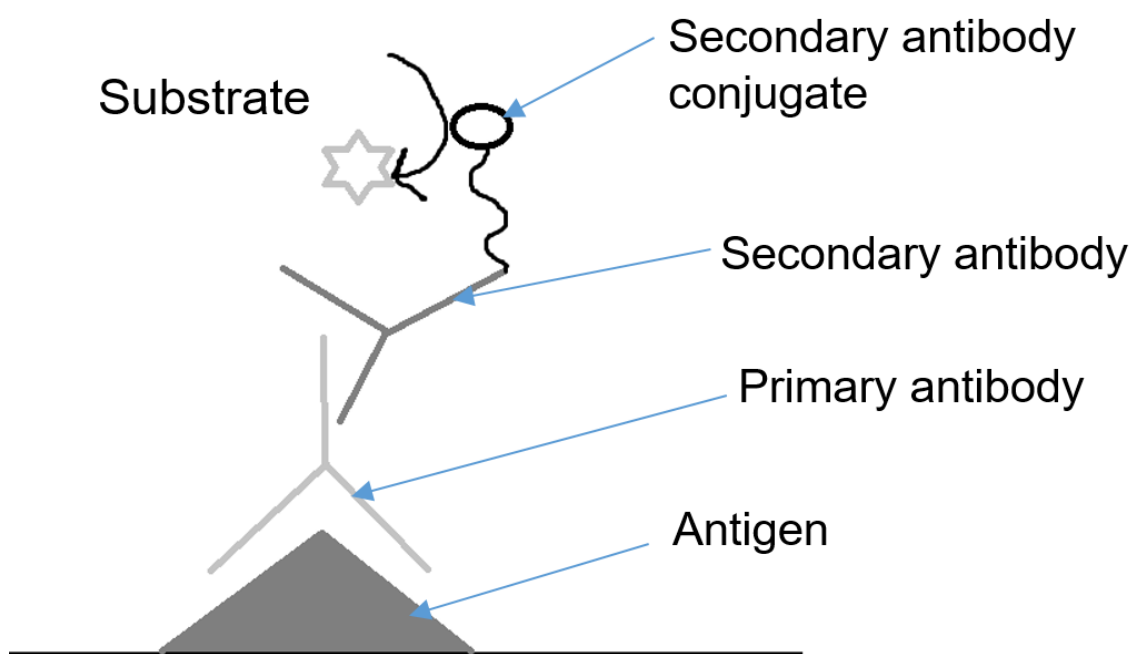


Figure 5.1.4.1: Diagram of the indirect ELISA

This diagram shows an illustration of the molecules making up the indirect ELISA in place where presence of the primary antibody is the antibody being detected. The antigen is fixed to the well bottom surface.

5.1.4.2: End point titre ELISA

Usually, in an ELISA assay, standard samples will be included. These contain the molecule of interest at known concentrations so that the absorbance values from the test wells can be compared with absorbance values from the standard wells on a graph to determine the concentrations of the molecule of interest in the test wells (Whitehead et al., 2017). For experiments conducted in this study, a size-standard was not available therefore, the alternative method, the end point titre method, was used. The end point titre is arguably more accurate as the result is an estimation calculated from several test result points rather than one comparison to one size standard (Dey et al., 2008).

If the protein coating concentration is kept the same, as the sample is diluted, there is a specific corresponding absorbance pattern which can be plotted on a graph. Illustrated in figure 5.1.4.2.1, as the dilution factor increases, initially there is no change to the absorbance reading. This is because the equipment is only able to measure absorbance values up to a limited intensity, but also the sample may be so concentrated that all of the capture protein molecules on the well floor are completely saturated with antibody, so any additional antibody is washed away and is not read. This is shown by the initial plateau on the graph and is the first limitation. The next stage is the linear region where the capture protein becomes unsaturated because the concentration of the antibody in the sample no longer exceeds the capacity of the protein coating. In this region, ever increasing dilution gives a corresponding ever decreasing absorbance reading, as there are fewer subsequent detector antibodies to provide the output read as the absorbance reading, labelled 'linear region' in the graph (Kannian et al., 2007). Then there is another plateau where the antibody is diluted such that the signal is no longer distinguishable from background absorbance, illustrated as the second plateau in the graph, so ever-increasing dilution factors give no effect on the absorbance value. This is another limitation of the assay.

In order to carry out the end point titre ELISA, the linear region is of key importance because this is where there is a proportional relationship which can be exploited for predictive calculations (Dey et al., 2008). If there was no limitation in the capacity of the equipment to measure absorbance values based on dilution, this linearity would be apparent throughout the graph line. As the concentration of the antibody cannot be directly measured or inferred in the capacity of this study, there is another method used to directly compare relative amounts of antibody within samples. If there were no limitations described above, then theoretically, a sample could be diluted down until a zero absorbance value is reached (Miura et al., 2008). Therefore, the amounts of dilution required for each sample to reach this zero-absorbance value can be compared between samples and are directly related to the amount of antibody in the sample. The amount of dilution required to achieve this hypothetical zero absorbance value is the end point titre (Dey et al., 2008). Calculation of the end point titre is illustrated in figure 5.1.4.2.2, there the axis have been switched such that the graph resembles the form $y=-mx+c$. The y intercept, where $x=0$, then corresponds to the hypothetical zero absorbance value (Frey et al., 1998).

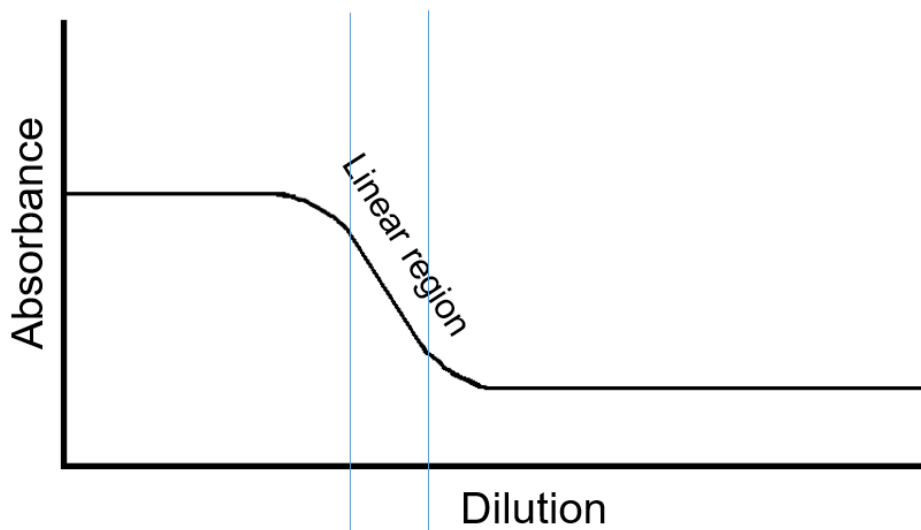


Figure 5.1.4.2.1: Illustration of a graph of dilution of sample against absorbance reading for end point titre ELISA.

The illustration depicts the normal curve established when increasing dilutions of sample are plotted against ELISA absorbance readings. There are 2 plateau regions, representative of limitations of the assay, and one linear region, labelled, representative of an inverse proportion relationship between the dilution of the sample and the absorbance read value.

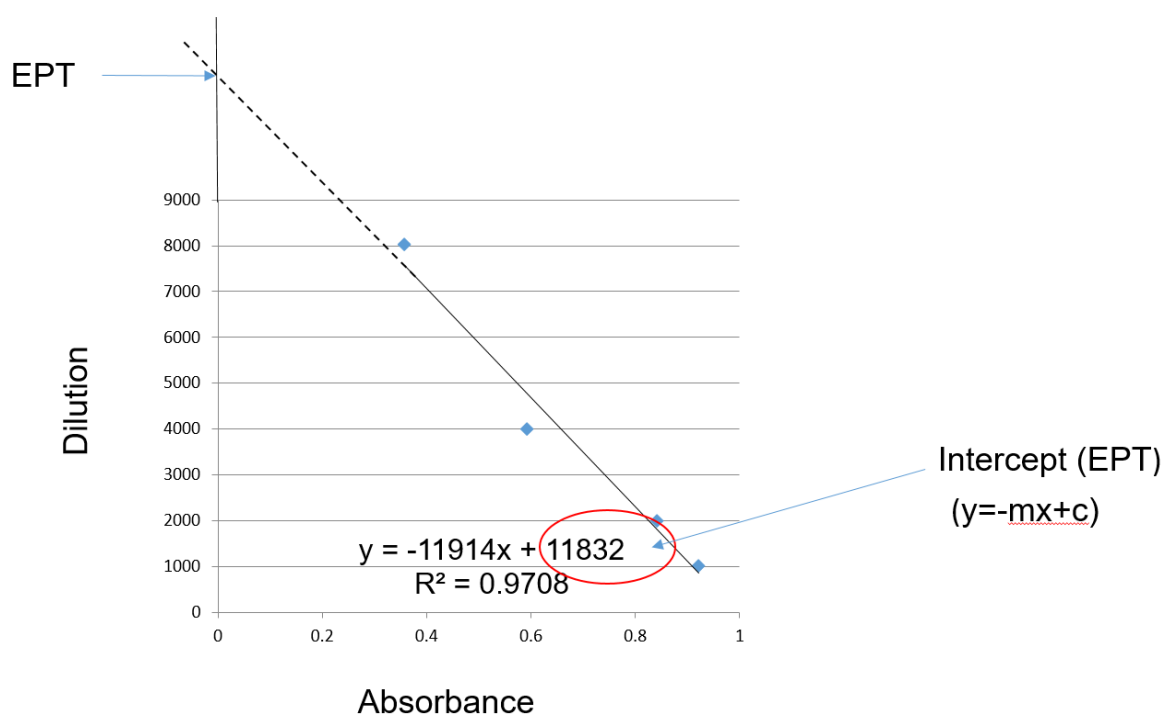


Figure 5.1.4.2.2: Graph of sample absorbance read against initial sample dilution value for end point titre calculation

This is an example graph to show how the end point titre, or EPT, is established from a graph of different dilutions of the sample. The end point titre is read off the graph when the linear line of the form $y = -mx + c$ is extrapolated back to the $x = 0$ value, or the y axis.

5.1.4.3: Optimisation of the protein coating concentration

The ELISA assay must be optimised for antigen coating concentration. The ideal coating concentration is not so low that all protein quickly becomes saturated and does not give a true reading but also the ELISA reader has an upper limit as to what intensity can be read, therefore the protein coating cannot be too high that the machine cannot distinguish different values.

The ideal plate coating concentration will be such that a dilution of the original sample applied to this ELISA will give a reading that is in the linear range of dilution values, such that the well surface is not saturated which would be wasteful of product but also such that the concentration is not so low that the read values are negligible. The dilution factor chosen should be within the linear range. For this study, due to there not being an exhaustive supply of antigen as it was generously supplied by Newcastle University and not generated on site, the dilution factor was established such that it would be efficient use of the proteins available: not excessive or wasteful.

5.1.5: Aims of this chapter

The evidence discussed above suggests that there may be subtypes of PBC patients. Given that some of the genes highlighted by the GWAS study cited are known to influence isotype switching, it is possible that different isotype patterns of specific autoantibodies may be seen in patients from different groups. The primary aim of this experiment is development of an assay which will be used to determine accurate autoantigen specific antibody titres from patient serum. The results from these assays will be analysed along with patient data; statistical data and analysis of the data is in chapter 6.

5.2: Methods

5.2.1: Isolation of bE2/E3BP and recombinant human proteins

Biochemical disassociation of bE2/E3BP was performed by the Dr Jeremy Palmer group, Newcastle University. Bovine heart tissue was mechanically disrupted before the tissue was lysed using a high sucrose concentration, Glaspergen beads and a magnetic stirrer. The sample was centrifuged 3 times at 1000 x g for ten minutes each with discarding of the

pellet, then at 14500 x g for fifteen minutes to obtain the mitochondrion fraction. This fraction was resuspended in 10% glycerol 10mM potassium phosphate and tosyl-L-lysyl chloromethane hydrochloride then frozen for 24h at -50°C. Mitochondria were then freeze thawed to disrupt the membranes and then centrifuged at 27000g for 30 minutes and the pellet resuspended in 10% glycerol 10mM potassium phosphate with 1 mM-dithiothreitol and centrifuged again. The pellet was then discarded and the supernatant pH-adjusted before further centrifugation steps to isolate the mitochondrial pellet. Then, to purify the mitochondrial pellet, it was first resuspended in 10% glycerol 10 mM potassium phosphate with 1 m-dithiothreitol and 1 mM Na-p-tosyl-L-lysine chloromethyl ketone (TLCK) to give a final protein concentration of 8-12 mg/ml. This was then stored at -50°C.

The recombinant human proteins E2, E2ILD and E3BP were grown in recombinant *E. coli* then purified, method not provided. Final concentrations were: bovine heart isolated E2/E3BP complex, bE2/E3BP (9mg/ml); rhE2 (1.5mg/ml); rhE2ILD (7mg/ml); rhE3BP (1.4mg/ml).

5.2.2: Optimisation of the protein coating concentration

First, an initial screen was carried out using an estimated coating concentration of antigen for all patients using the IgG-all secondary antibody from Sigma Aldrich, which is a pool of subtypes of IgG antibody. This is the antigen currently used in clinical PBC diagnostic AMA assays, therefore was likely to give high readings. The dilution of the first antigen, rhE2, was 1 in 100 of the initial 1.5mg/ml and the patient serum was screened at 1 in 25 dilution by the method in section 3.3. The patient with the highest screen result was then chosen for protein coat optimisation. This is important because the optimisation must aim to take into account the maximum achievable result for a given coating concentration and must be designed to be relevant for the highest response patient. The ELISA was repeated using patient serum at concentration 1 in 25 and different protein coat concentrations. A low dilution of patient serum ensured saturation of the coating antigen would be established in order to be able to visualise the full graph pattern for protein coating and most accurately establish the ideal coating concentration.

This was repeated for all test antigens.

5.2.3: ELISA screen

Each plate was coated with protein coat solution, with its protein concentration established in the protein coat optimisation stage, at a volume of 50µl/well. 96 well Nunc-Immuno™ MicroWell™ immunoassay plates were used throughout, obtained from Sigma Aldrich. Plates were incubated overnight at 4°C. The plates were then washed three times with PBST and 200µl blocking solution was added to each well. This was then incubated for one hour at room temperature. The plates were then washed with PBST 3 times and the samples diluted 1 in 25 were added, 50µl per well. Samples consisted of the diluted serum of 77 PBC patients and 34 healthy volunteers, all in duplicate, plus at least 4 blank wells for normalising. The plates were left at room temperature to incubate for one hour. The plates were then emptied into virkon solution and washed 6 times with PBST. The secondary antibodies were then added to required concentration (as outlined below). The plates were then incubated at room temperature for 1 hour. The plates were then washed in PBST 6 times. The plates were then developed according to the procedure for the particular secondary antibody.

Secondary IgG_{all}, IgA or IgM:

The substrate was made up of 25ml citrate phosphate buffer, 1 20mg tablet of OPD and 20µl H₂O₂. 100µl substrate was added to each well and the plate was incubated for 10 minutes. 25µl H₂SO₄ was added to each well to stop the reaction and the plate was read on the plate reader.

Secondary IgG1, IgG2, IgG3 or IgG4:

The particular types of secondary antibodies used of these antibodies did not contain the horseradish peroxidase conjugate, therefore this had to be added. These are biotinylated antibodies.

The avidin-HRP conjugate was added at a concentration of 1 in 10000, 50µl to each well. The plate was incubated at room temperature for 1 hour. The plate was then washed for one hour and developed using the substrate, consisting of 25ml citrate phosphate buffer, 1 x 20mg tablet of OPD and 20µl H₂O₂. 100µl substrate is added to each well and the plate was incubated for 10 minutes. 25µl H₂SO₄ was added to each well to stop the reaction and the plate was read on the plate reader.

Secondary IgE:

The IgE secondary antibody used had a different substrate and different mechanism of action to all others. Development required p-nitrophenyl phosphate, PNPP, rather than OPD. The PNPP tablet was dissolved at 1.0mg/ml in Mg²⁺ substituted diethanolamine. 200µl was added to each well and then allowed to incubate for 30 minutes. The reaction was then stopped by addition of 50µl NaOH per well and plates were read at 405nm on the plate reader.

5.2.4: Short dilutions

Only the secondary antibody of IgG_{all}, a pool of antibodies for all of the IgG isotypes, was used in the end point titre assays. End point titre results were to be compared with results from the screens to determine if the screen alone is an accurate representation of the end point titre results, such that screens alone could be used in future analysis.

The values from the initial screen were used to estimate the start dilution for the short dilution for each patient. The method used was the same as in section 5.2.3, however using 1 in 2 serial dilutions of serum from each patient, in duplicate. This stage required an element of trial and error but resulted in graphs showing in linear regions for all patients for graphs of dilution against absorbance. The R² value of the line of each graph was calculated on Microsoft Excel, using the correlation coefficient function, described in 5.2.5.1. This was to ensure that the lines were linear such that EPT could accurately be estimated. For this to be possible, the R² value needed to be above 0.6, as this is the generally recognised cut off for strong linear correlations.

5.2.5: Statistics

5.2.5.1: Linear regression

Linear regression was carried out for all short dilution graphs. The correlation of dilution against absorbance is found using the function in Microsoft Excel software, however can also be calculated using the formula below:

$$R = \frac{\sum(x - \bar{x})(y - \bar{y})}{\sqrt{(\sum(x - \bar{x})^2 \sum(y - \bar{y})^2)}}$$

R² is established by squaring the R value achieved using this formula (Colin Cameron and Windmeijer, 1997). (Data was first verified to be normally distributed – not shown.)

The R² value relates to how accurate the regression line is as an approximation of the real data points (Park et al., 2017).

5.2.5.2: Spearman's rank correlation coefficient

The Spearman's rank correlation coefficient is a statistical test to assess how closely the trend in one set of data can be expressed as a function of that of another. It explores whether there is a monotonic relationship between the two data sets or not (Spearman, 1904).

The data in each group is ranked in order of magnitude. Labelling one group x and the other y, the difference, d, between the ranks is calculated for each measurement, always in the order of d = x rank – y rank. As a test of accuracy, the total of the differences should be

zero. The differences in the ranks are then squared and then the squares are totalled. The Spearman's Rank value, r_s , is calculated using the following formula:

$$r_s = 1 - \frac{6 \sum d^2}{n(n^2 - 1)}$$

(Spearman, 1904).

This formula was then applied to the end point titre results for all short dilutions for all samples and their initial screen average value to determine if the screen alone would be an adequate assay, rather than having to use short dilution for the rest of the secondary antibodies.

5.3: Results

5.3.1: Optimisation of the protein coating

Figure 5.3.1 shows graphs of dilution of protein coating against absorbance for a constant primary antibody concentration. Arrows show where the dilution of protein coating has been established based on criteria from methods, section 5.2.2. 1/1000 dilution was decided for rhE2 and rhE2ILD and 1/500 for E3BP and bE2/E3BP.

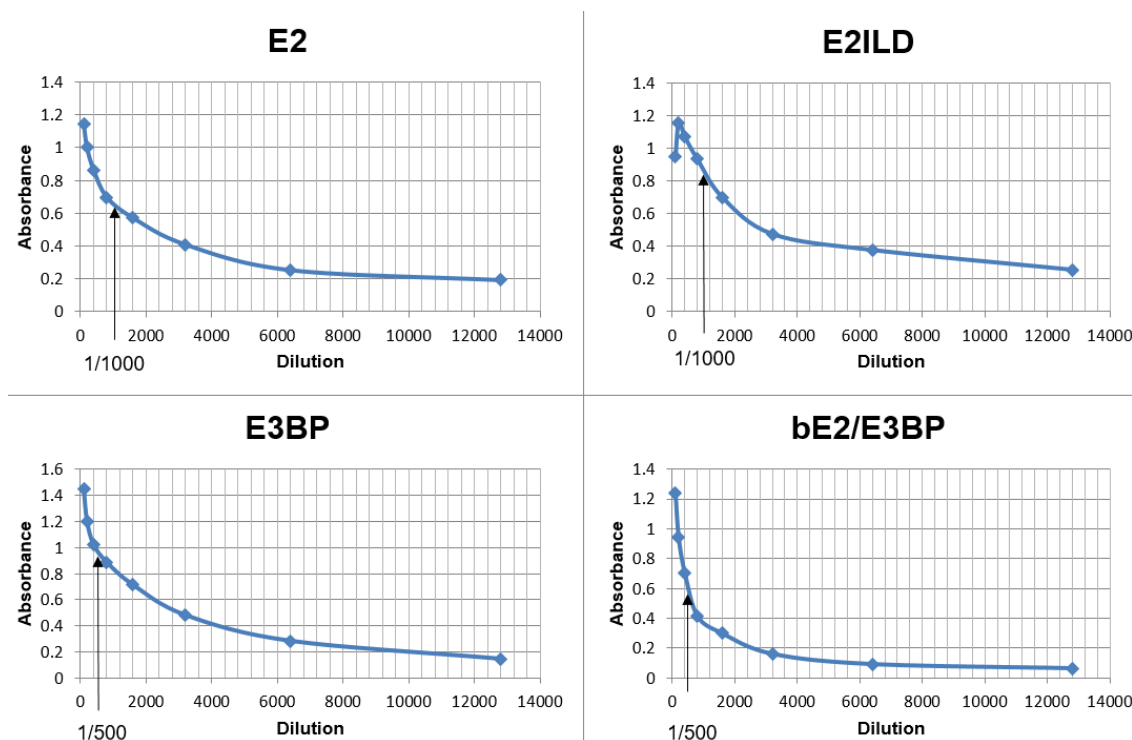


Figure 5.3.1: Graphs of dilution of the protein coating for each of the PBC antigens. The graphs show the plotted values for dilution of antigen against absorbance value read. The arrows show where the region of the graph is tracked to the x axis to establish the corresponding dilution factor.

5.3.2: Initial screen results and end point titre tabularised results

Results from screens and end point titres are displayed in combined tables, figure 8.4 (appendix). The R^2 values are listed to indicate the strength of the relationship between end point titre and initial screen average amount. The initial screen average was calculated by first removing the average blank value, then averaging the 2 screen readings. Graphs for each patient are also shown in the appendix displaying the R^2 value.

The tables (figure 8.4, appendix) shows all of the screen values, normalised by subtraction of the average blank reading. The blank reading average was calculated by averaging the screen values for 10 wells which only contained well protein coating and diluent used to dilute the serum, rather than diluted serum, and these were developed as normal. Normalised screen results were averaged and displayed under the heading 'Average Screen'. Where there is no entry in the table indicates a patient eliminated by being unable to satisfy the criteria of being able to give an end point titre value. For the antigen rhE2, patients 28 and 31 were eliminated; for rhE2ILD patients 51, 58, 69 and 74-78 were eliminated; for rhE3BP, patients 19, 25, 31, 42, 51, 66, 68, 69, 74 and 75 were eliminated; for bE2/E3BP, patients 5, 7, 10, 18, 20, 21, 23, 25, 28, 31, 34, 42, and 58 were eliminated. Patients eliminated at this stage were only eliminated for the Spearman's Rank correlation analysis against screen values for IgGall, but were included in further analysis as they could still show high levels of other isotypes.

Volunteer number	IgGall			
	rhE2	rhE2ILD	rhE3BP	bE2/E3BP
	Avg. Screen	Avg. Screen	Avg. Screen	Avg. Screen
1	0.0255	0.0465	0.0220	0.1320
2	0.0000	0.0160	0.0000	0.0835
3	0.0000	0.0000	0.0000	0.0225
4	0.0175	0.0140	0.0000	0.0905
5	0.0470	0.0400	0.0125	0.1180
6	0.0400	0.0475	0.0000	0.0865
7	0.0000	0.0000	0.0000	0.0000
8	0.0310	0.0270	0.0190	0.0810
9	0.0000	0.0000	0.0000	0.1065
10	0.0190	0.0300	0.0870	0.1110
11	0.0765	0.1320	0.1135	0.0970
12	0.0365	0.0395	0.0350	0.1405
13	0.0580	0.0555	0.0690	0.1175
14	0.0820	0.0400	0.0290	0.0965
15	0.0505	0.1130	0.0760	0.1125
16	0.0380	0.0465	0.0200	0.1180
17	0.0000	0.0000	0.0000	0.5100
18	0.0865	0.1310	0.0305	0.1235
19	0.0275	0.0175	0.0500	0.2090
20	0.1230	0.0055	0.0290	0.1545
21	0.0970	0.0180	0.0775	0.1220
22	0.1250	0.0370	0.0590	0.0630
23	0.0710	0.0000	0.0365	0.1650
24	0.0360	0.0000	0.0010	0.1540
25	0.0000	0.0000	0.0000	0.8280
26	0.0390	0.1485	0.1400	0.1210
27	0.0500	0.0065	0.0025	0.1415
28	0.0375	0.0390	0.0585	0.1235
29	0.0645	0.0170	0.0520	0.0760
30	0.0715	0.0515	0.0595	0.1030
31	0.0295	0.0170	0.0020	0.0645
32	0.0335	0.0115	0.0000	0.1735
33	0.0000	0.0000	0.0000	0.5245
34	0.0890	0.0630	0.0000	0.1915

Table 5.3.2: Lists of averaged, corrected absorbance values for IgGall Healthy Volunteer screens.

This table displays all averaged, corrected absorbance values for IgGall antibodies and shows those needing to be 'cut-off' in bold. This includes volunteer 20 for rhE2IgGall; 11, 15 and 26 for rhE2ILD IgGall; 11 and 26 for rhE3BP IgGall; 25 and 33 for bE2/E3BP IgGall. These readings were too high as per the cut-off criteria.

5.3.3: Cut-offs

A cut-off was required to determine if any healthy volunteers should be excluded as positive outliers. Equipment and materials for diagnosis of PBC in healthy volunteers was not available so healthy volunteers could not be excluded based on our determination of them being formerly undiagnosed PBC patients. Many studies involving ELISA assays in the past have excluded negative sera based on them being outliers based on their values being over 2 or 3x the standard deviation away from the mean for negative sera, however this method is often unnecessarily high and may therefore lower the sensitivity of the assay. Instead, a specific factor can be applied to the standard deviation based on the required confidence value and the number of controls. This method is especially beneficial when many controls are used, as number of controls negatively influences the factor. The cut-off can be calculated by:

$$\text{Cut-off} = \bar{x} + \text{SD}(f)$$

where $f = t\sqrt{(1+(1/n))}$,

where patients are excluded if their average absorbance is $>$ this cut-off value. \bar{x} is the averaged screen value for the measurements of all patients for the particular antibody, t is the minimum t value corresponding to the required confidence interval and n is the number of measurements, or number of controls in this case (Adair *et al.*, 1989). As shown in table 5.3.3 (and also in chapter 6), those eliminated for Spearman's Rank correlation coefficient comparison of EPT and screen were: volunteer 20 for rhE2IgGall; 11, 15 and 26 for rhE2ILD IgGall; 11 and 26 for rhE3BP IgGall; 25 and 33 for bE2/E3BP IgGall.

For healthy volunteers, it was important to eliminate outlier values because they could be indicative of undiagnosed PBC, however all patients have been given confirmed diagnosis of PBC, therefore assuming all diagnoses to be correct, it was important to keep all patient data as this chapter aims to establish conclusions based on the PBC population, which will include patients negative for certain antibodies. Given that PBC is diagnosed based on other factors than only antibody presence, it is unlikely that a negative outlier could be indicative of a wrongly-diagnosed PBC patient, who is actually disease-free. Therefore, it is more accurate to maintain patient outliers and instead use statistical analyses not sensitive to outliers, i.e. non-parametric analyses.

		\bar{x}	SD	1.756xSD	Cut-off	List HVs to cut off
rhE2	IgGall	0.0441	0.035	0.0614	0.1056	20
	IgG1	0.0213	0.0575	0.1009	0.1222	17, 26.
	IgG2	0.0350	0.0406	0.0713	0.1063	32, 34.
	IgG3	0.0459	0.1056	0.1855	0.2313	11
	IgG4	0.0192	0.0213	0.0374	0.0566	1, 6, 14.
	IgA	0.0753	0.1132	0.1988	0.2741	30
	IgM	0.1224	0.1788	0.3140	0.4364	(None)
	IgE	0.0002	0.0011	0.0020	0.0022	16
rhE2ILD	IgGall	0.0356	0.0404	0.0709	0.1064	11, 15, 26.
	IgG1	0.0489	0.0495	0.0870	0.1359	11, 16, 30, 33.
	IgG2	0.1483	0.1326	0.2328	0.3811	6
	IgG3	0.0664	0.0963	0.1692	0.2356	11, 22, 30.
	IgG4	0.0167	0.0154	0.0270	0.0437	14, 19.
	IgA	0.0417	0.0629	0.1104	0.1521	18, 26.
	IgM	0.1226	0.1648	0.2894	0.4121	5
	IgE	0.0147	0.0189	0.0333	0.0480	10, 12, 16.
rhE3BP	IgGall	0.0319	0.0367	0.0644	0.0962	26, 11.
	IgG1	0.0493	0.0706	0.1239	0.1732	19, 30.
	IgG2	0.0832	0.1157	0.2031	0.2863	13, 19.
	IgG3	0.0284	0.1040	0.1827	0.2111	11
	IgG4	0.0105	0.0241	0.0422	0.0528	1, 2, 6, 11.
	IgA	0.0441	0.0467	0.0819	0.126	2
	IgM	0.1312	0.0907	0.1593	0.2903	5, 14.
	IgE	0.0206	0.0475	0.0833	0.1039	2, 27.
be2/E3BP	IgGall	0.1577	0.1585	0.2783	0.436	25, 33.

Table 5.3.3: Table of calculations and exclusions for healthy volunteer screens.

This table lists the values calculated required to determine patients to cut off for each antibody, as per the formulae:

$$\text{Cut-off threshold} = \bar{x} + \text{SD}(f)$$

where $f = t\sqrt{(1+(1/n))}$.

The table then lists the patient numbers for those cut offs deemed outliers as per these calculations.

\bar{x} is the average absorbance value across all healthy volunteers for this antibody; SD is the standard deviation from the mean; 1.756 is the calculated SD multiplier as per $f = t\sqrt{(1+(1/n))}$; the cut-off is the minimum average absorbance 'cut off' as an outlier; 'HV' stands for Healthy Volunteer and the final column lists all 'cut' healthy volunteers.

5.3.4: Outliers in patient data

The patient data screens were all checked for normality and outliers. These are all shown in chapter 6. Software SPSS was used to calculate normal distribution. At the stage of comparing screen values to EPT, all outliers were kept in because the study aims to be as inclusive of all PBC patients as possible and this data will be used to investigate grouping of the patients, therefore it is important to keep outliers and use Spearman's Rank correlation, which is not sensitive to outliers.

5.3.5: End point titre graphs

All end point titre graphs are shown in combined figures 8.5 (appendix) and include correlation coefficients. R^2 values to show how strongly the data points used for the extrapolation to $x=0$ are included on each graph. The R^2 value shows how strong a linear relationship there is between the dilution and the absorbance. Some short dilutions, for example for patient 28 for the rhE2 antigen, the R^2 value was below 0.6 even when many different dilution series were investigated, therefore it was determined that the linear region for the curve for these patients could not be established, perhaps because there was too little of the antibody in question in their serum, therefore they were excluded from EPT calculations. All patients giving a linear region with R^2 value above 0.6 were kept for EPT analysis.

The EPT strategy was applied to healthy volunteers to establish the cut-off end point titre value for EPT, such that all values calculated in patients which were considered not significantly different from healthy volunteers could be excluded from further analysis. Healthy volunteers were subjected to long dilutions of their sera and measured for absorbance using the same method as in section 3.4, however no healthy controls showed a negative linear region, the strength of which measurable by an R^2 value above 0.6 for 4 consecutive points, in their plotted graphs of absorbance against dilution. Therefore, the end point titre as per the method applied in this chapter could not be calculated. The healthy volunteers all likely had no detectable levels of the antibodies in question in their sera. Some patients also failed to show any such linear region for some antibodies, and so were excluded from the Spearman's rank calculation with screen averages, as they, too, likely did not have a detectable level of the particular antibody in question.

5.3.6: Spearman's Rank Correlation Coefficient results

To determine the relationship between end point titre and antibody screen, a Spearman's rank correlation test was carried out on end point titre results and average screen results. Patients were excluded by 2 criteria: failing to show a linear region with $R^2 > 0.6$ in the dilution ELISA or failing to exceed the cut-off screen value.

Prior to Spearman's rank correlation coefficient, the EPT data and average screen data were tested using SPSS for normal distribution and outliers. The data was not normally distributed based on Shapiro-Wilk and Kolmogorov-Smirnov tests, both described in chapter 6. For EPT data, the Shapiro-Wilks normality statistic was 0.847 ($p=0.000$) and the Kolmogorov-Smirnov 0.183 ($p=0.000$). Results for screen data were 0.920 ($p=0.000$) and 0.153 ($p=0.000$) respectively, which causes for rejection of the null hypothesis of the data fitting the normal distribution. Skewness z values were 4.921 and -2.545, which show high skewness in opposite directions, further indicating the data were not normally distributed. These data are contained in chapter 6.

Table 5.3.6 shows the results of the calculation of spearman's rank correlation coefficient for comparing screen results with EPTs. The results for rhE2, rhE2ILD and rhE3BP show strong correlations with r_s values of 0.624, 0.805 and 0.805, however bE2/E3BP gave an r_s value of 0.592. As the bovine protein is less representative of the human protein and represents a complex of proteins which the recombinant human version are used, this is the least relevant of the antigens used. This protein was excluded from further analysis. The high r_s values indicate there is a relationship between the data, however the normal distribution test data indicates that the relationship is not linear and non-parametric tests must be used.

Antigen	r_s	p
rhE2	0.624	<0.0005
rhE2ILD	0.805	<0.0005
rhE3BP	0.805	<0.0005
bE2/E3BP	0.592	<0.0005

Table 5.3.6: Table of Spearman's Rank correlation coefficient values and the relevant p values.

The table shows the results from the Spearman's rank correlation coefficient when the relationship between the end point titre and the average normalised screen values is investigated.

5.4: Discussion

5.4.1: Aims

The aim of this chapter was to develop an assay which could be used to compare levels of different isotypes of antibodies against the autoantigens in PBC in PBC patients. This involved analysing the optimisation procedure to determine if using the average screen value was sufficient or if carrying out a short dilution was always required.

5.4.2: Discussion of results

End point titre (EPT) ELISAs were carried out on each patient for an accurate estimation of their dilution required to give a hypothetical zero absorbance value for antibodies of the IgG isotype pool, IgGall, against rhE2, rhE2ILD and rhE3BP. This is the most accurate and reliable method of ELISA to use as it gives a method for direct comparison between patients. A minimum of 4 data points are used to calculate the EPT, rather than an average of 2 or 3, giving it greater accuracy (Dey et al., 2008). It is important that measurements are taken using the linear fraction of the dilution against absorbance graph, and this can be verified by a high R^2 value of correlation coefficient which assesses the linear nature of the data points. In addition, a high R^2 value gives increased likelihood that the extrapolation of the line will be accurate and lead to an accurate EPT value.

ELISA plates were coated with the antigens as per ideal concentrations established in the plate coating optimisation assay. Duplicated screens were carried out to obtain an average screen value rather than one value to minimise error. Screen results were then compared to EPT results by Spearman's Rank correlation coefficient statistical analysis. This analysis was chosen to explore if there is a monotonic relationship between results of the screens and EPT results, such that for all other experiments screen could be used rather than the serum consuming EPT method. As shown in table 5.3.6, all antigens except bE2/E3BP showed a significant relationship between EPT values and normalised screen averages, therefore it was decided that the screen values would be used for future experiments. Table 5.3.6 also shows p values of the spearman's rank correlation coefficient. The r_s value assesses the strength of the relationship where 0.6 or above is generally considered a strong relationship. The p value suggests the confidence interval, such that for example a p value of 0.05 gives a confidence interval of 95% so it can be assumed with 95% confidence that the correlation described in strength by the magnitude of the r_s value is accurate for the data. The p values for the Spearman's rank correlation coefficients are all rounded to 0.000, therefore it can be estimated that at least 99.95% of the data points can be assumed to follow the relationship (Spearman, 1904). Therefore, it can be assumed with high confidence that conducting screen only calculations to investigate levels of IgM, IgA,

IgE and the IgG subtypes will strongly follow results which would have been obtained in carrying out end point titre dilution experiments.

The screen only tests are favourable because there is a limited supply of protein provided by Newcastle University. Additionally, there could be diagnostic implications which will be favoured by using only the screen method. If, in chapter 6 it is shown that there are levels of the antibodies tested for in this study that they could be used in PBC diagnoses in the future then it is less time consuming and more cost effective for hospital diagnostics to do screens rather than serial dilutions as the serial dilutions use considerably more reagents and involve more calculations. Similarly, if it is found that there are antibodies of significantly different levels between responders and non-responders, such that an assay similar to this is used in the future to distinguish responders from non-responders, the same cost and time effective advantage applies.

5.4.3: Discussion Summary

The implications of practise for this research will be its eventual use towards a potentially diagnostic tool for early determination of the type of PBC the patient has. The EPT correlated with the screen values such that by screening all patients for all antigens and using the range of secondary antibodies outlined in the methods, there is a large amount of data which can now be further analysed for any significant differences between responders and non-responders.

5.4.4: Limitations

A limitation of the screen average rather than using the EPT is that unlike EPT, the screen uses only 2 data points and it cannot be made certain that the linear portion of the graph is being represented. However, patient serum and coating antigen are in limited supply, therefore, it would be impractical to carry out short dilutions for every patient for every antigen and secondary antigen. Upon testing of this assay, if there are any significant findings, as in any differences between responder group and non-responder group, those antigens and discovered to be of interest could in future work be re-analysed using the end point titre method.

Chapter 6: Investigating differences in immune responses between PBC patients that are responders and non-responders to UDCA

Abstract

Recent research suggests that PBC should be treated as two or more separate disease subsets due to apparent differences in severity, clinical biochemical parameters and response to Ursodeoxycholic Acid (UDCA). UDCA is the current blanket therapy given in PBC, however it is ineffective in 20% of patients: “non-responders”. Categorisation as a non-responder requires inability of the drug to significantly lower a patient’s blood AST, ALP and bilirubin levels during a significant period of time, usually one year after UDCA is first administered. It is likely that these patients have a more severe autoimmune disease and that the failure of treatment may reduce the effectiveness of any potential anti-inflammatory drugs. Further elucidation of these subsets is crucial to stratify patients and potentially allow the development of differential therapies which may benefit these “non-responders”. Multiple indirect enzyme-linked immunosorbent assays (ELISAs) were carried out to measure antibody titre and therefore detect patterns of auto-antibody isotypes in serum from PBC patients known to be “responders” (62) or “non-responders” (15) to UDCA. Recombinant human PBC autoantigens E2, E2 inner lipoyl domain (E2ILD) and E3 binding protein (E3BP) were used to uncover statistically significant differences in antibody responses. Using Mann Whitney analysis, it was found that compared to responders, non-responders have higher levels of anti-E2 IgE ($p=0.025$), anti-E2ILD IgA ($p=0.047$) and anti-E2ILD IgG3 ($p=0.01$). The study also found that men with PBC, generally considered non-responders, have significantly lower levels of some antibodies, which are normally higher in non-responders: anti-E2IgE ($p=0.003$) and anti-E2ILD IgG3 ($p=0.05$). This is further evidence that men with PBC may constitute their own sub group of non-responders. Differences in antibody isotype to dominant autoantigens suggests that there may be significant functional differences in T helper cell subsets in each patient group. Further investigation into the differences between these subsets could in the future provide a diagnostic tool which could be used early on in diagnosis to categorise patients for stratified treatment.

6.1: Introduction

6.1.1: Background

Chapters 1 and 5 outline a study carried out in 2013 by Carbone and colleagues which found that there are key differences between patients that respond and those that do not respond to therapy of ursodeoxycholic acid (UDCA), normally given to all patients. Studies have shown that as many as 20% of patients may not respond to this blanket therapy, in that there is insufficient slowing of disease progression and levels of enzymes in the blood which can indicate liver damage fail to drop to what are considered 'normal' levels, outlined in the main introduction (Carbone et al., 2013).

In the study investigating differences between groups, the main difference of interest was age, whereby patients who are younger at diagnosis were more likely to fit the criteria for non-response and patients who are older at diagnosis are more likely to fit the criteria for non-response (Carbone et al., 2013). Figure 6.1.1 displays this suggested grouping system in a flow chart format. 'Response status' was determined by Paris I criteria, which groups patients based on their serum levels of known biological markers indicative of liver damage. These compounds are further outlined in section 6.1.2. According to the Paris I classification criteria, a PBC patient is considered a 'responder' to UDCA if, after 1 year of monitoring while taking UDCA, they satisfy the following: their alkaline phosphatase level is $\leq 3x$ the upper normal limit, their aspartate transaminase level $\leq 2x$ the upper normal limit and bilirubin level within the normal range. The accepted 'normal' limit or range of these factors can differ depending on the laboratory or geographical area, although some values quoted frequently in the literature are within this chapter. As outlined in chapters 1 and 5, the Carbone and colleagues study also identified that males may make up their own sub-group, with an aggressive form of the disease but different characteristics to female non-responders, and also sub-classified the non-responders based on different liver biochemistry (Carbone et al., 2013).

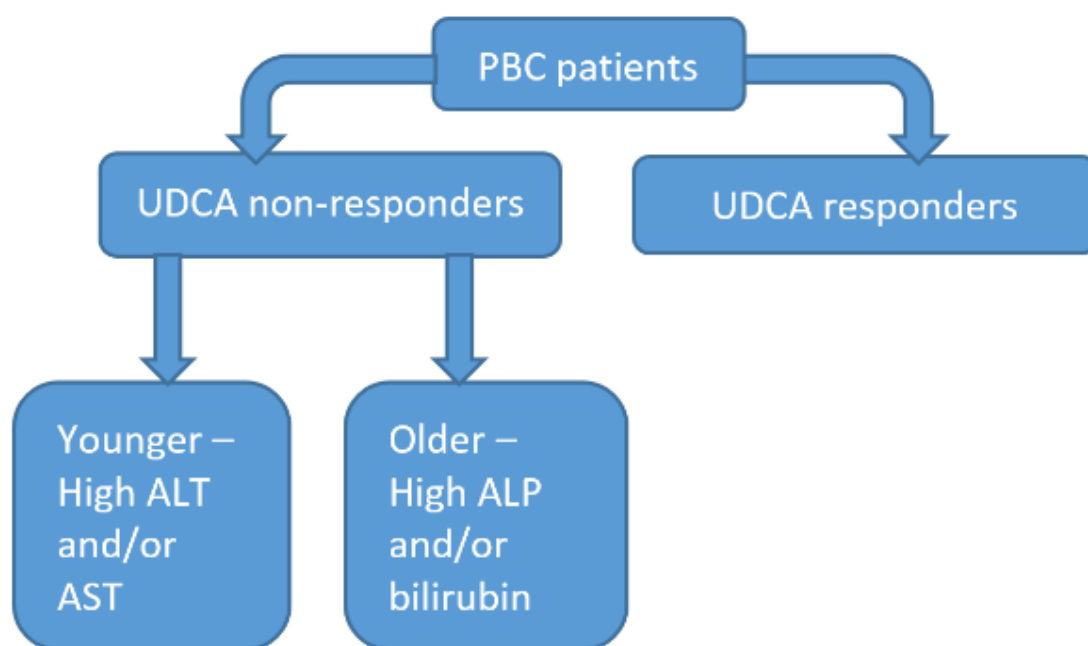


Figure 6.1.1: Hypothetical grouping diagram of PBC patients

This figure depicts the proposed grouping of PBC patients in recent literature (Carbone et al., 2013). PBC patients, according to their analysis, can be split into those who respond to UDCA, ‘responders,’ and those who do not, ‘non-responders.’ Non-responders can be further subdivided based on their blood biochemistry where younger non-responders tend to be classified as ‘non-reponders’ based on ALT and AST levels, whereas the older non-responders tend to be so-classified based on high ALP or bilirubin adapted from Carbone et al. 2013 (Carbone et al., 2013).

It is important to acknowledge that PBC patients have been grouped based on whether or not they ‘respond’ to current therapy. This was one of the first studies to attempt to provide statistical backing to the idea that PBC may be made up of different sub groups which may require their own therapies, however it is important to provide a biological reasoning why some patients ‘respond’ and others do not (Carbone et al., 2013). Therapy for the disease will continue to improve and be further stratified based on what is discovered which can more accurately define the groups of PBC patients, and possibly there are more groups within PBC patients to be discovered. Further elucidation between the subgroups of the patients will not only allow better understanding of and the development of better treatment for PBC patients, but it will also enable the subgroups to be more accurately defined such that they will no longer be defined based on response to a drug but can be identified based on biological properties of the patients.

It has been well-documented that PBC is likely a multi-factorial disease. Factors such as environment, history of infection, genetics and others may all contribute to development of the disease (Jones, 2003). This is outlined in further detail, such as possible pollutants which may contribute to PBC formation, in the main introduction (Jones, 2003). Additionally, presence of anti-mitochondrial antibodies, which is hallmark to most PBC patients, seems to be insufficient to cause disease on its own (Ozaslan et al., 2016). Factors which

contribute to PBC are explored more in chapter 1, Introduction. Previous results chapters further outlines a potential genetic input from data obtained in a genome-wide association study. The GWAS data, as well as other environmental factors outlined in chapter 1, introduction, has yet to be analysed in the responder/non-responder context, but may be of importance in the sub-grouping of PBC patients.

One potential argument for a reason why there are phenotypically different groups within the PBC population is that there could be different T cell responses to the antigen leading to one more aggressive disease form and another less aggressive form. Chapter 1, Introduction, suggests other diseases where the type of helper T cell response can be critical in determining whether the patient has an active or resistant disease state. There could be measurably different T cell profiles between patient groups in PBC giving rise to different disease phenotypes. In order to measure and compare the T cell profiles in PBC patients, T cells from patient blood can be counted and classified within their subtypes, as described in chapters 3 and 4, however patient cells were not available for this study. Previous results chapters outline how the different cytokines released by different T cells could lead to different characteristic antibody profiles which could be measurable by ELISA. For example, as outlined in chapter 5, a prominent Th1 response could lead to a predominant IgG3 profile, with low levels of IgG1 and IgE (Mitsdoerffera *et al.*, 2010). A predominant Th2 response could show abundant IgG4, IgE and/or IgG1 (Lebmann and Coffman 1988). A predominant Th17 response could show raised IgG1 and IgG3 (Mitsdoerffera *et al.*, 2010). If there are different antibody profiles for different subgroups of PBC then this may direct further studies such as what might be the influence of other factors, such as a genetic or environmental influence, on these antibody profiles.

Studies have shown that cytokines produced by Tregs, IL-10 and TGF- β , together induce switching to IgA1 and IgA2; Th2 cytokines IL-4 and IL-13 induce class switching to IgG4 and IgE; Th1-released IFN- γ favours IgG3 switching (Tangye et al.2002).

Elucidating any antibody patterns between groups is one step towards understanding on a cellular level why there are different groups within the disease.

6.1.2: Clinical liver evaluation

When a patient has a blood liver panel assessment, the levels of many enzymes and proteins are measured. This is because levels outside of normal parameters can indicate PBC but also other illnesses. A specific range of different characteristics must be measured in order to determine the correct illness while ruling out other potential illnesses.

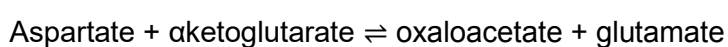
PBC is either diagnosed from a blood test carried out because PBC is suspected or from a routine blood test. Therefore, symptoms at diagnosis can range from none to some or all of: lethargy, pruritis, joint pain, dryness of the mouth, yellowing of the skin and eyes(Gatselis et al.).

A liver panel assessment will be carried out on the patient's blood and many different factors will be assessed to help determine the disease status. Blood alkaline phosphatase (ALP), aspartate aminotransferase (AST), alanine aminotransferase (ALT), bilirubin, antimitochondrial antibodies (AMA) and antinuclear antibodies (ANA) are measured and often a liver biopsy will also be taken (Patel and Seetharam, Song et al.). The test for PBC consists of serum AMA titres over 1 in 40, (rest of PBC identifiers),

This chapter includes clinical data regarding these parameters for the patients in this study therefore a brief overview of the components tested is incorporated below.

6.1.2.1: Aspartate Transaminase (AST)

AST catalyses the reversible reaction of:



In amino acid catabolism, this reaction involves formation of glutamate which is then broken down by oxidative deamination forming ammonium ions which are then excreted in the urine. This reaction is also important in anabolism of the non-essential amino acid of glutamate used in protein synthesis (Sookoian and Pirola, 2012).

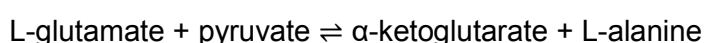
AST is associated with parenchymal cells therefore damage to parenchymal cells of the liver can cause its excessive release into the blood stream to above normal levels (6-34IU/L for females; 8-40IU/L in males) (Nyblom et al., 2006, Chen et al., 2016). Therefore, raised AST is a biomarker in PBC.

6.1.2.2: Alkaline Phosphatase (ALP)

Alkaline phosphatases are present in many tissues, including the liver and bile duct. It is a membrane bound enzyme which catalyses the removal of a phosphate group from another protein and may also carry out a transphosphorylase reaction if there is high concentration of phosphate accepting sites. In the context of PBC, damage to the bile ducts and later the liver causes the release of the enzyme into the bloodstream, which can cause an ALP level to rise above the normal 20-140IU/L (Millán, 2006).

6.1.2.3: Alanine Transaminase (ALT)

ALT is an enzyme which catalyses the reaction:



This reaction is the biosynthesis of alanine from pyruvate and a branched amino acid, in this case glutamate. This method can also synthesise valine, leucine and isoleucine. In the reverse direction, an amino group is removed from alanine and added to α -ketoglutarate for L-glutamate biosynthesis.

Although present in many tissues, ALT is most prevalent in the liver. Raised ALT of 34 IU/L for females or 52 IU/L for males is hallmark for hepatocellular injury (Farrell and Larter, 2006).

6.1.2.4: Bilirubin

A normal blood bilirubin level is between 0.3mg/dL to 1.0mg/dL. A breakdown product of red blood cells, biliurubin in circulation is taken up by healthy hepatocytes to be conjugated to glucuronic acid and excreted in bile. A liver functioning less than normally will be able to take up less bilirubin and so lead to greater levels in the blood (VanWagner and Green, 2015).

6.1.2.5: Anti-mitochondrial antibodies (AMA)

AMAs are discussed in greater detail in (reference the section of my introduction). PBC is not the only disease in which AMAs have been identified in the patients. A list of antigens has been discovered and categorised into groups M1-M2 depending on the type of disease they are relevant to. The M2 group contains the autoantigens relevant in PBC, these being proteins of the α -ketoacid dehydrogenase complex family of enzymes found in the inner membrane of mitochondria, including 2-oxoglutarate dehydrogenase complex (2-OGDC), branched chain 2-oxoacid dehydrogenase complex (BCOADC) and pyruvate dehydrogenase complex (PDC)(Fussey et al., 1991b). All of these enzymes are important in respiration. Presence of AMA is assessed using an ELISA panel screening for the M2 antigens.

AMA is detected by ELISA. There is a series of autoantigens which can indicate liver autoimmune disease, denoted M1-9. M2 contains those antigens relevant in PBC: the 2-oxo acid dehydrogenase complex (2-OADHC) enzymes which are located in the inner mitochondrial membrane and contain PDC (Berg and Klein). It has been reported that 90-95% of PBC patients test positive for AMA.

6.1.2.6: Anti-nuclear antibodies (ANA)

ANA is detected by ELISA(I Peene, 2001). Occuring in approximately 50% of patients, ANAs relevant in PBC include: anti-gp210 antibodies, anti-sp100 antibodies and other ANAs. Gp210 is a nuclear pore protein and sp100 is a nuclear body protein. Others include ANAs against centromere proteins, histones and nuclear lamins but anti-gp210 and anti-sp100 are the main ANAs in PBC and most exclusive to PBC (Worman and Courvalin).

6.1.2.7: Biopsy

Although rarely required today, a biopsy may confirm PBC in those patients with markedly raised AST (>5x normal) without the expected corresponding marked raise in ALP (<1.5x normal), however if both ALP and AST are markedly raised as expected to the thresholds for PBC diagnosis then a biopsy is not required(Zein et al.). The biopsy is carried out to visually confirm small bile duct damage in the absence of the adequate blood data.

Non-response to treatment with UDCA is usually defined by Paris I criteria which states that to have clinically responded to treatment, readings must satisfy: $ALP \leq 3x$ normal, $AST \leq 2x$ normal and normalised bilirubin level (Trivedi et al.).

The factors measured to test for PBC could be indicative of another liver disease, therefore the results must be compared to those for other liver diseases before a PBC diagnosis is decided on.

6.1.3: The use of liver damage enzymes in diagnosis of PBC

6.1.3.1: Aspartate transaminase and Alanine transaminase: AST, ALT.

When the AST level is higher than ALT, this is not necessarily indicative of liver disease because muscle damage from a myopathy disease, disease of the skeletal muscles lowering their function, could also cause increased blood AST(Cobbold et al., 2010). To rule this out, often another muscle damage indicating enzyme such as creatine kinase will also be measured (Cobbold et al., 2010). Creatine kinase is raised in myopathies but is not known to be raised in PBC. When AST is twice as high or more (2:1 ratio or higher) than ALT, this is suggestive of alcohol liver disease and is supported by high gamma glutamyl transferase, not known to be raised in PBC (Moussavian Sn Fau - Becker et al.). A high AST:ALT ratio could also be present in a cirrhotic hepatitis C patient with alcoholic liver disease(Sheth et al.). ALT is found predominantly in the liver and is therefore a more accurate indicator of liver inflammation than AST, however the list of diseases elevated ALT could indicate is extensive. AST and ALT are not accurate measures of liver function without also measuring other components.

6.1.3.2: Bilirubin

High bilirubin is also suggestive of liver disease or damage but has an extensive list of diseases which could account for it, including Gilbert's syndrome, a genetic disorder causing jaundice and hyperbilirubinemia(Bosma et al., 1995) for small increases, hepatitis, a viral infection, for moderate increases or severe liver failure from cirrhosis or Crigler-Najjar Syndrome, a genetically inherited inability to metabolise bilirubin(Jansen, 1999), with very high bilirubin.

6.1.4: Chapter Aims

Chapter 5 outlines development of an assay which can be used to elucidate differences in antibody patterns between the different PBC subgroups. The next logical step is to use a multitude of statistical analyses in attempt to discover if there may be statistically significant differences in antibody patterns between different types of PBC patients, or their clinical parameters. Patient serum used in chapter 5 was provided alongside patient data such as: age, age at diagnosis, date of recruitment to the study, months since recruitment of blood draw, sex, ethnicity, years since UDCA start. This data will be included in analysis in attempt to further subdivide the patient groups and test if our patient data is a fit for the model outlined by Carbone et al (Carbone et al., 2013).

This chapter aims to:

- Elucidate key differences between groups of non-responder and responder patients regarding their serum levels of different autoantibody isotypes.
- Provide statistical backing, where possible, to any discovered differences between responder/non-responder sub-grouping.
- Explore the differences between males and females.
- Explore the impact phenotypic data measured before this study compared with the impact of any further differences discovered in this study.
- Discuss wider implications of the data found in this study and discuss how further studies can refine that discovered in this chapter.

6.2: Methods

6.2.1: Methods introduction

6.2.1.1: Samples provided

Samples were kindly provided by Dr Vinod Hegade at Newcastle University as part of a larger study. Staff at Newcastle University had carried out various tests on the serum and also gathered background information on the patients.

6.2.1.2: Information provided

Patient information includes some gaps in place for some data sets. Patients were asked to give consent for their information to be used. Gaps in the data indicates where a patient has not provided consent for a certain piece of data to be used in this study or where data

could be inaccurate or was not yet measured on the date of sample collection. All patient data is provided in figure 8.1-8.3 in the appendix.

This study was a blind study in that this patient data was only made available after all serum ELISA data had been collected.

6.2.1.2.1: Responder/Non-responder

Arguably the most important information, a patient's responder or non-responder status is provided. This is calculated based on Paris I criteria, which uses the ALP, AST and bilirubin level of the patient after one year on UDCA, as per section 6.1, introduction of this chapter, to determine if the patient's liver biochemistry has adequately 'normalised' for them to be considered a 'responder'. It is unknown the exact 'normal' values for bilirubin, ALP and ALT used, but they likely resemble those values in section 6.1.

6.2.1.2.2: Sex

Sex of patient was provided. This is important because some data has indicated that men and women with PBC have some striking dissimilar characteristics (Lucey et al., 1986). It is important to obtain gender information to investigate if there are differences in antibody isotypes between gender which could further elucidate these potential different types of PBC.

6.2.1.2.3: Age

Age of patient is provided which is important because age is thought to be a key predictor of response, with older patients much more likely to respond to the current therapy than younger patients, who tend to have a more aggressive disease type (Carbone et al., 2013). Age refers to age at date blood was drawn.

6.2.1.2.4: Ethnicity

Ethnicity is provided because studies have shown that there may be differences in symptoms and disease severity between different ethnic groups. United States PBC patients were divided into Caucasian, African-American and Hispanic groups and it was found that non-caucasians had significantly more severe liver disease, more decreased physical activity and worse pruritis than Caucasians, not explained by another factor such as age (Peters et al., 2007). Therefore this data is collected for use in this study where possible.

6.2.1.2.5: Cohort

Some patients included in the study were UDCA-naïve. These patients were to be compared with those administered UDCA because any difference in these groups based

on antibody isotype patterns may suggest a direct effect on the immune system of UDCA which may be causing this effect. Data has shown that UDCA may have a direct effect on the T cells *in vitro*, specifically affecting the proliferation of CD8+ T cells (chapter 4). The UDCA-naïve patients are Cohort B while all taking UDCA are Cohort A.

6.2.1.2.6: Weight

Little has been found linking weight and PBC severity, however it has been suggested that UDCA administration may be associated with weight gain (Siegel et al.). Weight is not provided as a series of values over time so this will not be further explored in this study. Weight is mostly important in this study as it allows calculation of UDCA dosage per unit weight of the patient (see methods).

6.2.1.2.7: AMA and ANA

Data on whether the patient is AMA positive or negative is provided. Although it could be suggested that AMA negative patients should be eliminated from the study as this is a study testing for AMA, the panel which will be used is far more thorough than that currently used for PBC diagnosis so AMA negative patients are kept in this study in case any anti-mitochondrial antibodies not currently tested for are found in those patients. ANA status is important because the ANA antigens differ from the AMA antigens and so may illicit a different immune response which could be detected in the pattern of antibodies screened for in this study.

6.2.1.2.8: Blood Biochemistry

The patients' ALT, ALP and bilirubin blood levels are provided. These are all relevant in establishing a PBC diagnosis but also have been implicated in the responder/non-responder proposed grouping (Carbone et al., 2013). Patients used in this study were categorised as 'responder' and 'non-responder' based on their measurements of these levels and how they fit Paris I criteria, however it is unknown the exact normal limits that were used in calculating this. Additionally, as 'response' and 'non-response' is a fairly new concept, it is unknown exactly when the patients were classified as 'responder' and 'non-responder' and if they were all classified at the same time or not. Additionally, past ALT, ALP and bilirubin measurements are not included, only those of at the time the sera provided were drawn and analysed.

6.2.1.2.9: Other

The dosage of UDCA is dependent on the patient's weight, therefore any investigation into the effect of UDCA dosage on antibodies produced or other characteristics such as liver

biochemistry must also take weight into account. An estimate of the patient's dose per unit weight is calculated by dividing their dosage of UDCA, which is provided in mg, by their measured weight in kg. This is an estimate because studies have shown that weight may increase with UDCA therefore with a potentially changing weight it is impossible to have a thoroughly accurate weight measurement for a patient.

Other factors which require further calculation refer to those referring to time. Date of diagnosis and date of start of UDCA treatment are provided, along with date blood was drawn. Time since UDCA start and time since diagnosis are calculated based on this data.

6.2.2: Statistical Analyses

6.2.2.1: Normal distribution

A normal distribution test is carried out to determine if magnitudes of data follow a bell-shaped curve pattern or not. The bell-shaped curve pattern is suggestive of a 'normal' set of data, meaning data is spread about the mean in a pattern which can be expected, therefore it is likely there may be little of interest in the patterning of the data. The normal distribution is carried out on dependent variables, or the data sets which are measured against another factor, or with another factor in consideration: the independent variable.

There are two main tests for normal distribution, each with their strengths and weaknesses. In general, for sample sizes above 50, the Kolmogorov-Smirnov test for normality is applied and for sample sizes under 50 the Shapiro Wilk test for normality is applied. An alternative method for the Shapiro Wilk test has been developed and applied to software packages such as SPSS, therefore it can be used for sample sizes of up to 2000. In addition to this, the kurtosis and skewness of sample can also be measured for more information regarding the distribution of the data. The kurtosis refers to the heaviness of the tails of the data, or the proportion of the samples that resides in the tails, and the skewness refers to the symmetry, or lack thereof, of the data. In this context, normal distribution is assessed in order to determine which statistical tests may be used to analyse relationships within the data, therefore the Kolmogorov-Smirnov will be the only necessary information (Ghasemi and Zahediasl, 2012).

The Kolmogorov-Smirnov test compares the data with a standard normally distributed data set and assesses how close a fit the data is to this model. This is applied to all dependent variable data in order to highlight data of interest and to help determine which further statistical analyses may be used.

When the test is carried out, a p-value is provided. P-values of less than 0.05 suggest that the data is not normally distributed and therefore there is likely an external factor influencing the data causing a skew or unexpected patterning. This data is of interest in analysis.

6.2.2.2: Mann Whitney

The Mann Whitney U-test is a statistical test which determines whether an independent group of values is significantly greater or lower than another. The data within the groups must measure a dependent variable and be ordinal or continuous and not normally distributed. There are two proposed hypotheses, the null hypothesis, N_0 , and the alternative hypothesis, N_1 , as described below.

N_0 : It is equally likely that a randomly selected value from 1 group will be greater or less than a randomly selected value from the other group.

N_1 : It is not equally likely that a randomly selected value from 1 group will be greater or less than a randomly selected value from the other group.

The data in each group is ranked in order of magnitude. If there is a repeated value, all rank numbers covered by this value are averaged and this average is the rank assigned to this value. Points are then assigned to each group. For every sample in a group, a point is given to the group for every sample in the other group which is greater in magnitude than this sample. This is applied to every sample in every group. The sum of points for each group is calculated and the smaller of the two values is designated 'U'. The z value is calculated from the following formula where 1 and 2 refer to each group:

$$z = \frac{U - \frac{n_A n_B}{2}}{\sqrt{\frac{n_A n_B (n_A + n_B + 1)}{n_{tot}}}}$$

The confidence interval is 0.05, so 0.9750 Area in body is used in the z table, giving a z value of 1.96. If the calculated z is < -1.96 or $> +1.96$, the null hypothesis is rejected and the alternative hypothesis is taken (DeLong et al., 1988). The Kruskal-Wallis is a similar test used for comparison of more than 2 groups, or 'k' groups. The test is applied to give an overall statistic for differences between the k groups, then another statistic for each single group to group comparison is also calculated.

2.2.3: Spearman's rank correlation coefficient

The Spearman's rank correlation coefficient is a statistical test to assess how closely the trend in one set of data can be expressed as a function of that of another. It explores whether there is a monotonic relationship between the two data sets or not (Choi, 1977).

The data in each group is ranked in order of magnitude. Labelling one group x and the other y, the difference, d, between the ranks is calculated for each measurement, always in the order of $d = x \text{ rank} - y \text{ rank}$. As a test of accuracy, the total of the differences should be zero. The differences in the ranks are then squared and then the squares are totalled. The Spearman's Rank value, r_s , is calculated using the following formula:

$$r_s = 1 - \frac{6 \sum d^2}{n(n^2 - 1)}$$

The Spearman's Rank table displays the minimum required r_s value for a certain confidence interval required and for a given number of values, n . If the calculated r_s is greater than that displayed in the table, then there is a statistically significant monotonic relationship between the 2 data sets (Rozeboom).

This test is used when data is not normally distributed or has outliers because the outcome is based rank rather than data values (Choi, 1977).

6.2.3: Methods Implementation

All statistical analysis are carried out using IBM SPSS Statistics 24 software.

Tests for normality including skewness, kurtosis, Kolmogorov-Smirnov and Shapiro Wilk were carried out on all continuous data sets to determine the types of follow-up analyses which could be used.

The Mann Whitney test was carried out on all nominal data, this being: cohort, gender, ANA status, AMA status and responder/non-responder status, to compare differences between groups within this data set.

Spearman's Rank correlation was carried out on all scale data sets, those being all continuous data sets, in order to assess all correlations between data.

A multivariate regression and multinomial logarithmic regression were then carried out to determine the extent of the importance of factors discovered to be significant in previous analyses and to assess the relevance of the data.

6.2.3.1: Regression analysis using R and R studio

Once preliminary statistical analyses have been carried out, including Mann Whitney and Spearman's Rank, then those factors deemed significant can be selected for regression analysis. A multivariate linear regression is carried out when the dependent variable, for example response, can be considered numerical, or continuous data, whereas a multinomial logarithmic regression is carried out if the dependent variable is binary or nominal, for example one of 2 possibilities: 'responder' or 'not responder'. These analyses can indicate the weight that certain factors can have in ascertaining the likelihood of the independent variable outcome.

6.2.3.2: Error correction

The more statistical comparisons that are made, the greater the chance is of a 'Type 1 error'. A type 1 error occurs when a null hypothesis is wrongly rejected, or a difference is taken to be significant when it is not. The likelihood of obtaining a type 1 error increases with the number of comparisons made on a data set. For comparison between groups, the

significance level must be altered based on the number of comparisons. For a number, k , of groups, the original significance level is divided by the answer to $k(k-1)/2$, to give the new significance level, α . For Mann Whitney analysis where only 2 groups are compared, this is $2(2-1)/2 = 1$, so the p value is maintained. For Kruskal-Wallis, if there are 3 groups then the α for 95% confidence becomes $0.05/(3(3-1)/2) = 0.0167$.

6.3: Results

6.3.1: Normal Distribution

Normal distribution tests were carried out on absorbance values from ELISA screens outlined in chapter 5, and were also carried out on data for dependent variables in data obtained in the patient information.

Tables 6.3.1.1 to 6.3.1.5 show the results for calculation of normal distribution criteria. Skewness and Kurtosis are considered such that normal distribution can be considered for rejection if the z value, calculated by the statistic divided by standard error, is below -1.96 or above $+1.96$ for 95% confidence. Shapiro-Wilk (S-W) and Kolmogorov-Smirnov (K-S) tests for normality are factors which can be used for rejection of the null hypothesis for normally distributed data if the p value is below 0.05, indicating there is only a 5% chance that the data happen to be unlike the normal distribution model by chance and not because they do not actually fit the model. Values which can be used to consider rejection of the null hypothesis for a data set of normal distribution are shown with a grey background. To carry out parametric analysis between responder and non-responder groups, both responder and non-responder data must satisfy the null hypothesis. Normal distribution for all data ungrouped was also carried out to determine if parametric correlation analyses could be carried out. Data was also tested for outliers. Outliers were kept in for analysis because the eventual aim of the grouping of PBC patients across all studies is to eventually design therapies which can work for all PBC patients. Therefore, they must be taken into consideration when attempting to sub-group patients.

As can be seen by tables 6.3.1.1 to 6.3.1.5, for most data sets there is at least one criterion which is suggestive that the null hypothesis for normal distribution should be rejected. For example, bilirubin levels for responder patients have an extremely high kurtosis statistic of 37.045, and a relatively low standard error of 0.668, and corresponding z value of 55.457. The kurtosis is a measure of how much of the data resides within the tails of the distribution, therefore a high kurtosis indicates that much of the data resides in the tails. 55.457 is far out of the range of $-1.96 < z < +1.96$, therefore the null hypothesis cannot be assumed as the data does not enough resemble the 'bell shape' with such a heavy distribution of data at the extremes. ALP for all patients has a skewness value of 2.407 and a standard error of 0.291, therefore the z value of skewness per unit standard error is 8.271, again outside the range

of $-1.96 < z < +1.96$, therefore the data shows too much of a positive skew for it to be classified as normally distributed. rhE2IgE data for responders is one example of a data set where the data do not fit the normal distribution by K-S or S-W criteria ($p=0.000$; $p=0.000$ respectively). Therefore, when calculations are carried out to determine if the data are similar enough to hypothetical normal distribution data, there is a less than 0.1% likelihood of observing the data in its distribution if the data is in fact normally distributed, therefore with a confidence interval of 95% the null hypothesis is rejected and this data is assumed to be not normally distributed.

As there are very few data sets which do fit the normal distribution, non-parametric tests will be carried out throughout this chapter.

		All patients											
		Skewness			Kurtosis			K-S.		S-W.		Outliers	
		Stat.	S.E.	z	Stat.	S.E.	z	Stat	p	Stat	p	Upper	Lower
rhE2	IgGall	-0.982	0.302	-3.25166	0.564	0.595	0.947899	0.142	0.003	0.914	0		2,4,38,34,3.
	IgG1	0.144	0.302	0.476821	-1.174	0.595	-1.97311	0.095	0.2	0.951	0.014		None
	IgG2	-0.183	0.302	-0.60596	-1.071	0.595	-1.8	0.121	0.023	0.956	0.016		None
	IgG3	-0.479	0.302	-1.58609	-1.51	0.595	-2.53782	0.208	0	0.827	0		None
	IgG4	2.614	0.302	8.655629	8.852	0.595	14.87731	0.257	0	0.649	0	57,71,76,79,16,64,59.	
	IgA	0.737	0.302	2.440397	-0.603	0.595	-1.01345	0.158	0	0.891	0		None
	IgM	0.12	0.302	0.397351	-1.61	0.595	-2.70588	0.197	0	0.886	0		None
	IgE	1.239	0.302	4.102649	0.238	0.595	0.4	0.277	0	0.762	0		45
rhE2ILD	IgGall	-0.697	0.302	-2.30795	-0.188	0.595	-0.31597	0.103	0.092	0.948	0.01		None
	IgG1	0.431	0.302	1.427152	-1.267	0.595	-2.12941	0.169	0	0.885	0		None
	IgG2	0.72	0.302	2.384106	-0.764	0.595	-1.28403	0.162	0	0.889	0		None
	IgG3	-0.631	0.302	-2.0894	-1.423	0.595	-2.3916	0.253	0	0.781	0		None
	IgG4	2.437	0.302	8.069536	6.222	0.595	10.45714	0.237	0	0.674	0	64,76,16,55,71,77.	
	IgA	0.326	0.302	1.07947	-1.197	0.595	-2.01176	0.119	0.028	0.917	0		None
	IgM	-0.711	0.302	-2.3543	-0.712	0.595	-1.19664	0.203	0	0.898	0		None
	IgE	0.463	0.302	1.533113	-1.247	0.595	-2.0958	0.187	0	0.877	0		None
rhE3BP	IgGall	-0.539	0.302	-1.78477	-0.359	0.595	-0.60336	0.123	0.019	0.959	0.036		None
	IgG1	2.779	0.302	9.201987	8.336	0.595	14.01008	0.316	0	0.585	0	55,57,76,79,60,71.	
	IgG2	1.277	0.302	4.228477	1.09	0.595	1.831933	0.175	0	0.861	0	7, 57.	
	IgG3	1.618	0.302	5.357616	1.76	0.595	2.957983	0.24	0	0.749	0	21,59,71,65,77.	
	IgG4	1.031	0.302	3.413907	0.008	0.595	0.013445	0.281	0	0.831	0		None
	IgA	1.32	0.302	4.370861	1.182	0.595	1.986555	0.191	0	0.859	0	27,7,16.	
	IgM	0.064	0.302	0.211921	-1.365	0.595	-2.29412	0.117	0.032	0.934	0.002		None
	IgE	5.477	0.302	18.13576	35.755	0.595	60.09244	0.305	0	0.436	0	21,18,45,76,40,64,55.	
bE2/E3BP	IgGall	-0.388	0.302	-1.28477	-0.32	0.595	-0.53782	0.097	0.2	0.977	0.285		None

Table 6.3.1.1: Normal distribution assessment of autoantibody readings for all PBC patients

Assessments of normal distribution were carried out using the Kolmogorov-Smirnov (K-S) test and the Shapiro-Wilks (S-W) test.

Assessments for skewness and kurtosis were also carried out to assess whether the data was weighted towards one side or not and the weight of the data in the tails were also carried out.

Values in grey squares indicate criteria for which the null hypothesis of normally distributed data is rejected.

		Responders													
		Skewness			Kurtosis			K-S.		S-W.		Outliers			
		Stat.	S.E.	z	Stat.	S.E.	z	Stat	p	Stat	p	Upper	Lower		
	IgGall	-0.722	0.374	-1.93048	0.148	0.733	0.20191	0.131	0.079	0.944	0.049	None			
	IgG1	0.414	0.374	1.106952	-1.047	0.733	-1.42838	0.128	0.094	0.931	0.018	None			
	IgG2	0.188	0.374	0.502674	-1.104	0.733	-1.50614	0.129	0.091	0.95	0.073	None			
	IgG3	-0.219	0.374	-0.58556	-1.753	0.733	-2.39154	0.203	0.000	0.831	0.000	None			
	IgG4	2.723	0.374	7.280749	9.393	0.733	12.81446	0.253	0.000	0.651	0.000	57, 55, 79, 76.			
	IgA	0.977	0.374	2.612299	-0.219	0.733	-0.29877	0.176	0.003	0.852	0.000	None			
	IgM	0.458	0.374	1.224599	-1.449	0.733	-1.97681	0.228	0.000	0.86	0.000	None			
rhE2	IgE	1.813	0.374	4.847594	2.463	0.733	3.360164	0.314	0.000	0.685	0.000	45, 29, 55, 64.			
	IgGall	-0.534	0.374	-1.42781	-0.67	0.733	-0.91405	0.128	0.097	0.945	0.051	None			
	IgG1	0.399	0.374	1.066845	-1.22	0.733	-1.66439	0.149	0.025	0.906	0.003	None			
	IgG2	0.667	0.374	1.783422	-0.958	0.733	-1.30696	0.202	0.000	0.878	0.000	None			
	IgG3	-0.333	0.374	-0.89037	-1.777	0.733	-2.42428	0.229	0.000	0.796	0.000	None			
	IgG4	2.618	0.374	7	7.415	0.733	10.11596	0.235	0.000	0.671	0.000	64, 76, 55.			
	IgA	0.512	0.374	1.368984	-1.074	0.733	-1.46521	0.14	0.048	0.895	0.001	None			
	IgM	-0.744	0.374	-1.9893	-0.626	0.733	-0.85402	0.191	0.001	0.893	0.001	None			
rhE2ILD	IgE	0.559	0.374	1.494652	-1.274	0.733	-1.73806	0.209	0.000	0.842	0.000	None			
	IgGall	-0.322	0.374	-0.86096	-0.302	0.733	-0.41201	0.091	0.200	0.979	0.658	None			
	IgG1	2.307	0.374	6.168449	5.332	0.733	7.274216	0.275	0.000	0.653	0.000	55, 57, 76, 79, 60.			
	IgG2	1.27	0.374	3.395722	1.168	0.733	1.593452	0.184	0.001	0.864	0.000		57		
	IgG3	1.875	0.374	5.013369	3.155	0.733	4.304229	0.25	0.000	0.73	0.000	70, 76, 65, 59.			
	IgG4	1.287	0.374	3.441176	1.199	0.733	1.635744	0.289	0.000	0.811	0.000		67		
	IgA	1.311	0.374	3.505348	0.374	0.733	0.510232	0.178	0.003	0.853	0.000	45, 29, 5, 33, 47.			
	IgM	0.185	0.374	0.494652	-1.169	0.733	-1.59482	0.1	0.200	0.942	0.042	None			
rhE3BP	IgE	2.075	0.374	5.548128	4.276	0.733	5.833561	0.207	0.000	0.743	0.000	76, 46, 64, 55.			
bE2/E3BP	IgGall	-0.627	0.374	-1.67647	0.056	0.733	0.076398	0.094	0.200	0.96	0.162	None			

Table 6.3.1.2: Normal distribution assessment of autoantibody readings for the responder group of PBC patients.

Assessments of normal distribution were carried out using the Kolmogorov-Smirnov (K-S) test and the Shapiro-Wilks (S-W) test.

Assessments for skewness and kurtosis were also carried out to assess whether the data was weighted towards one side or not and the weight of the data in the tails were also carried out.

Values in grey squares indicate criteria for which the null hypothesis of normally distributed data is rejected.

Non-responders		Skewness			Kurtosis			K-S.		S-W.		Outliers	
		Stat.	S.E.	z	Stat.	S.E.	z	Stat	p	Stat	p	Upper	Lower
	IgGall	-2.826	0.616	-4.58766	8.597	1.191	7.218304	0.306	0.002	0.615	0.000		20, 49.
	IgG1	0.124	0.616	0.201299	-1.1	1.191	-0.92359	0.147	0.200	0.979	0.658	None	
	IgG2	-0.909	0.616	-1.47565	0.705	1.191	0.59194	0.198	0.170	0.926	0.302		50
	IgG3	-1.741	0.616	-2.8263	1.984	1.191	1.665827	0.307	0.002	0.725	0.001		49, 26.
	IgG4	1.472	0.616	2.38961	0.505	1.191	0.424013	0.328	0.000	0.665	0.000	50, 77, 61.	
	IgA	0.061	0.616	0.099026	-1.713	1.191	-1.43829	0.179	0.200	0.884	0.082	None	
	IgM	-0.604	0.616	-0.98052	-1.496	1.191	-1.25609	0.244	0.033	0.832	0.017	None	
rhE2	IgE	0.499	0.616	0.810065	-1.368	1.191	-1.14861	0.199	0.165	0.888	0.092		
	IgGall	-1.204	0.616	-1.95455	2.37	1.191	1.989924	0.168	0.200	0.899	0.131		49
	IgG1	0.335	0.616	0.543831	-1.724	1.191	-1.44752	0.22	0.087	0.84	0.021	None	
	IgG2	1.28	0.616	2.077922	0.154	1.191	0.129303	0.277	0.007	0.771	0.003	50, 61.	
	IgG3	-2.067	0.616	-3.35552	2.934	1.191	2.463476	0.414	0.000	0.595	0.000		49, 26.
	IgG4	1.823	0.616	2.959416	3.761	1.191	3.157851	0.273	0.009	0.757	0.002	None	
	IgA	0.028	0.616	0.045455	-1.351	1.191	-1.13434	0.126	0.200	0.94	0.461	None	
	IgM	-1.085	0.616	-1.76136	-0.09	1.191	-0.07557	0.286	0.005	0.828	0.015	None	
rhE2ILD	IgE	0.157	0.616	0.25487	-0.708	1.191	-0.59446	0.141	0.200	0.976	0.952	None	
	IgGall	-0.985	0.616	-1.59903	1.773	1.191	1.488665	0.189	0.200	0.927	0.311	21	49
	IgG1	1.785	0.616	2.897727	1.958	1.191	1.643997	0.334	0.000	0.672	0.000	61, 77.	
	IgG2	2.094	0.616	3.399351	5.37	1.191	4.508816	0.187	0.200	0.792	0.005	7	
	IgG3	1.038	0.616	1.685065	-0.115	1.191	-0.09656	0.238	0.042	0.845	0.025	None	
	IgG4	1.607	0.616	2.608766	2.107	1.191	1.769102	0.329	0.000	0.773	0.003	22	
	IgA	0.744	0.616	1.207792	-0.732	1.191	-0.61461	0.196	0.181	0.89	0.096	7	
	IgM	-0.372	0.616	-0.6039	-1.568	1.191	-1.31654	0.188	0.200	0.88	0.071	None	
rhE3BP	IgE	3.041	0.616	4.936688	9.775	1.191	8.207389	0.35	0.000	0.54	0.000	18, 21.	
bE2/E3BP	IgGall	-0.065	0.616	-0.10552	0.055	1.191	0.04618	0.152	0.200	0.977	0.963	None	

Table 6.3.1.3: Normal distribution assessment of autoantibody readings for the Non-responder group of PBC patients

Assessments of normal distribution were carried out using the Kolmogorov-Smirnov (K-S) test and the Shapiro-Wilks (S-W) test.

Assessments for skewness and kurtosis were also carried out to assess whether the data was weighted towards one side or not and the weight of the data in the tails were also carried out.

Values in grey squares indicate criteria for which the null hypothesis of normally distributed data is rejected.

Healthy volunteers		Skewness			Kurtosis			K-S.		S-W.		Outliers	
		Stat.	S.E.	z	Stat.	S.E.	z	Stat	p	Stat	p	Upper	Lower
	IgGall	0.6	0.403	1.488834	-0.175	0.788	-0.22208	0.135	0.135	0.936	0.048	None.	
	IgG1	3.612	0.403	8.962779	13.814	0.788	17.53046	0.366	0	0.438	0	26, 17, 10, 34, 7.	
	IgG2	1.783	0.403	4.424318	3.579	0.788	4.541878	0.188	0.004	0.81	0	32, 32.	
	IgG3	4.605	0.403	11.4268	23.672	0.788	30.04061	0.324	0	0.443	0	11, 22.	
	IgG4	1.165	0.403	2.890819	1.184	0.788	1.502538	0.226	0	0.844	0	6	
	IgA	3.615	0.403	8.970223	16.109	0.788	20.44289	0.244	0	0.609	0	30	
	IgM	3.303	0.403	8.19603	13.17	0.788	16.7132	0.25	0	0.62	0	24, 33, 19, 23.	
rhE2	IgE	3.038	0.403	7.538462	18.924	0.788	24.01523	0.472	0	0.39	0	16, 6.	
	IgGall	1.571	0.403	3.898263	1.94	0.788	2.461929	0.177	0.008	0.801	0	26, 18, 11, 15.	
	IgG1	0.967	0.403	2.399504	-0.236	0.788	-0.29949	0.189	0.003	0.86	0	None	
	IgG2	0.945	0.403	2.344913	0.464	0.788	0.588832	0.191	0.003	0.884	0.002	6, 15.	
	IgG3	2.244	0.403	5.568238	5.424	0.788	6.883249	0.297	0	0.711	0	11, 30, 22.	
	IgG4	1.286	0.403	3.191067	1.583	0.788	2.008883	0.18	0.007	0.882	0.002	14, 19.	
	IgA	2.021	0.403	5.014888	3.97	0.788	5.038071	0.233	0	0.717	0	18, 26.	
	IgM	1.897	0.403	4.707196	4.835	0.788	6.135787	0.256	0	0.745	0	5	
rhE2ILD	IgE	1.731	0.403	4.295285	2.663	0.788	3.379442	0.221	0	0.788	0	16, 10, 3, 12, 34.	
	IgGall	1.184	0.403	2.937965	1.014	0.788	1.286802	0.181	0.006	0.852	0	None	
	IgG1	1.171	0.403	2.905707	-0.118	0.788	-0.14975	0.294	0	0.727	0	19	
	IgG2	2.824	0.403	7.007444	10.426	0.788	13.23096	0.236	0	0.697	0	13	
	IgG3	5.384	0.403	13.3598	30.163	0.788	38.27792	0.378	0	0.29	0	11, 12, 8, 18, 6.	
	IgG4	2.413	0.403	5.987593	4.928	0.788	6.253807	0.4	0	0.534	0	2, 11, 1, 6, 3, 7.	
	IgA	2.837	0.403	7.039702	11.308	0.788	14.35025	0.171	0.013	0.74	0	2, 25.	
	IgM	1.29	0.403	3.200993	1.695	0.788	2.151015	0.189	0.003	0.896	0.004	5	
rhE3BP	IgE	3.486	0.403	8.650124	12.655	0.788	16.05964	0.306	0	0.491	0	4, 27, 6.	

Table 6.3.1.4: Normal distribution assessment of autoantibody readings for all healthy volunteers

Assessments of normal distribution were carried out using the Kolmogorov-Smirnov (K-S) test and the Shapiro-Wilks (S-W) test.

Assessments for skewness and kurtosis were also carried out to assess whether the data was weighted towards one side or not and the weight of the data in the tails were also carried out.

Values in grey squares indicate criteria for which the null hypothesis of normally distributed data is rejected.

Responders:	Skewness			Kurtosis			K-S.		S-W.		Outliers	
	Stat.	S.E.	z	Stat.	S.E.	z	Stat	p	Stat	p	upper	lower
Age	-0.087	0.350	-0.24857	0.461	0.688	0.670058	0.118	0.114	0.976	0.439	20	
Weight	2.036	0.383	5.315927	8.195	0.750	10.92667	0.163	0.012	0.841	0.000	42	
Yrs diagnosed	0.522	0.347	1.504323	-0.699	0.681	-1.02643	0.112	0.176	0.944	0.025	None	
Age Diagnosed	-1.088	0.536	-2.02985	1.406	1.038	1.354528	0.207	0.040	0.916	0.112		39
Yrs on UDCA	0.458	0.357	1.282913	-0.974	0.702	-1.38746	0.130	0.062	0.933	0.013	None	
UDCA mg/kg	-0.45	0.388	-1.15979	0.627	0.759	0.826087	0.106	0.200	0.971	0.429	None	
Bilirubin	5.762	0.340	16.94706	37.045	0.668	55.45659	0.290	0.000	0.396	0.000	29, 76.	
ALP	1.633	0.340	4.802941	5.389	0.668	8.067365	0.113	0.154	0.886	0.000	76	
ALT	0.694	0.340	2.041176	-0.282	0.668	-0.42216	0.122	0.068	0.941	0.017	39	
Non-responders	Skewness			Kurtosis			K-S.		S-W.		Outliers	
	Stat.	S.E.	z	Stat.	S.E.	z	Stat	p	Stat	p	upper	lower
Age	1.205	0.687	1.754003	2	1.334	1.49925	0.149	0.2	0.914	0.31	13, 44, 47.	2
Weight	0.548	0.717	0.764296	-0.407	1.4	-0.29071	0.175	0.2	0.938	0.56	50	
Yrs diagnosed	2.378	0.717	3.316597	6.235	1.4	4.453571	0.273	0.053	0.71	0.002	49	
Age Diagnosed	0.085	0.913	0.0931	-1.981	2	-0.9905	0.257	0.2	0.904	0.435	None	
Yrs on UDCA	1.317	0.717	1.83682	1.593	1.4	1.137857	0.209	0.2	0.888	0.19	22	
UDCA mg/kg	-1.364	0.717	-1.90237	1.394	1.4	0.995714	0.255	0.094	0.848	0.072	None	
Bilirubin	0.277	0.58	0.477586	8.322	1.121	7.423729	0.282	0.002	0.657	0	61	
ALP	1.93	0.58	3.327586	4.086	1.121	3.64496	0.224	0.041	0.793	0.003	7, 77.	
ALT	0.521	0.58	0.898276	-0.894	1.121	-0.7975	0.134	0.2	0.926	0.24	None	
All Patients	Skewness			Kurtosis			K-S.		S-W.		Outliers	
	Stat.	S.E.	z	Stat.	S.E.	z	Stat	p	Stat	p	upper	lower
Age	-0.102	0.293	-0.34812	-0.167	0.578	-0.28893	0.095	0.200	0.983	0.515	None	
Weight	1.853	0.319	5.808777	8.095	0.628	12.89013	0.127	0.025	0.869	0	42	
Yrs diagnosed	0.755	0.291	2.594502	0.051	0.574	0.08885	0.105	0.062	0.942	0.004	49	
Age Diagnosed	-0.334	0.427	-0.7822	-0.62	0.833	-0.7443	0.169	0.029	0.964	0.381	None	
Yrs on UDCA	0.611	0.306	1.996732	-0.762	0.604	-1.26159	0.136	0.007	0.92	0.001	None	
UDCA mg/kg	-1.469	0.325	-4.52	2.961	0.639	4.633803	0.144	0.007	0.885	0	15, 7.	
Bilirubin	4.974	0.291	17.09278	29.157	0.574	50.79617	0.277	0.000	0.475	0	76, 61, 26, 40, 29.	
ALP	2.407	0.291	8.271478	7.886	0.574	13.73868	0.201	0.000	0.766	0	7, 77, 18, 10, 11.	
ALT	2.05	0.291	7.044674	4.008	0.574	6.982578	0.216	0.000	0.746	0	78, 10, 18, 40, 61, 77, 7, 58.	

Table 6.1.3.5: Normal distribution assessment of hospital-recorded data for all PBC patients and the groups of responders and non-responders.

Assessments of normal distribution were carried out using the Kolmogorov-Smirnov (K-S) test and the Shapiro-Wilks (S-W) test.

Assessments for skewness and kurtosis were also carried out to assess whether the data was weighted towards one side or not and the weight of the data in the tails were also carried out.

Values in grey squares indicate criteria for which the null hypothesis of normally distributed data is rejected.

6.3.2: Spearman's Rank Correlation Coefficient

All variables were tested against each other for a significant positive or negative correlation by Spearman's Rank Correlation Coefficient. Coefficients and p-values are shown in tables 6.3.2.1 and 6.3.2.2 and scatter graphs with the line of best fit indicating the relevant R^2 value are included in the appendix.

Significant findings for patient data are positive correlations between age and years since diagnosis; age and age at diagnosis; age and years since UDCA treatment began; bilirubin and ALT; bilirubin and ALP; ALT and ALP. There were significant negative correlations between age and ALP; age and ALT.

Comparing each data set with the others can indicate relationships which may be of interest in responder/non-responder categorising.

Spearman's rank correlation was carried out to compare all continuous data with other continuous data. This stage is equivalent to carrying out a 'scatter plot matrix' which precedes a multivariate or multinomial regression analysis. To have insight into which characteristics may be exerting an influence on each other before factoring in the grouping of interest, for example whether a patient is a responder or non-responder, can highlight where inclusion of more than one of these factors may be redundant and also which factors are likely influencing the outcome on their own. For example, if age correlates strongly and positively with weight, then weight and age may not necessarily contribute an original influence into whether or not a patient is a responder to UDCA and it would be redundant to use both age and weight in the regression stage.

Table 6.3.2.1 shows the results of patient data gathered at the Freeman hospital where all factors are analysed against each other in Spearman's Rank correlation analysis. Generally, where the r_s value is between 0.00-0.19, there is a very weak correlation, between 0.2-0.39 indicates weak correlation, 0.4-0.59 indicates a moderate correlation, 0.6-0.79 indicates a strong correlation and 0.8-1 indicates a very strong correlation. The p value indicates the likelihood of observing this correlation if the null hypothesis of no correlation were true. Age shows a positive correlation with years since diagnosis, age at diagnosis and years since UDCA therapy began, with p values all below 0.05 ($p=0.012$, 0.000, 0.022 respectively) but only weak correlations with years since diagnosis and years since UDCA therapy began, ($r_s= 0.309$ and 0.295 respectively) but a very strong correlation with age at diagnosis ($r_s = 0.819$).

Years since diagnosis correlates strongly with a significant p value with years since UDCA therapy began ($r_s=0.722$, $p=0.000$).

Bilirubin shows a moderate positive correlation with both ALP and ALT ($r_s= 0.418$ and 0.445; $p=0.000$ and 0.000 respectively). ALP and ALT show a strong positive correlation ($r_s=0.727$, $p=0.000$).

No other factors appeared to show a significant correlation with each other.

Patient serum hospital-measured criteria were also correlated against serum antibody levels for an idea of if any antibodies being investigated might correlate with these data due to factors not necessarily relating to their response. For example, there is a weak negative correlation between weight and 2 IgG1 isotype antibodies, rhE2ILD ($r_s=-0.274$, $p=0.049$) and rhE3BP ($r_s=-0.351$, $p=0.016$), therefore there could be a tendency for levels of IgG1 antibody to drop as weight increases due to weight-related factors not necessarily related to disease.

Those antibody levels which appear to correlate with bilirubin, ALP and ALT may be of interest in PBC response grouping because UDCA response is assessed based on bilirubin, ALP and ALT. The table shows many potentially interesting correlations, highlighted in bold, with significant p values and weak-to-moderate correlation coefficients.

Although interesting on its own, to address the main question of this chapter, this data must be analysed in the context of the results from the Mann Whitney analysis.

Correlations										
		Weight	Age	Years since diagnosis	Age at diagnosis	Years since UDCA start	UDCA dose per kg weight	Bilirubin	ALP	ALT
Weight	Corr.Coeff.		-0.184	-0.050	-0.298	0.189	-0.137	-0.093	-0.095	-0.085
	Sig. (2-		0.178	0.715	0.157	0.176	0.323	0.522	0.511	0.558
	N		55	56	24	53	54	50	50	50
Age	Corr.Coeff.	-0.184		.309*	.819**	.295*	-0.022	-0.054	-.315*	-.348**
	Sig. (2-	0.178		0.012	0.000	0.022	0.877	0.683	0.014	0.006
	N	55		66	30	60	53	60	60	60
Years since diagnosis	Corr.Coeff.	-0.050	.309*		-0.239	.722**	-0.173	0.140	-0.047	-0.101
	Sig. (2-	0.715	0.012		0.204	0.000	0.211	0.285	0.721	0.442
	N	56	66		30	61	54	60	60	60
Age Diagnosis	Corr.Coeff.	-0.298	.819**	-0.239		-0.217	-0.234	-0.163	-0.289	-0.375
	Sig. (2-	0.157	0.000	0.204		0.278	0.271	0.425	0.152	0.059
	N	24	30	30		27	24	26	26	26
Years since UDCA start	Corr.Coeff.	0.189	.295*	.722**	-0.217		0.055	0.109	-0.083	-0.164
	Sig. (2-	0.176	0.022	0.000	0.278		0.698	0.424	0.545	0.227
	N	53	60	61	27		52	56	56	56
UDCA dose per kg weight	Corr.Coeff.	-0.137	-0.022	-0.173	-0.234	0.055		-0.069	0.002	0.145
	Sig. (2-	0.323	0.877	0.211	0.271	0.698		0.638	0.989	0.320
	N	54	53	54	24	52		49	49	49
Bilirubin	Corr.Coeff.	-0.093	-0.054	0.140	-0.163	0.109	-0.069		.418**	.445**
	Sig. (2-	0.522	0.683	0.285	0.425	0.424	0.638		0.000	0.000
	N	50	60	60	26	56	49		68	68
ALP	Corr.Coeff.	-0.095	-.315*	-0.047	-0.289	-0.083	0.002	.418**		.727**
	Sig. (2-	0.511	0.014	0.721	0.152	0.545	0.989	0.000		0.000
	N	50	60	60	26	56	49	68		68
ALT	Corr.Coeff.	-0.085	-.348**	-0.101	-0.375	-0.164	0.145	.445**	.727**	
	Sig. (2-	0.558	0.006	0.442	0.059	0.227	0.320	0.000	0.000	
	N	50	60	60	26	56	49	68	68	

*. Correlation is significant at the 0.05 level (2-tailed).

** Correlation is significant at the 0.01 level (2-tailed).

Table 6.3.2.1: Table of correlations for patient data

This table shows the results from Spearman's Rank Correlation Coefficient analysis between patient data. 2-tailed analysis is used because both positive and negative relationships are being investigated. 'Tails' can be likened to a skew in the data and a skew in either direction would be relevant.

Significant findings are shown in bold.

Key –

Corr.Coeff.: Correlation Coefficient

Sig.(2-: Statistical significance, or p-value, based on 2-tailed analysis.

N: Number of data sets in the analysis.

Correlations

	rHE2 IgGall	rHE2IL2 IgGall	rHE3BP IgGall	rHE2 IgG1	rHE2IL2 IgG1	rHE3BP IgG1	rHE2 IgG2	rHE2IL2 IgG2	rHE3BP IgG2	rHE2 IgG3	rHE2IL2 IgG3	rHE3BP IgG3	rHE2 IgG4	rHE2IL2 IgG4	rHE3BP IgG4	rHE2 IgA	rHE2IL2 IgA	rHE3BP IgA	rHE2 IgM	rHE2IL2 IgM	rHE3BP IgM	rHE2 IgE	rHE2IL2 IgE	rHE3BP IgE
Age	Corr.Coeff. 0.031	Corr.Coeff. 0.047	Corr.Coeff. 0.023	Corr.Coeff. 0.074	Corr.Coeff. 0.027	Corr.Coeff. 0.074	Corr.Coeff. -0.145	Corr.Coeff. -0.185	Corr.Coeff. -0.030	Corr.Coeff. -0.029	Corr.Coeff. -0.038	Corr.Coeff. 0.015	Corr.Coeff. 0.024	Corr.Coeff. 0.054	Corr.Coeff. 0.011	Corr.Coeff. 0.011	Corr.Coeff. 0.011	Corr.Coeff. -0.095	Corr.Coeff. -0.106	Corr.Coeff. -0.087	Corr.Coeff. -0.091	Corr.Coeff. -0.070	Corr.Coeff. -0.008	
	Sig.(2-tailed) 0.806	Sig.(2-tailed) 0.705	Sig.(2-tailed) 0.853	Sig.(2-tailed) 0.833	Sig.(2-tailed) 0.833	Sig.(2-tailed) 0.833	Sig.(2-tailed) 0.250	Sig.(2-tailed) 0.153	Sig.(2-tailed) 0.827	Sig.(2-tailed) 0.817	Sig.(2-tailed) 0.773	Sig.(2-tailed) 0.912	Sig.(2-tailed) 0.794	Sig.(2-tailed) 0.667	Sig.(2-tailed) 0.930	Sig.(2-tailed) 0.930	Sig.(2-tailed) 0.847	Sig.(2-tailed) 0.444	Sig.(2-tailed) 0.411	Sig.(2-tailed) 0.485	Sig.(2-tailed) 0.462	Sig.(2-tailed) 0.937	Sig.(2-tailed) 0.946	
	N 67	N 67	N 67	N 63	N 65	N 61	N 65	N 61	N 57	N 65	N 60	N 57	N 62	N 67	N 67	N 62	N 67	N 67	N 62	N 67	N 67	N 67	N 67	
UDCAdo sepe/kg weight	Corr.Coeff. 0.120	Corr.Coeff. 0.076	Corr.Coeff. 0.201	Corr.Coeff. 0.055	Corr.Coeff. 0.187	Corr.Coeff. 0.187	Corr.Coeff. 0.093	Corr.Coeff. 0.156	Corr.Coeff. 0.328*	Corr.Coeff. 0.236	Corr.Coeff. 0.176	Corr.Coeff. 0.293	Corr.Coeff. 0.132	Corr.Coeff. 0.154	Corr.Coeff. -0.006	Corr.Coeff. 0.072	Corr.Coeff. 0.037	Corr.Coeff. 0.047	Corr.Coeff. 0.059	Corr.Coeff. -0.016	Corr.Coeff. 0.328*	Corr.Coeff. 0.254	Corr.Coeff. 0.255	
	Sig.(2-tailed) 0.366	Sig.(2-tailed) 0.566	Sig.(2-tailed) 0.146	Sig.(2-tailed) 0.700	Sig.(2-tailed) 0.194	Sig.(2-tailed) 0.194	Sig.(2-tailed) 0.312	Sig.(2-tailed) 0.288	Sig.(2-tailed) 0.028	Sig.(2-tailed) 0.091	Sig.(2-tailed) 0.232	Sig.(2-tailed) 0.051	Sig.(2-tailed) 0.204	Sig.(2-tailed) 0.275	Sig.(2-tailed) 0.964	Sig.(2-tailed) 0.607	Sig.(2-tailed) 0.689	Sig.(2-tailed) 0.737	Sig.(2-tailed) 0.689	Sig.(2-tailed) 0.306	Sig.(2-tailed) 0.016	Sig.(2-tailed) 0.064	Sig.(2-tailed) 0.062	
	N 54	N 54	N 54	N 52	N 48	N 45	N 52	N 48	N 45	N 52	N 47	N 45	N 49	N 54	N 54	N 49	N 54	N 54	N 49	N 54	N 54	N 54	N 54	
Weight	Corr.Coeff. -0.116	Corr.Coeff. -0.061	Corr.Coeff. -0.032	Corr.Coeff. -0.070	Corr.Coeff. -0.274*	Corr.Coeff. -0.351*	Corr.Coeff. 0.014	Corr.Coeff. -0.212	Corr.Coeff. -0.056	Corr.Coeff. -0.081	Corr.Coeff. -0.152	Corr.Coeff. -0.287	Corr.Coeff. -0.042	Corr.Coeff. 0.124	Corr.Coeff. -0.006	Corr.Coeff. 0.124	Corr.Coeff. 0.124	Corr.Coeff. 0.100	Corr.Coeff. 0.205	Corr.Coeff. -0.112	Corr.Coeff. -0.112	Corr.Coeff. 0.015	Corr.Coeff. 0.000	
	Sig.(2-tailed) 0.395	Sig.(2-tailed) 0.656	Sig.(2-tailed) 0.501	Sig.(2-tailed) 0.614	Sig.(2-tailed) 0.043	Sig.(2-tailed) 0.043	Sig.(2-tailed) 0.919	Sig.(2-tailed) 0.133	Sig.(2-tailed) 0.711	Sig.(2-tailed) 0.559	Sig.(2-tailed) 0.232	Sig.(2-tailed) 0.936	Sig.(2-tailed) 0.642	Sig.(2-tailed) 0.775	Sig.(2-tailed) 0.364	Sig.(2-tailed) 0.364	Sig.(2-tailed) 0.361	Sig.(2-tailed) 0.770	Sig.(2-tailed) 0.464	Sig.(2-tailed) 0.409	Sig.(2-tailed) 0.409	Sig.(2-tailed) 0.915	Sig.(2-tailed) 0.998	
	N 56	N 56	N 56	N 54	N 52	N 47	N 54	N 50	N 47	N 54	N 49	N 47	N 56	N 51	N 56									
YrsSinc e/Day	Corr.Coeff. 0.256	Corr.Coeff. 0.232	Corr.Coeff. 0.278	Corr.Coeff. 0.242	Corr.Coeff. 0.178	Corr.Coeff. 0.242	Corr.Coeff. 0.128	Corr.Coeff. 0.083	Corr.Coeff. -0.029	Corr.Coeff. 0.194	Corr.Coeff. 0.182	Corr.Coeff. -0.069	Corr.Coeff. -0.038	Corr.Coeff. 0.234	Corr.Coeff. 0.127	Corr.Coeff. 0.122	Corr.Coeff. 0.063	Corr.Coeff. 0.039	Corr.Coeff. 0.001	Corr.Coeff. 0.179	Corr.Coeff. 0.174	Corr.Coeff. 0.071	Corr.Coeff. 0.200	
	Sig.(2-tailed) 0.035	Sig.(2-tailed) 0.057	Sig.(2-tailed) 0.022	Sig.(2-tailed) 0.050	Sig.(2-tailed) 0.160	Sig.(2-tailed) 0.160	Sig.(2-tailed) 0.305	Sig.(2-tailed) 0.522	Sig.(2-tailed) 0.827	Sig.(2-tailed) 0.118	Sig.(2-tailed) 0.156	Sig.(2-tailed) 0.607	Sig.(2-tailed) 0.762	Sig.(2-tailed) 0.070	Sig.(2-tailed) 0.341	Sig.(2-tailed) 0.323	Sig.(2-tailed) 0.607	Sig.(2-tailed) 0.759	Sig.(2-tailed) 0.994	Sig.(2-tailed) 0.144	Sig.(2-tailed) 0.156	Sig.(2-tailed) 0.585	Sig.(2-tailed) 0.102	
	N 68	N 68	N 68	N 66	N 64	N 58	N 66	N 62	N 58	N 66	N 62	N 58	N 66	N 61	N 58	N 68	N 68	N 68	N 63	N 68	N 68	N 68	N 68	
Age/Day nosis	Corr.Coeff. -0.258	Corr.Coeff. -0.266	Corr.Coeff. -0.256	Corr.Coeff. -0.139	Corr.Coeff. -0.007	Corr.Coeff. -0.125	Corr.Coeff. -0.429*	Corr.Coeff. 0.018	Corr.Coeff. -0.274	Corr.Coeff. -0.307	Corr.Coeff. -0.249	Corr.Coeff. -0.023	Corr.Coeff. -0.163	Corr.Coeff. -0.253	Corr.Coeff. -0.150	Corr.Coeff. -0.166	Corr.Coeff. -0.172	Corr.Coeff. -0.435*	Corr.Coeff. -0.260	Corr.Coeff. -0.173	Corr.Coeff. -0.369*	Corr.Coeff. -0.350	Corr.Coeff. -0.060	
	Sig.(2-tailed) 0.168	Sig.(2-tailed) 0.155	Sig.(2-tailed) 0.171	Sig.(2-tailed) 0.463	Sig.(2-tailed) 0.969	Sig.(2-tailed) 0.533	Sig.(2-tailed) 0.077	Sig.(2-tailed) 0.166	Sig.(2-tailed) 0.099	Sig.(2-tailed) 0.932	Sig.(2-tailed) 0.932	Sig.(2-tailed) 0.311	Sig.(2-tailed) 0.390	Sig.(2-tailed) 0.185	Sig.(2-tailed) 0.454	Sig.(2-tailed) 0.381	Sig.(2-tailed) 0.384	Sig.(2-tailed) 0.018	Sig.(2-tailed) 0.166	Sig.(2-tailed) 0.362	Sig.(2-tailed) 0.045	Sig.(2-tailed) 0.058	Sig.(2-tailed) 0.751	
	N 30	N 27	N 30	N 29	N 27	N 30	N 29	N 27	N 30	N 29	N 27	N 30	N 30	N 29	N 30									
YrsSinc e/UDCAS tart	Corr.Coeff. 0.291	Corr.Coeff. 0.325	Corr.Coeff. 0.322	Corr.Coeff. 0.181	Corr.Coeff. 0.130	Corr.Coeff. -0.019	Corr.Coeff. -0.002	Corr.Coeff. 0.026	Corr.Coeff. 0.257*	Corr.Coeff. 0.221	Corr.Coeff. 0.159	Corr.Coeff. 0.024	Corr.Coeff. 0.157	Corr.Coeff. 0.151	Corr.Coeff. 0.168	Corr.Coeff. 0.190	Corr.Coeff. 0.190	Corr.Coeff. 0.015	Corr.Coeff. 0.168	Corr.Coeff. 0.015	Corr.Coeff. 0.206	Corr.Coeff. 0.206	Corr.Coeff. 0.093	
	Sig.(2-tailed) 0.023	Sig.(2-tailed) 0.010	Sig.(2-tailed) 0.011	Sig.(2-tailed) 0.170	Sig.(2-tailed) 0.335	Sig.(2-tailed) 0.891	Sig.(2-tailed) 0.932	Sig.(2-tailed) 0.990	Sig.(2-tailed) 0.050	Sig.(2-tailed) 0.004	Sig.(2-tailed) 0.251	Sig.(2-tailed) 0.866	Sig.(2-tailed) 0.228	Sig.(2-tailed) 0.245	Sig.(2-tailed) 0.213	Sig.(2-tailed) 0.912	Sig.(2-tailed) 0.143	Sig.(2-tailed) 0.912	Sig.(2-tailed) 0.912	Sig.(2-tailed) 0.011	Sig.(2-tailed) 0.111	Sig.(2-tailed) 0.111	Sig.(2-tailed) 0.476	
	N 61	N 61	N 61	N 59	N 57	N 52	N 59	N 55	N 52	N 59	N 55	N 52	N 59	N 54	N 52	N 61	N 61	N 61	N 57	N 61	N 61	N 61	N 61	
Bilirubin	Corr.Coeff. 0.265	Corr.Coeff. 0.258	Corr.Coeff. 0.283	Corr.Coeff. 0.213	Corr.Coeff. 0.213	Corr.Coeff. 0.000	Corr.Coeff. 0.272	Corr.Coeff. 0.247	Corr.Coeff. 0.051	Corr.Coeff. 0.265	Corr.Coeff. 0.375**	Corr.Coeff. 0.122	Corr.Coeff. -0.099	Corr.Coeff. 0.137	Corr.Coeff. 0.137	Corr.Coeff. 0.265	Corr.Coeff. 0.265	Corr.Coeff. 0.044	Corr.Coeff. 0.145	Corr.Coeff. 0.213	Corr.Coeff. 0.144	Corr.Coeff. 0.304*	Corr.Coeff. 0.116	
	Sig.(2-tailed) 0.029	Sig.(2-tailed) 0.034	Sig.(2-tailed) 0.020	Sig.(2-tailed) 0.000	Sig.(2-tailed) 0.093	Sig.(2-tailed) 0.999	Sig.(2-tailed) 0.026	Sig.(2-tailed) 0.055	Sig.(2-tailed) 0.703	Sig.(2-tailed) 0.030	Sig.(2-tailed) 0.003	Sig.(2-tailed) 0.358	Sig.(2-tailed) 0.201	Sig.(2-tailed) 0.131	Sig.(2-tailed) 0.131	Sig.(2-tailed) 0.285	Sig.(2-tailed) 0.285	Sig.(2-tailed) 0.044	Sig.(2-tailed) 0.237	Sig.(2-tailed) 0.081	Sig.(2-tailed) 0.241	Sig.(2-tailed) 0.347		
	N 68	N 68	N 68	N 67	N 63	N 59	N 67	N 61	N 59	N 67	N 61	N 59	N 68											
ALP	Corr.Coeff. 0.045	Corr.Coeff. 0.102	Corr.Coeff. 0.167	Corr.Coeff. 0.226	Corr.Coeff. 0.112	Corr.Coeff. -0.015	Corr.Coeff. 0.163	Corr.Coeff. 0.283	Corr.Coeff. 0.286*	Corr.Coeff. 0.266	Corr.Coeff. 0.453**	Corr.Coeff. -0.093	Corr.Coeff. -0.182	Corr.Coeff. 0.252	Corr.Coeff. 0.252	Corr.Coeff. 0.252	Corr.Coeff. 0.252	Corr.Coeff. 0.320**	Corr.Coeff. 0.320**	Corr.Coeff. 0.194	Corr.Coeff. 0.159	Corr.Coeff. 0.284*	Corr.Coeff. 0.024	
	Sig.(2-tailed) 0.719	Sig.(2-tailed) 0.410	Sig.(2-tailed) 0.173	Sig.(2-tailed) 0.066	Sig.(2-tailed) 0.382	Sig.(2-tailed) 0.909	Sig.(2-tailed) 0.171	Sig.(2-tailed) 0.027	Sig.(2-tailed) 0.028	Sig.(2-tailed) 0.030	Sig.(2-tailed) 0.000	Sig.(2-tailed) 0.021	Sig.(2-tailed) 0.452	Sig.(2-tailed) 0.794	Sig.(2-tailed) 0.166	Sig.(2-tailed) 0.038	Sig.(2-tailed) 0.007	Sig.(2-tailed) 0.008	Sig.(2-tailed) 0.008	Sig.(2-tailed) 0.113	Sig.(2-tailed) 0.195	Sig.(2-tailed) 0.019	Sig.(2-tailed) 0.846	
	N 68	N 68	N 68	N 67	N 63	N 59	N 67	N 61	N 59	N 67	N 61	N 59	N 68											
ALT	Corr.Coeff. 0.198	Corr.Coeff. 0.204	Corr.Coeff. 0.273	Corr.Coeff. 0.216	Corr.Coeff. 0.140	Corr.Coeff. 0.053	Corr.Coeff. 0.244	Corr.Coeff. 0.366**	Corr.Coeff. 0.271	Corr.Coeff. 0.308*	Corr.Coeff. 0.454**	Corr.Coeff. -0.064	Corr.Coeff. -0.157	Corr.Coeff. 0.147	Corr.Coeff. 0.363**	Corr.Coeff. 0.147	Corr.Coeff. 0.363**	Corr.Coeff. 0.258*	Corr.Coeff. 0.293*	Corr.Coeff. 0.314**	Corr.Coeff. 0.256*	Corr.Coeff. 0.359**	Corr.Coeff. 0.129	
	Sig.(2-tailed) 0.106	Sig.(2-tailed) 0.096	Sig.(2-tailed) 0.024	Sig.(2-tailed) 0.078	Sig.(2-tailed) 0.274	Sig.(2-tailed) 0.688	Sig.(2-tailed) 0.047	Sig.(2-tailed) 0.004	Sig.(2-tailed) 0.038	Sig.(2-tailed) 0.011	Sig.(2-tailed) 0.000	Sig.(2-tailed) 0.100	Sig.(2-tailed) 0.437	Sig.(2-tailed) 0.262	Sig.(2-tailed) 0.235	Sig.(2-tailed) 0.231	Sig.(2-tailed) 0.002	Sig.(2-tailed) 0.041	Sig.(2-tailed) 0.015	Sig.(2-tailed) 0.003	Sig.(2-tailed) 0.001	Sig.(2-tailed) 0.003	Sig.(2-tailed) 0.294	
	N 68	N 68	N 68	N 67	N 63	N 59	N 67	N 61	N 59	N 67	N 61	N 59	N 68											

** Correlation is significant at the 0.01 level (2-tailed).
* Correlation is significant at the 0.05 level (2-tailed).

Table 6.3.2.2: Table of correlations for ELISA absorbance data

This table shows the results from Spearman’s Rank Correlation Coefficient analysis of patient data against ELISA data for absorbance values for the different isotypes of antibody against the different autoantigens. 2-tailed analysis is used because both positive and negative relationships are being investigated. ‘Tails’ can be likened to a skew in the data and a skew in either direction would be relevant. Significant findings are shown in bold.

Key -
Corr.Coeff.: Correlation Coefficient
Sig.(2-: Statistical significance, or p-value, based on 2-tailed analysis.
N: Number of data sets in the analysis.

6.3.3: Mann Whitney

Mann Whitney analysis was carried out as a non-parametric comparison of means based on ranked data, between nominal data groups, most importantly between responder/non-responder groups, but also to determine if AMA negative patients should be kept in for analysis and if there was likely a gender difference.

Results from the Mann Whitney are in figures 6.3.3.1 to 6.3.3.6 and also tables 6.3.3.1 and 6.3.3.2.

Firstly, antibody levels across PBC patients on the whole were carried out against healthy volunteers to determine which antibody isotypes against which antigens were raised in PBC and which were insignificant. It was found that all except the IgG4 isotypes showed significantly higher levels in PBC patients compared to healthy volunteers, therefore all except IgG4 isotypes were kept in for further analysis. Table 6.3.3.1 shows p values of 0.542, 0.958 and 0.323 comparing PBC patient levels of antirhE2IgG4, antirhE2ILD IgG4 and antirhE3BPIgG4 respectively, whereas all other p values comparing PBC patient levels to healthy control levels were 0.000 or 0.001 (rhE3BPIgG1). Then levels of the remaining antibodies were further investigated for differences between responders and non-responders. Table 6.3.3.2 shows that those showing significantly different levels between responders and non-responders are then rhE2ILD IgG3 ($p=0.010$), rhE2ILD IgA ($p=0.047$) and rhE2IgE ($p=0.025$).

Mann Whitney analysis was also carried out on hospital-obtained data and those factors where there was a difference between responder and groups were Age($p=0.002$), Age at diagnosis($p=0.030$), ALP($p=0.000$) and ALT($p=0.000$).

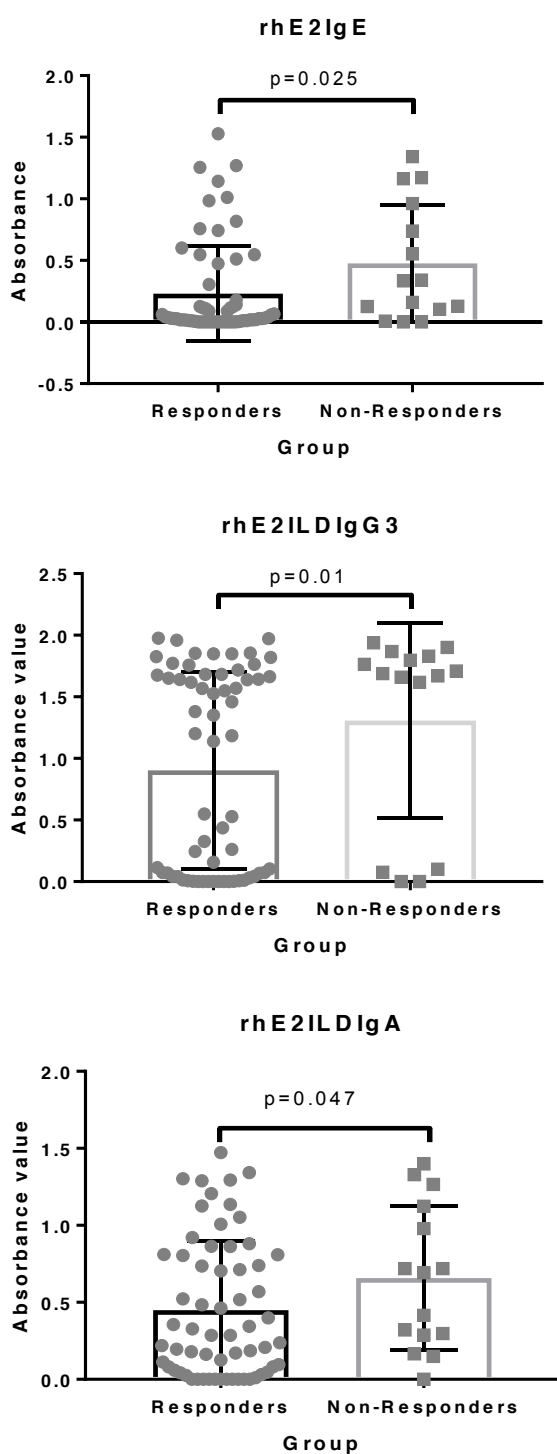


Figure 6.3.3.1: Bar charts for autoantibodies showing significant difference by Mann-Whitney comparison

The absorbance for antibodies in the ELISA assay are plotted, grouped into responders and non-responders. Those shown are those where the p value was <0.05 , giving a significant difference.

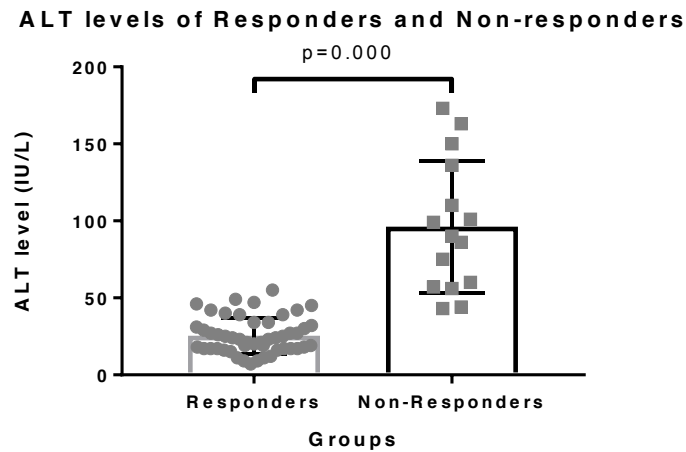
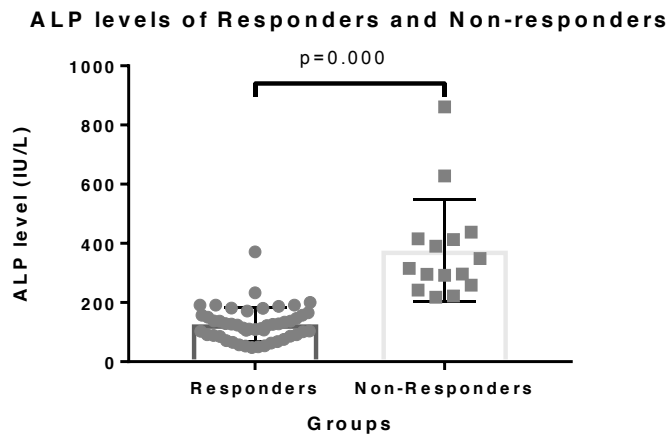
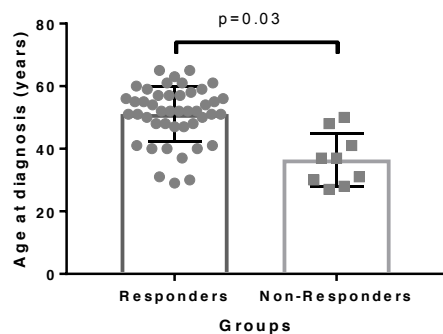
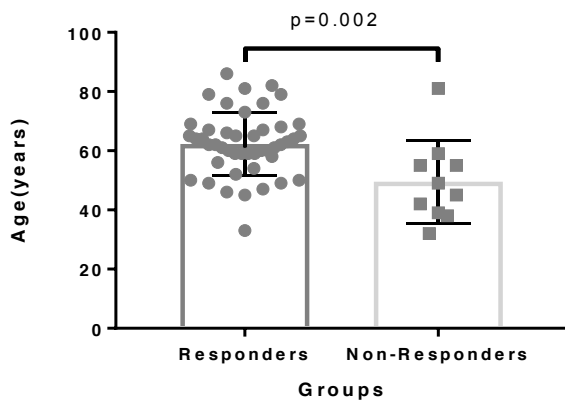


Figure 6.3.3.2: Bar charts for liver biochemistry measurements

The clinical liver data were plotted grouped into responders and non-responders. Those shown are those where the p value was <0.05 , giving a significant difference.

Ages at diagnosis of Responders and Non-responders**Ages of Responders and Non-responders****Figure 6.3.3.5: Boxplots and mean bar charts for age criteria**

The age at diagnosis and age at time of sample collection are plotted grouped into responder and non-responder groups. Those characteristics shown have a significant difference between responders and non-responders where $p < 0.05$.

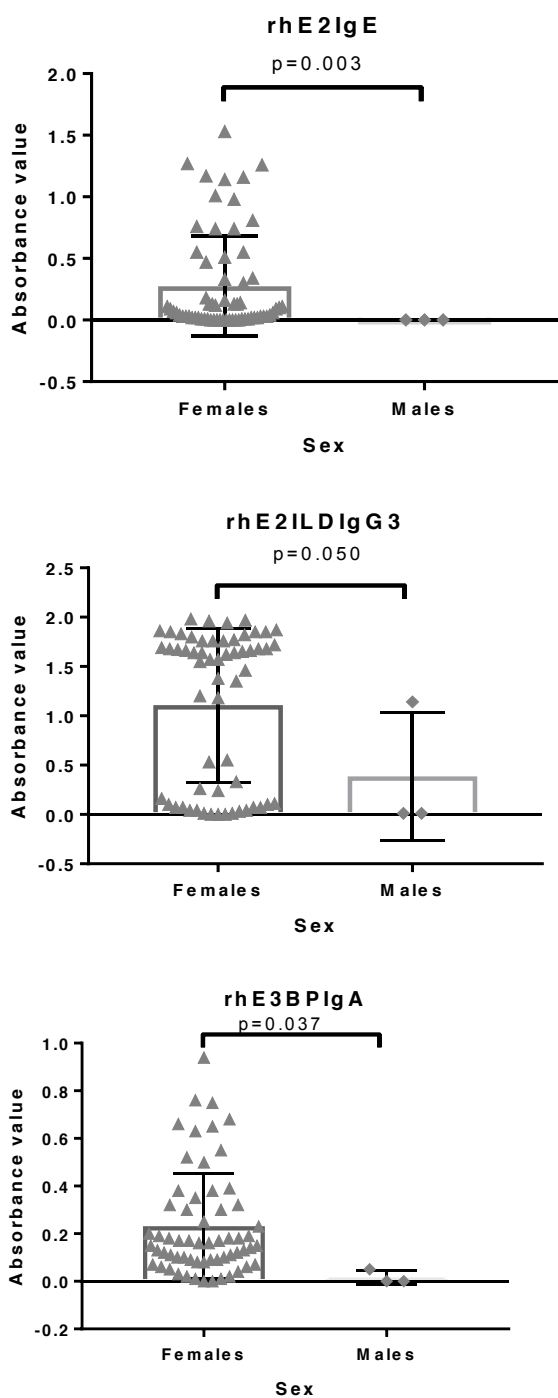


Figure 6.3.3.6: Male and female significant differences for autoantibody levels

These figures show the autoantibodies found to be significantly different in levels between males and females where $p < 0.05$.

Antibody	Healthy Controls vs PBC P value	UDCA responders vs Healthy Controls P value	Non-responders vs Healthy Controls P value	UDCA responders vs Non-responders P value
α rhE2 IgG _{all}	<0.0005	<0.0005	<0.0005	0.375
α rhE2ILD IgG _{all}	<0.0005	<0.0005	<0.0005	0.330
α rhE3BP IgG _{all}	<0.0005	<0.0005	<0.0005	0.059
α rhE2 IgG ₁	<0.0005	<0.0005	<0.0005	0.142
α rhE2ILD IgG ₁	<0.0005	<0.0005	0.003	0.845
α rhE3BP IgG ₁	0.001	0.004	0.008	0.985
α rhE2 IgG ₂	<0.0005	<0.0005	<0.0005	0.197
α rhE2ILD IgG ₂	<0.0005	<0.0005	<0.0005	0.068
α rhE3BP IgG ₂	<0.0005	<0.0005	0.002	0.774
α rhE2 IgG ₃	<0.0005	<0.0005	<0.0005	0.054
α rhE2ILD IgG ₃	<0.0005	<0.0005	<0.0005	0.010
α rhE3BP IgG ₃	<0.0005	<0.0005	<0.0005	0.076
α rhE2 IgG ₄	0.542	0.840	0.333	0.421
α rhE2ILD IgG ₄	0.958	0.689	0.849	0.774
α rhE3BP IgG ₄	0.323	0.475	0.672	0.924
α rhE2 IgA	<0.0005	<0.0005	<0.0005	0.251
α rhE2ILD IgA	<0.0005	<0.0005	<0.0005	0.047
α rhE3BP IgA	<0.0005	<0.0005	<0.0005	0.098
α rhE2 IgM	<0.0005	<0.0005	<0.0005	0.058
α rhE2ILD IgM	<0.0005	<0.0005	<0.0005	0.271
α rhE3BP IgM	<0.0005	<0.0005	<0.0005	0.552
α rhE2 IgE	<0.0005	<0.0005	<0.0005	0.025
α rhE2ILD IgE	<0.0005	<0.0005	<0.0005	0.070
α rhE3BP IgE	<0.0005	<0.0005	<0.0005	0.491

Table 6.3.3.1: Table of p-values for Mann Whitney analysis

This table shows the p value data for figures 3.1.1-3.1.8. Significant finds are in bold with the comparison in question at the top of the column and the antibody isotype and autoantigen it is against at the left hand side of each row.

		p values on Mann Whitney Analysis				
		Responder	Sex	Cohort	AMA	ANA
rhE2	IgGall	0.375	0.341	0.64	0.002	0.086
	IgG1	0.142	0.867	0.601	0.023	0.806
	IgG2	0.197	0.559	0.712	0.026	0.291
	IgG3	0.054	0.123	0.625	0.069	0.291
	IgG4	0.421	1	0.322	0.592	0.976
	IgA	0.251	0.356	0.815	0.262	0.91
	IgM	0.058	0.778	0.907	0.082	0.376
	IgE	0.025	0.003	0.498	0.094	0.533
	IgGall	0.33	0.422	0.593	0.023	0.313
rhE2ILD	IgG1	0.845	0.858	0.085	0.252	0.737
	IgG2	0.068	0.251	0.068	0.568	0.476
	IgG3	0.01	0.05	0.427	0.079	0.312
	IgG4	0.774	0.264	0.367	0.672	0.942
	IgA	0.047	0.388	0.993	0.082	0.971
	IgM	0.271	0.911	0.483	0.178	0.78
	IgE	0.07	0.439	0.947	0.035	0.483
	IgGall	0.059	0.245	0.646	0.171	0.512
	IgG1	0.985	0.483	0.94	0.967	0.351
rhE3BP	IgG2	0.774	0.483	0.789	0.45	0.937
	IgG3	0.076	0.793	1	0.612	0.627
	IgG4	0.924	0.276	0.499	0.961	0.761
	IgA	0.098	0.037	0.992	0.234	0.535
	IgM	0.552	0.866	0.764	0.067	0.88
	IgE	0.491	0.475	0.385	0.345	0.24
	Age	0.002	0.749	0.889	0.189	0.199
	Age Diagnosis	0.03	0.257	0.086	0.376	0.501
	Weight	0.514	0.06	0.314	0.297	0.71
Patient Data	mg/kg dosage	0.703	0.287	0.565	0.046	0.549
	Bilirubin	0.054	0.8	0.866	0.747	0.822
	ALP	0.000	0.8	1	0.306	0.815
	ALT	0.000	0.667	0.651	0.262	0.663

Table 6.3.3.2: Table of p value results for all Mann Whitney analysis

This table shows the p values for all Mann Whitney assessments carried out with the most important also being displayed in chart form in other figures. All findings are explained in the discussion section.

Significant findings are in bold.

The criteria being analysed for differences between subgroups thereof is denoted at the top of each column with the criteria being measured and compared to the left of each row.

6.3.4: Power of the study

The power of the study can indicate if the sample size is large enough to rely on conclusions gathered from a study and can also indicate the likelihood of there being type II errors, as in null hypotheses maintained when they ought to have been rejected. Statistical power is defined as 'the probability that an effect will be detected if there is one' and is mathematically related to the standardised error, which is the difference between the 2 means per unit standard deviation; the threshold probability for rejecting the null hypothesis (α); if there are different sized groups, the proportion of subjects in each group. Power can also be expressed as $1-\beta$, where β is the probability of making a type 2 error, or the probability that a null hypothesis is not rejected when it ought to be.

As the effect size before the study is unknown, it is difficult to calculate the power of a study, however it can be calculated the effect size that can be confidently detected based on power of 0.8. With a power of 0.8, it can be estimated that 80% of effects will be detected given the sample size and gives a 20% chance of a type II error. As the variance of each data set is different to the next, it is less useful to calculate the actual statistical power of each different variable, as this will provide different values for each element of the study, and more useful to compare, at each point, whether or not the power is as good as 0.8, which is generally accepted in the literature for giving a low type II error rate.

Table 6.3.4 shows the minimum standardised effect (SE) detectable given 0.8 power and the numbers of participants used. All values in the calculated SE column are lower than those in the minimum required for 0.8 power column except for ALP and ALT. For example, for anti-rhE2IgE, which was discovered to be significantly different between groups, the standard effect was 0.597, whereas it may usually take a minimum difference with a standard effect of greater than this (0.8) to confidently detect this difference. This implies that the study is underpowered for the sizes of effect being detected. This means that conclusions may still be drawn from the data, however there is a high chance of type II error and it is likely that some of the variables would be found to give significant differences between responders and non-responders had there been more participants in each category. If there is a significant difference in the minimum standard error detected in this study, being 0.110 for anti-rhE2ILD IgM, given 20% non-responders and 80% non-responders within patients, this would require 4054 participants to detect using the sample size calculator at <http://www.sample-size.net/sample-size-means/>, before correcting for using non-parametric analyses.

6.3.4.1: Antibody levels

Using <http://www.sample-size.net/sample-size-means/> it was calculated that given 15 non-responders and 62 responders, 80% of real relationships with a standardised effect size of approximately 0.8696 and over can be detected, meaning samples with a mean difference per unit standard deviation of 0.8696 and over can be detected. A smaller standard deviation allows for a smaller mean difference to be detected and a larger standard deviation requires a larger mean difference to be detected.

6.3.4.2: Other Patient Data

As there are some missing values for patient data, a new minimum standardised error exists for every comparison. The minimum effect size confidently detectable for a power of 0.8 are in table 6.3.4. The values show that any significant differences in age (SE=1.042, >0.980), age at diagnosis (SE=1.411, >0.980), ALP (SE=1.767, >0.893) and ALT (SE=1.925, >0.893) discovered would come from adequately powered studies such that should any of these show differences which are insignificant, this is unlikely to be due to a type II error. However, other criteria such as weight (SE=0.257, <1.042) do not come from adequately powered studies to be able to confidently determine whether they have insignificant differences between groups or have a significantly different difference which cannot be detected due to the low power of this study.

		Used in study:					S.E.	Min. SE for power 0.8
		N _R	N _{NR}	μ_R	μ_{NR}	σ		
rhE2	IgG1	62	15	0.891	1.178	0.679	0.423	0.800
	IgG2	62	15	0.443	0.522	0.305	0.261	0.800
	IgG3	62	15	0.757	1.162	0.676	0.598	0.800
	IgG4	62	15	0.027	0.018	0.045	0.209	0.800
	IgA	62	15	0.374	0.459	0.377	0.227	0.800
	IgM	62	15	0.590	0.832	0.507	0.477	0.800
	IgE	62	15	0.228	0.475	0.414	0.597	0.800
rhE2IL D	IgGall	62	15	0.696	0.758	0.271	0.229	0.800
	IgG1	62	15	0.339	0.461	0.375	0.326	0.800
	IgG2	62	15	0.653	0.810	0.624	0.251	0.800
	IgG3	62	15	0.903	1.308	0.785	0.516	0.800
	IgG4	62	15	0.030	0.021	0.051	0.170	0.800
	IgA	62	15	0.450	0.658	0.455	0.458	0.800
	IgM	62	15	0.982	1.035	0.474	0.110	0.800
rhE3BP	IgE	62	15	0.600	0.911	0.644	0.483	0.800
	IgGall	62	15	0.618	0.697	0.287	0.272	0.800
	IgG1	62	15	0.247	0.141	0.487	0.217	0.800
	IgG2	62	15	0.270	0.326	0.319	0.175	0.800
	IgG3	62	15	0.254	0.520	0.466	0.570	0.800
	IgG4	62	15	0.007	0.013	0.021	0.309	0.800
	IgA	62	15	0.189	0.285	0.211	0.456	0.800
Age Age Diagnosis Weight Years since Diag. Yrs on UDCA UDCA dose/kg Bilirubin ALP	IgM	62	15	0.723	0.803	0.476	0.167	0.800
	IgE	62	15	0.070	0.168	0.152	0.646	0.800
	IgGall	62	15	0.543	0.667	0.259	0.478	0.800
	Age	46	10	62.300	49.500	12.280	1.042	0.980
	Age Diagnosis	46	10	51.090	36.560	10.300	1.411	0.980
	Weight	38	9	75.880	71.490	17.051	0.257	1.042
	Years since Diag.	47	9	11.640	10.330	6.825	0.192	1.020
Yrs on UDCA	44	9	10.700	8.000	6.571	0.411	1.020	
UDCA dose/kg	37	9	12.550	11.470	3.667	0.295	1.053	
Bilirubin	49	15	9.143	12.270	10.146	0.308	0.893	
ALP	49	15	126.22	375.53	141.08	1.767	0.893	
				0	0	2		

Table 6.3.4: Table of effect size.

This table shows the effect size confidently detectable by this study based on a desired statistical power of 0.8. This is the power level usually strived for in the literature as it leads to only a 20% chance of type II error. The observed effect size, SE, can be compared to the maximum SE detectable if power level were at 0.8. Where SE is greater than Min. SE for power 0.8, the study can be considered 'adequately' powered assuming 20% type II error rate which is generally accepted in the literature.

6.3.4.3: Male and Female

There were differences discovered between male and female groups, disregarding responder/non-responder grouping.

With only 3 males and 62 females, the minimum standard error for confident detection of 80% of relationships is 1.621. The standard errors between males and female groups are 0.915 for rhE2ILDlgG3, 0.974 for rhE2ILDlgA and 0.685 for rhE2lgE (not shown), therefore there may be other significant antibody differences between males and females that this study is not powerful enough to uncover. Additionally, to require confident detection of these 3 differences given a likelihood of 20% of other comparisons to also be actually significant but undetected, the number of females would be required to be at least 195 and males 10, as calculated using <http://www.sample-size.net/sample-size-means/>.

6.3.5: Kruskal-Wallis

The Kruskal-Wallis would be useful if in this study it was of interest if the groups differ compared to each other and also to healthy volunteers. In a question regarding if there are any significant differences between Healthy Volunteers, Responders and Non-responders, a Kruskal-Wallis determines whether there is a significant difference between the means of the 3 groups of healthy volunteers, responders and non-responders. Results are shown in table 6.3.5. rhE3BP1gG3 appears of significant interest, with chi-squared value of 6.261 and p value of 0.012, showing a large difference with high significance.

Difference between 3 groups																								
Test Statistics^{a,b}																								
	E2IggAll	ILDiggAll	E3IggAll	E2Igg1	ILDigg1	E3Igg1	E2Igg2	ILDigg2	E3Igg2	E2Igg3	E3Igg3	E2Igg4	ILDigg4	E3Igg4	E2IggA	ILDiggA	E3IggA	E2IggM	ILDiggM	E3IggM	E2IggE	ILDiggE	E3IggE	
Chi-Square	69.621	68.124	68.252	62.509	18.084	7.260	51.594	26.114	11.656	39.595	26.583	31.369	0.404	0.772	1.220	29.770	33.114	27.949	35.993	57.924	51.249	50.728	70.406	40.751
df	2	2	2	2	2	2	2	2	2	2	2	2	2	2	2	2	2	2	2	2	2	2	2	2
Asymp. Sig.	0.000	0.000	0.000	0.000	0.000	0.027	0.000	0.000	0.003	0.000	0.000	0.817	0.680	0.543	0.000	0.000	0.000	0.000	0.000	0.000	0.000	0.000	0.000	0.000
a. Kruskal-Wallis Test																								
b. Grouping Variable: Response																								
Responders vs non-responders																								
Test Statistics^{a,b}																								
	E2IggAll	ILDiggAll	E3IggAll	E2Igg1	ILDigg1	E3Igg1	E2Igg2	ILDigg2	E3Igg2	E2Igg3	E3Igg3	E2Igg4	ILDigg4	E3Igg4	E2IggA	ILDiggA	E3IggA	E2IggM	ILDiggM	E3IggM	E2IggE	ILDiggE	E3IggE	
Chi-Square	0.233	0.616	2.523	1.966	0.406	1.337	0.906	1.672	1.052	4.053	3.753	6.261	0.185	0.060	0.906	2.742	2.996	2.710	0.657	0.180	5.104	3.478	0.430	
df	1	1	1	1	1	1	1	1	1	1	1	1	1	1	1	1	1	1	1	1	1	1	1	
Asymp. Sig.	0.630	0.433	0.112	0.161	0.524	0.248	0.341	0.196	0.305	0.044	0.053	0.012	0.667	0.806	0.341	0.088	0.083	0.100	0.418	0.671	0.024	0.062	0.512	
a. Kruskal-Wallis Test																								
b. Grouping Variable: Response																								
Responders vs Healthy volunteers																								
Test Statistics^{a,b}																								
	E2IggAll	ILDiggAll	E3IggAll	E2Igg1	ILDigg1	E3Igg1	E2Igg2	ILDigg2	E3Igg2	E2Igg3	E3Igg3	E2Igg4	ILDigg4	E3Igg4	E2IggA	ILDiggA	E3IggA	E2IggM	ILDiggM	E3IggM	E2IggE	ILDiggE	E3IggE	
Chi-Square	30.688	30.017	30.949	33.322	7.517	7.020	27.962	17.277	10.371	22.165	15.421	26.542	0.406	0.690	16.114	23.846	18.647	21.568	23.335	17.170	33.885	30.736	18.826	
df	1	1	1	1	1	1	1	1	1	1	1	1	1	1	1	1	1	1	1	1	1	1	1	
Asymp. Sig.	0.000	0.000	0.000	0.000	0.006	0.008	0.000	0.000	0.001	0.000	0.000	0.000	0.524	0.406	0.000	0.000	0.000	0.000	0.000	0.000	0.000	0.000	0.000	
a. Kruskal-Wallis Test																								
b. Grouping Variable: Response																								
Non-responders vs Healthy volunteers																								
Test Statistics^{a,b}																								
	E2IggAll	ILDiggAll	E3IggAll	E2Igg1	ILDigg1	E3Igg1	E2Igg2	ILDigg2	E3Igg2	E2Igg3	E3Igg3	E2Igg4	ILDigg4	E3Igg4	E2IggA	ILDiggA	E3IggA	E2IggM	ILDiggM	E3IggM	E2IggE	ILDiggE	E3IggE	
Chi-Square	64.481	62.904	61.511	55.892	16.808	3.779	44.539	19.944	7.327	31.568	20.040	18.478	0.108	0.485	25.372	23.918	20.296	28.351	54.695	50.541	43.671	63.514	37.622	
df	1	1	1	1	1	1	1	1	1	1	1	1	1	1	1	1	1	1	1	1	1	1	1	
Asymp. Sig.	0.000	0.000	0.000	0.000	0.000	0.052	0.000	0.000	0.007	0.000	0.000	0.742	0.486	0.296	0.000	0.000	0.000	0.000	0.000	0.000	0.000	0.000	0.000	
a. Kruskal-Wallis Test																								
b. Grouping Variable: Response																								

Table 6.3.5: Chi-squared values and relevant p values for Kruskal-Wallis comparison of means.

This table shows the chi-squared values and relevant p values for Kruskal-Wallis analysis between 3 groups of Responders, Non-responders and Healthy volunteers. The IgG3 isotypes appear to be

of most relevance looking at the disease of PBC as a whole and taking healthy volunteers into consideration.

6.3.6: Multinomial analysis

In this stage, factors of significance in the previous sections were taken and further analysed for their relative influence on a patient's response status to determine if the response of a patient could be accurately predicted given the data from previous sections. As blood levels of all independent variables were not available and based on all data which was available, the best formula which could be established was one which may predict whether a patient would have been designated a responder or non-responder one year after diagnosis, given data available at time of blood draw.

Response was initially calculated using ALP, ALT and bilirubin criteria, presumably 1 year after UDCA treatment was commenced, as outlined in section 6.1. Exact blood levels of these at diagnosis were not made available to this group, therefore it is unknown if these levels have altered, and by how much, since the patient was designated a responder or non-responder. A prediction can be made on if the ALP and ALT measurements, at time of blood draw, of the PBC patients in this study as a whole are reflective of those at diagnosis. Table 6.3.2.1 indicates that on Spearman's Rank correlation, there is no significant correlation between years since diagnosis and ALP (All PBC – $r_s = -0.047$, $p = 0.721$; Responders – $r_s = 0.018$, $p = 0.903$; Non-responders – $r_s = 0.075$, $p = 0.847$) or ALT (All PBC – $r_s = -0.101$, $p = 0.442$; Responders – $r_s = -0.035$, $p = 0.847$; Non-responders – $r_s = 0.142$, $p = 0.715$). Therefore, it can be assumed that ALP and ALT are not significantly different to at the time of diagnosis and it would be unfair to include ALP and ALT in predicting a patient's UDCA responder status, given response/non-reponse was first allocated based on these levels. Therefore, those factors of interest are Age, age at diagnosis, anti-rhE2ILDlgG3 level, anti-rhE2ILDlgA level and anti-rhE2lgE level.

Those factors which were found to be of interest in Mann Whitney analysis (age, age at diagnosis, rhE2lgE, rhE2ILDlgG3, rhE2ILDlgA) are referred to on table 6.3.3.2 and were carried forward to look for correlations between these. Spearman's rank correlation coefficient indicates that there is a very strong positive correlation between age at blood draw and age at diagnosis ($r_s = 0.819$, $p = 0.000$). rhE2lgE, rhE2ILDlgG3 and rhE2ILDlgA do not correlate with age, however rhE2lgE shows a weak negative correlation with age at diagnosis ($r_s = -0.369$, $p = 0.045$). Additionally, there was found to be positive correlations between rhE2lgE, rhE2ILDlgG3 and rhE2ILDlgA. Positive correlations between factors does not necessarily mean that they are not contributing independently to response status, but indicates there could be an underlying factor governing those factors that correlate strongly with each other.

The factors of age, age at diagnosis, rhE2lgE, rhE2ILDlgG3 and rhE2lgA could, then, be brought forward for multinomial regression. Based on the data available, the multinomial regression formula would be designed to predict if a patient would have been designated

'responder' or 'non-responder' by Paris criteria one year after their diagnosis given their age at time of blood draw, so for example time 'T'; their age at diagnosis; their anti-rhE2ILDlgG3 level at time T; their anti-rhE2ILDlgA level at time T; their anti-rhE2lgE level at time T.

$$Y \sim x_0 + b_1x_1 + b_2x_2 + b_3x_3 + b_4x_4 + b_5x_5$$

For $\ln[P(\text{non-responder})/P(\text{responder})]$, to give the probability that a patient is a non-responder, rather than a responder, given the combined products of the levels of the independent variables and their co-efficients.

where:

x_1 is age, b_1 is the co-efficient for age;

x_2 is age at diagnosis, b_2 is its coefficient;

x_3 is rhE2ILDlgG3 level, b_3 is its co-efficient;

x_4 is the rhE2ILDlgA level, b_4 is the co-efficient;

x_5 is the rhE2lgE level, b_5 is the co-efficient;

x_0 is the Y intercept.

The data is input in table form into R studio and the R command of
`> multinom(formula = out ~ Age + Agediag + rhE2lge + rhE2ILDlgg3,
 data = Patientdata).`

where 'out' is the pre-defined name for Responder/non-responder category with Responder as the reference.

The formula which can be inferred by the intercepts and coefficients provided by R:

$$\ln[P(\text{Non-responder})/P(\text{Responder})=$$

$$11.694 - (-0.154 \times \text{Age}) + (-0.158 \times \text{Age at diagnosis}) + (2.023 \times \text{rhE2ILDlgG3}) + (0.1541 \times \text{rhE2ILDlgA}) - (-1.835 \times \text{rhE2lgE}) \quad \text{at}$$

The significance of each independent variable in the formula of each of these is by finding the z statistic and converting this to a p value. The z statistic can be calculated by dividing the coefficient by the standard error.

$$\text{Intercept: } z = 11.694 / 5.802 = 2.016, p = 0.044$$

$$\text{Age: } z = -0.154 / 0.106 = -1.459, p = 0.145.$$

$$\text{Age at diagnosis: } z = -0.158 / 0.107 = -1.475, p = 0.141.$$

$$\text{rhE2ILDlgG3: } z = 2.023 / 1.367 = 1.480, p = 0.139.$$

$$\text{rhE2ILDlgA: } 0.154 / 1.343 = 0.115, p = 0.909.$$

$$\text{rhE2lgE: } z = -1.835 / 2.215 = -0.828, p = 0.408.$$

When the z values are converted to p values, it can be determined that no criteria input into the equation provide any significant 'strength' to the equation as all of the p values are greater than 0.05.

This information is also available using the commands:

```
> z <- summary(mymodel5)$coefficients/summary(mymodel5)$standard.errors
```

```
> p <- (1 - pnorm(abs(z),0,1))*2
```

As none of the p values are significant, it is not necessary to test the formula, however if there were variables providing significant strength to the formula it would then be appropriate to remove those not providing significant strength, recalculate the formula and then test the new formula by the steps below.

If p values for antibodies were found to be significant, and were subsequently kept in the formula and a working formula for prediction of whether a patient is a responder or non-responder had been established, the formula would then have to be tested. As none of the p values were under 0.05 (explained in discussion), this was not the case and therefore it can be determined that although significant differences between means by Mann Whitney analysis were found, these antibody levels on their own do not significantly define whether a patient is a responder or non-responder. If there were significant p values, the formula's accuracy would then be tested as below.

The assessment of percentage of accurate guesses by the formula based on how many of the actual results can the formula estimate would then be carried out. The R command for this is:

```
> predict([model name],[data name])
```

which produces probabilities of the values being the observation value, rather than the reference value, in this case the probability of being a non-responder rather than a responder, given the formula.

The commands:

```
> cm <- table(predict([model name]),[data name]${[Reference factor]})
```

```
> print(cm)
```

then provide a table of the numbers of correct guesses and number of incorrect guesses.

Odds-ratio calculation would then be calculated for relative correctness of the formula by:

$$OR = (a/c) / (b/d)$$

Where OR is odds ratio and (a/c) is (actual number of non-responders/actual number of responders) and (b/d) is (formula's guessed number of non-responders/formula's guessed number of responders).

This would give an estimate of how reliable the formula is for predicting the outcome, or predicting the dependent variable.

6.4: Discussion

6.4.1.1 Patient Data – Spearman’s Rank Correlation Coefficient

Using all patients, Spearman’s rank correlation showed strong positive correlations between bilirubin, ALT and ALP ($p < 0.001$ across the board), as shown in table 6.3.2.1. These markers are all known to be indicative of liver damage. In addition, age correlated negatively with ALP ($p = 0.014$) and ALT ($p = 0.006$) which implies a strong association between age and liver damage. This association is indicative that patients at a lower age at time of serum draw and also diagnosis may have worse liver function, which is in agreement with the observation in the literature that younger patients are more likely to be non-responders regarding the current therapy with a more aggressive disease.

ALP and ALT did not, however, correlate significantly with age at diagnosis apparent in table 6.3.2.1 ($p = 0.152$ and 0.059 respectively), however this could be due to the fact that most patients are at a very early disease state at diagnosis, therefore do not yet have raised ALP or ALT. The age range at which patients can be diagnosed is large and up to 60% of patients are asymptomatic at diagnosis therefore patients across all ages at diagnosis may have liver function tests only just within the diagnostic range (Prince et al., 2004). Even early non-responders may have ALP and ALT only just in the diagnostic range, but then their disease goes on to progress more quickly than the responders.

Age at date drawn and age at diagnosis correlate positively ($p < 0.001$, shown in table 6.3.2.1) meaning the older any given patient is at the time of blood drawn, the older they likely were when diagnosed. This could indicate that there are narrow parameters of length of time a patient in this study has been diagnosed with PBC for. This could be because eventually patients require a new liver or perhaps die of an unrelated cause, to do with old age.

Some factors correlate positively due to their relation to time, such as age at diagnosis and years since UDCA administration: UDCA is usually administered early in diagnosis. These factors were not taken into account during analysis because correlation may be a result of relation to time.

6.4.1.2 Patient Data - Mann Whitney

Patients of different nominal groups were also compared, by Mann Whitney analysis, based on information provided alone to investigate any phenotypic grouping.

There were no significant differences in different gender groups regarding age at draw, age at diagnosis, weight, UDCA dosage, bilirubin, ALT or ALP. There were few male participants giving limited statistical power so a future study should aim to recruit more men with PBC. A surprising find was no significant difference regarding weight between the genders ($p = 0.06$, table 6.3.3.2), as it would be expected for men to have a significantly greater weight

than females, suggestive that there may have been limited significance power or women in the study are significantly heavier than the normal population whereas men are not, or men are lighter than the general population of men whereas the women were not. The average weight of PBC females in the study was 76.1kg compared to the national average of 70.2kg, whereas the average weight of PBC males in this study was 87.1kg compared to 83.6kg (table 8.1-8.3, appendix). It could be argued that there could be an element of males being underweight whereby females are overweight, but another study gathering weight of age matched healthy volunteers and more males to increase the statistical power would be required in order to give real evidence for this. It has been discussed in this chapter that the power of this study is limited, therefore if the weights of patients in this study do mimic the normal population with a difference between males and females, it may not be detectable in this study.

There were no significant differences across cohort A and B groups regarding age at draw, age at diagnosis, weight, UDCA dosage, bilirubin, ALT or ALP, shown in table 3.3.2 where all p values exceed 0.05. One surprising find is that UDCA naïve patients did not show any difference in liver biochemistry results (bilirubin – $p=0.866$; ALT – $p=1.000$; AST – $p=0.651$) compared with those already taking UDCA, when UDCA is thought to normalise liver function tests in most patients. On further investigation, many of these patients were missing liver biochemistry results, but additionally therefore were likely very early in disease state, therefore only minor liver damage had yet occurred. Cohort B patients were likely not yet on UDCA due to their only having just been diagnosed and only in monitoring stage of treatment.

As all patients were either white or with non-disclosed ethnicity, no comparison between ethnic groups could be carried out which is one limitation of the study.

There were no significant differences between AMA and ANA positive and negative groups regarding age at draw, age at diagnosis, weight, UDCA dosage, bilirubin, ALT or ALP, shown by p values in table 3.3.2. This might imply that a patient's AMA or ANA status is not indicative of their liver function, and therefore potentially also disease severity, or age or weight, therefore it is not likely a determining factor of their response or non-response status based on predictions by Carbone and colleagues (Carbone et al., 2013), according to the data in this study.

The most interesting find of this strand of the study was the key differences in groups within the response/non-response comparison. There was no difference in weight, UDCA dosage or bilirubin between responder/non-responder groups, indicated by p values in table 6.3.3.2. The result for weight was not surprising as there has been little or no evidence to suggest that weight differs in these groups. Regarding dosage, the lack of a difference suggests that physicians have not increased patients' dosage based on non-response. This is likely due to the growing understanding that there are different sub-types of the disease and no evidence suggests it would be beneficial to raise UDCA beyond currently applied levels in

a patient suspected to be a non-responder. Bilirubin does not appear to differ between responders and non-responders. A higher bilirubin would have been suspected in the younger patients with more aggressive disease, however blood serum bilirubin has been found to increase with age which may explain the insignificant result (Boland et al., 2014). Patients denoted responders had a significantly higher age at time of draw ($p=0.002$) and diagnosis ($p=0.02$) than those denoted non-responder, shown by p values in table 6.3.3.2 and shown in graphical form in figure 6.3.4.2. Non-responders have significantly higher ALP ($p<0.001$) and ALT ($p<0.001$) than responders, shown in p value in table 6.3.3.2 and in graphical form in figure 3.4.1. This is congruent with the grouping system suggested by Carbone and colleagues, established by their statistical analysis of responders and non-responders. That our data can replicate their grouping system is largely important because confidence in this system and reliance on a study with 2353 participants provides confidence to the data in this study and any differences in antibody subtypes we find between responders and non-responders based on these criteria (Carbone et al., 2013). It was intended to further divide the non-responders to investigate if they can be further subdivided into the older and the younger non-response groups to verify the claim the older group of non-responders are likely to fail to meet response criteria because of raised alkaline phosphatase and bilirubin whereby younger non-responders fail to do so due to raised ALT/AST. All attempts to further categorise the non-responders and gain significant results were unsuccessful. This is likely due to there being few non-responding patients in the study: only 15. Some of these patients were missing data, leaving the usable non-responders in this context at only 8. Although this is a large enough group to compare with the non-responder group and obtain significant results, this is insufficient data to further divide and achieve significant results and therefore inadequate statistical power. In addition, many patients were missing data, for example there were two non-responders whose age was missing. Further studies should work to specifically recruit the non-responder cohort and stringent patient data should be kept. This is a limitation which could not be surmounted in this study as serum was obtained from an external source and therefore patients were recruited and patient data was obtained by an external group.

One limitation of the study was in that clinical data established from patient blood was unavailable for the healthy volunteers due to lack of assays for detecting ANA, ALP, ALT and also as none of the healthy volunteers have a PBC diagnosis, they cannot be categorised as responders or non-responders; similarly none are taking UDCA, therefore years since UDCA start cannot be taken into account. The healthy volunteers are crucial as they allow comparison of antibody levels against the non-PBC group, such that those isotypes higher than the healthy level can be selected for further analysis. The IgG4 isotype of all autoantigens was found to be of levels in PBC patients not significantly higher than in healthy controls therefore this isotype was excluded from further analysis.

6.4.3 ELISA results

Data from Chapter 5 were analysed using statistical analysis as below.

6.4.3.1 Normal distribution

Firstly, the presence of each dependent variable was checked for normal distribution and levels were compared with healthy controls. Data that is not normally distributed or is skewed is more likely to be of interest because it implies a change in the level in response to another factor, rather than patients generally having levels clustered around the most common value which would be expected under uninfluenced conditions.

Regarding serum antibody levels, it is important to firstly compare patient levels with healthy controls to determine which types of antibody appear to be unimportant in PBC regarding if their levels are raised in PBC. Those with an insignificant difference in Mann Whitney analysis between patients and healthy controls are likely antibodies not important in PBC and therefore can be disregarded. The IgG4 isotypes were the only isotypes found to be present in levels not significantly greater than in the PBC patients when compared by Mann Whitney analysis: anti-rhE2 IgG4 ($p=0.542$), anti-rhE2ILD IgG4 ($p=0.958$), rhE3BP IgG4 ($p=0.323$), indicated in figure 6.3.3.2. This suggests that IgG4 class switching is not an important factor in PBC. This may also imply that cytokines which cause IgG4 switching are also unimportant, such as IL-4, produced by Th2 cells. This seems to contradict one study which has suggested that IgG4 should be measured as standard in PBC diagnosis when the patient does not respond to UDCA based on a case study of one patient (Takemoto et al.), however the data in this study shows no significant difference between non-responders and healthy volunteers thus refuting this suggestion. The study is an example of overlap with PBC and IgG4-related disease (IgG4-RD), which is an inflammatory disease involving infiltration of lymphocytes into tissues which could be one or more of many throughout the body, and PBC. Both are rare diseases and so overlap between these two diseases is extremely rare. Although there are more documented cases (Takasumi et al.), there is insufficient evidence in the literature or this study to suggest that IgG4 levels should be measured as a standard diagnostic protocol for PBC or PBC overlap with IgG4-RD.

6.4.3.2 Spearman's Rank Correlation Coefficient

Many antibody isotypes correlate positively with bilirubin, ALT and ALP. This indicates which antibodies are likely to be important in disease progression. The greater the autoimmune response the more tissue destruction there is so those isotypes which correlate to known signs of liver injury, such as raised ALT, ALP and bilirubin, are likely to be involved in or indicative of the autoimmune response. In particular, anti-rhE2 IgG3, anti-rhE2ILD IgG3, anti-rhE2ILD IgA, anti-rhE3BP IgA and anti-rhE2IgE are of interest as their serum

levels appear to correlate positively with ALP, ALT and bilirubin (p values shown in figure 3.2.2, for example: anti-rhE2IgG3, $p=$; anti-rhE2ILD IgG3, moderate correlation with ALT, $p=0.000$; anti-rhE2ILD IgA, weak correlation with ALT, $p=0.002$; anti-rhE3BP IgA, moderate correlation with ALP, $p=0.001$; anti-rhE2IgE, weak correlation with ALT, $p=0.001$). As none of these correlations are considered strong based on $r_s > 0.6$, possibly there are multifactorial relationships between the variables.

Although there was insufficient statistical power to further subdivide the non-responders based on criteria outlined by Carbone and colleagues, our data does indicate which particular isotypes could be associated with the particular criteria which Carbone and colleagues suggest could be indicative of further subdivisions of the non-responders. According to the literature, the non-responders can be further subdivided into the younger non-responders usually with higher ALT and the older non-responders usually with higher bilirubin and higher ALP. Therefore investigating which isotypes are associated with these specific increases could highlight pathways for future investigation in elucidating the differences between the separate non-responder groups. Anti-rhE2ILD IgG1 level correlated positively with bilirubin level and anti-rhE2 IgA correlated positively with ALP level, associated with the older non-responders, whereby levels of anti-rhE3BP IgM was shown to correlate positively with ALT, associated with the younger non-responders, therefore the underlying mechanisms causing isotype switching to IgG1 and IgA, and also lack of switching, resulting in IgM, could contain a differentiating factor between these groups which are within the non-responder group. Therefore, further work into elucidating the differences in the non-responder sub groups could focus on pathways leading to IgM and IgA or IgG1. Interestingly the difference was only observed with the specific autoantigen stated and not across the panel of autoantigens, therefore different autoantigens could be elucidating different responses in terms of antibody isotype switching.

6.4.3.3: PBC vs Healthy volunteers: Mann whitney and Kruskal-Wallis.

Comparisons of PBC patients and healthy volunteers were carried out as an initial test to assess which antibodies may be of interest in overall disease. One main investigation into this study is if there may be differences in isotype switching in responders and non-responders. If non-responders undergo isotype switching in a different way to responders, then likely there may be some levels of isotypes within a PBC group which are low levels, like healthy volunteers, but raised in the other groups to a significantly higher level than healthy volunteers, but these difference may be difficult to detect when comparing PBC patients to healthy volunteers. For this reason, Mann Whitney data comparing only responders and non-responders was used for the bulk of the analysis. Kruskal-Wallis data indicates which autoantibodies may be of interest if those used in this study were of such different levels among the 3 groups that they could be used for diagnosis not only of PBC

but also on response to UDCA likelihood. PBC is already considered diagnosable, so for this chapter to add to the field of PBC diagnosis would require subgroup diagnosis, which has been shown not to be possible using data gathered in this study. The Kruskal-Wallis data, shown in table 6.3.5, indicates that if comparison between the 3 groups were feasible that the IgG3 isotype against the E3BP antigen may be of interest, given a p value of 0.012 for significance between responders and non-responders considering 3 groups. The multinomial regression analysis indicates that differences of antibodies between responders and no-responders are not significant for diagnosis or prediction of response alone, therefore likely more data would be required to postulate an assay for diagnosis including sub-grouping. Further work to possibly establish a diagnostic assay which could sub-group patients is described within the multinomial analysis sections of this chapter.

6.4.3.3.1: Mann Whitney

There were no significant differences in levels of any isotype between ANA positive and negative groups.

Only some antibodies were shown to have significantly lower levels in AMA negative patients compared to AMA positive patients, therefore AMA negative patients were kept in for full analysis. These were: anti-rhE2 IgGall ($p=0.002$), anti-rhE2 IgG1 ($p=0.023$), anti-rhE2 IgG2 ($p=0.026$), anti-rhE2ILD IgGall ($p=0.023$), anti-rhE2ILD IgE ($p=0.035$), displayed in table 3.3.2. It should be noted that these isotypes were not considered relevant in other finds of this study therefore the inclusion of AMA negative patients did not affect other finds. The IgGall is a secondary antibody which recognises all IgG isotypes, and the IgG1 is the only which is statistically negative so it is possible that in this instance IgGall is representative of raised IgG1 and not all IgG subtypes, as the rest of the IgG subtypes are not raised.

The most important find was when comparing responder and non-responder groups. The non-responders were shown to have significantly higher levels of the antibodies anti-rhE2ILD IgG3 ($p=0.01$), anti-rhE2ILD IgA ($p=0.047$) and anti-rhE2 IgE ($p=0.025$) indicated by p values in table 6.3.3.2 and data shown in figures 6.3.3.4, 6.3.3.6 and 6.3.3.8. Clear differences in the spread of data is apparent in the box plots and bar charts show clear differences in the average absorbance values across responder and non-responder groups. Furthermore, these are all antibodies found to correlate with liver damage blood biomarkers ALP, ALT and bilirubin. This is the first instance of an antibody pattern difference being discovered between responder and non-responder groups and could indicate a potential difference in the underlying mechanisms.

Further ELISAs must be carried out to monitor patients at various different disease stages. For example, patients very early in diagnosis yet late enough to obtain responder/non-responder status may form one group, patients at middle-stage of disease progression may

form another group and late stage patients a third group in order to compare antibody patterning at the different stages throughout disease progression and determine if there is a change in antibody patterning as the disease progresses. Data obtained in this study uses patients at various disease stages, some diagnosed as early as 1992; and also some only newly diagnosed; some patients with liver function tests as high as 13mg/dL bilirubin, 438IU/L ALP and 150IU/L ALT; some with 5mg/dL bilirubin, 54IU/L ALP and 9IU/LALT. Symptomatic disease state and liver function would be an appropriate grouping factor rather than years since diagnosis as years since diagnosis does not take into account the disease history pattern, whereby patients experience a steep drop off in health at a given time (Jones, 2003) and the fact that patients do not necessarily enter the disease progression stage at a constant time. The reason for this study would be to monitor any changes in antibody differences between responders and non-responders as the disease progresses but also because if a diagnostic tool is to be developed then it is most important to elucidate any antibody differences early on in the disease such that a patient can be placed on an appropriate treatment course as early as possible to have maximum impact in slowing or stopping disease progression. The data which was available for this study was insufficient to characterise a patient as early, mid or late disease state, therefore this analysis could not be carried out as an extension of the completed study described.

There were no significant differences between cohorts A and B, indicated by p values in table 6.3.3.2 which all exceed 0.05 (the smallest being 0.068 for rhE2ILDlgG2), for comparison by Mann-Whitney analysis, comparing cohort A, patients on UDCA, and cohort B, UDCA naïve patients. This may suggest that expression of all of the isotypes neither increases nor decreases after commencing UDCA treatment, however this is not supported in the Spearman's Rank correlation coefficient results, from table 6.3.2.2, which does suggest a related change in levels of certain antibodies with time taking UDCA. These are anti-rhE2lgGall ($rs=0.291, p=0.023$), anti-rhE2ILDlgGall($rs=0.325, p=0.01$), rhE3BPlgGall($rs=0.322, p=0.011$), anti-rhE2lgG3($rs=0.257, p=0.05$) and anti-rhE2ILDlgE($rs=0.276, p=0.050$). All of these relationships have rs values of below 0.4, therefore indicate weak relationships which may not be directly governed by UDCA use over time but another factor which may also correlate with UDCA over time. Notably, there was no difference between UDCA naïve and UDCA-taking patients of the antibodies found to be of interest comparing responders and non-responders: anti-rhE2ILD IgG3($p=0.05$), anti-rhE2ILD IgA($p=0.037$) and anti-rhE2 IgE($p=0.025$). This is an area of interest for the future: to uncover if a difference in antibody profiles between responders and non-responders is similar to that of patients pre- and post- UDCA. More on this is covered in the future work section.

Males are significantly less likely to respond to UDCA therapy, however they do not appear to fit the same response/non-response phenotypic pattern as females. For example, it has been found in early phenotyping studies that females tend to experience more pruritus,

abdominal pain and weight loss than males, however males experience more jaundice, jaundice-associated pruritus and upper gastrointestinal bleeding than females (Rubel et al., 1984). Males have also been shown to have significantly higher bilirubin levels even when normal gender differences are taken into account (Carbone et al., 2013). Data from this study also suggests that men may not fit the same responder/non-responder patterning as females. There are only three antibodies which differ significantly in levels between males and females in this study: anti-rhE2 IgE ($p=0.003$), anti-rhE2ILD IgG3 ($p=0.05$) and anti-rhE3BP IgA ($p=0.037$). All of these are lower in males, however two of these are those antibodies identified as being higher in non-responders than responders: anti-rhE2 IgE ($p=0.025$) and anti-rhE2ILD ($p=0.01$). This then poses the question of where males fit in the ever branching PBC picture. Section 6.3 outlines how there is likely high type II error in the comparison of responders and non-responders and of males and females. A study containing more participants, ideally inclusive of a more even ratio of males/females, would increase the statistical power of the study and the relative differences between males and females and how these may differ from differences between 'responders' and 'non-responders'.

In addition, none of the males had recorded whether they are a responder or non-responder to UDCA, therefore the effect of response on gender could not be investigated in this future study. Males were therefore all left out of analysis comparing responders and non-responders, without this necessary data.

Overall, the Mann-Whitney analysis carried out in this study shows that there are some detectable large differences between certain different antibody levels, however the study likely lacks statistical power required to detect all significant differences. This has to do with number of participants but also the variance of the data, which could not be predicted before this study.

Given that the differences between responders and non-responders uncovered in this study were particularly relevant as their mean differences per unit standard deviations were relatively high, suggesting a large mean difference and/or a low data variance, both factors which suggest a relevant difference. It is therefore important to consider a reason for the difference in these antibodies between groups of PBC patients and consider any underlying T cell activity which could be influencing this patterning, relating to previous chapters.

IgE

Firstly, focussing on IgE, although IgE class switching can in some circumstances be attributed to T follicular helper cells releasing IL-4 (Meli et al.), this is unlikely to be the case in this context because IL-4 released by TFH has also been shown to increase class switching to IgG4 (Akiyama et al.) and there is no evidence of there being raised IgG4 in PBC in this study. IL-13 levels have been shown to be raised in sera of PBC patients (Landi et al., 2014). IL-13 is primarily produced by Th2 but may also be produced by Th1 or Th17 cells.

IgG3

IFN-gamma and IL-10:

IgG3 isotype class switching is associated with a Th1 response, whereby Th1 cells release IFN- γ which induces antibody isotype switching to IgG3 (Mortensen et al., 2015). In addition, it has long been established that IL-10, produced by a plethora of different leucocytes, can also induce isotype switching to IgG1 and IgG3 (1994, Saxena et al., 2015).

IgA

It is known that release of IL-5 by Th2 cells can induce isotype switching to IgA (Harriman et al.). However, TGF- β released by Tregs may also induce class switching to IgA (Dedobbeleer et al.).

As there could be many different underlying mechanisms causing the isotype switching to the isotypes in question, it raises the question of which of these mechanisms and underlying cell action could be important in PBC. Utilisation of the Flow Cytometry assay optimised in chapter 3 on PBC patients could begin to answer this question.

To explore why these particular isotypes of antibodies against particular autoantigens, and not across the board of all autoantigens explored, seems to differentiate responders and non-responders, an ELISpot experiment should be carried out, as per the method in chapter 4. The ELISpot would use PBMCs isolated from PBC patient blood, and also use healthy controls. This ELISpot would include wells coated with antibodies against the different cytokines known to cause switching to certain isotypes of antibody. The PBMCs would then be added and challenged with autoantigens such that there is a challenge in at least triplicate of every cytokine-antigen combination. The response by T cells in terms of the cytokines released when challenged with the autoantigens can then be quantified by counting and analysing the number of spots produced in each well. If the experiment is carried out across many patients, a tendency towards the type of antibody response against that antigen may be apparent, which could not only determine if the different autoantigens can illicit different responses but also explore a T cell basis to the antibody isotype patterning seen in the data in this chapter. If the PBMCs are stained with CFSE prior to the ELISpot, then they may then be harvested and analysed by flow cytometry using the assay designed and optimised in chapter 3. Post-ELISpot, the cells would be stained for extracellular markers to allow their discrimination based on their T cell subtype and their proliferation in response to the different autoantigens may be compared.

6.4.4: Multinomial regression

Section 6.3.6 outlines a multinomial regression which was designed to determine if, given the data available, the patients' responder/non-responder categorisation could be

predicted, with a particular interest in how important the antibody levels found to be significantly different between responders and non-responders were.

Although the levels of rhE2ILD IgG3, rhE2ILD IgA and rhE2 IgE appear to be significantly different in non-responders compared to non-responders, they possibly carry insufficient strength to be considered for diagnostic purposes. At this stage it may often be appropriate to consider testing for homogeneity of variance of all of the independent variables and if this is not satisfied, data can be transformed, and then it may fit the multinomial regression formula, but in this study it has already been established that there are likely many type II errors so this is best saved for a more highly powered study, such that more independent variables may be carried forward for multinomial regression. A more highly powered study involving more participants, i.e. more responders and more non-responders, may be less sensitive to type II errors and would possibly detect more antibodies of interest in terms of different levels between responders and non-responders, which could then be used in multinomial regression.

6.4.5: Future work and limitations of this chapter

Something not covered in this chapter is any relationship between the autoantigens recognised by a patient and the isotypes of antibodies produced in response to each antigen. There may be a relationship between isotypes of antibodies produced and the autoantigen(s) recognised by the patient. In order to answer this question, first a competitive ELISA experiment would have to be carried out to estimate the amount of response to an antigen that is measured due to antibody cross-over. For this chapter, there was not enough available autoantigen for coating of the ELISA plates to cover this. The competitive ELISA answers the question of if one antibody may be promiscuously binding to other antigens. In this context, some anti-rhE2ILD-recognising antibodies in patient sera may be binding to the rhE2 protein coat. Therefore it is unknown in this chapter what proportion of the results from ELISA screens were from contributions made by other antibodies than that being tested at the time. The competitive ELISA involves incubating the patient serum with an autoantigen then detecting for the presence of all autoantigens being used, separately, by the indirect ELISA technique used in this study. An autoantigen should 'inhibit' itself such that when a certain concentration of autoantigen is added to the serum and incubated before ELISA, there will be no response. Then other autoantigens incubated with this serum will give less than 'normal' readings if they are competing for the protein coat with the antibody in question. The extent of competition exerted by an antibody against an autoantigen on another can be quantified by using different dilutions of autoantigen in the patient serum, or different serum dilutions for a fixed autoantigen concentration, and the extent of this competition indicates the extent of cross-reactivity between antibodies.

Once this has been established, then antibody isotype responses for individual autoantigens can be investigated, correcting for cross-reactivity, using the Kruskal-Wallis comparison for k groups test. It is important to consider the importance of power of the experiment, as using Kruskal-Wallis involves dividing the p value for confidence by $k(k-1)/2$, so for example investigating 8 different isotypes would involve an alpha level of $0.05/28 = 0.00179$. Section 6.3 outlines the importance of consideration of power in an experiment.

It is important to note that this study assumes minimal cross-reactivity, as it is not corrected for, and this is due to there being a limited amount of autoantigen protein available, but further studies should carry out cross-reactivity experiments as standard.

Additionally, it is important to acknowledge that this study does not take advantage of all autoantigens found to be of importance in PBC, only those which were available, so a larger scale study could use a wider range of autoantigens.

6.4.6: Concluding remarks: The future for PBC diagnosis?

A future study to generate a diagnostic formula for PBC could involve large groups of UDCA-naïve PBC patients and healthy volunteers with no detectable PBC by diagnostic criteria or raised AMAs above the 'cut-off' for negative sera. ALP, ALT and levels of different isotypes of the autoantibodies would be gathered. Sera from these same PBC patients one year on, at the point of 'response/non-response' categorisation based on ALP and ALT, would then have the same results gathered from these 1-year-on sera. Comparison of ALP, ALT and autoantibodies from pre- and post- UDCA levels and analysing any responder/non-responder differences could indicate if the different antibody profiles may be due to a response to UDCA or already present. If it is established that there is a notable difference in antibody levels in the UDCA-naïve sera between those who would go on to be responders compared with those who would go on to be non-responders, then this would be indicative of there being a potential diagnostic difference between these patients.

The above experiment could also include other factors of PBC-predictive interest. Those found to show significant difference between healthy volunteers, those that go on to be responders and those that go on to be non-responders found in early serum samples can be applied used in multinomial regressions after adjustment of p values based on 3 groups. Comparisons to the healthy control would be carried out with those who would go on to be responders and those who would go on to be non-responders. Those factors with significant z-calculated p values from multinomial regression would be kept in the formula and the formulae would be tested. The resultant formulae would be:

$$YR = \ln[P(\text{responder})/P(\text{Healthy})] = x_0 + x_1b_1 + x_2b_2 \dots$$

$$YN = \ln[P(\text{Non-responder})/P(\text{Healthy})] = x_0 + x_1b_1 + x_2b_2 \dots$$

(where the 'x' and 'b' values are specific for each formula).

Taking exponentials to both sides gives:

$$P(\text{Responder})/P(\text{Healthy}) = e^{YR} \text{ and } P(\text{Non-responder})/P(\text{Healthy}) = e^{YN}.$$

These can be combined to give:

$$P(\text{Healthy}) = 1/(1+e^{YR}+e^{YN})$$

Given that $P(\text{Healthy})+P(\text{Responder})+P(\text{Non-responder})$ must total 1 (all possible outcomes),

$$(1-P(\text{Healthy}))/P(\text{Healthy}) = e^{YR} + e^{YN}$$

$$\text{and } 1/P(\text{Healthy}) = 1 + e^{YR} + e^{YN}$$

$$P(\text{Healthy}) = 1/(1+e^{YR}+e^{YN})$$

$$P(\text{Responder}) = e^{YR}/(1+e^{YR}+e^{YN})$$

$$P(\text{Non-responder}) = e^{YN}/(1+e^{YR}+e^{YN})$$

Once this formula is designed with the relevant coefficients and intercepts, and tested on large groups of patients, a computer programme calculation could be designed in which the measurements of characteristics found to be significant predictors of no PBC, response and non-response in all previous stages could be entered and a probability for someone suspected of having PBC for them being healthy, a PBC UDCA responder or a PBC non-responder would be given based on these criteria.

Alternatively, for a formula which applied to only PBC-confirmed patients could be expressed as:

$$Y = \ln[P(\text{Non-responder})/P(\text{Responder})] = x_0 + x_1b_1 + x_2b_2 + \dots$$

can give

$$P(\text{Non-Responder})/P(\text{Responder}) = e^Y$$

$$P(\text{Non-responder}) + P(\text{Responder}) = 1$$

$$\text{Substitute in } P(\text{Non-responder}) = 1 - P(\text{Responder})$$

$$(1 - P(\text{Responder}))/P(\text{Responder}) = e^Y$$

$$1 - P(\text{Responder}) = P(\text{Responder})(e^Y)$$

$$1 = P(\text{Responder})(e^Y) + P(\text{Responder})$$

$$1/P(\text{Responder}) = 1 + e^Y$$

$$P(\text{Responder}) = 1/(1 + e^Y).$$

This could also be calculated to find $P(\text{Non-responder})$ rather than $P(\text{Responder})$.

This would then give the probability of a PBC patient being a non-responder or a responder, depending on how the equations are rearranged, provided all of the factors are shown to be accurate responder/non-responder predictors.

7: General Discussions

7.1: Results Summary

7.1.1: Chapter 3: Design of an assay which can distinguish between different subsets of T cell for use in categorising patient subgroup T cell populations and to investigate any skewing ability of UDCA on T cell populations.

One aim of this chapter was to design a method for the distinguishing of different T cell subsets. This assay would have two primary applications. Patient T cell subsets could be investigated for any potential difference pertaining to their response/non-response status and potentially also their length of time on the drug ursodeoxycholic acid (UDCA). This assay would also be used on PBMCs isolated from healthy volunteers to investigate the effect on the T cell population under proliferative

conditions and in the presence of UDCA, to determine if UDCA may be altering the population of activated T cell subsets.

Data from this assay would be useful because it would potentially help to underpin the differences between patients that do respond to the current therapy and those who do not. It is important not only to identify if there are specific T cell profiles identifiable of the different PBC subgroups but also if this could be UDCA-directed or the result of another factor. There are many potential factors which can contribute towards PBC development, such as genetics and environmental factors, discussed in chapter 1, therefore it is important to distinguish if these differences could be a direct impact of the drug or genetic or environmental and if they can be controlled. Additionally, if it were discovered that there are different T cell subsets important in the different PBC subsets, this could lead to measurably different antibody concentrations in patient serum, discussed in chapter 1 and also this chapter.

This assay is useful to help elucidate the role of CD4+ T cells in PBC. Studies already carried out have investigated the role of CD4+ T cells in immunological dysfunction. One such study investigated the importance of the *ras* gene in TCR signalling and have identified microRNAs (miRNAs) which can dysregulate TCR expression and dampen the CD4+ T cell response in PBC (Nakagawa *et al.*, 2017). Other studies have gone so far as to investigate CD4+ subsets and their potential importance in PBC in mouse models and have found that hepatic Th2 and Treg cell populations are increased in disease mice (Zhang *et al.*, 2017), however none have used human PBC patient blood samples and compared CD4+ T cell profiles in the comparison of responders with non-responders.

The design and testing of an assay to identify T cell subsets was successful, with a flow cytometric panel designed which could identify Th1, Th2, Th17 and Treg cells. Patient blood samples were initially anticipated which would allow for the completion of this aim, however administration difficulties led to their being unavailable for the time frame of this project. The panel was, however, used in the following chapter to investigate if UDCA influences proliferation of T cell subsets in healthy volunteers.

7.1.2: Chapter 4: Further elucidating the mechanism of action of UDCA in PBC: investigating a direct effect on T cells in the cholangiocytes

One aim of this chapter was to implement the assay designed in the chapter '**Design of an assay which can distinguish between different subsets of T cell for use in categorising patient subgroup T cell populations and to investigate any skewing ability of UDCA on T cell populations.**' This entailed investigation into if there may be any differences in T cell subsets having differential impacts in patients of the different subgroups in PBC. Additionally, this chapter investigated if there was a UDCA influence in a T cell's ability to carry out essential functions such as surmount a response to antigen or proliferate. Finally, the chapter investigated if UDCA influences the proliferation of cholangiocytes lining the small bile ducts, but also if it influences the types of cytokines they release which may then influence proliferation of the T cells.

Investigating any effect of UDCA which could be of clinical relevance is important because the identification of different subgroups of patients was initially carried out based on response to this drug, therefore investigating the impact of the drug in responders may uncover key pathways and processes which differ between responders and non-responders. It is important to directly study the impact of UDCA on the cholangiocytes as these are the primary cells damaged in this disease and the initial site of inflammation. Protection of the structural integrity of the small bile ducts is key to prolonging liver survival and therefore patient wellbeing and survival. The disease is amplified by the auto-reactive immune cells causing and perpetuating inflammation in the disease site. It has been reported that removal of the stimulus can render a patient able to regenerate organ health (Jones 1999). As the disease is autoimmune and removal of the stimulus is impossible, dampening down the immune response becomes the key method for therapeutic intervention. If UDCA has an impact on dampening down the immune response, this is of clinical importance because uncovering the specific biological impact could highlight areas for investigation for elucidating responder/non-responder differences.

Studies into the effect of UDCA on the cholangiocytes have been carried out, some focussing on their proliferation, and data in this study further confirm this. It has been known for some time that UDCA can reduce proliferation in rat cholangiocytes by activation of Ca^{2+} -dependent signalling (Marzioni *et al.* 2006). Data in this thesis investigates if there is a similar attenuation of proliferation on human cholangiocyte cell-line H69 cells by UDCA and confirms a significant decrease compared with the ethanol control at concentrations of 0.25mM ($p=0.031$), 0.5mM ($p=0.004$) and 1mM ($p=0.026$). The data in this thesis goes further and suggests that the cholangiocytes may also alter their cytokine secreting profile in response to UDCA, as T cells incubated in the supernatant of previously UDCA-treated cholangiocyte cell line (H69) cells show significantly less proliferation compared with untreated H69 cell culture. The effect was measurable with culture 1 and 2 days post-wash ($p<0.05$; $p<0.001$).

Importantly, data in this thesis have shown that there is a significant reduction of CD8+ T cell proliferation as a direct effect of UDCA ($p=0.03$). Many studies have outlined the importance of CD8+ T cells in PBC. It has been known for some time that infiltration into the liver of autoreactive CD4+ and CD8+ T cells is an early event in PBC and infiltrating CD8+ T cells have been known for some time to be key mediators of tissue damage (Palmer *et al.*, 1999). Taken alongside the data from the ELISpot assays, that responsiveness of some CD4+ T cells to antigen may be

attenuated in the presence of UDCA (at 0.5mM, $p=0.002$; at 1mM, $p=0.0006$), this could suggest that the drug has an effect on both CD4+ and CD8+ T cells, but the effects may be different.

7.1.3: Chapter 5: The development of an ELISA assay using End Point Titre to compare serum levels of anti-PDC autoantibodies in UDCA responder and non-responder PBC patients.

This chapter aimed to design an assay which would allow the quantification of anti-PDC autoantibodies in patient blood for their direct comparison. Importantly, it needed to be determined if patient anti-PDC titres could be accurately quantified using a screening method rather than the more time consuming short dilution end point titre method. An assay which can be carried out quickly and in a cost-effective method is important for if this method could go on to have diagnostic applications. This assay could identify differences in the antibody profiles of different patient subsets to be identified to further elucidate key differences between the sub groups of PBC patients. If patient blood samples had been received from patients and their T cell subset profiles had been established, the data in this chapter may have been able to confirm the impact of the T cell with the antibodies produced by the plasma cells acting as a read out of the cytokine instructions received from the T cells.

Additionally, this assay could allow for the determination of if responders and non-responders have antibodies targeting different epitopes of PDC subunits.

The primary aim of this chapter was to determine if screening patient serum with optimised protein concentration is accurate enough a representation of their autoantibody titre for the use of screens to be used in further experiments to determine significant differences between autoantibody levels of different patient groups. This was achieved, with screen duplicate results following Spearman's Rank correlations of $r_s > 0.6$ and $p > 0.0005$ for the antigens of rhE2, rhE2ILD and rhE3BP.

7.1.4: Chapter 6: Investigating differences in immune responses between PBC patients that are responders and non-responders to UDCA

The aim of this chapter was to apply statistical analysis to all patient data including that obtained in the autoantibody screens from the previous chapter and attempt to uncover some statistically significant differences in patient subgroups, with the particular focus on any difference between UDCA responders and non-responders. The data uncovered in this chapter does provide the first instance of levels of autoantibodies which are significantly different between responders and non-responders.

While current research focuses on development of new drugs which can be used instead of or in conjunction with UDCA (Suraweera *et al.* 2017), this chapter focusses on starting to underpin the biological reasoning behind why patient subgrouping was initially discovered.

This chapter was successful, most importantly in that there were some antibodies discovered which are significantly overproduced in non-responders compared to responders, which were anti-rhE2ILD IgG3 ($p=0.01$), anti-rhE2ILD IgA ($p=0.047$) and

anti-E2IgE ($p=0.025$). Additionally, there was a difference in antibody profiles discovered between males and females whereby males with PBC were found to have significantly underproduced anti-rhE2IgE ($p=0.003$), anti-rhE2ILD IgE ($p=0.05$) and anti-rhE3BP IgA ($p=0.037$) compared to females. These data indicate that although there may be an underlying B- or T-cell difference orchestrating the difference in antibody profiles uncovered here between responders and non-responders, the difference in disease severity between males and females is possibly differently orchestrated. This is novel data which is the first to identify a significant difference in disease phenotype between patient groups in PBC.

7.2: Further work

There is considerable expansion on this body of work which can help further the progression of this disease to one which has treatments in line with stratified medicine.

Individual results chapters outline how each separate piece of work can be furthered, but to take all chapters together there are some key questions which are arisen from the findings in this thesis.

One such question stems from findings that UDCA may be affecting proliferation of different T cells differently. It then becomes important to consider why this might be the case. It becomes important to consider the proliferation mechanisms of CD4+ T cells and CD8+ T cells. Propagation of the T cell signal intracellularly, once there has been a TCR antigen recognition event and complex formation at the cell surface (outlined in general introduction), with the tyrosine phosphorylation of immunoreceptor tyrosine-based activation motifs (ITAMs) in the cytoplasmic domains of CD3. The TCR-CD3 complex contains 10 functional ITAMs, allowing for functional differentiation from ITAMS of other immune cells (Guy *et al.*, 2013). Further differentiation in downstream signalling can arise with the inclusion of CD4

or CD8 and whether the cell is memory or effector (Guy *et al.*, 2013). To elucidate why UDCA may be having a differential impact on CD4+ and CD8+ T cells, the inclusion of a flow cytometric panel which also distinguishes effector and memory could uncover further differences and then allow postulation of why this differential effect is seen, and thus further uncover pathways of interest in the mechanism of action of UDCA. Such a panel would include CCR7 and CD45RA antibodies, where CCR7+CD45RA+ are naïve, CCR7+CD45RA- cells are effector, CCR7-CD45RA+ cells are central memory and CCR7-CD45RA- cells are effector memory. The flow panel for determining the impact of UDCA on T cell subsets would be repeated using a larger number of volunteers and the inclusion of these markers. Further flow cytometry assays could intracellularly stain for cytokines known to induce class switching in B cells.

Additionally, as the impact of UDCA can vary between patients, establishing the extent of this which could be due to the body's ability to metabolise the drug could be investigated. If responders and non-responders metabolise the drug differently, this could help explain the large discrepancy seen in its effectiveness between patient groups. In 2012, Dilger and colleagues carried out pharmacokinetic profiling of the bile acids entering the duodenum from the liver to investigate UDCA metabolism and its enrichment (Dilger *et al.*, 2012). This experiment repeated in the context of responders and non-responders could offer some insight into any differential metabolism of UDCA between the response/non-response groups. Taking findings from this experiment could bring into contextual relevance some findings in this thesis: UDCA appears to attenuate T cell proliferation, particularly CD8+ T cells and may also render CD4+ T cells less able to recognise antigen, so if some patients are unable to metabolise UDCA in such a way that it can be effective, then different UDCA analogues could be investigated for those individuals. The largest improvement which could be made to this work would be the inclusion of patient cells. This would potentially allow for all experiments carried out in this thesis to be done so with the aim of directly elucidating differences between patient subgroups. Although some progress has been made towards elucidating potential differences in the comparison of autoantibody profiles between responders and non-responders and also males and females, with the inclusion of blood cells there could be comparison of the impact of UDCA on proliferation and antigen recognition of T cells between responder and non-responder groups. If no difference were discovered, then this would point towards a potential other impact such as a liver or microbiome metabolomic influence whereby the drug is less accessible to the non-

responders, to do with how it is processed. Inclusion of patient cells would also give the potential for those genes of interest in the GWAS carried out by Mells and colleagues in 2013 to be sequenced and analysed for the SNPs, in the context of a responders and non-responders comparison to determine if an SNP profile may possibly dictate response (Mells *et al.*, 2013). Most importantly, flow cytometric analysis of the T cells in patient blood including intracellular staining of cytokines could help elucidate the reason why the different antibody profiles were discovered between patient groups and if there is influence from T cell cytokines.

The era of stratified medicine calls for personalisation of therapy. While much research is being carried out into new drugs which are effective on a greater percentage of PBC patients, outlined in the main introduction, these in general are only prescribed after up to a year of the patient on UDCA, an ineffective drug for up to 20% of patients (Carbone *et al.*, 2013) and additionally a new study suggests the onset of jaundice is a risk with rapid switching of UDCA to obeticholic acid, an FXR ligand effective in the UDCA non-responding population (Quigley *et al.*, 2018). It is imperative to further work to establish a diagnostic assay which can allow for early application of the appropriate therapy. For this to be possible, a large-scale comparison study must be undertaken of a large number of patients taking into account their response or lack thereof to UDCA. UDCA is known to be metabolised by bacteria in the gut, and a recent study has analysed the microbiome of PBC patients and found that the microbiome is altered in PBC and partly restored after UDCA therapy (Tang *et al.*, 2017). This data in light of whether or not a patient was classified as a 'responder' to UDCA could highlight some microbiomal differences and possibly areas where microbiome manipulation could be therapeutically beneficial. Additionally, if the GWAS by Dilger and colleagues in 2013 were extended to include a comparison of responders and non-responders then this could reveal some SNPs which may predispose a particular disease phenotype (Dilger *et al.*, 2012).

7.3: General remarks

This thesis has made considerable progress in untangling the differences between the elusive subgroups of PBC, helping take this disease into the era of stratified medicine. The concept of response/non-response was first conceptualised given comparisons between patients and their response to UDCA. The impact of UDCA has been investigated and has highlighted key potential mechanisms of action,

namely on proliferation of CD8⁺ T cells and antigen recognition of CD4⁺ T cells. Additionally, a discrepancy between responders and non-responders in antibody titre has been identified in that non-responders have higher levels of rhE2ILDlgG3 and rhE2ILDlgA, so taking this antigen on its own could indicate IFN- γ and TGF- β influence, but further work has been suggested which could confirm this in the way of flow cytometry of patient T cells. Overall, this thesis is the first piece of work to suggest biological reasoning behind the detected phenotypic differences between groups of PBC patients and highlights the importance of directing further research into this disease down a stratified approach.

Chapter 8: Appendix

BANC study ID	Date Recruited	Months since recruit	Age	Sex	Ethnicity	Weight	Date of diagnosis	Yrs since drawn	Yrs since diagnosis	Age at diagnosis	Date UDCA started	Yrs since UDCA start	Current UDCA dose	mg/kg dosage	Cohort	AMA	ANA	UDCA responder	Bilirubin	ALP	ALT
BANC00185	15/01/2015	24	58	F	W	68.8	2008	2	9	52	2008	9	900	13.081	A	1		R	8	107	27
BANC00385	22/01/2015	24	33	F	W	56	01/10/2014	2	3	56	01/01/2014	3	750	13.393	A	1		R	10	109	42
BANC00285	22/01/2015	24	76	F	W	85.6	1996	2	11	56	20/02/96	21	1000	11.682	A	1		R	6	157	11
BANC004C5	29/01/2015	24	67	F	W	81.2	29/01/2015	2	?	?	?	?	?	?	B						
BANC00585	05/02/2015	23	62	F	W	64	2000	2	16	48	01/03/2002	15	900	14.063	A	1		R	12	191	27
BANC00685	12/02/2015	23	61	F	W	87	01/09/2010	2	6	50	01/10/2010	7	1250	14.368	A	1		R	7	127	39
BANC00785	19/02/2015	23	55	F	W	58.9	01/12/2010	2	6	50	01/12/2010	7	0	0	A	1		NR	10	861	99
BANC00885	26/02/2015	23	35	F	W	104.8	01/07/2014	2	3	34	2012	5	1500	14.313	A	1			4	74	16
BANC00985	26/02/2015	23		F			2014	2	3		/				B	1					
BANC01085	12/02/2015	23	45	F	W	71	01/10/2006	2	11	37	17/01/2007	10	900	12.676	A	1		NR	8	413	163
BANC01185	05/03/2015	22	49	F	W	65.8	2009	2	8		31/10/2011	6	1000	15.198	A	1		NR	6	415	75
BANC01285	05/03/2015	22	73	F	W	87.6	1995	2	22		1996	21	1000	11.416	A	1		R	5	71	19
BANC01385	05/03/2015	22	86			46.6	1992	2	25		1992	25	500	10.73	A	1		R	10	233	23
BANC01485	12/03/2015	22						2					750	0	A	1		R	7	124	9
BANC0158	19/03/2015	22	68	M	W	85	2001	2	16	55	?	?			A			Post OLT			
BANC0168	19/03/2015	22	53	F	W	77.6	01/05/1998	2	19	37	01/05/1998	19	900	11.598	A			Post OLT			
BANC0178	20/03/2015	22						1.5							B	1					
BANC0188	23/07/2015	18	42	F	W	84	2004	1.5	13	30	2004	13	1250	14.881	A	1		NR	13	438	150
BANC0198	30/07/2015	18	56	F	W	77	2011	1.5	6	52	30/07/2015	2	1000	12.987	B			R	5	157	25
BANC0208	30/07/2015	18	81	F	W			1.5					900		A	1		NR	10	295	60
BANC0218	30/07/2015	18						1.5					1000		A	1		NR	6	292	57
BANC0228	30/07/2015	18	55	F	W	74.2	2008	1.5	9	48	2008	19	1000	13.477	A	1		NR	5	222	44
BANC0238	30/07/2015	18	54	F	W		2015	1.5	2	54	2015	2	900		A	1		?R	5	181	24
BANC0248	30/07/2015	18	69	F	W		2005	1.5	12	59			1000		A	2		R	7	65	27
BANC0258	06/08/2015	17	60	F	W		2005	1.5	12	50	2005	12	900		A	2		R	5	180	17
BANC0268	13/08/2015	17						1.5					750		A	1		NR	20	218	86
BANC0278	13/08/2015	17	52	F	W	81.4	2007	1.5	10	44	2007	10	1250	15.356	A	1		/	14	358	49
BANC0288	13/08/2015	17	76	F	W	90.1	2002	1.5	15		2002	15	600	6.6593	A	2		R	6	68	7
BANC0298	13/08/2015	17	50	F	W	82	07/12/2012	1.5	5	48	07/12/2012	5	750	9.1463	A	1		R	18	200	46
BANC0308	13/08/2015	17	59	F	W	84	01/06/2006	1.5	11	50	2010	7	1000	11.905	A	1		R	9	85	17
BANC0318	14/08/2015	17	62	M	W	84.5	2011	1.5	6		2011	6	1000	11.834	A						
BANC0328	20/08/2015	17	65	F	W		2009	1.5	8				1000		A	1		R	5	54	9
BANC0338	20/08/2015		64	F	W		2004	1.5	13				900		A	1		R	5	187	19
BANC0348	27/08/2015		52	F	W	72.2	01/03/2014	1.5	3	51	01/03/2014	3	750	10.388	A	1		R	6	110	19
BANC0358	27/08/2015		50	F	W		2006	1.5	11	41	2006	11	1000		A	1		R	17	150	49

Figure 8.1: Raw patient data provided by freeman hospital, patients 1-35. W indicates white; F indicates female; M indicates male; NR indicates non-responder; R indicates responder; A indicates not UDCA-naïve; B indicates UDCA-Naïve.

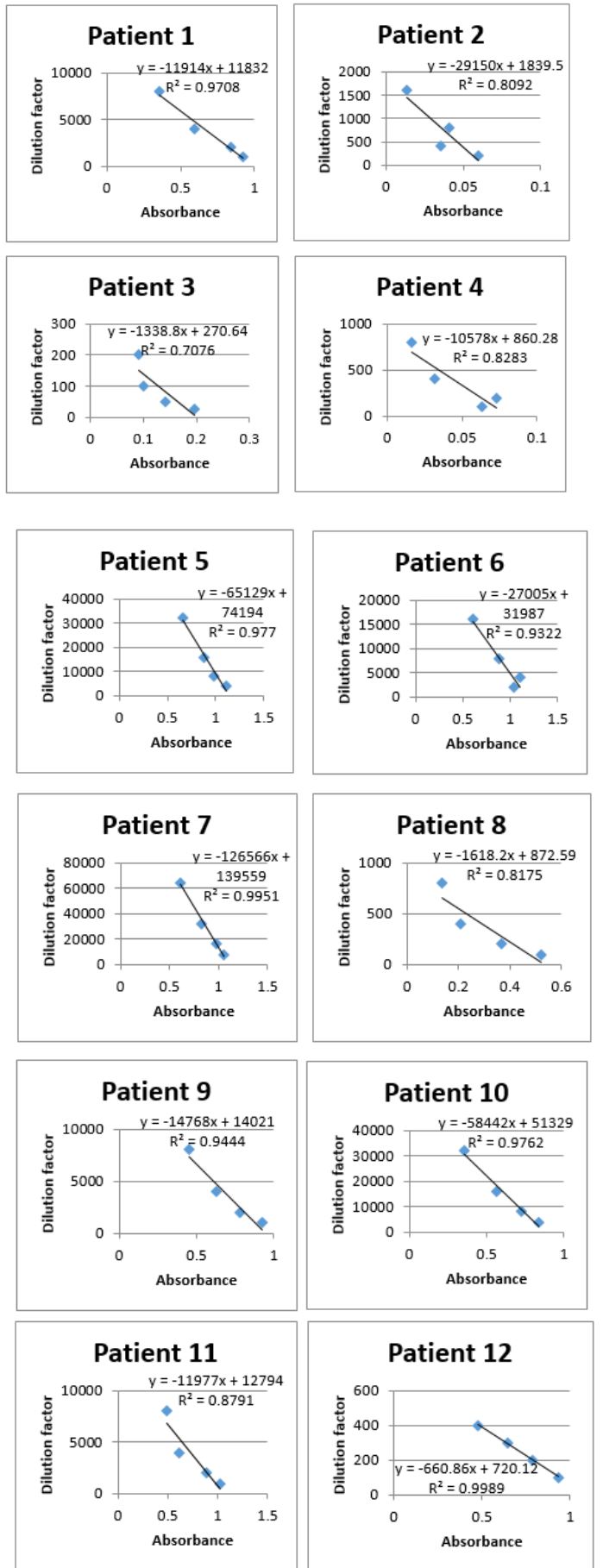
BANC study ID	Date recruited	Months since recruit	Age	Sex	Ethnicity	Weight	Date of diagnosis	Yrs since drawn	Yrs since diagnosis	Age at diagnosis	Date UDCA started	Yrs since UDCA start	Current UDCA dose	mg/kg dosage	Cohort	AMA	ANA	UDCA responder	ALT	AlP	Bilirubin		
BANC036B	27/08/2015		47	F	W	75	1998	1.5	19		27/08/2015	2	500	6.6667	B			R			4	48	26
BANC038B	10/09/2015		65	F	W	80.2	2009	1.5	8		2009	8	1500	18.703	A	1		R			11	191	55
BANC039B	10/09/2015		49	F	W	101	1996	1.5	21	29	1999	18	1250	12.376	A	1		R			20	349	136
BANC040B	10/09/2015							1.5					1500		A	1		NR					
BANC041B	17/09/2015		64	F	W		01/07/2015	1	2	64	18/09/2015	2	2000		B								
BANC042B	01/10/2015		49	F	W	157	01/05/2005	1	12		2005	12	2000	12.739	A	1	2	R			5	146	24
BANC044B	08/10/2015		81	F	W	75.9	2001	1	16		2001	16	1000	13.175	A	1	2	R			9	112	16
BANC045B	08/10/2015		79	F	W	85.8	1997	1	20		1998	19	1200	13.986	A	?	?	R			9	191	45
BANC046B	08/10/2015		45	F	W	81	01/07/2003	1	14		01/06/2005	12	600	7.4074	A	1	2	R			6	122	32
BANC047B	08/10/2015		82	F	W	62.1	1993	1	24		1993	24	1000	16.103	A	1	2	R			9	50	20
BANC048B	15/10/2015		64	F	W	70.8	2000	1	17		2000	17	1000	14.124	A	1	2	R			10	53	17
BANC049B	29/10/2015		59	F	W	59.2	01/12/1986	1	31		28/07/2015	2	500	8.4459	A	1	2	NR			9	296	56
BANC050B	05/11/2015		38	F	W	89.7	2010	1	7		2010	7	1500	16.722	A	1	2	NR			8	242	43
BANC051A	12/11/2015		59	F	W	84.6	2010	1	7		27/09/2010	7	500	5.9102	A	2	2	R			16	137	17
BANC053A	07/01/2016		49	F	W	57.8	2005	1	12	39	2005	12	900	15.571	A			Post-OLT			7	129	21
BANC054A	07/01/2016		60	F	W	79.6	2003	1	14	48	2003	14	1000	12.563	A	2	2	R			10	134	39
BANC055A	14/01/2016		59	F	W	102	01/01/1999	1	18	40	1999	18	1250	12.255	A	1	2	R			6	63	12
BANC056A	14/01/2016		60	F	W	61.2	2008	1	9		2008	9	600	9.8039	A	1	2	R			7	114	18
BANC057A	21/01/2016					54.8	2009	1	8		2009	6	900	16.423	A	1	2	R			8	242	43
BANC058A	28/01/2016		39	F	W	66.4	01/01/2014	1	3	37	01/01/2014	3	1000	15.06	A	1	2	NR			5	315	90
BANC059A	04/02/2016		67	F	W		2004	1	13	55	2004	13	600		A	1	2	R			5	128	18
BANC060A	25/02/2016		67	F	W	62.8	01/01/2013	1	4		01/01/2013	4	NA		A	1	2	R			5	106	17
BANC061A	25/02/2016		32	F	W	74.2	01/09/2012	1	5		2012	5	500	6.7385	A	1	2	NR			46	390	110
BANC062A	25/02/2016		47	F	W	87.2	01/05/2009	1	8	40	2011	6	1250	14.335	A	1	2	R			4	75	11
BANC063A	10/03/2016		46	F	W		2012	1	5		2012	5	1250		A	1	2	R			7	104	17
BANC064A	24/03/2016		62	F	W	75.8	2009	1	8		2009	6	1000	13.193	A	1	2	R			7	126	40
BANC065A	24/03/2016		62	F	W	71	2007	1	10		2007	10	1000	14.085	A	1	2	R			3	86	21
BANC066A	28/04/2016		69	F	W	67.2	2013	0.5	4		01/01/2016	1	1000	14.881	A	1	1	R			5	137	34
BANC067A	28/04/2016		64	F	W	70	1993	0.5	24		1996	21	750	10.714	A	?	?	R			4	57	16
BANC068A	12/05/2016		52	M	W	92.7	12/05/2016	0.5	1	52			1250	13.484	B	1	2	/			8	152	41
BANC069A	19/05/2016		59	F	W	76	14/09/2010	0.5	7		01/09/2010	7	750	9.8684	A	2	2	R			6	138	29
BANC070A	19/05/2016		65	F	W		2007	0.5	10		2013	4	600		A	2	1	R			11	89	42
BANC071A	26/05/2016		77	F	W		26/05/2016	0.5	1		26/05/2016	1	750		B	1	2	/			9	110	42
BANC072A	02/06/2016		63	F	W	55.8	01/07/2013	0.5	4	60	01/07/2013	4	750	13.441	A	1	2	R			5	91	30
BANC073A	07/04/2016		68	F	W	69	1996	0.5	21		1996	21	1000	14.493	A	1	2	R			7	101	31

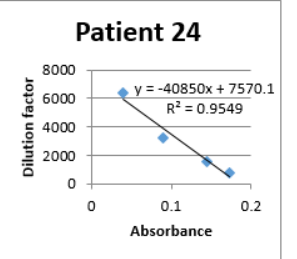
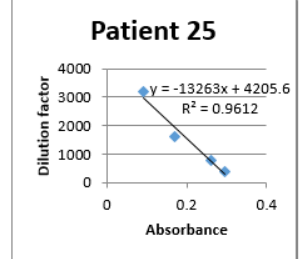
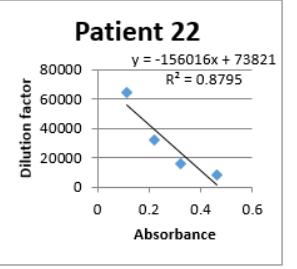
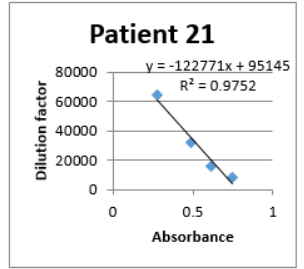
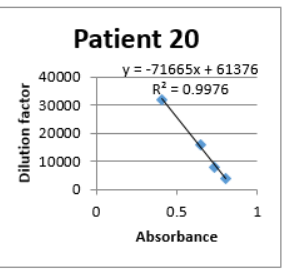
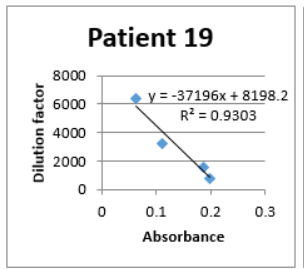
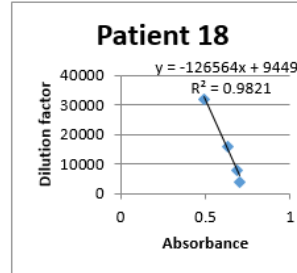
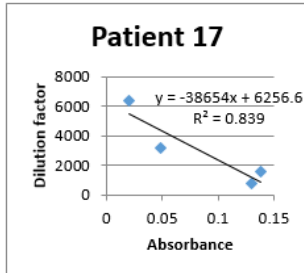
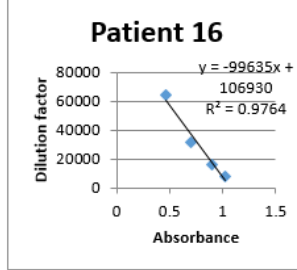
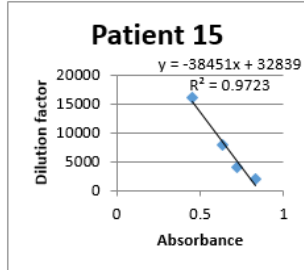
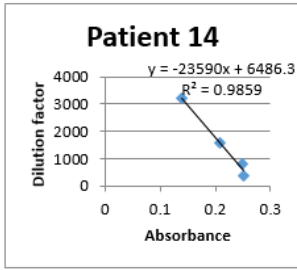
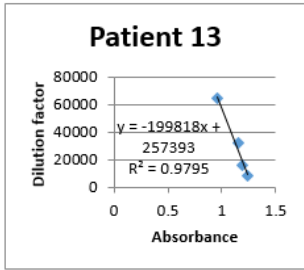
Figure 8.2: Raw patient data provided by freeman hospital, patients 36-73. W indicates white; F indicates female; M indicates male; NR indicates non-responder; R indicates responder; A indicates not UDCA-naïve; B indicates UDCA-Naïve.

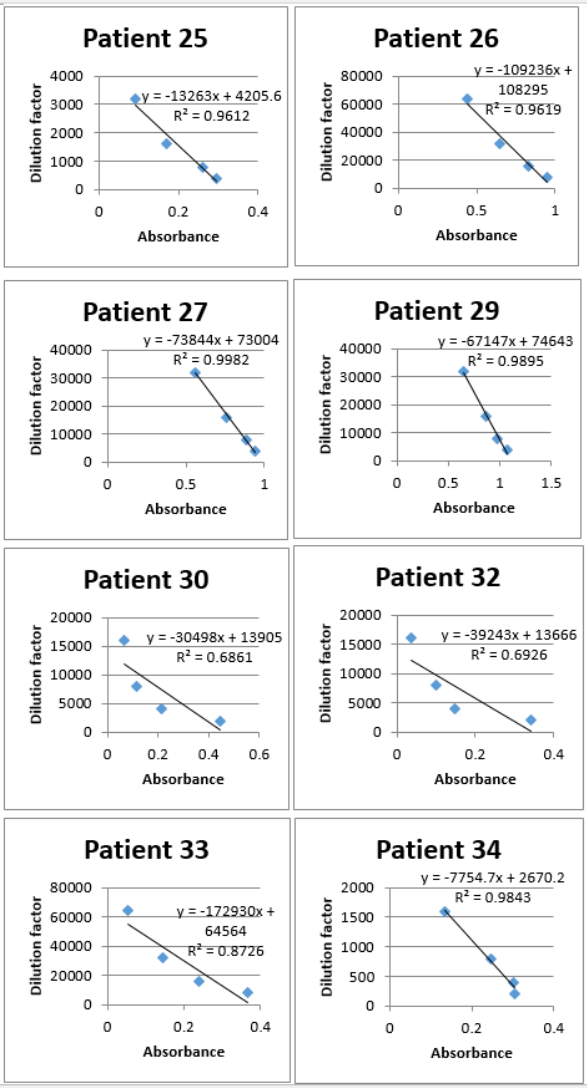
BANC study ID	Date Recruited	Months since recruit	Age	Sex	Ethnicity	Weight	Date of diagnosis	Yrs since drawn	Yrs since diagnosis	Age at diagnosis	Date UDCA started	Yrs since UDCA start	Current UDCA dose	mg/kg dosage	Cohort	AMA	AMA responder	UDCA responder	Bilirubin	ALP	ALT
BANC074A	09/06/2016		79	F	W	48	1995	0.5	22		2015	2	500	10.417	A	1	2	R	6	165	25
BANC075A	09/06/2016		65	F	W	67.8	2013	0.5	4		2013	4	1000	14.749	A	1	2	R	17	171	23
BANC076A	07/04/2016		66	F	W	55.5	01/11/2000	0.5	17	56	01/11/2000	17	900	16.216	A	1	2	R	76	371	47
BANC077A	23/06/2016							0.5					1000		A	1	2	NR	7	628	101
BANC078A	23/06/2016							0.5					1000		A	1	2	NR	11	259	173
BANC079A	23/06/2016							0.5					900		A	1	2	R	14	103	15
BANC080A	30/06/2016		61	F	W	80.6	2009	0.5	8		28/09/2009	8	1000	12.407	A	2	R	4	4	91	34

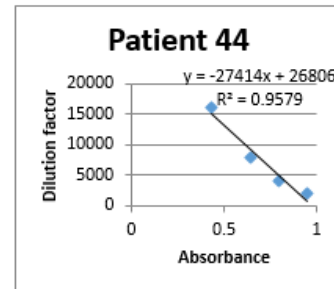
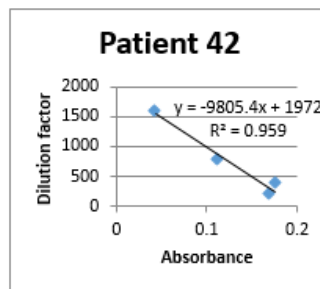
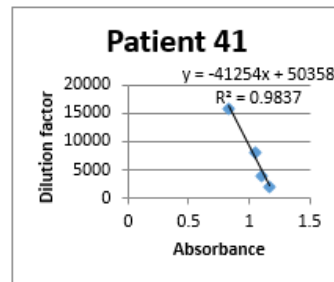
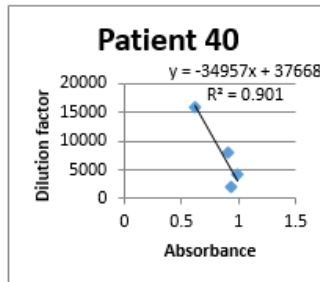
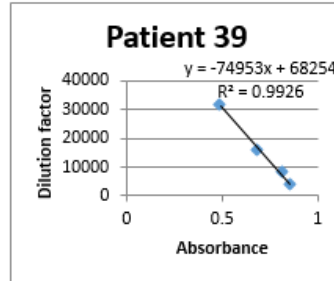
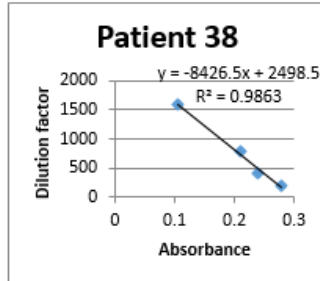
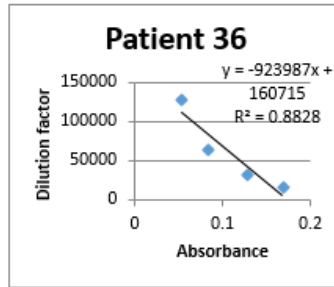
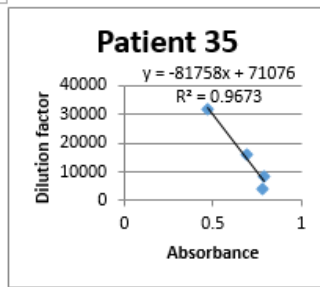
Figure 8.3: Raw patient data provided by freeman hospital, patients 74-80. W indicates white; F indicates female; M indicates male; NR indicates non-responder; R indicates responder; A indicates not UDCA-naïve; B indicates UDCA-Naïve.

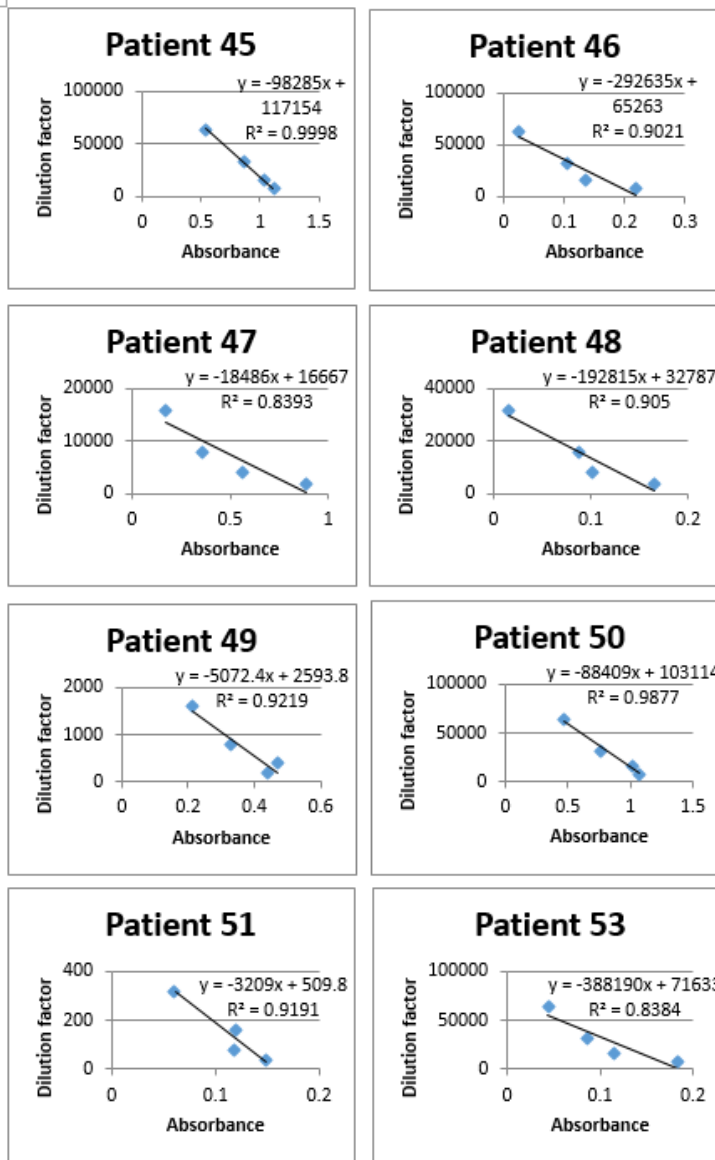
rhE2:

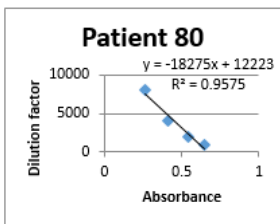
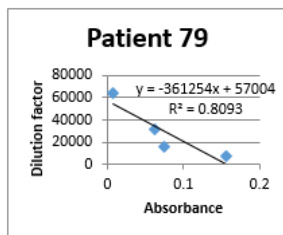
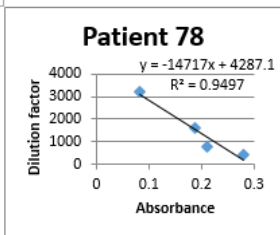
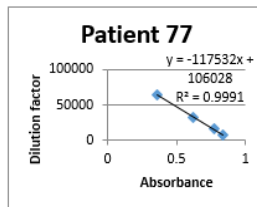
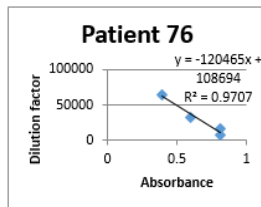
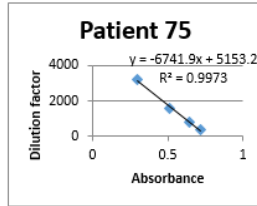
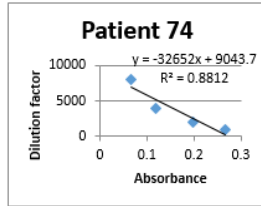
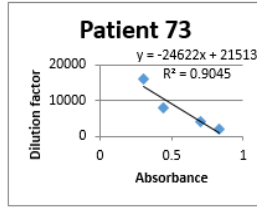
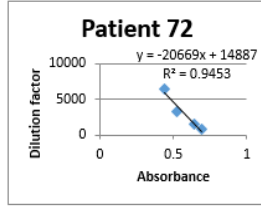
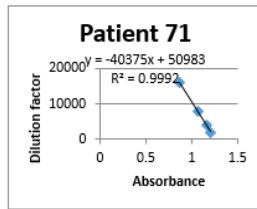
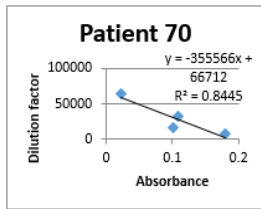




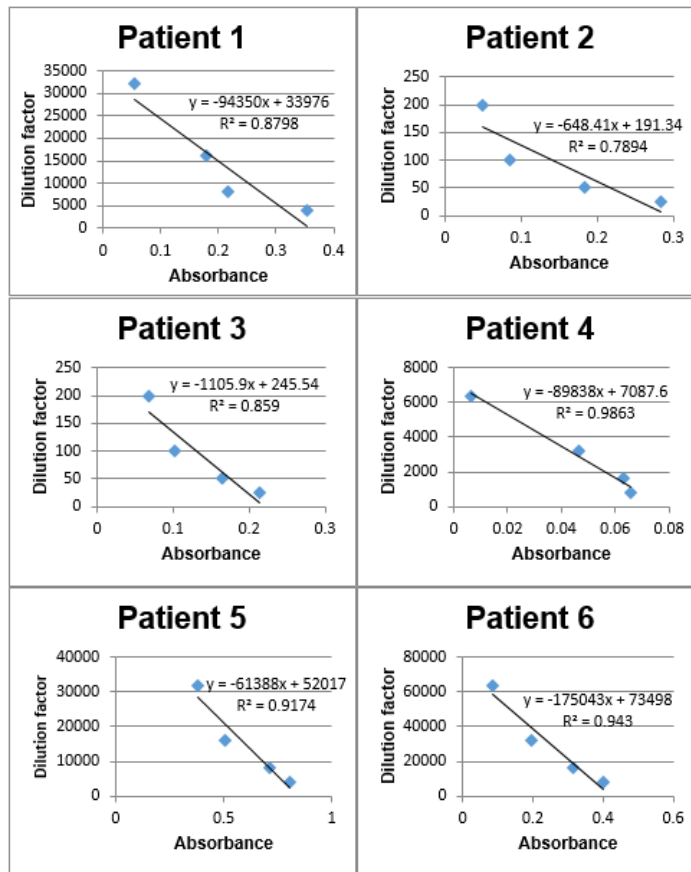


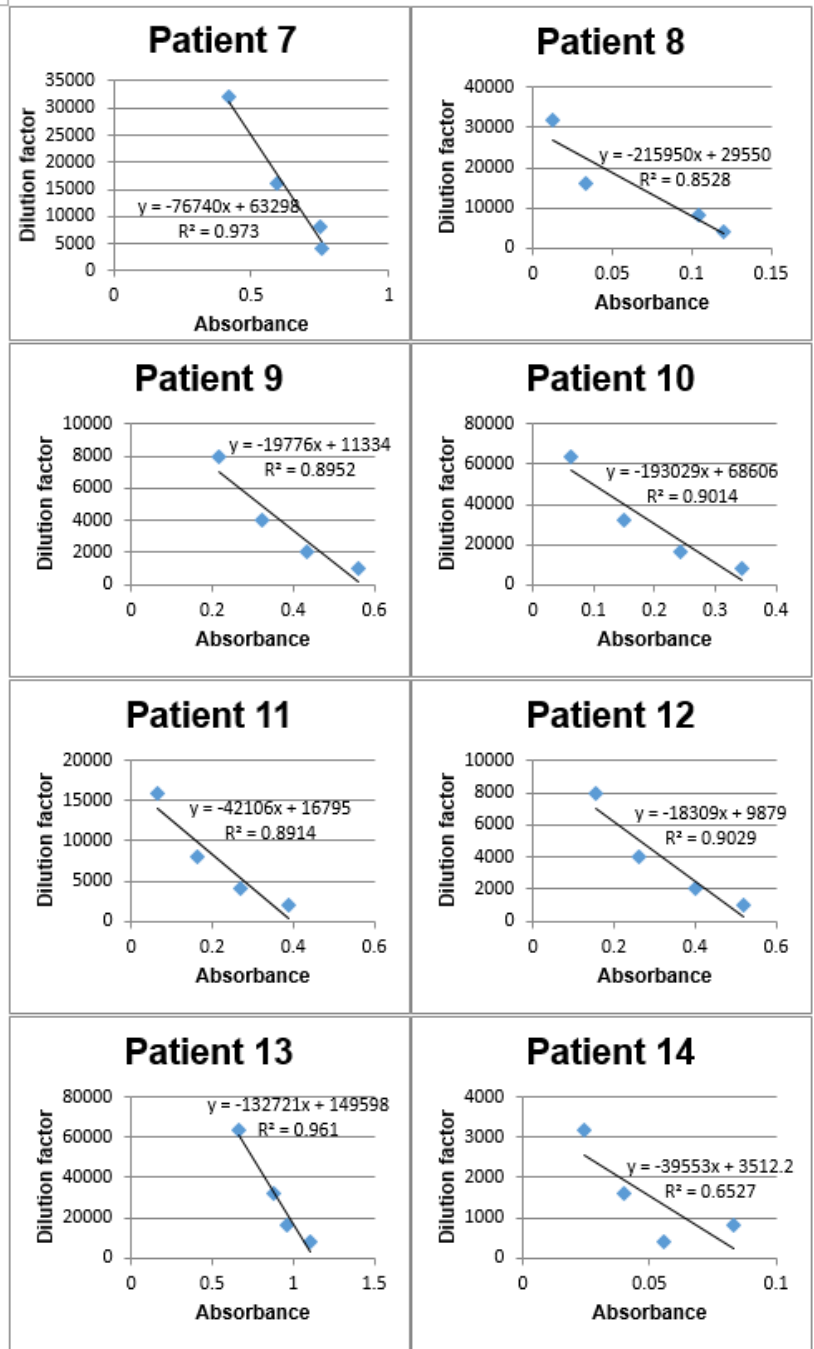


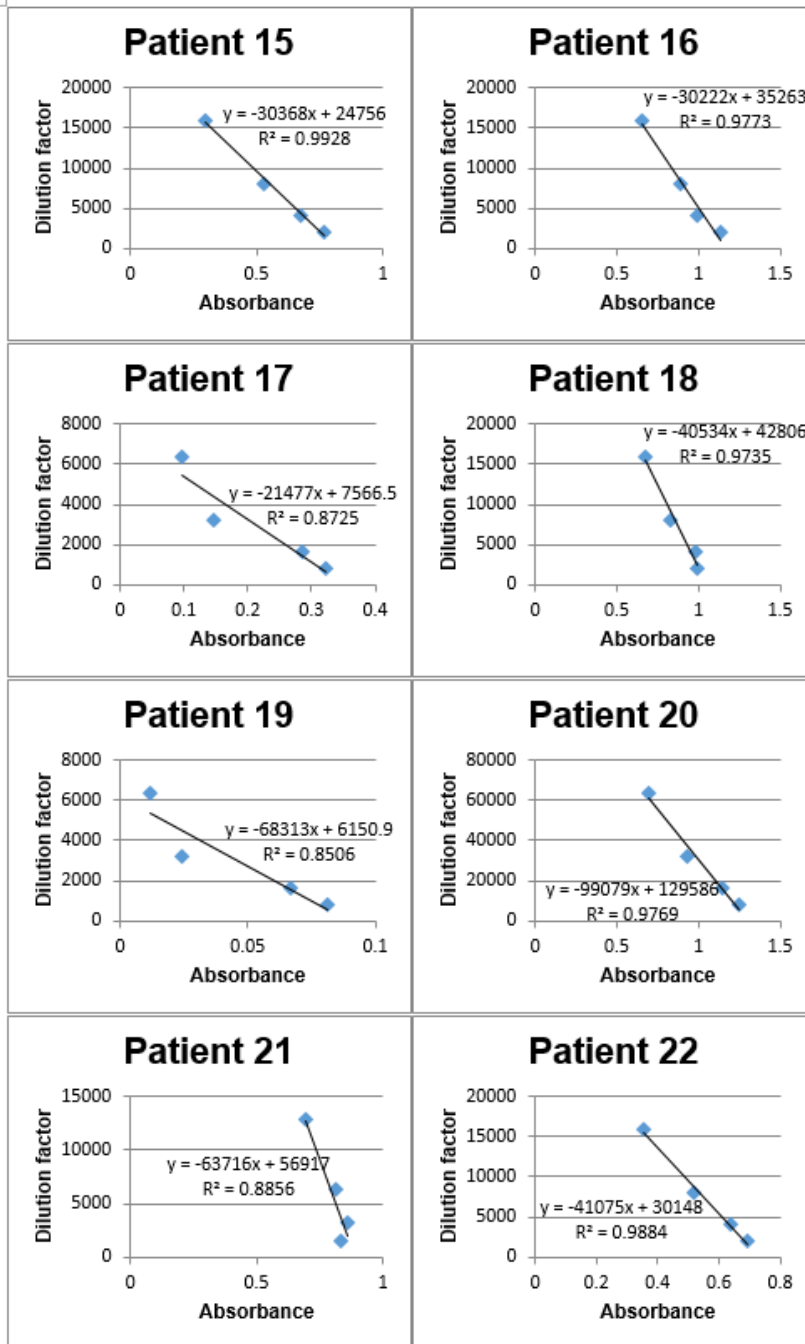


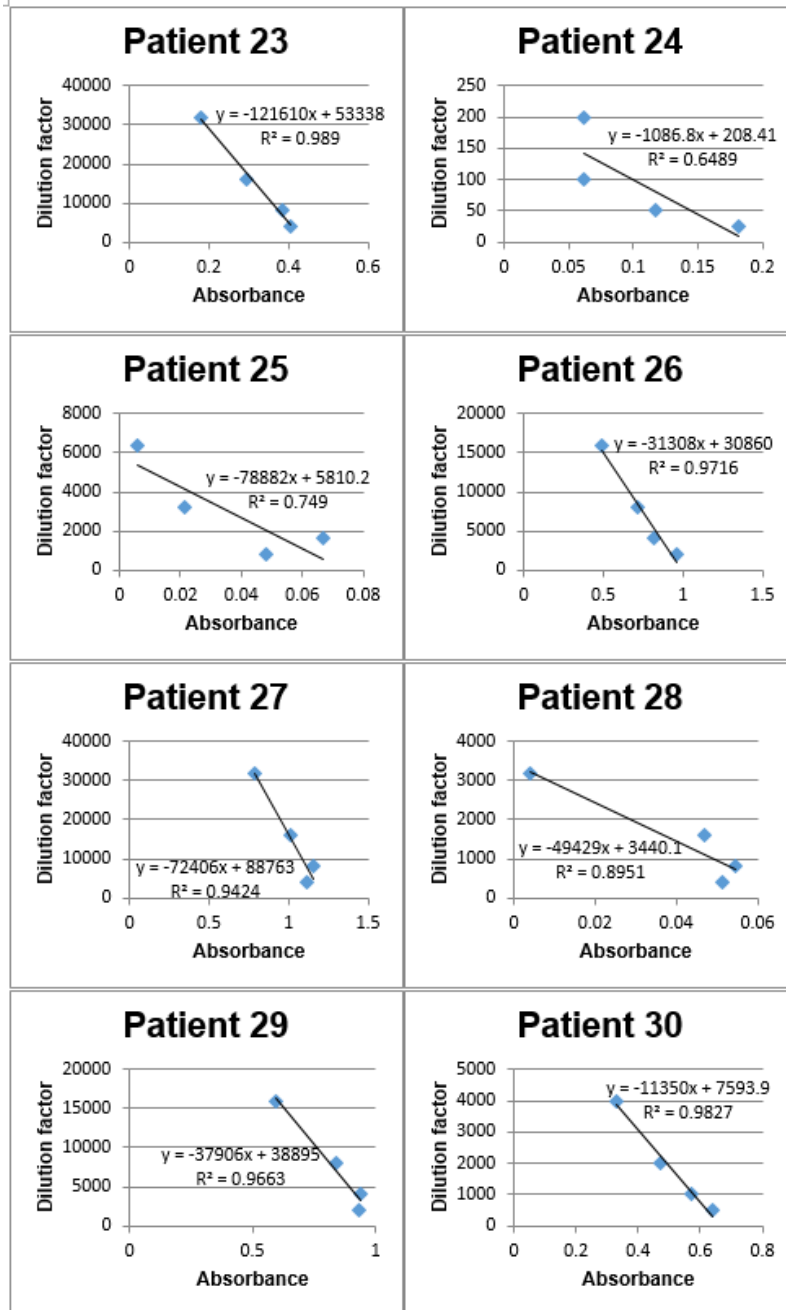


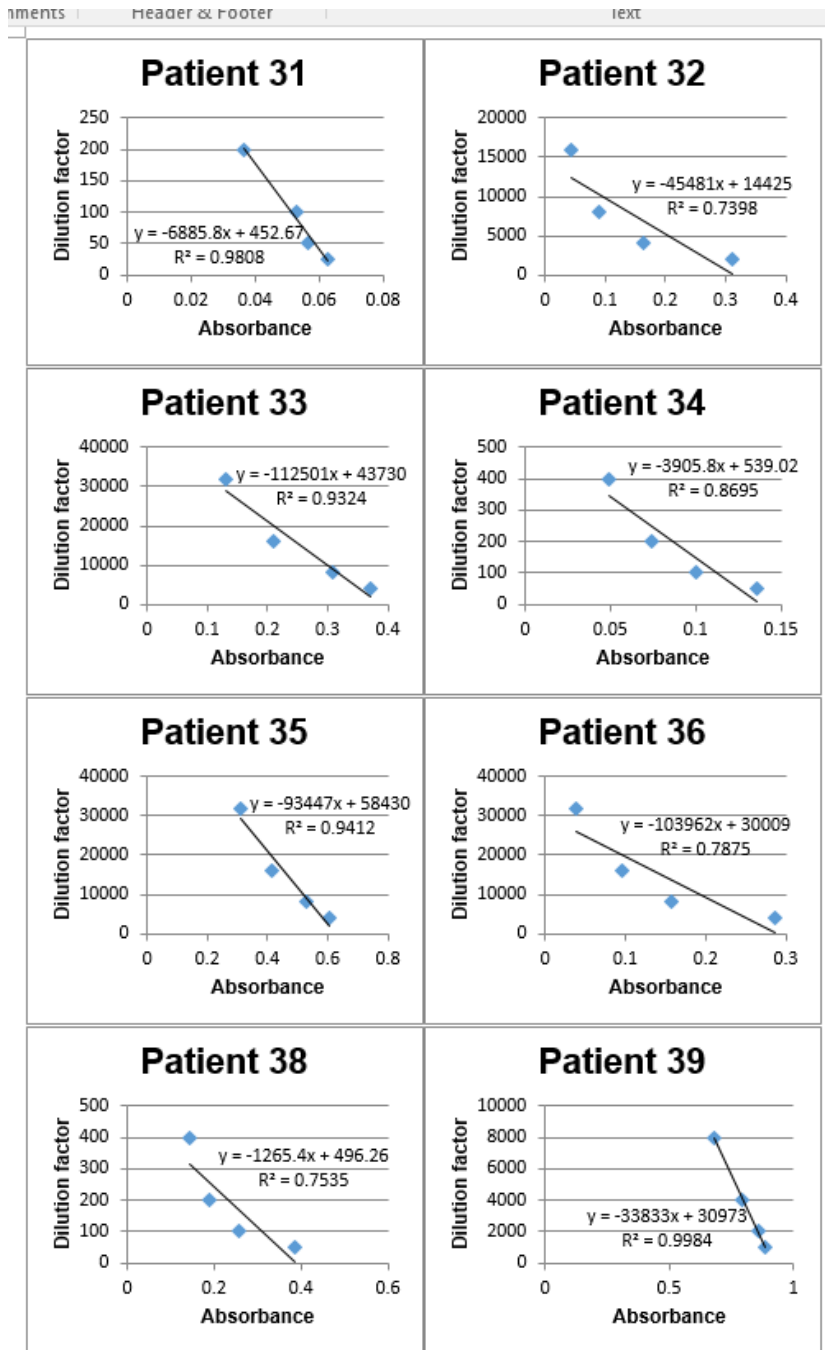
rhE2ILD:

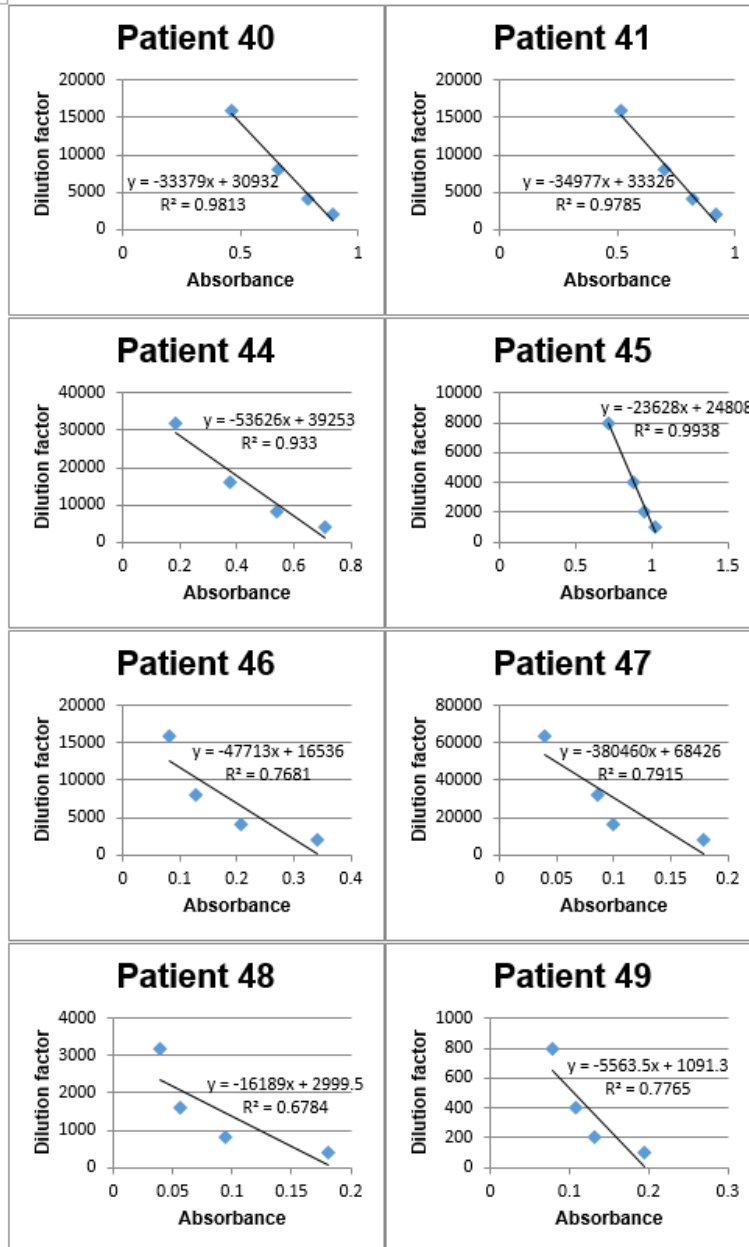


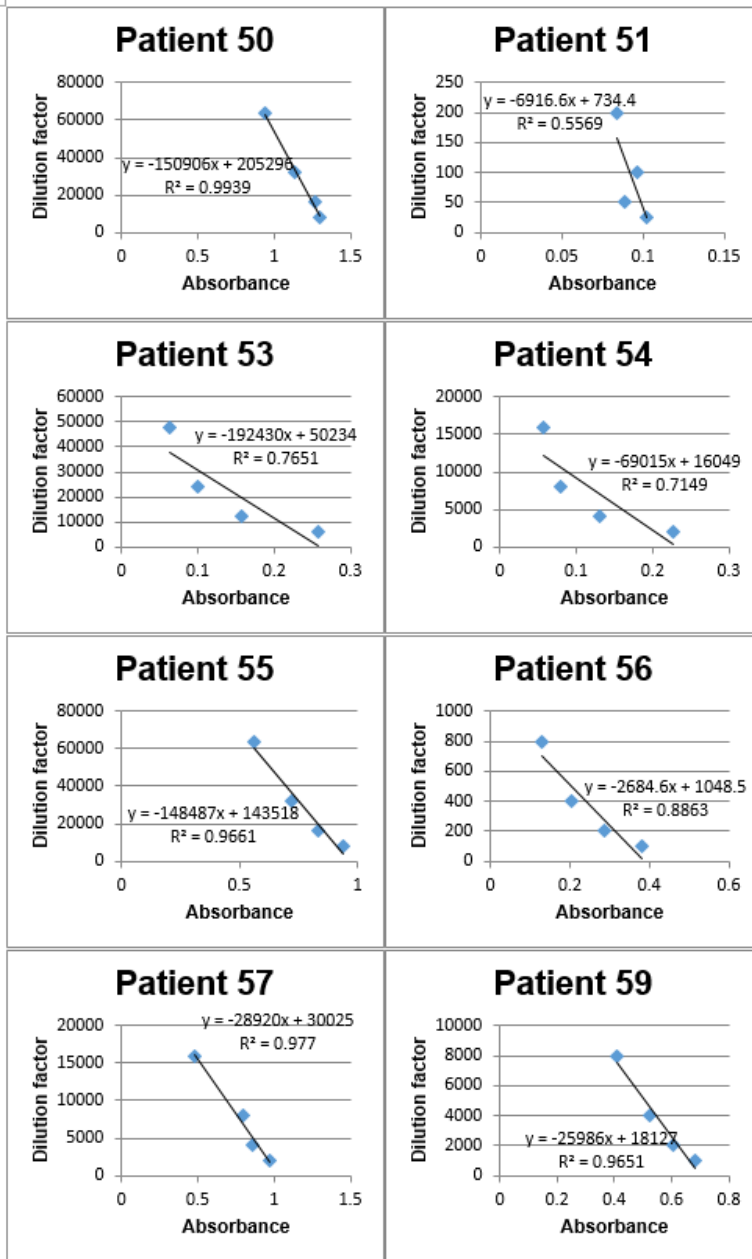


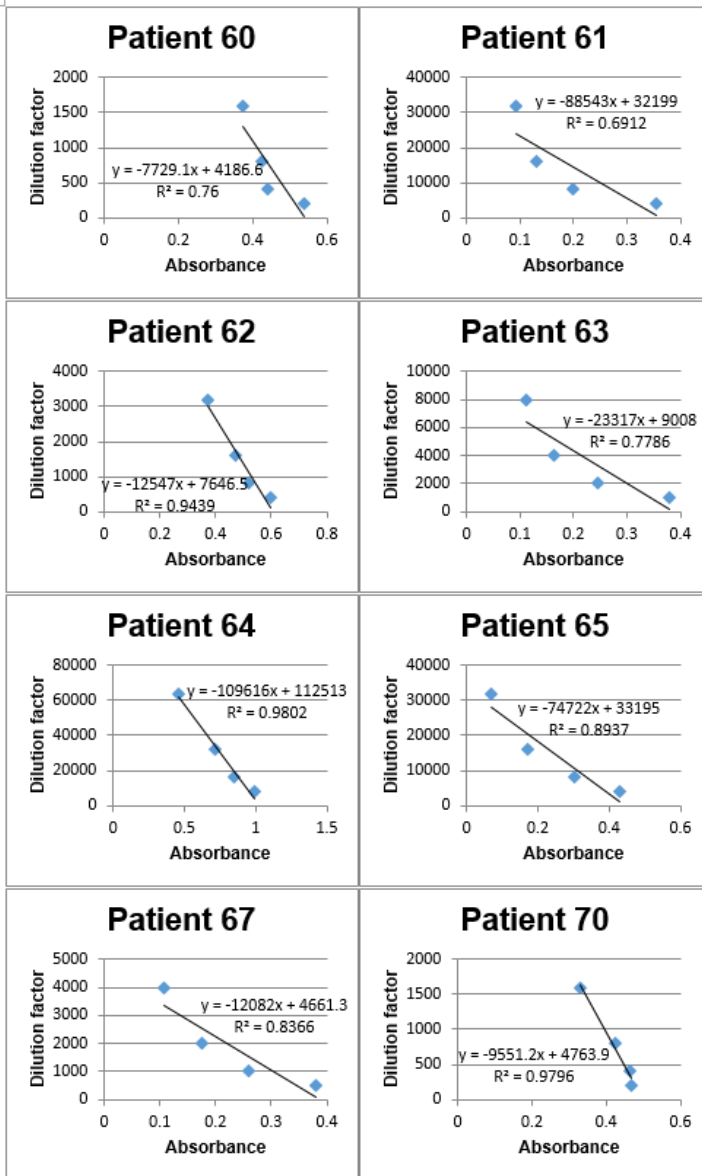


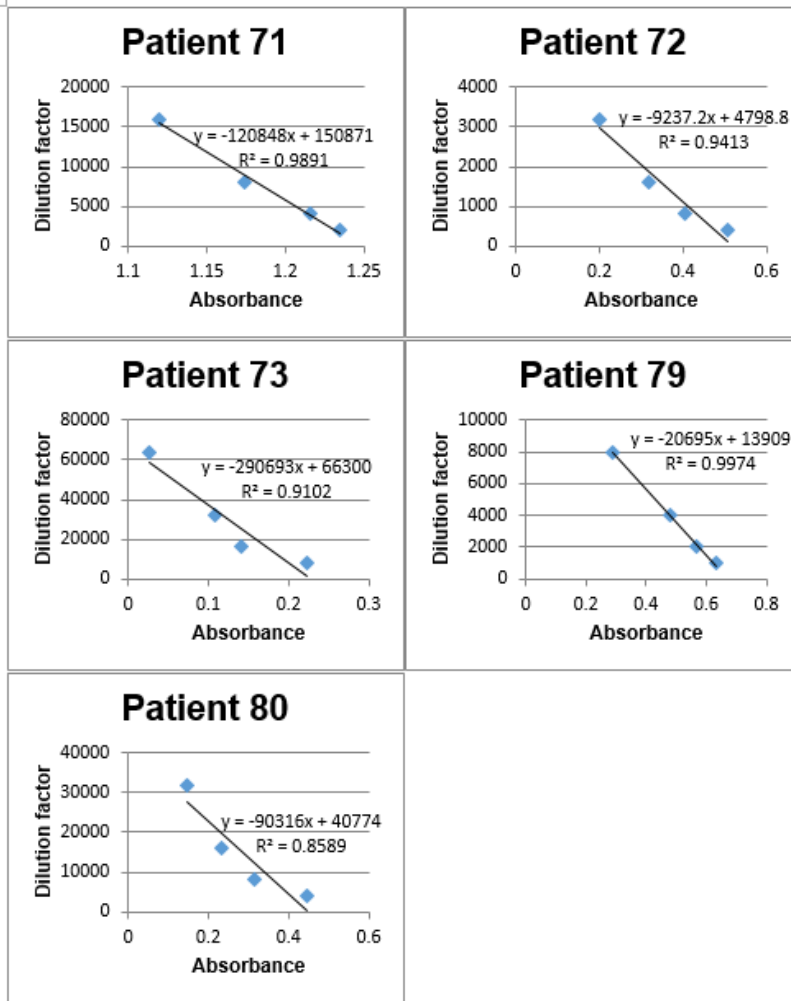




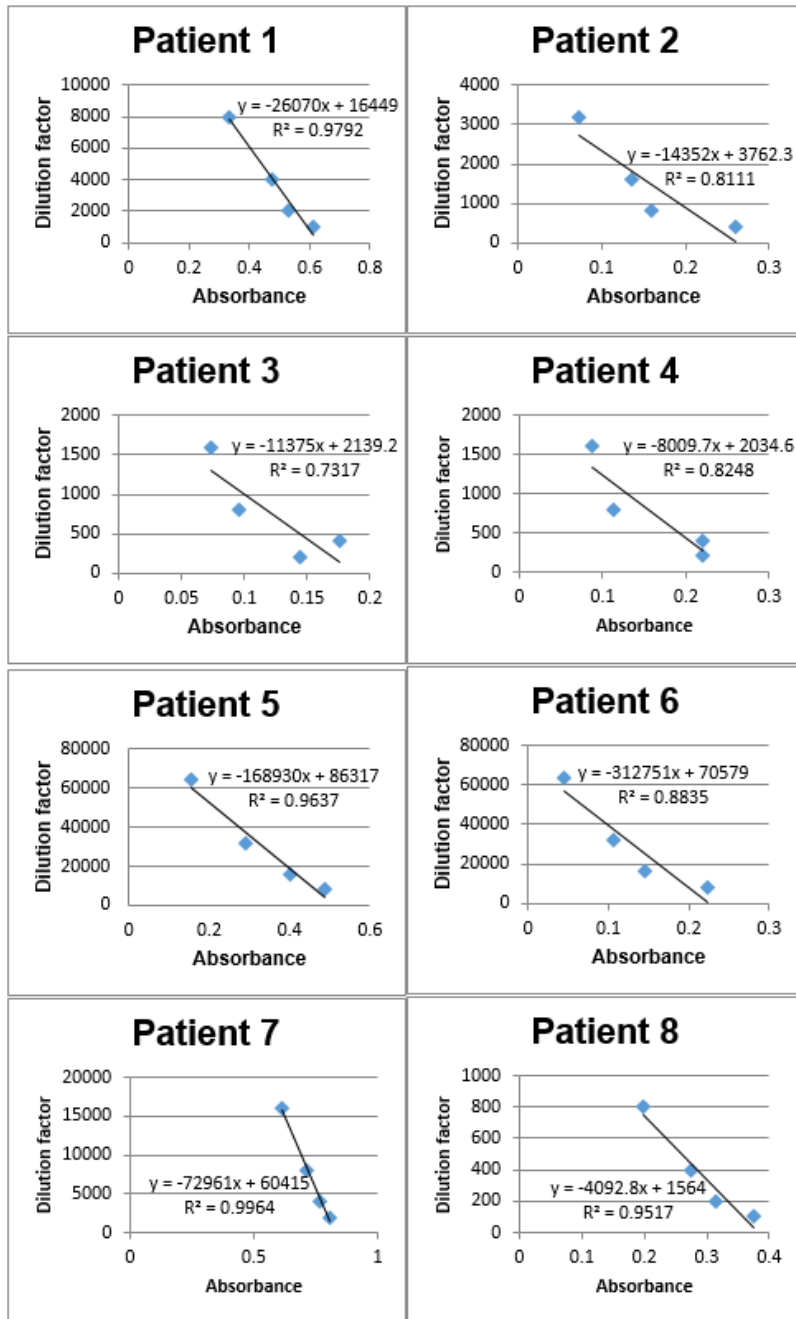


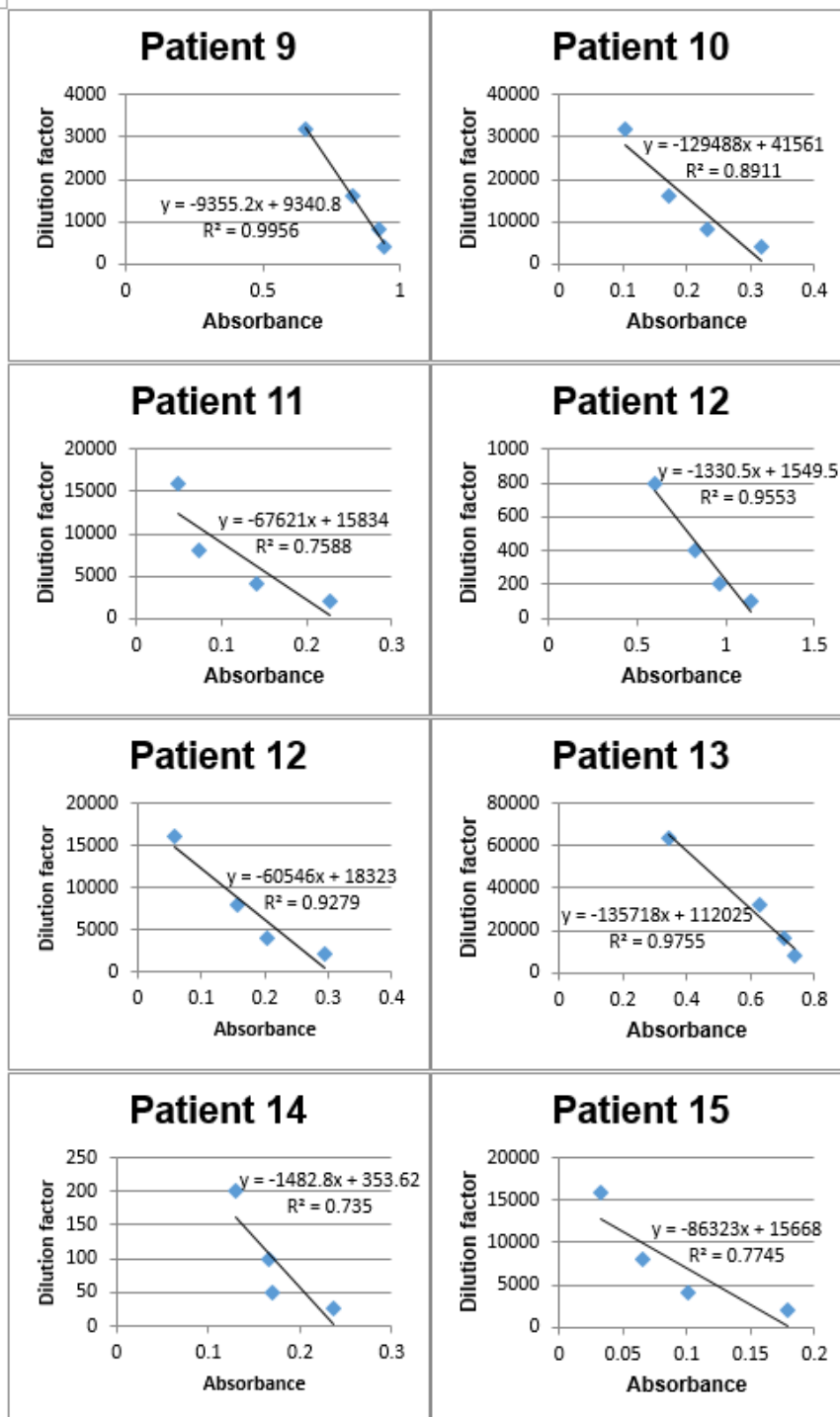


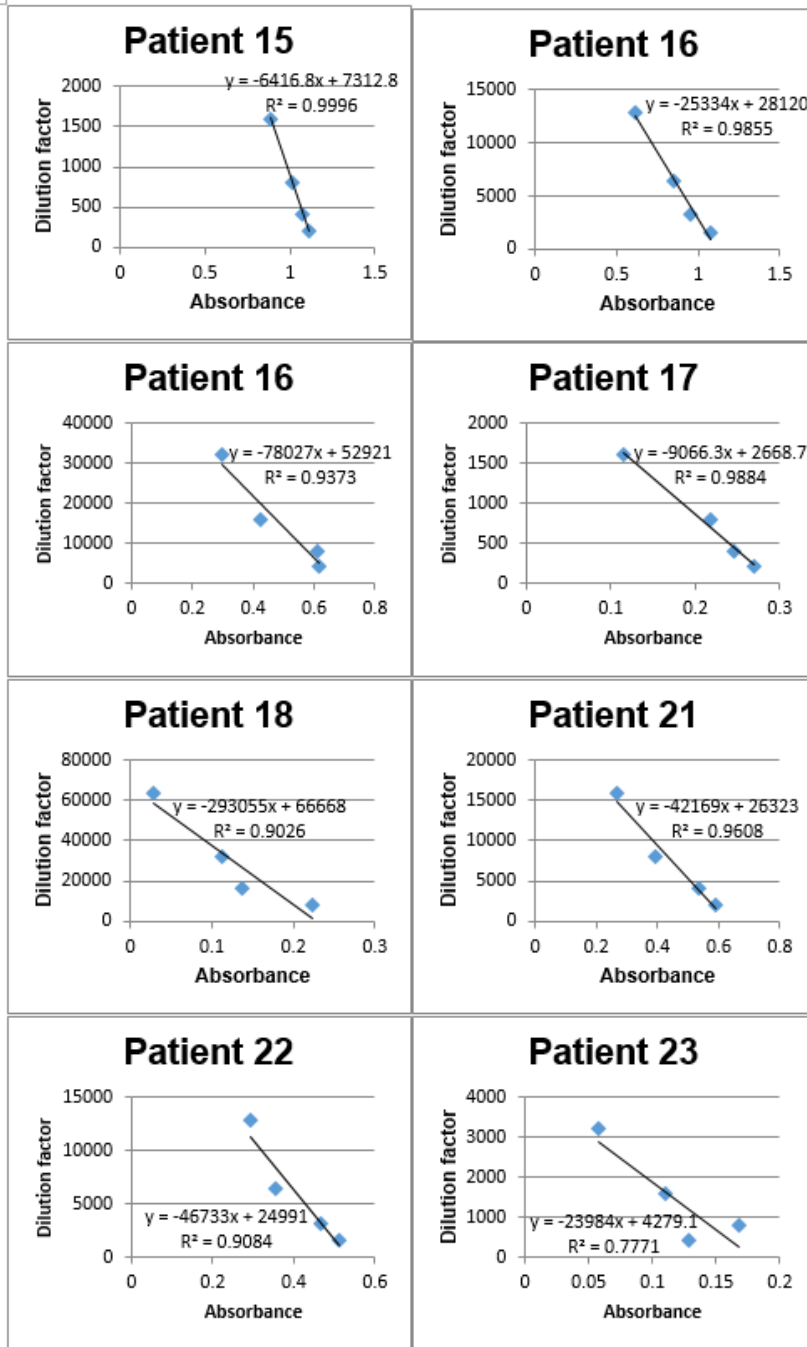


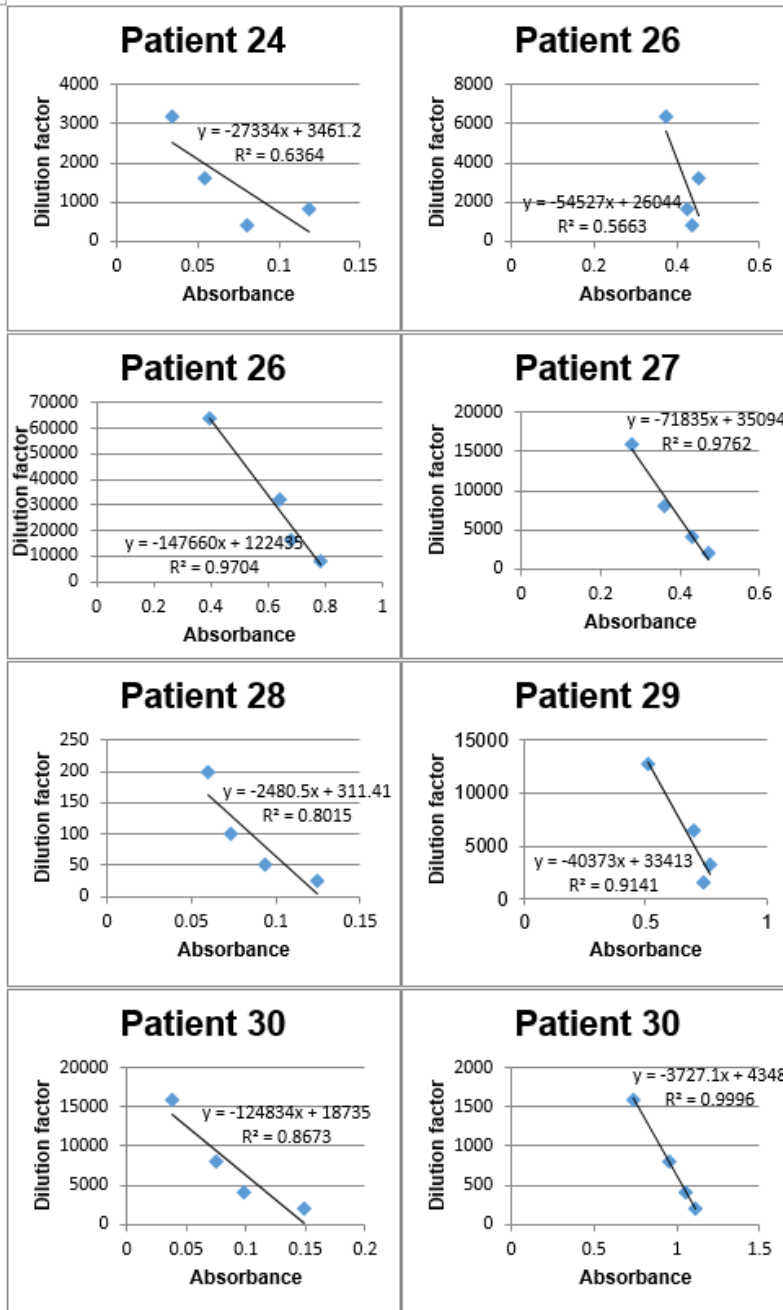


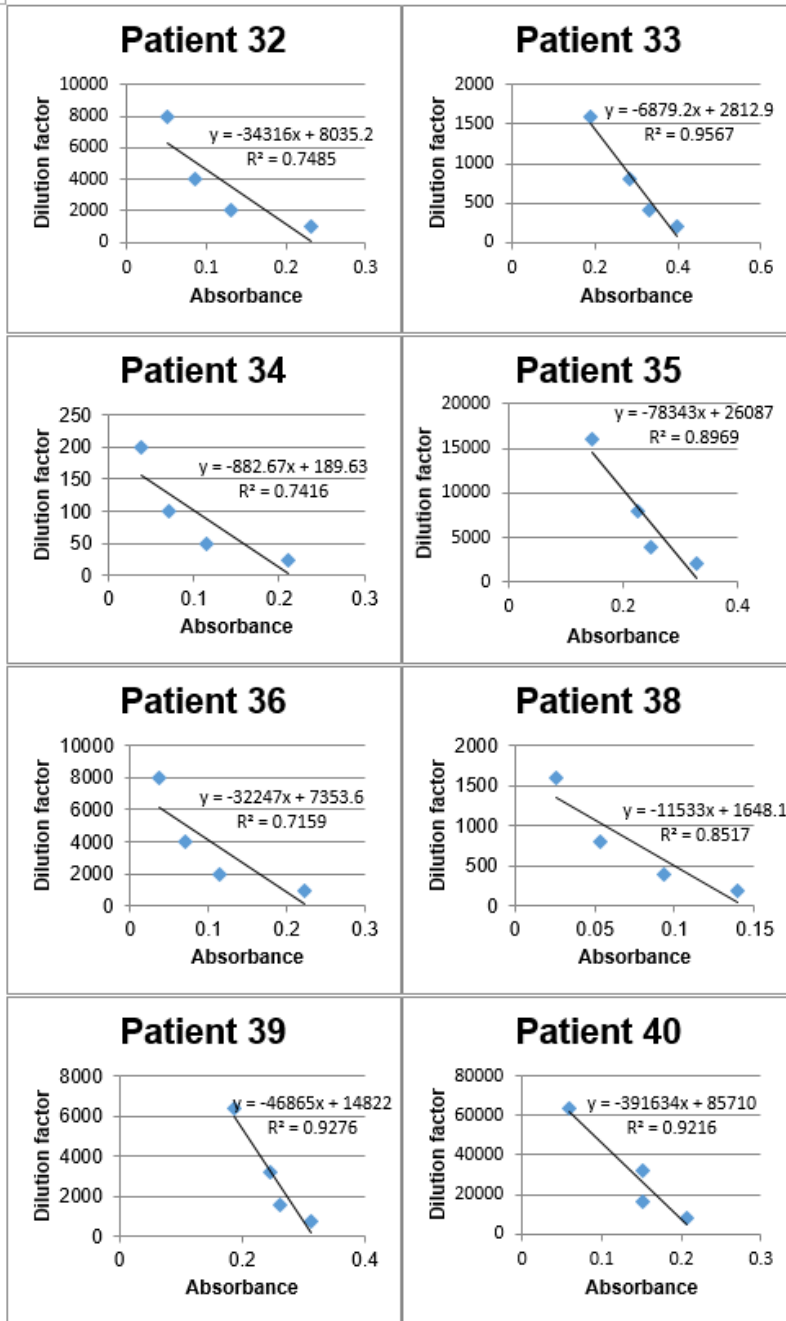
rne3BP

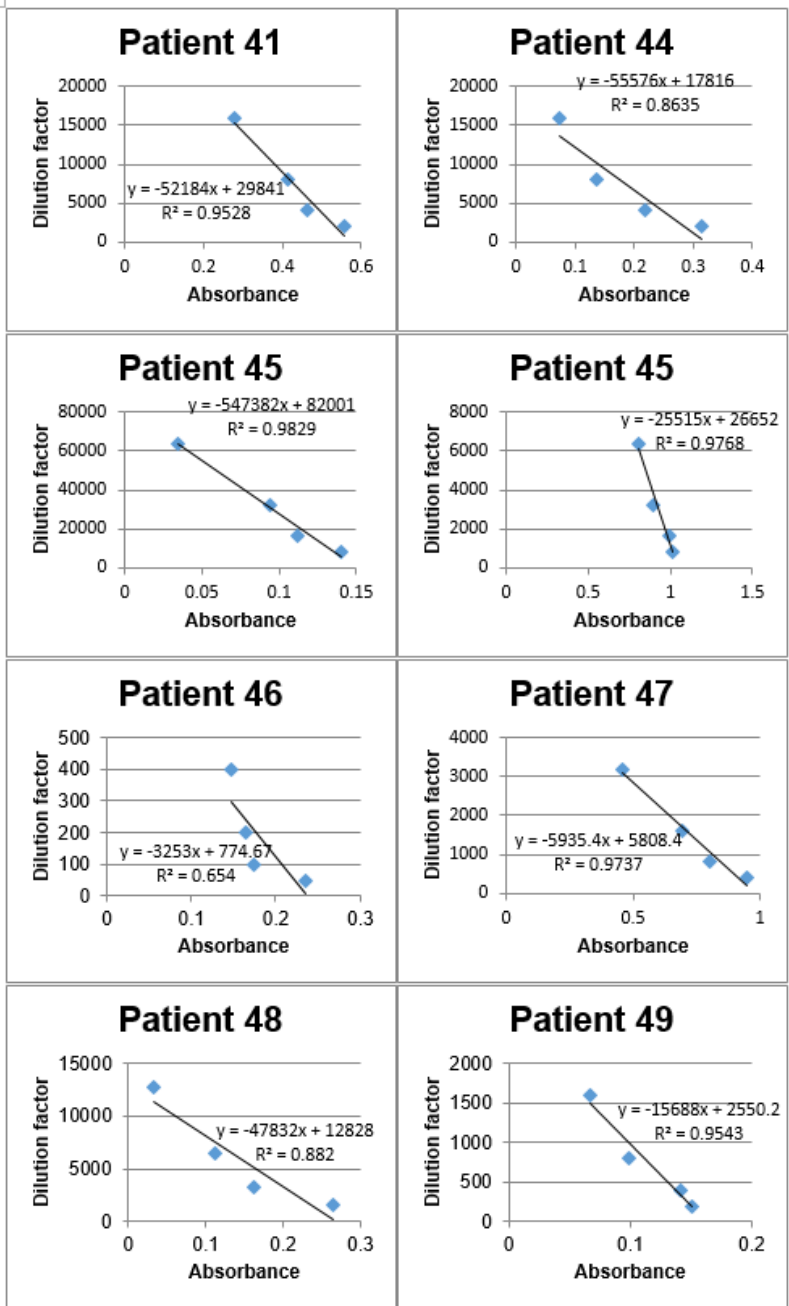


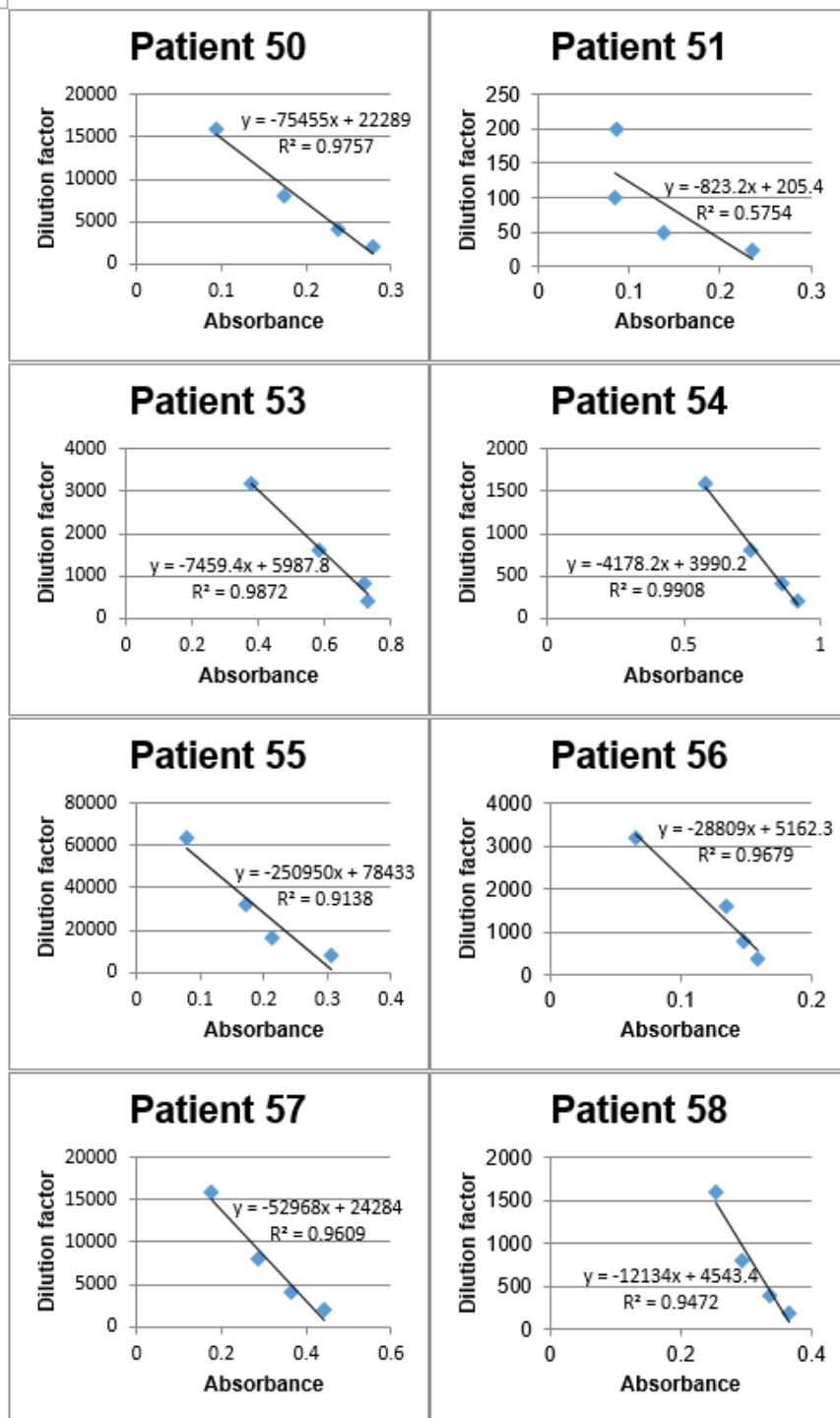


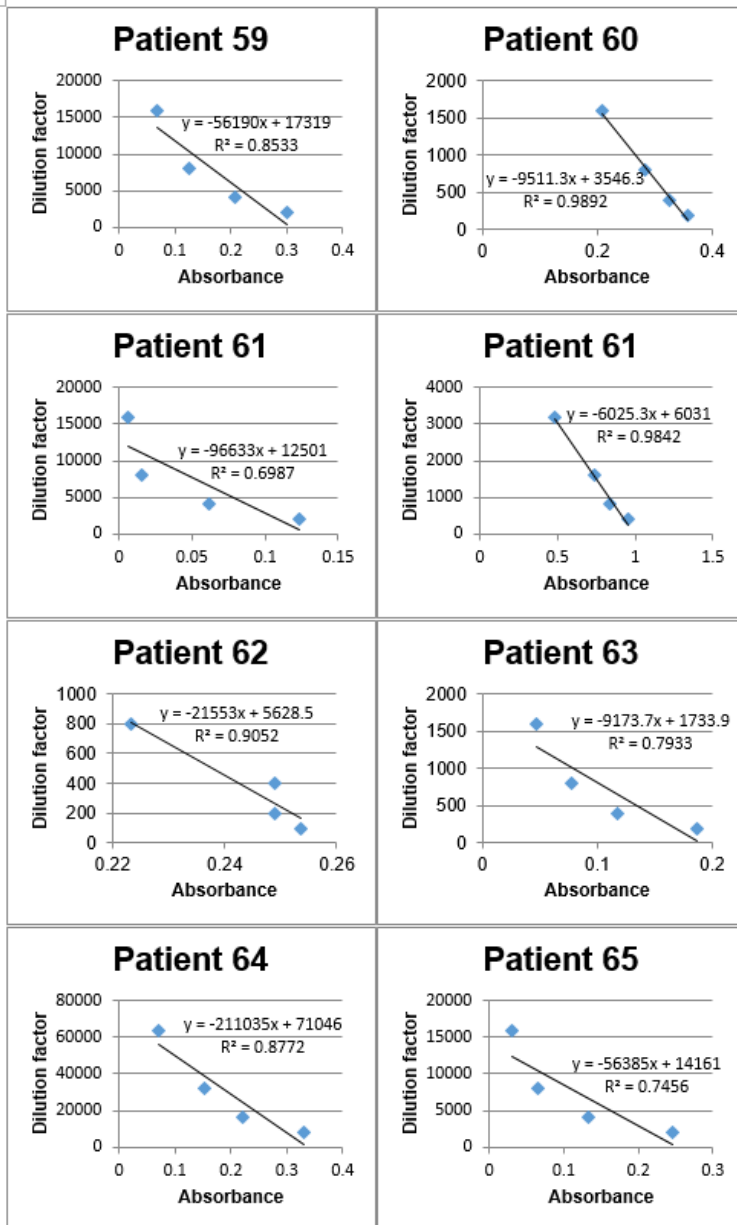


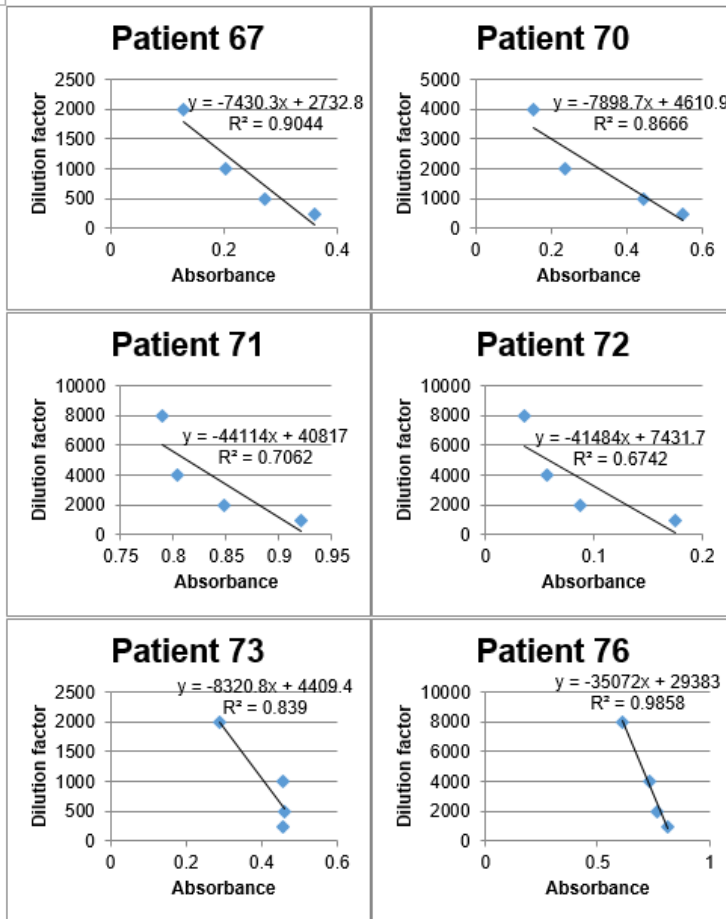












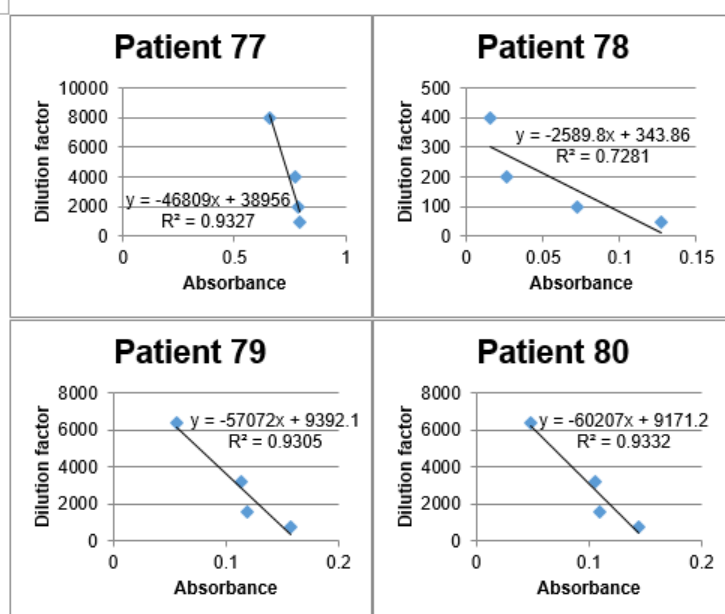


Figure 8.5: Graphs of absorbance against dilution factor to calculate end point titre

This figure shows line graphs of all patients which, in their end point titre experiment for the IgG_{all} antigen, gave an R^2 correlation coefficient of over 0.6. The intercept on the y axis shows the end point titre, or dilution of serum required to give a hypothetical zero absorbance. This is calculated in Microsoft Excel using the 'display line on graph' function where the line is given of the form $y = -mx + c$ and where 'c' is the end point titre. Shown are the line graphs of all patients who did not fail to give a linear region between 4 points, indicated by $R^2 > 0.6$.

rhE2

Patient	R ² value	Start dilution	Screen 1	Screen 1 Normalised	Screen 2	Screen 2 Normalised	Average screen	EPT	Ran k 1	Ran k 2
1	0.9708	1000	0.808	0.686	1.402	1.333	1.0095	11832	5	54
2	0.8092	200	0.323	0.201	0.528	0.459	0.33	1839.5	66	70
3	0.7076	25	0.44	0.318	0.189	0.12	0.219	270.64	73	75
4	0.8283	100	0.454	0.332	0.339	0.27	0.301	860.28	67	72
5	0.977	4000	0.663	0.541	1.324	1.255	0.898	74194	20	20
6	0.9322	2000	0.656	0.534	1.439	1.37	0.952	31987	15	37
7	0.9951	8000	0.621	0.499	1.282	1.213	0.856	139559	29	4
8	0.8175	100	0.794	0.672	1.237	1.168	0.92	872.59	18	71
9	0.9444	1000	0.829	0.707	1.09	1.021	0.864	14021	25	48
10	0.9762	4000	0.728	0.606	1.223	1.154	0.88	51329	22	31
11	0.8791	1000	0.687	0.565	1.257	1.188	0.8765	12794	23	52
12	0.9989	100	0.715	0.593	0.935	0.866	0.7295	720.12	48	73
13	0.9795	8000	0.796	0.674	1.281	1.212	0.943	257393	17	1
14	0.9859	400	0.898	0.776	0.449	0.38	0.578	6486.3	56	60
15	0.9723	2000	0.847	0.725	1.319	1.25	0.9875	32839	11	35
16	0.9764	8000	0.916	0.794	1.298	1.229	1.0115	106930	4	12
17	0.839	800	0.529	0.407	0.645	0.576	0.4915	6256.6	59	61
18	0.9821	4000	0.677	0.555	1.076	1.007	0.781	94498	41	17
19	0.9303	800	0.646	0.524	0.222	0.153	0.3385	8198.2	65	58
20	0.9976	2000	0.567	0.445	1.021	0.952	0.6985	61376	49	29
21	0.9752	8000	0.667	0.545	1.24	1.171	0.858	95145	28	16
22	0.8795	8000	0.716	0.594	1.193	1.124	0.859	73821	27	21
23	0.9058	1600	0.585	0.463	0.833	0.764	0.6135	17048	54	44
24	0.9549	800	0.528	0.406	0.534	0.465	0.4355	7570.1	60	59
25	0.9612	400	0.425	0.303	0.282	0.213	0.258	4205.6	70	64
26	0.9619	8000	0.653	0.531	1.319	1.25	0.8905	108295	21	11
27	0.9982	4000	0.571	0.449	1.228	1.159	0.804	73004	37	22
28	<0.6		0.479	0.357	0.071	0.002	0.1795		76	76
29	0.9895	4000	0.733	0.611	1.36	1.291	0.951	74643	16	19
30	0.6861	2000	0.599	0.477	1.162	1.093	0.785	13905	40	49
31	<0.6		0.524	0.402	0.248	0.179	0.2905		68	76
32	0.6926	2000	0.854	0.732	1.346	1.277	1.0045	13666	8	51
33	0.8726	8000	0.728	0.606	1.12	1.051	0.8285	64564	34	28
34	0.9843	200	0.479	0.357	0.227	0.158	0.2575	2670.2	71	65
35	0.9673	4000	0.697	0.575	1.559	1.49	1.0325	71076	3	24
36	0.8828	16000	0.744	0.622	1.139	1.07	0.846	160715	31	2
38	0.9863	200	0.672	0.55	0.098	0.029	0.2895	2498.5	69	67
39	0.9926	4000	0.756	0.634	1.019	0.95	0.792	68254	39	25
40	0.901	2000	0.74	0.618	1.081	1.012	0.815	37668	36	34

Patient	R ² value	Start dilution	Screen 1	Screen 1 Normalised	Screen 2	Screen 2 Normalised	Average screen	EPT	Ran k 1	Ran k 2
41	0.9837	2000	0.684	0.562	1.493	1.424	0.993	50358	10	33
42	0.959	200	0.557	0.435	0.092	0.023	0.229	1972	72	68
44	0.9579	2000	0.678	0.556	1.173	1.104	0.83	26806	33	39
45	0.9998	8000	0.9	0.778	1.622	1.553	1.1655	117154	1	7
46	0.9021	8000	0.545	0.423	1.114	1.045	0.734	65263	47	27
47	0.8393	2000	0.74	0.618	1.421	1.352	0.985	16667	13	45
48	0.905	4000	0.895	0.773	0.901	0.832	0.8025	32787	38	36
49	0.9219	200	0.594	0.472	0.369	0.3	0.386	2593.8	62	66
50	0.9877	8000	0.655	0.533	1.269	1.2	0.8665	103114	24	14
51	0.9191	40	0.593	0.471	0.369	0.3	0.3855	509.8	63	74
53	0.8384	8000	0.754	0.632	1.35	1.281	0.9565	71633	14	23
54	0.8898	16000	0.518	0.396	1.042	0.973	0.6845	131356	50	5
55	1	8000	0.861	0.739	1.142	1.073	0.906	147654	19	3
56	0.9402	2000	0.838	0.716	0.867	0.798	0.757	18134	43	43
57	0.9919	8000	0.658	0.536	1.08	1.011	0.7735	101959	42	15
58	0.9292	1600	0.386	0.264	0.632	0.563	0.4135	25018	61	40
59	0.9629	8000	0.41	0.288	1.275	1.206	0.747	77931	45	18
60	0.8749	1600	0.499	0.377	0.866	0.797	0.587	18408	55	42
61	0.8842	16000	0.523	0.401	1.31	1.241	0.821	117069	35	8
62	0.9727	2000	0.294	0.172	0.909	0.84	0.506	31247	58	38
63	0.9513	1000	0.503	0.381	0.953	0.884	0.6325	10851	52	55
64	0.9799	8000	0.783	0.661	1.418	1.349	1.005	115103	7	9
65	0.8997	16000	0.688	0.566	1.226	1.157	0.8615	118337	26	6
66	0.9929	800	0.26	0.138	0.672	0.603	0.3705	10284	64	56
67	0.7513	2000	0.595	0.473	1.567	1.498	0.9855	14431	12	47
68	0.8483	200	0.198	0.076	0.156	0.087	0.0815	1846.2	77	69
69	0.9359	1000	0.381	0.259	0.238	0.169	0.214	13692	74	50
70	0.8445	8000	0.49	0.368	1.205	1.136	0.752	66712	44	26
71	0.9992	2000	0.782	0.66	1.422	1.353	1.0065	50983	6	32
72	0.9453	800	0.79	0.668	0.765	0.696	0.682	14887	51	46
73	0.9045	2000	0.718	0.596	1.482	1.413	1.0045	21513	9	41
74	0.8812	1000	0.477	0.355	0.972	0.903	0.629	9043.7	53	57
75	0.9973	400	0.403	0.281	0.198	0.129	0.205	5153.2	75	62
76	0.9707	8000	0.668	0.546	1.235	1.166	0.856	108694	29	10
77	0.9991	8000	0.609	0.487	1.27	1.201	0.844	106028	32	13
78	0.9497	400	0.593	0.471	0.657	0.588	0.5295	4287.1	57	63
79	0.8093	8000	0.966	0.844	1.52	1.451	1.1475	57004	2	30
80	0.9575	1000	0.755	0.633	0.928	0.859	0.746	12223	46	53

rhE2ILD

Patient	R ² value	Start dilution	Screen 1	Screen 1 Normalised	Screen 2	Screen 2 Normalised	Average screen	EPT	Rank 1	Rank 2
1	0.8798	4000	1.046	0.96	0.954	0.827	0.8935	33976	17	24
2	0.7894	25	0.387	0.301	0.22	0.093	0.197	191.34	66	66
3	0.859	25	0.524	0.438	0.222	0.095	0.2665	245.54	65	64
4	0.9863	800	0.766	0.68	0.53	0.403	0.5415	7087.6	51	48
5	0.9174	4000	0.834	0.748	1.177	1.05	0.899	52017	15	16
6	0.943	8000	1.098	1.012	1.281	1.154	1.083	73498	1	8
7	0.973	4000	0.814	0.728	1.246	1.119	0.9235	63298	11	11
8	0.8528	4000	0.728	0.642	0.739	0.612	0.627	29550	42	30
9	0.8952	1000	0.899	0.813	0.903	0.776	0.7945	11334	24	38
10	0.9014	8000	0.869	0.783	1.177	1.05	0.9165	68606	11	8
11	0.8914	2000	0.895	0.809	1.032	0.905	0.857	16795	18	32
12	0.9029	1000	0.999	0.913	0.747	0.62	0.7665	9879	24	36
13	0.961	8000	1.082	0.996	1.067	0.94	0.968	149598	6	3
14	0.6527	400	0.39	0.304	0.388	0.261	0.2825	3512.2	54	46
15	0.9928	2000	1.129	1.043	1.152	1.025	1.034	24756	1	29
16	0.9773	2000	1.005	0.919	1.236	1.109	1.014	35263	1	18
17	0.8725	800	0.754	0.668	0.487	0.36	0.514	7566.5	41	36
18	0.9735	2000	0.736	0.65	0.968	0.841	0.7455	42806	24	14
19	0.8506	800	0.703	0.617	0.183	0.056	0.3365	6150.9	46	35
20	0.9769	8000	0.736	0.65	0.898	0.771	0.7105	129586	26	4
21	0.8856	1600	0.771	0.685	0.789	0.662	0.6735	56917	29	9
22	0.9884	2000	0.91	0.824	0.791	0.664	0.744	30148	24	21
23	0.989	4000	0.944	0.858	0.655	0.528	0.693	53338	25	9
24	0.6489	25	0.255	0.169	0.345	0.218	0.1935	208.41	45	44
25	0.749	800	0.558	0.472	0.245	0.118	0.295	5810.2	42	31
26	0.9716	2000	0.97	0.884	1.004	0.877	0.8805	30860	11	19
27	0.9424	4000	0.814	0.728	0.897	0.77	0.749	88763	22	5
28	0.8951	400	0.568	0.482	0.219	0.092	0.287	3440.1	40	34
29	0.9663	2000	0.929	0.843	1.041	0.914	0.8785	38895	12	12
30	0.9827	500	0.913	0.827	0.752	0.625	0.726	7593.9	21	27
31	0.9808	25	0.324	0.238	0.217	0.09	0.164	452.67	40	37
32	0.7398	2000	1.065	0.979	1.135	1.008	0.9935	14425	2	23
33	0.9324	4000	0.93	0.844	0.833	0.706	0.775	43730	16	9
34	0.8695	50	0.623	0.537	0.382	0.255	0.396	539.02	34	33
35	0.9412	4000	0.944	0.858	0.796	0.669	0.7635	58430	17	7
36	0.7875	4000	1.089	1.003	0.506	0.379	0.691	30009	18	16
38	0.7535	50	0.627	0.541	0.335	0.208	0.3745	496.26	32	31
39	0.9984	1000	0.962	0.876	0.947	0.82	0.848	30973	12	13
40	0.9813	2000	1.023	0.937	1.106	0.979	0.958	30932	3	13

Patient	R ² value	Start dilution	Screen 1	Screen 1 Normalised	Screen 2	Screen 2 Normalised	Average screen	EPT	Rank 1	Rank 2
41	0.9785	2000	0.959	0.873	1.23	1.103	0.988	33326	2	10
42	<0.6		0.219	0.133	0.115	0	0.0665	0	36	29
44	0.933	4000	0.898	0.812	0.966	0.839	0.8255	39253	10	9
45	0.9938	1000	1.087	1.001	0.915	0.788	0.8945	24808	6	12
46	0.7681	2000	0.914	0.828	0.632	0.505	0.6665	16536	16	13
47	0.7915	8000	1.114	1.028	1.093	0.966	0.997	68426	1	5
48	0.6784	400	0.7	0.614	0.629	0.502	0.558	2999.5	17	21
49	0.7765	100	0.712	0.626	0.295	0.168	0.397	1091.3	23	21
50	0.9939	8000	0.741	0.655	0.973	0.846	0.7505	205296	11	1
51	<0.6		0.314	0.228	0.22	0.093	0.1605		24	22
53	0.7651	6000	1.06	0.974	0.883	0.756	0.865	50234	7	5
54	0.7149	2000	0.919	0.833	0.672	0.545	0.689	16049	10	10
55	0.9661	8000	0.969	0.883	1.116	0.989	0.936	143518	3	2
56	0.8863	100	0.638	0.552	0.472	0.345	0.4485	1048.5	18	17
57	0.977	2000	0.98	0.894	1.038	0.911	0.9025	30025	3	7
58	<0.6		0.565	0.479	0.216	0.089	0.284		17	17
59	0.9651	1000	0.811	0.725	0.747	0.62	0.6725	18127	8	7
60	0.76	200	0.819	0.733	0.305	0.178	0.4555	4186.6	15	14
61	0.6912	4000	1.073	0.987	0.763	0.636	0.8115	32199	6	6
62	0.9439	400	0.831	0.745	0.569	0.442	0.5935	7646.5	9	8
63	0.7786	1000	0.886	0.8	0.429	0.302	0.551	9008	9	7
64	0.9802	8000	0.911	0.825	1.2	1.073	0.949	112513	1	2
65	0.8937	4000	0.989	0.903	0.983	0.856	0.8795	33195	3	4
66	0.9771	25	0.315	0.229	0.123	0	0.1145	79.49	14	9
67	0.8366	500	0.871	0.785	0.402	0.275	0.53	4661.3	8	8
68	0.9796	200	0.195	0.109	0.086	0	0.0545	4763.9	13	6
69	<0.6		0.259	0.173	0.21	0.083	0.128		11	7
70	0.9796	200	0.746	0.66	0.399	0.272	0.466	4763.9	8	6
71	0.9891	2000	0.858	0.772	0.986	0.859	0.8155	150871	3	1
72	0.9413	400	0.805	0.719	0.508	0.381	0.55	4798.8	6	4

71	0.9891	2000	0.858	0.772	0.986	0.859	0.8155	150871	3	1
72	0.9413	400	0.805	0.719	0.508	0.381	0.55	4798.8	6	4
73	0.9102	8000	1.102	1.016	1.004	0.877	0.9465	66300	1	1
74	<0.6		0.386	0.3	0.191	0.064	0.182		5	3
75	<0.6		0.336	0.25	0.128	0.001	0.1255		6	3
76	<0.6		0.742	0.656	0.725	0.598	0.627		4	3
77	<0.6		0.87	0.784	0.682	0.555	0.6695		3	3
78	<0.6		0.321	0.235	0.151	0.024	0.1295		3	3
79	0.9974	1000	1.073	0.987	0.919	0.792	0.8895	13909	1	2
80	0.8589	4000	0.996	0.91	0.758	0.631	0.7705	40774	1	1

rhE3BP

Patient	R ² value	Start dilution	Screen 1	Screen 1 Normalised	Screen 2	Screen 2 Normalised	Average screen	EPT	Rank 1	Rank 2
1	0.9792	1000	0.727	0.61	0.505	0.325	0.4675	16449	51	28
2	0.8111	400	0.369	0.252	0.217	0.037	0.1445	3762.3	71	50
3	0.7317	200	0.4	0.283	0.257	0.077	0.18	2139.2	69	56
4	0.8248	200	0.624	0.507	0.352	0.172	0.3395	2034.6	59	56
5	0.9637	8000	0.681	0.564	1.099	0.919	0.7415	86317	26	3
6	0.8835	8000	0.732	0.615	1.096	0.916	0.7655	70579	21	7
7	0.9964	2000	0.738	0.621	0.893	0.713	0.667	60415	34	8
8	0.9517	100	0.831	0.714	0.401	0.221	0.4675	1564	48	55
9	0.9956	400	0.803	0.686	0.918	0.738	0.712	9340.8	30	30
10	0.8911	4000	0.676	0.559	1.169	0.989	0.774	41561	19	9
11	0.7588	2000	0.766	0.649	1.026	0.846	0.7475	15834	23	24
12	0.9279	2000	0.849	0.732	0.925	0.745	0.7385	18323	24	21
13	0.9755	8000	0.832	0.715	1.549	1.369	1.042	112025	1	2
14	0.735	25	0.501	0.384	0.239	0.059	0.2215	353.62	57	51
15	0.9996	200	0.741	0.624	1.162	0.982	0.803	7312.8	12	30
16	0.9373	4000	0.933	0.816	0.972	0.792	0.804	52921	10	7
17	0.9884	200	0.448	0.331	0.378	0.198	0.2645	2668.7	52	44
18	0.9026	8000	0.72	0.603	1.108	0.928	0.7655	66668	17	6
19	<0.6		0.514	0.397	0.356	0.176	0.2865		48	50
20	0.667	800	0.638	0.521	0.686	0.506	0.5135	20337	36	17
21	0.9608	2000	0.79	0.673	1.445	1.265	0.969	26323	2	12
22	0.9084	1600	0.859	0.742	0.917	0.737	0.7395	24991	18	13
23	0.7771	400	0.686	0.569	0.268	0.088	0.3285	4279.1	44	34
24	0.6364	400	0.616	0.499	0.428	0.248	0.3735	3461.2	41	36
25	<0.6		0.674	0.557	0.303	0.123	0.34		42	45
26	0.9704	8000	0.717	0.6	0.854	0.674	0.637	122435	26	1
27	0.9762	2000	0.693	0.576	1.178	0.998	0.787	35094	12	7
28	0.8015	25	0.361	0.244	0.47	0.29	0.267	311.41	40	41
29	0.9141	1600	0.67	0.553	0.713	0.533	0.543	33413	31	7
30	0.9996	200	0.784	0.667	1.035	0.855	0.761	4348	15	30
31	<0.6		0.173	0.056	0.228	0.048	0.052		47	40
32	0.7485	1000	0.919	0.802	0.806	0.626	0.714	8035.2	18	19
33	0.9567	200	0.676	0.559	0.719	0.539	0.549	2812.9	28	31
34	0.7416	25	0.376	0.259	0.452	0.272	0.2655	189.63	36	37
35	0.8969	2000	0.769	0.652	1.165	0.985	0.8185	26087	7	9
36	0.7159	1000	0.923	0.806	0.804	0.624	0.715	7353.6	16	19
38	0.8517	200	0.696	0.579	0.365	0.185	0.382	1648.1	32	32
39	0.9276	800	0.8	0.683	0.809	0.629	0.656	14822	20	13
40	0.9216	8000	0.805	0.688	1.227	1.047	0.8675	85710	6	1



Patient	R ² value	Start dilution	Screen 1	Screen 1 Normalised	Screen 2	Screen 2 Normalised	Average screen	EPT	Ran k 1	Ran k 2
41	0.9528	2000	0.755	0.638	1.421	1.241	0.9395	29841	2	6
42	<0.6		0.226	0.109	0.178	0	0.0545		37	31
44	0.8635	2000	0.576	0.459	1.065	0.885	0.672	17816	15	9
45	0.9829	8000	0.843	0.726	1.034	0.854	0.79	82001	8	1
46	0.654	50	0.478	0.361	0.586	0.406	0.3835	774.67	26	27
47	0.9737	400	0.793	0.676	1.3	1.12	0.898	5808.4	3	16
48	0.882	1600	0.764	0.647	0.859	0.679	0.663	12828	14	10
49	0.9543	200	0.479	0.362	0.53	0.35	0.356	2550.2	24	23
50	0.9757	2000	0.633	0.516	1.297	1.117	0.8165	22289	4	7
51	<0.6		0.389	0.272	0.362	0.182	0.227		23	24
53	0.9872	400	1.086	0.969	1.014	0.834	0.9015	5987.8	2	13
54	0.9908	200	0.734	0.617	1.115	0.935	0.776	3990.2	6	18
55	0.9138	8000	0.774	0.657	1.472	1.292	0.9745	78433	1	1
56	0.9679	400	0.849	0.732	0.47	0.29	0.511	5162.3	15	13
57	0.9609	2000	0.722	0.605	1.172	0.992	0.7985	24284	3	5
58	0.9472	200	0.349	0.232	0.854	0.674	0.453	4543.4	16	13
59	0.8533	2000	0.582	0.465	1.258	1.078	0.7715	17319	4	5
60	0.9892	200	0.706	0.589	0.795	0.615	0.602	3546.3	9	13
61	0.9842	400	0.831	0.714	1.027	0.847	0.7805	6031	3	9
62	0.9052	100	0.551	0.434	0.592	0.412	0.423	5628.5	13	9
63	0.7933	200	0.768	0.651	0.653	0.473	0.562	1733.9	10	12
64	0.8772	8000	0.703	0.586	1.355	1.175	0.8805	71046	1	1
65	0.7456	2000	0.695	0.578	1.105	0.925	0.7515	14161	2	4
66	<0.6		0.206	0.089	0.243	0.063	0.076		14	11
67	0.9044	250	0.789	0.672	0.656	0.476	0.574	2732.8	7	9
68	<0.6		0.224	0.107	0.208	0.028	0.0675		13	10
69	<0.6		0.19	0.073	0.286	0.106	0.0895		12	10
70	0.8666	500	0.564	0.447	0.999	0.819	0.633	4610.9	5	7
71	0.7062	1000	0.761	0.644	1.144	0.964	0.804	40817	1	1
72	0.6742	1000	0.935	0.818	0.699	0.519	0.6685	7431.7	3	5
73	0.839	250	0.755	0.638	0.527	0.347	0.4925	4409.4	5	5
74	<0.6		0.34	0.223	0.3	0.12	0.1715		7	6
75	<0.6		0.38	0.263	0.37	0.19	0.2265		5	6
76	0.9858	1000	0.565	0.448	1.098	0.918	0.683	29383	2	2
77	0.9327	1000	0.759	0.642	0.974	0.794	0.718	38956	1	1
78	0.7281	50	0.395	0.278	0.302	0.122	0.2	343.86	3	3
79	0.9305	800	0.788	0.671	0.662	0.482	0.5765	9392.1	1	1
80	0.9332	800	0.725	0.608	0.569	0.389	0.4985	9171.2	1	1

bE2/E3BP

Patient	R ² value	Start dilution	Screen 1	Screen 1 Normalised	Screen 2	Screen 2 Normalised	Average screen	EPT	Ran k 1	Ran k 2
1	0.9913	1000	0.727	0.614	0.565	0.44	0.527	16797	44	26
2	0.8886	200	0.369	0.256	0.273	0.148	0.202	2697.1	69	53
3	0.9652	200	0.4	0.287	0.213	0.088	0.1875	2222.9	71	55
4	0.9882	200	0.624	0.511	0.262	0.137	0.324	2892.7	63	52
5	<0.6		0.681	0.568	0.303	0.178	0.373		59	61
6	0.7911	4000	0.732	0.619	0.393	0.268	0.4435	68747	49	12
7	<0.6		0.738	0.625	0.41	0.285	0.455		48	60
8	0.8892	2000	0.831	0.718	0.467	0.342	0.53	16038	42	28
9	0.821	2000	0.803	0.69	0.417	0.292	0.491	30052	45	17
10	<0.6		0.676	0.563	0.434	0.309	0.436		46	58
11	0.9544	2000	0.766	0.653	0.633	0.508	0.5805	22348	29	19
12	0.8296	2000	0.849	0.736	0.414	0.289	0.5125	16567	42	24
13	0.7687	4000	0.832	0.719	0.502	0.377	0.548	283695	35	2
14	0.9254	250	0.501	0.388	0.672	0.547	0.4675	2658.2	42	47
15	0.9557	1000	0.741	0.628	0.857	0.732	0.68	25577	18	17
16	0.8583	500	0.933	0.82	0.369	0.244	0.532	4223.6	37	40
17	0.728	100	0.448	0.335	0.188	0.063	0.199	727.27	56	50
18	<0.6		0.72	0.607	0.367	0.242	0.4245		41	51
19	0.9849	400	0.514	0.401	0.411	0.286	0.3435	14173	48	25
20	<0.6		0.638	0.525	0.407	0.282	0.4035		41	50
21	<0.6		0.79	0.677	0.512	0.387	0.532		37	50
22	0.7477	1000	0.859	0.746	0.482	0.357	0.5515	17409	33	19
23	<0.6		0.686	0.573	0.341	0.216	0.3945		40	49
24	0.739	100	0.616	0.503	0.218	0.093	0.298	835.26	47	47
25	<0.6		0.674	0.561	0.302	0.177	0.369		43	48
26	0.9391	1000	0.717	0.604	0.637	0.512	0.558	27350	30	16
27	0.9974	16000	0.693	0.58	0.632	0.507	0.5435	285450	33	1
28	<0.6		0.361	0.248	0.651	0.526	0.387		38	46
29	0.9853	16000	0.67	0.557	0.677	0.552	0.5545	261632	30	1
30	0.9904	500	0.784	0.671	0.588	0.463	0.567	8427.4	28	30
31	<0.6		0.173	0.06	0.288	0.163	0.1115		47	44
32	0.9618	500	0.919	0.806	0.805	0.68	0.743	8413.1	8	30
33	0.9874	4000	0.676	0.563	0.425	0.3	0.4315	46639	33	10
34	<0.6		0.376	0.263	0.62	0.495	0.379		35	42
35	0.9726	4000	0.769	0.656	0.953	0.828	0.742	101375	8	6
36	0.9866	1000	0.923	0.81	0.808	0.683	0.7465	15474	6	17
38	0.7686	500	0.696	0.583	0.599	0.474	0.5285	4062.2	29	30
39	0.9905	1000	0.8	0.687	0.691	0.566	0.6265	34411	20	10
40	0.7663	1000	0.805	0.692	0.542	0.417	0.5545	31956	25	10

Patient	R ² value	Start dilution	Screen 1	Screen 1 Normalised	Screen 2	Screen 2 Normalised	Average screen	EPT	Rank 1	Rank 2
41	0.9849	16000	0.755	0.642	0.704	0.579	0.6105	188306	21	1
42	<0.6		0.226	0.113	0.304	0.179	0.146		36	36
44	0.7432	1000	0.576	0.463	0.833	0.708	0.5855	17221	22	11
45	0.6428	2000	0.843	0.73	0.885	0.76	0.745	12051	6	18
46	0.6704	200	0.478	0.365	0.562	0.437	0.401	3712.5	25	26
47	0.9983	500	0.793	0.68	0.993	0.868	0.774	10755	4	19
48	0.7198	500	0.764	0.651	0.598	0.473	0.562	3927.9	20	24
49	0.8312	200	0.479	0.366	0.377	0.252	0.309	1914.1	25	26
50	0.9267	1000	0.633	0.52	0.81	0.685	0.6025	39120	19	8
51	0.7067	200	0.389	0.276	0.615	0.49	0.383	1402	22	26
53	0.9851	250	1.086	0.973	0.917	0.792	0.8825	5512.2	1	21
54	0.7877	1000	0.734	0.621	0.744	0.619	0.62	8139.4	17	20
55	0.6542	2000	0.774	0.661	0.89	0.765	0.713	85626	7	6
56	0.6532	2000	0.849	0.736	0.718	0.593	0.6645	13926	12	12
57	0.9962	4000	0.722	0.609	0.904	0.779	0.694	103837	8	3
58	<0.6		0.349	0.236	0.476	0.351	0.2935		19	23
59	0.982	2000	0.582	0.469	1.1	0.975	0.722	55638	5	5
60	0.9503	1000	0.706	0.593	0.89	0.765	0.679	11585	9	13
61	0.7077	2000	0.831	0.718	0.876	0.751	0.7345	16712	4	7
62	0.9013	1000	0.551	0.438	0.764	0.639	0.5385	14832	12	8
63	0.9146	2000	0.768	0.655	0.893	0.768	0.7115	19365	5	6
64	0.8644	4000	0.703	0.59	0.969	0.844	0.717	117195	4	2
65	0.87	1000	0.695	0.582	0.825	0.7	0.641	12998	6	8
66	0.9936	1600	0.206	0.093	0.258	0.133	0.113	20714	15	4
67	0.7107	2000	0.789	0.676	0.825	0.7	0.688	13708	5	5
68	0.6887	100	0.224	0.111	0.328	0.203	0.157	687.52	13	13
69	0.7134	200	0.19	0.077	0.721	0.596	0.3365	1329.2	9	12
70	0.8265	500	0.564	0.451	0.686	0.561	0.506	4904.6	8	8
71	0.9148	4000	0.761	0.648	0.991	0.866	0.757	101380	3	2
72	0.9882	500	0.935	0.822	1.039	0.914	0.868	9447.4	1	6
73	0.9659	500	0.755	0.642	1.036	0.911	0.7765	13316	1	4
74	0.8864	200	0.34	0.227	0.496	0.371	0.299	2673.7	5	6
75	0.6928	100	0.38	0.267	0.245	0.12	0.1935	3136.5	6	5
76	0.9908	4000	0.565	0.452	0.768	0.643	0.5475	100204	4	2
77	0.9782	8000	0.759	0.646	0.761	0.636	0.641	142095	2	1
78	0.8036	100	0.395	0.282	0.293	0.168	0.225	1793.2	3	3
79	0.7187	2000	0.788	0.675	0.831	0.706	0.6905	16212	1	1
80	0.8762	1000	0.725	0.612	0.786	0.661	0.6365	10118	1	1

Figure 8.4: Tables of results for screens and end point titres
Spearman's Rank Correlation coefficient was carried out to assess the relationship between columns Average Screen and EPT.

a. Antibodies

<u>Antibody against</u>	<u>Fluorochrome</u>	<u>Clone</u>	<u>Source</u>	<u>Cat. Number</u>
CD3	PerCPvio700	BW264/56	Miltenyi	130-100-458
CD3	BV421	OKT3	Biolegend	317344
CD3	BV510	OKT3	Biolegend	317331
CD4	APC	OKT4	eBiosciences	17-0048-41
CD4	PerCPCy5.5	OKT4	eBiosciences	45-0048-42
CD4	APC eFluor780	OKT4	eBiosciences	47-0048-41
CD4	APC-H7	RPA-T4	Biolegend	560158
CD4	APC-Cy7	A161A1	Biolegend	357416
CD4	BV510	SK3	BD	562970
CD4	APC eFluor780	RPA-T4	eBiosciences	47-0049-41
CD4	APC	M-T466	Miltenyi	130-098-133
CD8	PECy7	RPA-T8	eBiosciences	25-0088-42
CD8	FITC	BW135/80	Miltenyi	130-098-059
CD8	APC	OKT8	eBiosciences	17-0086-71
		1.1.1.1 TÜK4		
CD14	FITC		Miltenyi	130-098-063
CD25	PE	BC96	eBiosciences	12-0259-42
CD45RO	PerCPCy5.5	UCHL1	eBiosciences	46-6457-41
CCR6	APC	R6H1	eBiosciences	17-1969-41
CXCR3	BV421	G025H7	Biolegend	353715
CXCR3	PerCPCy5.5	ICS/CXCR3	BD	560832
FoxP3	PECy7	PCH101	eBiosciences	25-4776-41

b. Isotype controls

<u>Fluorochrome</u>	<u>Isotype</u>	<u>Clone</u>	<u>Source</u>	<u>Cat. Number</u>
BV421	IgG2 α mouse	MOPC-173	Biolegend	400267
PECy7	Rat IgG2 α κ	eBR2a	eBiosciences	25-4321-81
APC	Mouse IgG1 κ	P3.6.2.8.1	eBiosciences	17-4714-41
PE	Mouse IgG1 κ	P3.6.2.8.1	eBiosciences	12-4714-81
PerCPCy5.5	Mouse IgG2 α κ	eBM2a	eBiosciences	46-4724-80
APCeFluor780	Mouse IgG1 κ	P3.6.2.8.1	eBiosciences	46-4714-80
BV421	Mouse IgG1 κ	MOPC-21	Biolegend	400157

Table 8.6: Antibodies used for flow cytometry.

Tables show list of all antibodies used in flow cytometry and clones and sources, where a shows antibodies and b the isotype controls.

References

- Alanine Aminotransferase: Analyte Monograph. *Association for Clinical Biochemistry and Laboratory Medicine*.
1994. Human interleukin 10 induces naive surface immunoglobulin D+ (sIgD+) B cells to secrete IgG1 and IgG3. *The Journal of Experimental Medicine*, 179, 757-762.
- ABBEY, J. L. & O'NEILL, H. C. 2008. Expression of T-cell receptor genes during early T-cell development.
- AKIYAMA, M., SUZUKI, K., YASUOKA, H., KANEKO, Y., YAMAOKA, K. & TAKEUCHI, T. Follicular helper T cells in the pathogenesis of IgG4-related disease. LID - 10.1093/rheumatology/kex171 [doi].
- AL-HARTHY, N. & KUMAGI, T. 2012. Natural history and management of primary biliary cirrhosis. *Hepatic Medicine : Evidence and Research*, 4, 61-71.
- ALA, A., STANCA, C. M., BU-GHANIM, M., AHMADO, I., BRANCH, A. D., SCHIANO, T. D., ODIN, J. A. & BACH, N. 2006. Increased prevalence of primary biliary cirrhosis near Superfund toxic waste sites. *Hepatology*, 43, 525-31.
- ALPINI, G., BAIOCCHI, L., GLASER, S., UENO, Y., MARZIONI, M., FRANCIS, H., PHINIZY, J. L., ANGELICO, M. & LESAGE, G. 2002. Ursodeoxycholate and tauroursodeoxycholate inhibit cholangiocyte growth and secretion of BDL rats through activation of PKC alpha. *Hepatology*, 35, 1041-52.
- ATTILI, A. F., ANGELICO, M., CANTAFORA, A., ALVARO, D. & CAPOCACCIA, L. 1986. Bile acid-induced liver toxicity: relation to the hydrophobic-hydrophilic balance of bile acids. *Med Hypotheses*, 19, 57-69.
- BACHRACH, W. H. & HOFMANN, A. F. 1982. Ursodeoxycholic acid in the treatment of cholesterol cholelithiasis. *Digestive Diseases and Sciences*, 27, 737-761.
- BATALLER, R. & BRENNER, D. A. 2005. Liver fibrosis. *Journal of Clinical Investigation*, 115, 209-218.
- BEGUM, J., DAY, W., HENDERSON, C., PUREWAL, S., CERVEIRA, J., SUMMERS, H., REES, P., DAVIES, D. & FILBY, A. 2013. A method for evaluating the use of fluorescent dyes to track proliferation in cell lines by dye dilution. *Cytometry A*, 83, 1085-95.
- BELVIN, M. P. & ANDERSON, K. V. A conserved signaling pathway: the *Drosophila* toll-dorsal pathway.
- BENZ, C., ANGERMÜLLER, S., TÖX, U., KLÖTERS-PLACHKY, P., RIEDEL, H. D., SAUER, P., STREMMEL, W. & STIEHL, A. 1998. Effect of tauroursodeoxycholic acid on bile-acid-induced apoptosis and cytolysis in rat hepatocytes. *Journal of Hepatology*, 28, 99-106.
- BERG, P. A. & KLEIN, R. Antimitochondrial antibodies in primary biliary cirrhosis and other disorders: definition and clinical relevance.
- BEUERS, U. 2006. Drug insight: Mechanisms and sites of action of ursodeoxycholic acid in cholestasis.
- BEUERS, U., BILZER, M., CHITTATTU, A., KULLAK-UBLICK, G. A., KEPPLER, D., PAUMGARTNER, G. & DOMBROWSKI, F. 2001. Tauroursodeoxycholic acid inserts the apical conjugate export pump, Mrp2, into canalicular membranes and stimulates organic anion secretion by protein kinase C-dependent mechanisms in cholestatic rat liver. *Hepatology*, 33, 1206-16.

- BEUERS, U., NATHANSON, M. H., ISALES, C. M. & BOYER, J. L. 1993. Tauroursodeoxycholic acid stimulates hepatocellular exocytosis and mobilizes extracellular Ca⁺⁺ mechanisms defective in cholestasis. *Journal of Clinical Investigation*, 92, 2984-93.
- BEUERS, U., SPENGLER, U., KRUIS, W., AYDEMIR, U., WIEBECKE, B., HELDWEIN, W., WEINZIERL, M., PAPE, G. R., SAUERBRUCH, T. & PAUMGARTNER, G. 1992. Ursodeoxycholic acid for treatment of primary sclerosing cholangitis: a placebo-controlled trial. *Hepatology*, 16, 707-14.
- BOLAND, B. S., DONG, M. H., BETTENCOURT, R., BARRETT-CONNOR, E. & LOOMBA, R. 2014. Association of Serum Bilirubin with Aging and Mortality. *Journal of clinical and experimental hepatology*, 4, 1-7.
- BOSMA, P. J., CHOWDHURY, J. R., BAKKER, C., GANTLA, S., DE BOER, A., OOSTRA, B. A., LINDHOUT, D., TYTGAT, G. N. J., JANSEN, P. L. M., ELFERINK, R. P. J. O. & CHOWDHURY, N. R. 1995. The Genetic Basis of the Reduced Expression of Bilirubin UDP-Glucuronosyltransferase 1 in Gilbert's Syndrome. *New England Journal of Medicine*, 333, 1171-1175.
- BOYD, S. D., MARSHALL EL FAU - MERKER, J. D., MERKER JD FAU - MANIAR, J. M., MANIAR JM FAU - ZHANG, L. N., ZHANG LN FAU - SAHAF, B., SAHAF B FAU - JONES, C. D., JONES CD FAU - SIMEN, B. B., SIMEN BB FAU - HANCZARUK, B., HANCZARUK B FAU - NGUYEN, K. D., NGUYEN KD FAU - NADEAU, K. C., NADEAU KC FAU - EGHOLM, M., EGHOLM M FAU - MIKLOS, D. B., MIKLOS DB FAU - ZEHNDER, J. L., ZEHNDER JL FAU - FIRE, A. Z. & FIRE, A. Z. 2009. Measurement and clinical monitoring of human lymphocyte clonality by massively parallel VDJ pyrosequencing.
- BOYLSTON, A. 2012. The origins of inoculation.
- CARBONE, M., MELLS, G. F., PELLIS, G., DAWWAS, M. F., NEWTON, J. L., HENEGHAN, M. A., NEUBERGER, J. M., DAY, D. B., DUCKER, S. J., CONSORTIUM, U. P., SANDFORD, R. N., ALEXANDER, G. J. & JONES, D. E. 2013. Sex and age are determinants of the clinical phenotype of primary biliary cirrhosis and response to ursodeoxycholic acid. *Gastroenterology*, 144, 560-569 e7; quiz e13-4.
- CATALFAMO, M. & HENKART, P. A. 2003. Perforin and the granule exocytosis cytotoxicity pathway.
- CHAIYADET, S., SMOUT, M., JOHNSON, M., WHITCHURCH, C., TURNBULL, L., KAEWKES, S., SOTILLO, J., LOUKAS, A. & SRIPA, B. 2015a. Excretory/secretory products of the carcinogenic liver fluke are endocytosed by human cholangiocytes and drive cell proliferation and IL6 production. *Int J Parasitol*, 45, 773-81.
- CHAIYADET, S., SOTILLO, J., SMOUT, M., CANTACESSI, C., JONES, M. K., JOHNSON, M. S., TURNBULL, L., WHITCHURCH, C. B., POTRIQUET, J., LAOHAVIROJ, M., MULVENNA, J., BRINDLEY, P. J., BETHONY, J. M., LAHA, T., SRIPA, B. & LOUKAS, A. 2015b. Carcinogenic Liver Fluke Secretes Extracellular Vesicles That Promote Cholangiocytes to Adopt a Tumorigenic Phenotype. *J Infect Dis*, 212, 1636-45.
- CHEN, Y. N., HSU, S. L., LIAO, M. Y., LIU, Y. T., LAI, C. H., CHEN, J. F., NGUYEN, M. T., SU, Y. H., CHEN, S. T. & WU, L. C. 2016. Ameliorative Effect of Curcumin-Encapsulated Hyaluronic Acid-PLA Nanoparticles on Thioacetamide-Induced Murine Hepatic Fibrosis. *Int J Environ Res Public Health*, 14.
- CHOI, S. C. 1977. Tests of equality of dependent correlation coefficients. *Biometrika*, 64, 645-647.

- CHUGHTAI, M. I., MAQBOOL, U., IQBAL, M., SHAH, M. S. & FODEY, T. 2017. Development of in-house ELISA for detection of chloramphenicol in bovine milk with subsequent confirmatory analysis by LC-MS/MS.
- COBBOLD, J. F. L., ANSTEE, Q. M. & THOMAS, H. C. 2010. Investigating mildly abnormal serum aminotransferase values. *BMJ*, 341.
- COLIN CAMERON, A. & WINDMEIJER, F. A. G. 1997. An R-squared measure of goodness of fit for some common nonlinear regression models. *Journal of Econometrics*, 77, 329-342.
- CORTHAY, A. 2009. How do regulatory T cells work?
- COSSARIZZA, A., CHANG, H. D., RADBRUCH, A., AKDIS, M., ANDRA, I., ANNUNZIATO, F., BACHER, P., BARNABA, V., BATTISTINI, L., BAUER, W. M., BAUMGART, S., BECHER, B., BEISKER, W., BEREK, C., BLANCO, A., BORSELLINO, G., BOULAIS, P. E., BRINKMAN, R. R., BUSCHER, M., BUSCH, D. H., BUSHNELL, T. P., CAO, X., CAVANI, A., CHATTOPADHYAY, P. K., CHENG, Q., CHOW, S., CLERICI, M., COOKE, A., COSMA, A., COSMI, L., CUMANO, A., DANG, V. D., DAVIES, D., DE BIASI, S., DEL ZOTTO, G., DELLA BELLA, S., DELLABONA, P., DENIZ, G., DESSING, M., DIEFENBACH, A., DI SANTO, J., DIELI, F., DOLF, A., DONNENBERG, V. S., DORNER, T., EHRHARDT, G. R. A., ENDL, E., ENGEL, P., ENGELHARDT, B., ESSER, C., EVERTS, B., DREHER, A., FALK, C. S., FEHNIGER, T. A., FILBY, A., FILLATREAU, S., FOLLO, M., FORSTER, I., FOSTER, J., FOULDS, G. A., FRENETTE, P. S., GALBRAITH, D., GARBI, N., GARCIA-GODOY, M. D., GEGINAT, J., GHORESCHI, K., GIBELLINI, L., GOETTLINGER, C., GOODYEAR, C. S., GORI, A., GROGAN, J., GROSS, M., GRUTZKAU, A., GRUMMITT, D., HAHN, J., HAMMER, Q., HAUSER, A. E., HAVILAND, D. L., HEDLEY, D., HERRERA, G., HERRMANN, M., HIEPE, F., HOLLAND, T., HOMBRINK, P., HOUSTON, J. P., HOYER, B. F., HUANG, B., HUNTER, C. A., IANNONE, A., JACK, H. M., JAVEGA, B., JONJIC, S., JUELKE, K., JUNG, S., KAISER, T., KALINA, T., KELLER, B., KHAN, S., KIENHOFER, D., KRONEIS, T., et al. 2017. Guidelines for the use of flow cytometry and cell sorting in immunological studies. *Eur J Immunol*, 47, 1584-1797.
- DEDOBBELEER, O., STOCKIS, J. A.-O. H. O. O., VAN DER WONING, B., COULIE, P. G. & LUCAS, S. A.-O. H. O. O. Cutting Edge: Active TGF-beta1 Released from GARP/TGF-beta1 Complexes on the Surface of Stimulated Human B Lymphocytes Increases Class-Switch Recombination and Production of IgA.
- DEENICK, E. K., HASBOLD, J. & HODGKIN, P. D. 2005. Decision criteria for resolving isotype switching conflicts by B cells. *Eur J Immunol*, 35, 2949-55.
- DELONG, E. R., DELONG, D. M. & CLARKE-PEARSON, D. L. 1988. Comparing the Areas under Two or More Correlated Receiver Operating Characteristic Curves: A Nonparametric Approach. *Biometrics*, 44, 837-845.
- DEY, S., MOHAN CM FAU - RAMADASS, P., RAMADASS P FAU - NACHIMUTHU, K. & NACHIMUTHU, K. 2008. Diagnosis of leptospirosis by recombinant antigen based single serum dilution ELISA.
- DIENZ, O., EATON, S. M., BOND, J. P., NEVEU, W., MOQUIN, D., NOUBADE, R., BRISO, E. M., CHARLAND, C., LEONARD, W. J., CILIBERTO, G., TEUSCHER, C., HAYNES, L. & RINCON, M. 2009. The induction of antibody production by IL-6 is indirectly mediated by IL-21 produced by CD4+ T cells. *J Exp Med*, 206, 69-78.
- DILGER, K., HOHENESTER, S., WINKLER-BUDENHOFER, U., BASTIAANSEN, B. A., SCHAAP, F. G., RUST, C. & BEUERS, U. 2012. Effect of ursodeoxycholic acid on bile acid profiles and intestinal detoxification machinery in primary biliary cirrhosis and health. *J Hepatol*, 57, 133-40.

- ELGUETA, R., BENSON MJ FAU - DE VRIES, V. C., DE VRIES VC FAU - WASIUK, A., WASIUK A FAU - GUO, Y., GUO Y FAU - NOELLE, R. J. & NOELLE, R. J. 2009. Molecular mechanism and function of CD40/CD40L engagement in the immune system.
- ELIAS, H. & BENGELSDORF, H. 1952. The structure of the liver of vertebrates. *Acta Anat (Basel)*, 14, 297-337.
- EMMERICH, J., MUMM, J. B. & OFT, M. 2012. Autochthonous T cells to the rescue: IL-10 directly activates tumor-resident CD8(+) T cells. *Oncoimmunology*, 1, 1637-1639.
- FABBRI, M., SMART, C. & PARDI, R. 2003. T lymphocytes. *Int J Biochem Cell Biol*, 35, 1004-8.
- FARRELL, G. C. & LARTER, C. Z. 2006. Nonalcoholic fatty liver disease: from steatosis to cirrhosis. *Hepatology*, 43, S99-s112.
- FICKERT, P., ZOLLNER, G., FUCHSBICHLER, A., STUMPTNER, C., POJER, C., ZENZ, R., LAMMERT, F., STIEGER, B., MEIER, P. J., ZATLOUKAL, K., DENK, H. & TRAUNER, M. 2001. Effects of Ursodeoxycholic and Cholic Acid Feeding on Hepatocellular Transporter Expression in Mouse Liver. *Gastroenterology*, 121, 170-183.
- FLAJNIK, M. F. 2002. Comparative analyses of immunoglobulin genes: surprises and portents.
- FREY, A., DI CANZIO, J. & ZURAKOWSKI, D. 1998. A statistically defined endpoint titer determination method for immunoassays. *Journal of Immunological Methods*, 221, 35-41.
- FUJIEDA, S., SAXON A FAU - ZHANG, K. & ZHANG, K. 1998. Direct evidence that gamma 1 and gamma 3 switching in human B cells is interleukin-10 dependent.
- FUSSEY, S. P., WEST, S. M., LINDSAY, J. G., RAGAN, C. I., JAMES, O. F., BASSENDINE, M. F. & YEAMAN, S. J. 1991a. Clarification of the identity of the major M2 autoantigen in primary biliary cirrhosis. *Clinical Science*, 80, 451-5.
- FUSSEY, S. P., WEST, S. M., LINDSAY, J. G., RAGAN, C. I., JAMES, O. F., BASSENDINE, M. F. & YEAMAN, S. J. 1991b. Clarification of the major M2 autoantigen primary biliary cirrhosis. *Clinical Science*, 80, 451-455.
- GASCAN, H., GAUCHAT, J. F., RONCAROLO, M. G., YSSEL, H., SPITS, H. & DE VRIES, J. E. 1991. Human B cell clones can be induced to proliferate and to switch to IgE and IgG4 synthesis by interleukin 4 and a signal provided by activated CD4+ T cell clones. *The Journal of Experimental Medicine*, 173, 747.
- GATSELIS, N. K., ZACHOU, K., LYGOURA, V., AZARIADIS, K., ARVANITI, P., SPYROU, E., PAPADAMOU, G., KOUKOULIS, G. K., DALEKOS, G. N. & RIGOPOULOU, E. I. Geoepidemiology, clinical manifestations and outcome of primary biliary cholangitis in Greece. *European Journal of Internal Medicine*.
- GHASEMI, A. & ZAHEDIASL, S. 2012. Normality Tests for Statistical Analysis: A Guide for Non-Statisticians. *International Journal of Endocrinology and Metabolism*, 10, 486-489.
- GOLDSTEIN, J. I., KOMINSKY, D. J., JACOBSON, N., BOWERS, B., REGALIA, K., AUSTIN, G. L., YOUSEFI, M., FALTA, M. T., FONTENOT, A. P., GERICH, M. E., GOLDEN-MASON, L. & COLGAN, S. P. 2011. Defective Leukocyte GM-CSF Receptor (CD116) Expression and Function in Inflammatory Bowel Disease. *Gastroenterology*, 141, 208-216. .
- GOSSELIN, A., MONTEIRO P FAU - CHOMONT, N., CHOMONT N FAU - DIAZ-GRIFFERO, F., DIAZ-GRIFFERO F FAU - SAID, E. A., SAID EA FAU - FONSECA,

- S., FONSECA S FAU - WACLECHE, V., WACLECHE V FAU - EL-FAR, M., EL-FAR M FAU - BOULASSEL, M.-R., BOULASSEL MR FAU - ROUTY, J.-P., ROUTY JP FAU - SEKALY, R.-P., SEKALY RP FAU - ANCUTA, P. & ANCUTA, P. Peripheral blood CCR4+CCR6+ and CXCR3+CCR6+CD4+ T cells are highly permissive to HIV-1 infection.
- GRAY PW FAU - GOEDEL, D. V. & GOEDEL, D. V. 1982. Structure of the human immune interferon gene.
- GRIFFIN, A. S., PREECE, S. R., RONALD, J., SMITH, T. P., SUHOCKI, P. V. & KIM, C. Y. 2017. Hemorrhage risk with transjugular intrahepatic portosystemic shunt (TIPS) insertion at the main portal vein bifurcation with stent grafts. LID - S2211-5684(17)30196-1 [pii] LID - 10.1016/j.diii.2017.07.006 [doi].
- GROOM, J. R. & LUSTER, A. D. 2011a. CXCR3 in T cell function. *Experimental cell research*, 317, 620-631.
- GROOM, J. R. & LUSTER, A. D. 2011b. CXCR3 in T cell function. *Exp Cell Res*, 317, 620-31.
- GRUBMAN, S. A., PERRONE, R. D., LEE, D. W., MURRAY, S. L., ROGERS, L. C., WOLKOFF, L. I., MULBERG, A. E., CHERINGTON, V. & JEFFERSON, D. M. 1994. Regulation of intracellular pH by immortalized human intrahepatic biliary epithelial cell lines. *Am J Physiol*, 266, G1060-70.
- GULZAR, N. & COPELAND, K. F. 2004. CD8+ T-cells: function and response to HIV infection.
- HA, S. G., GE, X. N., BAHAI, N. S., KANG, B. N., RAO, A., RAO, S. P. & SRIRAMARAO, P. 2013. ORMDL3 promotes eosinophil trafficking and activation via regulation of integrins and CD48. *Nat Commun*, 4, 2479.
- HAMEL, K. M., MANDAL, M., KARKI, S. & CLARK, M. R. 2014. Balancing Proliferation with Igk Recombination during B-lymphopoiesis. *Frontiers in Immunology*, 5, 139.
- HAN, E., JO, S. J., LEE, H., CHOI, A.-R., LIM, J., JUNG, E.-S. & OH, E.-J. 2017. Clinical relevance of combined anti-mitochondrial M2 detection assays for primary biliary cirrhosis. *Clinica Chimica Acta*, 464, 113-117.
- HARRIMAN, G. R., KUNIMOTO DY FAU - ELLIOTT, J. F., ELLIOTT JF FAU - PAETKAU, V., PAETKAU V FAU - STROBER, W. & STROBER, W. The role of IL-5 in IgA B cell differentiation.
- HEIT, J. J., APELQVIST, A. A., GU, X., WINSLOW, M. M., NEILSON, J. R., CRABTREE, G. R. & KIM, S. K. 2006. Calcineurin/NFAT signalling regulates pancreatic [beta]-cell growth and function. *Nature*, 443, 345-349.
- HIRBOD-MOBARAKEH, A., AGHAMOHAMMADI, A. & REZAEI, N. 2014. Immunoglobulin class switch recombination deficiency type 1 or CD40 ligand deficiency: from bedside to bench and back again. *Expert Rev Clin Immunol*, 10, 91-105.
- HWANG, T.-C. & KIRK, K. L. 2013. The CFTR Ion Channel: Gating, Regulation, and Anion Permeation. *Cold Spring Harbor Perspectives in Medicine*, 3, a009498.
- I PEENE, L. M., E M VEYS, F DE KEYSER 2001. Detection and identification of Anti-nuclear antibodies (ANA) in a large and consecutive cohort of serum samples referred for ANA testing. *Ann Rheum Dis*, 60, 1131-1136.
- INAMURA, K., TSUJI, H., NAKAMOTO, Y., SUZUKI, M. & KANEKO, S. 2006. Transgenic mice aberrantly expressing pyruvate dehydrogenase complex E2 component on biliary epithelial cells do not show primary biliary cirrhosis. *Clin Exp Immunol*, 145, 93-100.
- INVERNIZZI, P., PODDA, M., BATTEZZATI, P. M., CROSIGNANI, A., ZUIN, M., HITCHMAN, E., MAGGIONI, M., MERONI, P. L., PENNER, E. & WESIERSKA-

- GADEK, J. 2001. Autoantibodies against nuclear pore complexes are associated with more active and severe liver disease in primary biliary cirrhosis. *Journal of Hepatology*, 34, 366-371.
- JANSEN, P. L. M. 1999. Diagnosis and management of Crigler-Najjar syndrome. *European Journal of Pediatrics*, 158, S089-S094.
- JEANNIN, P., DELNESTE, Y., LECOANET-HENCHOZ, S., GREENER, D. & BONNEFOY, J.-Y. 1998. Interleukin-7 (IL-7) Enhances Class Switching to IgE and IgG4 in the Presence of T Cells Via IL-9 and sCD23. *Blood*, 91, 1355.
- JENTSCH-ULLRICH, K., KOENIGSMANN, M., MOHREN, M. & FRANKE, A. 2005. Lymphocyte subsets' reference ranges in an age- and gender-balanced population of 100 healthy adults--a monocentric German study. *Clin Immunol*, 116, 192-7.
- JONES, D. E. J. 2000. Autoantigens in primary biliary cirrhosis. *Journal of Clinical Pathology*, 53, 813-821.
- JONES, D. E. J. 2003a. Addison's other disease: Primary biliary cirrhosis as a model autoimmune disease *Clinical Medicine*, 3, 351-356.
- JONES, D. E. J. 2003b. Pathogenesis of primary biliary cirrhosis. *Journal of Hepatology*, 39, 639-648.
- JONES, D. E. J., PALMER, J. M., BENNETT, K., ROBE, A. J., YEAMAN, S. J., ROBERTSON, H., BASSENDINE, M. F., BURT, A. D. & KIRBY, J. A. 2002. Investigation of a Mechanism for Accelerated Breakdown of Immune Tolerance to the Primary Biliary Cirrhosis-Associated Autoantigen, Pyruvate Dehydrogenase Complex. *Lab Invest*, 82, 211-219.
- KAMIHIRA, T., SHIMODA, S., NAKAMURA, M., YOKOYAMA, T., TAKII, Y., KAWANO, A., HANDA, M., ISHIBASHI, H., GERSHWIN, M. E. & HARADA, M. 2005. Biliary epithelial cells regulate autoreactive T cells: implications for biliary-specific diseases. *Hepatology*, 41, 151-9.
- KANNIAN, P., MCHUGH, G., JOHNSON, B. J. B., BACON, R. M., GLICKSTEIN, L. J. & STEERE, A. C. 2007. Antibody responses to *Borrelia burgdorferi* in patients with antibiotic-refractory, antibiotic-responsive, or non-antibiotic-treated lyme arthritis. *Arthritis & Rheumatism*, 56, 4216-4225.
- KAWATA, K., TSUDA, M., YANG, G. X., ZHANG, W., TANAKA, H., TSUNAYAMA, K., LEUNG, P., HE, X. S., KNECHTLE, S., ANSARI, A. A., COPPEL, R. L. & GERSHWIN, M. E. 2013. Identification of potential cytokine pathways for therapeutic intervention in murine primary biliary cirrhosis. *PLoS One*, 8, e74225.
- KENNEL, A. S. M., GOULD, K. G. & SALAMAN, M. R. 2014. Proliferation assay amplification by IL-2 in model primary and recall antigen systems. *BMC Research Notes*, 7, 662.
- KIM, K. A. & JEONG, S. H. 2011. The diagnosis and treatment of primary biliary cirrhosis. *The Korean journal of hepatology*, 17, 173-9.
- KOULENTAKI, M., MANTAKA, A., SIFAKI-PISTOLLA, D., THALASSINOS, E., TZANAKIS, N. & KOUROUMALIS, E. 2014. Geoepidemiology and space-time analysis of Primary Biliary Cirrhosis in Crete, Greece. *Liver Int*.
- KOUSOULIS, A. A., ECONOMOPOULOS KP FAU - POULAKOU-REBELAKOU, E., POULAKOU-REBELAKOU E FAU - ANDROUTSOS, G., ANDROUTSOS G FAU - TSIODRAS, S. & TSIODRAS, S. 2012. The plague of Thebes, a historical epidemic in Sophocles' Oedipus Rex.
- KRÄHENBÜHL, S., FISCHER, S., TALOS, C. & REICHEN, J. 1994. Ursodeoxycholate protects oxidative mitochondrial metabolism from bile acid toxicity: dose-response study in isolated rat liver mitochondria. *Hepatology*, 20, 1595-601.

- KRAUSGRUBER, T., BLAZEK, K., SMALLIE, T., ALZABIN, S., LOCKSTONE, H., SAHGAL, N., HUSSELL, T., FELDMANN, M. & UDALOVA, I. A. 2011. IRF5 promotes inflammatory macrophage polarization and TH1-TH17 responses. *Nat Immunol*, 12, 231-8.
- LANDI, A., WEISMULLER, T. J., LANKISCH, T. O., SANTER, D. M., TYRRELL, D. L. J., MANNS, M. P. & HOUGHTON, M. 2014. Differential Serum Levels of Eosinophilic Eotaxins in Primary Sclerosing Cholangitis, Primary Biliary Cirrhosis, and Autoimmune Hepatitis. *Journal of Interferon & Cytokine Research*, 34, 204-214.
- LEBMAN, D. A. & COFFMAN, R. L. 1988a. Interleukin 4 causes isotype switching to IgE in T cell-stimulated clonal B cell cultures.
- LEBMAN, D. A. & COFFMAN, R. L. 1988b. Interleukin 4 causes isotype switching to IgE in T cell-stimulated clonal B cell cultures. *J Exp Med*, 168, 853-62.
- LEPERCQ, P., HERMIER, D., DAVID, O., MICHELIN, R., GIBARD, C., BEGUET, F., RELANO, P., CAYUELA, C. & JUSTE, C. 2005. Increasing ursodeoxycholic acid in the enterohepatic circulation of pigs through the administration of living bacteria. *British Journal of Nutrition*, 93, 457-469.
- LINTERMAN, M. A., RIGBY RJ FAU - WONG, R. K., WONG RK FAU - YU, D., YU D FAU - BRINK, R., BRINK R FAU - CANNONS, J. L., CANNONS JL FAU - SCHWARTZBERG, P. L., SCHWARTZBERG PL FAU - COOK, M. C., COOK MC FAU - WALTERS, G. D., WALTERS GD FAU - VINUESA, C. G. & VINUESA, C. G. 2009. Follicular helper T cells are required for systemic autoimmunity.
- LIU, J. Z., ALMARRI, M. A., GAFFNEY, D. J., MELLS, G. F., JOSTINS, L., CORDELL, H. J., DUCKER, S. J., DAY, D. B., HENEGHAN, M. A., NEUBERGER, J. M., DONALDSON, P. T., BATHGATE, A. J., BURROUGHS, A., DAVIES, M. H., JONES, D. E., ALEXANDER, G. J., BARRETT, J. C., THE UK PRIMARY BILIARY CIRRHOSIS (PBC) CONSORTIUM, THE WELLCOME TRUST CASE CONTROL CONSORTIUM 3, SANDFORD, R. N. & CARL A ANDERSON, C. A. 2012. Dense fine-mapping study identifies new susceptibility loci for primary biliary cirrhosis. *Nature Genetics*, 44, 1137-1141.
- LUC, S., LUIS, T. C., BOUKARABILA, H., MACAULAY, I. C., BUZA-VIDAS, N., BOURIEZ-JONES, T., LUTTEROPP, M., WOLL, P. S., LOUGHRAN, S. J., MEAD, A. J., HULTQUIST, A., BROWN, J., MIZUKAMI, T., MATSUOKA, S., FERRY, H., ANDERSON, K., DUARTE, S., ATKINSON, D., SONEJI, S., DOMANSKI, A., FARLEY, A., SANJUAN-PLA, A., CARELLA, C., PATIENT, R., DE BRUIJN, M., ENVER, T., NERLOV, C., BLACKBURN, C., GODIN, I. & JACOBSEN, S. E. W. 2012. The Earliest Thymic T Cell Progenitors Sustain B Cell and Myeloid Lineage Potentials. *Nature immunology*, 13, 412-419.
- LUCEY, M. R., NEUBERGER, J. M. & WILLIAMS, R. 1986. Primary biliary cirrhosis in men. *Gut*, 27, 1373-1376.
- LUPARDUS, P. J. & GARCIA, K. C. 2008. The structure of interleukin-23 reveals the molecular basis of p40 subunit sharing with interleukin-12. *J Mol Biol*, 382, 931-41.
- MAECKER, H. T. & TROTTER, J. 2006. Flow cytometry controls, instrument setup, and the determination of positivity. *Cytometry A*, 69, 1037-42.
- MARRACK P FAU - KAPPLER, J. W. & KAPPLER, J. W. Antigen-specific and nonspecific mediators of T cell/B cell cooperation. II. Two helper T cells distinguished by their antigen sensitivities.
- MATSUMOTO, A., DOBASHI H FAU - OHNISHI, H., OHNISHI H FAU - TANAKA, T., TANAKA T FAU - KUBOTA, Y., KUBOTA Y FAU - KITANAKA, A., KITANAKA A FAU - ISHIDA, H., ISHIDA H FAU - TOKUDA, M., TOKUDA M FAU - WAKI, M., WAKI M FAU - KUBO, A., KUBO A FAU - ISHIDA, T. & ISHIDA, T. Tyrosine

- phosphorylation of a novel 100-kDa protein coupled to CD28 in resting human T cells is enhanced by a signal through TCR/CD3 complex.
- MCINTYRE, T. M., KLINMAN, D. R., ROTHMAN, P., LUGO, M., DASCH, J. R., MOND, J. J. & SNAPPER, C. M. 1993. Transforming growth factor beta 1 selectivity stimulates immunoglobulin G2b secretion by lipopolysaccharide-activated murine B cells. *J Exp Med*, 177, 1031-7.
- MELERO, S., SPIRLI, C., ZSEMBERY, A., MEDINA, J. F., JOPLIN, R. E., DUNER, E., ZUIN, M., NEUBERGER, J. M., PRIETO, J. & STRAZZABOSCO, M. 2002. Defective regulation of cholangiocyte Cl⁻/HCO₃⁻ and Na⁺/H⁺ exchanger activities in primary biliary cirrhosis. *Hepatology*, 35, 1513-21.
- MELI, A. P., FONTES, G., LEUNG SOO, C. & KING, I. L. T Follicular Helper Cell-Derived IL-4 Is Required for IgE Production during Intestinal Helminth Infection.
- MELLS, G. F., KASER, A. & KARLSEN, T. H. 2013. Novel insights into autoimmune liver diseases provided by genome-wide association studies. *Journal of autoimmunity*, 46, 41-54.
- MILLÁN, J. L. 2006. Alkaline Phosphatases: Structure, substrate specificity and functional relatedness to other members of a large superfamily of enzymes. *Purinergic Signalling*, 2, 335-341.
- MIOZZO, M., SELMI, C., GENTILIN, B., GRATI, F. R., SIRCHIA, S., OERTELT, S., ZUIN, M., GERSHWIN, M. E., PODDA, M. & INVERNIZZI, P. 2007. Preferential X chromosome loss but random inactivation characterize primary biliary cirrhosis. *Hepatology*, 46, 456-62.
- MITSDOERFFER, M., LEE, Y., JAGER, A., KIM, H. J., KORN, T., KOLLS, J. K., CANTOR, H., BETTELLI, E. & KUCHROO, V. K. 2010. Proinflammatory T helper type 17 cells are effective B-cell helpers. *Proc Natl Acad Sci U S A*, 107, 14292-7.
- MITSDOERFFER, M., LEE, Y., JÄGER, A., HYE-JUNG, K., KORN, T., KOLLS, J. K., CANTOR, H., BETTELLI, E. & KUCHROO, V. K. 2010. Proinflammatory T helper Type 17 cells are effective B cell helpers. *PNAS*, 107, 14292-14297.
- MIURA, K., ORCUTT, A. C., MURATOVA, O. V., MILLER, L. H., SAUL, A. & LONG, C. A. 2008. Development and Characterization of a Standardized ELISA Including a Reference Serum on Each Plate to Detect Antibodies Induced by Experimental Malaria Vaccines. *Vaccine*, 26, 193-200.
- MOHAMMADINEJAD, P., ABOLHASSANI, H., AGHAMOHAMMADI, A., POURHAMDI, S., GHOSH, S., SADEGHI, B., KALMARZI, R. N., DURANDY, A. & BORKHARDT, A. 2014. CLASS SWITCH RECOMBINATION PROCESS IN ATAXIA TELANGIECTASIA PATIENTS WITH ELEVATED SERUM LEVELS OF IgM. *Journal of immuniassay immunochemistry*.
- MORTENSEN, R., NISSEN, T. N., BLAUENFELDT, T., CHRISTENSEN, J. P., ANDERSEN, P. & DIETRICH, J. 2015. Adaptive Immunity against *Streptococcus pyogenes* in Adults Involves Increased IFN- γ and IgG3 Responses Compared with Children. *The Journal of Immunology*, 195, 1657.
- MOUSSAVIAN SN FAU - BECKER, R. C., BECKER RC FAU - PIEPMEYER, J. L., PIEPMEYER JL FAU - MEZEY, E., MEZEY E FAU - BOZIAN, R. C. & BOZIAN, R. C. Serum gamma-glutamyl transpeptidase and chronic alcoholism. Influence of alcohol ingestion and liver disease.
- NEDWIN GE FAU - NAYLOR, S. L., NAYLOR SL FAU - SAKAGUCHI, A. Y., SAKAGUCHI AY FAU - SMITH, D., SMITH D FAU - JARRETT-NEDWIN, J., JARRETT-NEDWIN J FAU - PENNICA, D., PENNICA D FAU - GOEDEL, D. V., GOEDEL DV FAU - GRAY, P. W. & GRAY, P. W. 1985. Human lymphotoxin

- and tumor necrosis factor genes: structure, homology and chromosomal localization.
- NELSON, M. & ROY, K. 2015. Bone-marrow mimicking biomaterial niches for studying hematopoietic stem and progenitor cells. *Journal of Material Chemistry B*, 4, 3490-3503.
- NEMAZEE, D. 2006. Receptor editing in lymphocyte development and central tolerance.
- NEUBERGER, J. M., JOPLIN, R. E., WALLACE, L. L., LINDSAY, J. G., PALMER, J. M. & YEAMAN, S. J. 1997. The Human Biliary Epithelial Cell Plasma Membrane Antigen
- in Primary Biliary Cirrhosis: Pyruvate Dehydrogenase X? *Gastroenterology*, 1727-1733.
- NEWPORT, M. 2003. A schematic representation of the interleukin-12 receptor (IL-12R) and its signalling pathway. *Expert Reviews in Molecular Medicine by Cambridge University Press*, 5.
- NEZASA, K., TIAN, X., ZAMEK-GLISZCZYNSKI, M. J., PATEL, N. J., RAUB, T. J. & BROUWER, K. L. R. 2006. ALTERED HEPATOBILIARY DISPOSITION OF 5 (AND 6)-CARBOXY-2',7'-DICHLOROFLUORESCEIN IN Abcg2 (Bcrp1) AND Abcc2 (Mrp2) KNOCKOUT MICE. *Drug Metabolism and Disposition*, 34, 718-723.
- NYBLOM, H., BJORNSSON, E., SIMREN, M., ALDENBORG, F., ALMER, S. & OLSSON, R. 2006. The AST/ALT ratio as an indicator of cirrhosis in patients with PBC. *Liver Int*, 26, 840-5.
- O'FLYNN, K., RUSSUL-SAIB, M., ANDO, I., WALLACE, D. L., BEVERLEY, P. C., BOYLSTON, A. W. & LINCH, D. C. 1986. Different pathways of human T-cell activation revealed by PHA-P and PHA-M. *Immunology*, 57, 55-60.
- PAGEAUX, G. P., BLANC, P., PERRIGAULT, P. F., NAVARRO, F., FABRE, J. M., SOUCHE, B., DOMERGUE, J., LARREY, D. & MICHEL, H. 1995. Failure of ursodeoxycholic acid to prevent acute cellular rejection after liver transplantation. *J Hepatol*, 23, 119-22.
- PARK, K., KIM J FAU - LEE, J. & LEE, J. 2017. Reproducibility of Bruch's Membrane Opening-minimum Rim Width Measurements with Spectral Domain Optical Coherence Tomography. LID - 10.1097/IJG.0000000000000787 [doi].
- PATEL, A. & SEETHARAM, A. Primary Biliary Cholangitis: Disease Pathogenesis and Implications for Established and Novel Therapeutics.
- PAUMGARTNER, G. & BEUERS, U. 2002. Ursodeoxycholic acid in cholestatic liver disease: mechanisms of action and therapeutic use revisited. *Hepatology*, 36, 525-31.
- PELLICORO, A., RAMACHANDRAN, P. & IREDALE, J. 2012. Reversibility of liver fibrosis. *Fibrogenesis & Tissue Repair*, 5, S26.
- PETERS, M. G., DI BISCEGLIE, A. M., KOWDLEY, K. V., FLYE, N. L., LUKETIC, V. A., MUNOZ, S. J., GARCIA-TSAO, G., BOYER, T. D., LAKE, J. R., BONACINI, M., COMBES, B. & FOR THE, P. G. 2007. Differences Between Caucasian, African American, and Hispanic Patients with Primary Biliary Cirrhosis in the United States. *Hepatology (Baltimore, Md.)*, 46, 769-775.
- PINHEIRO, R. O., DE SOUZA SALLES, J., SARNO, E. N. & SAMPAIO, E. P. 2011. Mycobacterium leprae-host-cell interactions and genetic determinants in leprosy: an overview. *Future microbiology*, 6, 217-230.
- POUPON, R. E., BALKAU, B., ESCHWÈGE, E. & POUPON, R. 1991. A multicenter, controlled trial of ursodiol for the treatment of primary biliary cirrhosis. UDCA-PBC Study Group. *New England Journal of Medicine*, 30, 1548-54.

- POUPON, R. E., LINDOR, K. D., CAUCH-DUDEK, K., DICKSON, E. R., POUPON, R. & HEATHCOTE, E. J. 1997. Combined analysis of randomized controlled trials of ursodeoxycholic acid in primary biliary cirrhosis. *Gastroenterology*, 113, 884-90.
- PRINCE, M. I., CHETWYND, A., CRAIG, W. L., METCALF, J. V. & JAMES, O. F. W. 2004. Asymptomatic primary biliary cirrhosis: clinical features, prognosis, and symptom progression in a large population based cohort. *Gut*, 53, 865-870.
- PRINCE, M. I., CHETWYND, A., DIGGLE, P., JARNER, M., METCALF, J. V. & JAMES, O. F. 2001. The geographical distribution of primary biliary cirrhosis in a well-defined cohort. *Hepatology*, 34, 1083-8.
- RICKEN, T., WERNER, D., G HOLZHÜTTER, H., KÖNIG, M., DAHMEN, U. & DIRSCH, O. 2014. *Modeling function-perfusion behavior in liver lobules including tissue, blood, glucose, lactate and glycogen by use of a coupled two-scale PDE-ODE approach.*
- RODRIGUES, C. M. P., FAN, G., MA, X., KREN, B. T. & STEER, C. J. 1998a. A Novel Role for Ursodeoxycholic Acid in Inhibiting Apoptosis by Modulating Mitochondrial Membrane Perturbation. *Journal of Clinical Investigation*, 101, 2790-2799.
- RODRIGUES, C. M. P., FAN, G., WONG, P. Y., KREN, B. T. & STEER, C. J. 1998b. Ursodeoxycholic Acid May Inhibit Deoxycholic Acid-Induced Apoptosis by Modulating Mitochondrial Transmembrane Potential and Reactive Oxygen Species Production. *Molecular Medicine*, 4, 165-178.
- ROMAGNANI, S. 2000. T-cell subsets (Th1 versus Th2).
- ROZEBOOM, W. W. The theory of abstract partials: an introduction.
- RUBEL, L. R., RABIN, L., SEEFF, L. B., LICHT, H. & CUCCHERINI, B. A. 1984. Does Primary Biliary Cirrhosis in Men Differ from Primary Biliary Cirrhosis in Women? *Hepatology*, 4, 671-677.
- RUSSELL, L. M., STRIKE, P., BROWNE, C. E. & JACOBS, P. A. 2007. X chromosome loss and aging. *Cytogenetic Genome Research*, 116, 181-5.
- SADEGH-NASSERI, S. 2016. A step-by-step overview of the dynamic process of epitope selection by major histocompatibility complex class II for presentation to helper T cells. LID - 10.12688/f1000research.7664.1 [doi] LID - F1000 Faculty Rev-1305 [pii].
- SAXENA, A., KHOSRAVIANI, S., NOEL, S., MOHAN, D., DONNER, T. & HAMAD, A. R. A. 2015. Interleukin-10 paradox: A potent immunoregulatory cytokine that has been difficult to harness for immunotherapy. *Cytokine*, 74, 27-34.
- SHETH, S. G., FLAMM SL FAU - GORDON, F. D., GORDON FD FAU - CHOPRA, S. & CHOPRA, S. AST/ALT ratio predicts cirrhosis in patients with chronic hepatitis C virus infection.
- SHIMOKURA, G. H., MCGILL, J. M., SCHLENKER, T. & FITZ, J. G. 1995. Ursodeoxycholate increases cytosolic calcium concentration and activates Cl⁻ currents in a biliary cell line. *Gastroenterology*, 109, 965-72.
- SIEGEL, J. L., JORGENSEN R FAU - ANGULO, P., ANGULO P FAU - LINDOR, K. D. & LINDOR, K. D. Treatment with ursodeoxycholic acid is associated with weight gain in patients with primary biliary cirrhosis.
- SLEIMAN, P. M., FLORY, J., IMIELINSKI, M., BRADFIELD, J. P., ANNAIAH, K., WILLIS-OWEN, S. A., WANG, K., RAFAELS, N. M., MICHEL, S., BONNELYKKE, K., ZHANG, H., KIM, C. E., FRACKELTON, E. C., GLESSNER, J. T., HOU, C., OTIENO, F. G., SANTA, E., THOMAS, K., SMITH, R. M., GLABERSON, W. R., GARRIS, M., CHIAVACCI, R. M., BEATY, T. H., RUCZINSKI, I., ORANGE, J. S., ALLEN, J., SPERGEL, J. M., GRUNDMEIER, R., MATHIAS, R. A., CHRISTIE, J. D., VON MUTIUS, E., COOKSON, W. O.,

- KABESCH, M., MOFFATT, M. F., GRUNSTEIN, M. M., BARNES, K. C., DEVOTO, M., MAGNUSSON, M., LI, H., GRANT, S. F., BISGAARD, H. & HAKONARSON, H. 2010. Variants of DENND1B associated with asthma in children. *N Engl J Med*, 362, 36-44.
- SMYK, D., MYTILINAIIOU, M. G., RIGOPOULOU, E. I. & BOGDANOS, D. P. 2010. PBC triggers in water reservoirs, coal mining areas and waste disposal sites: from Newcastle to New York. *Dis Markers*, 29, 337-44.
- SONG, Y., LIU, C., LIU, X., TROTTIER, J., BEAUDOIN, M., ZHANG, L., POPE, C., PENG, G., BARBIER, O., ZHONG, X., LI, L. & WANG, L. H19 promotes cholestatic liver fibrosis by preventing ZEB1-mediated inhibition of EpCAM. LID - 10.1002/hep.29209 [doi].
- SOOKOIAN, S. & PIROLA, C. J. 2012. Alanine and aspartate aminotransferase and glutamine-cycling pathway: Their roles in pathogenesis of metabolic syndrome. *World Journal of Gastroenterology : WJG*, 18, 3775-3781.
- SPEARMAN, C. 1904. The Proof and Measurement of Association between Two Things. *The American Journal of Psychology*, 15, 72-101.
- SPOLSKI, R. & LEONARD, W. J. 2010. IL-21 and T follicular helper cells. *International Immunology*, 22, 7-12.
- SWANN, J. R., WANT, E. J., GEIER, F. M., SPAGOU, K., WILSON, I. D., SIDAWAY, J. E., NICHOLSON, J. K. & HOLMES, E. 2011. Systemic gut microbial modulation of bile acid metabolism in host tissue compartments. *Proc Natl Acad Sci U S A*, 108 Suppl 1, 4523-30.
- TABARKIEWICZ, J., POGODA, K., KARCZMARCZYK, A., POZAROWSKI, P. & GIANNOPOULOS, K. 2015. The Role of IL-17 and Th17 Lymphocytes in Autoimmune Diseases. *Archivum Immunologiae et Therapiae Experimentalis*, 63, 435-449.
- TAKABA, H. & TAKAYANAGI, H. 2017. The Mechanisms of T Cell Selection in the Thymus.
- TAKASUMI, M., MIYATA M FAU - KURODA, M., KURODA M FAU - TERASHIMA, K., TERASHIMA K FAU - ABE, K., ABE K FAU - TAKAHASHI, A., TAKAHASHI A FAU - KOBAYASHI, H., KOBAYASHI H FAU - TAZAKI, K., TAZAKI K FAU - WATANABE, H., WATANABE H FAU - OHIRA, H. & OHIRA, H. Overlap of IgG4-related Disease and Primary Biliary Cirrhosis Complicated with Autoimmune Thrombocytopenia.
- TAKEMOTO, R., MIYAKE Y FAU - HARADA, K., HARADA K FAU - NAKANUMA, Y., NAKANUMA Y FAU - MORIYA, A., MORIYA A FAU - ANDO, M., ANDO M FAU - HIROHATA, M., HIROHATA M FAU - YAMAMOTO, K. & YAMAMOTO, K. Overlap of IgG4-related sclerosing cholangitis and primary biliary cirrhosis.
- TANI-ICHI, S., SHIMBA, A., WAGATSUMA, K., MIYACHI, H., KITANO, S., IMAI, K., HARA, T. & IKUTA, K. 2013. Interleukin-7 receptor controls development and maturation of late stages of thymocyte subpopulations. *Proc Natl Acad Sci U S A*, 110, 612-7.
- THIEL, N., ZISCHKE, J., ELBASANI, E., KAY-FEDOROV, P. & MESSERLE, M. 2015. Viral Interference with Functions of the Cellular Receptor Tyrosine Phosphatase CD45. *Viruses*, 7, 1540-1557.
- TODRYK, S. M., PATHAN, A. A., KEATING, S., PORTER, D. W., BERTHOUD, T., THOMPSON, F., KLENERMAN, P. & HILL, A. V. S. 2009. The relationship between human effector and memory T cells measured by ex vivo and cultured ELISPOT following recent and distal priming. *Immunology*, 128, 83-91.
- TOELLNER, K.-M., LUTHER, S. A., SZE, D. M. Y., CHOY, R. K. W., TAYLOR, D. R., MACLENNAN, I. C. M. & ACHA-ORBEA, H. 1998. T Helper 1 (Th1) and Th2

- Characteristics Start to Develop During T Cell Priming and Are Associated with an Immediate Ability to Induce Immunoglobulin Class Switching. *The Journal of Experimental Medicine*, 187, 1193-1204.
- TRAUNER, M., MEIER, P. J. & BOYER, J. L. 1998. Molecular Pathogenesis of Cholestasis. *New England Journal of Medicine*, 339, 1217-1227.
- TRINCHIERI, G. & SHER, A. 2007. Cooperation of Toll-like receptor signals in innate immune defence. *Nat Rev Immunol*, 7, 179-90.
- TRIVEDI, P. J., LAMMERS, W. J., VAN BUUREN, H. R., PARES, A., FLOREANI, A., JANSSEN, H. L., INVERNIZZI, P., BATTEZZATI, P. M., PONSIOEN, C. Y., CORPEchot, C., POUAPON, R., MAYO, M. J., BURROUGHS, A. K., NEVENS, F., MASON, A. L., KOWDLEY, K. V., LLEO, A., CABALLERIA, L., LINDOR, K. D., HANSEN, B. E. & HIRSCHFIELD, G. M. Stratification of hepatocellular carcinoma risk in primary biliary cirrhosis: a multicentre international study.
- TZANG, B. S., LIU, C. H., HSU, K. C., CHEN, Y. H., HUANG, C. Y. & HSU, T. C. 2017. Effects of oral Lactobacillus administration on antioxidant activities and CD4+CD25+forkhead box P3 (FoxP3)+ T cells in NZB/W F1 mice. *Br J Nutr*, 118, 333-342.
- VANWAGNER, L. B. & GREEN, R. M. 2015. Evaluating elevated bilirubin levels in asymptomatic adults. *JAMA*, 313, 516-7.
- VARIKUTI, S., OGHUMU, S., NATARAJAN, G., KIMBLE, J., SPERLING, R. H., MORETTI, E., KAPLAN, M. H. & SATOSKAR, A. R. STAT4 is required for the generation of Th1 and Th2, but not Th17 immune responses during monophosphoryl lipid A adjuvant activity.
- VON BEHRING E FAU - KITASATO, S. & KITASATO, S. 1991. The mechanism of diphtheria immunity and tetanus immunity in animals. 1890.
- WADA, H., MASUDA K FAU - SATOH, R., SATOH R FAU - KAKUGAWA, K., KAKUGAWA K FAU - IKAWA, T., IKAWA T FAU - KATSURA, Y., KATSURA Y FAU - KAWAMOTO, H. & KAWAMOTO, H. 2008. Adult T-cell progenitors retain myeloid potential.
- WAHLSTROM, A., SAYIN, S. I., MARSCHALL, H. U. & BACKHED, F. 2016. Intestinal Crosstalk between Bile Acids and Microbiota and Its Impact on Host Metabolism. *Cell Metab*, 24, 41-50.
- WALDEN, H. R., KIRBY, J. A., YEAMAN, S. J., GRAY, J., JONES, D. E. & PALMER, J. M. 2008. Xenobiotic incorporation into pyruvate dehydrogenase complex can occur via the exogenous lipoylation pathway. *Hepatology*, 48, 1874-84.
- WANG, X. X., WANG, F. X., LI, Z. G., WEN, Y. J., WANG, X., SONG, N. & WU, H. 2017. Development of an indirect enzyme-linked immunosorbent assay (ELISA) to differentiate antibodies against wild-type porcine reproductive and respiratory syndrome from the vaccine strain TJM-F92 based on a recombinant Nsp2 protein. LID - S0166-0934(16)30320-2 [pii] LID - 10.1016/j.jviromet.2017.09.001 [doi].
- WESSELBORG, S., PRÜFER, U., WILD, M., SCHRAVEN, B., MEUER, S. C. & KABELITZ, D. 1993. Triggering via the alternative CD2 pathway induces apoptosis in activated human T lymphocytes. *European Journal of Immunology*, 23, 2707-2710.
- WHITEHEAD, T. J., AVILA, C. O. C. & SUNDARARAGHAVAN, H. G. 2017. Combining Growth Factor Releasing Microspheres within Aligned Nanofibers Enhances Neurite Outgrowth. LID - 10.1002/jbm.a.36204 [doi].
- WORMAN, H. J. & COURVALIN, J. C. Antinuclear antibodies specific for primary biliary cirrhosis.

- XIA, X., FRANCIS, H., GLASER, S., ALPINI, G. & LESAGE, G. 2006. Bile acid interactions with cholangiocytes. *World Journal of Gastroenterology* : *WJG*, 12, 3553-3563.
- XU, J., YANG, Y., QIU, G., LAL, G., YIN, N., WU, Z., BROMBERG, J. S. & DING, Y. 2011. Stat4 is critical for the balance between Th17 cells and regulatory T cells in colitis. *J Immunol*, 186, 6597-606.
- YEAMAN, S. J., KIRBY, J. A. & JONES, D. E. 2000. Autoreactive responses to pyruvate dehydrogenase complex in the pathogenesis of primary biliary cirrhosis. *Immunol Rev*, 174, 238-49.
- YU, H. A.-O. H. O. O., BORSOTTI, C., SCHICKEL, J. N., ZHU, S., STROWIG, T., EYNON, E. E., FRLETA, D., GURER, C., MURPHY, A. J., YANCOPOULOS, G. D., MEFFRE, E., MANZ, M. G. & FLAVELL, R. A. A.-O. H. O. O. A novel humanized mouse model with significant improvement of class-switched, antigen-specific antibody production.
- ZAN, H., CERUTTI, A., DRAMITINOS, P., SCHAFFER, A. & CASALI, P. 1998. CD40 Engagement Triggers Switching to IgA1 and IgA2 in Human B Cells Through Induction of Endogenous TGF- β : Evidence for TGF- β But Not IL-10-Dependent Direct $S_{\mu} \rightarrow S_{\alpha}$ and Sequential $S_{\mu} \rightarrow S_{\gamma}$, $S_{\gamma} \rightarrow S_{\alpha}$ DNA Recombination. *The Journal of Immunology*, 161, 5217.
- ZAVALA-CERNA, M. G., MARTINEZ-GARCIA, E. A., TORRES-BUGARIN, O., RUBIO-JURADO, B., RIEBELING, C. & NAVA, A. 2014. The Clinical Significance of Posttranslational Modification of Autoantigens. *Clin Rev Allergy Immunol*.
- ZEIN, C. O., ANGULO P FAU - LINDOR, K. D. & LINDOR, K. D. When is liver biopsy needed in the diagnosis of primary biliary cirrhosis?
- ZHANG, L., WEETMAN, A. P., BASSENDINE, M. & OLIVEIRA, D. B. 1994. Major histocompatibility complex class-II alleles in primary biliary cirrhosis. *Scandinavian Journal of Immunology*, 39, 104-6.
- ZHANG, Q., NAKAKI, T., IWAMI, D., NIIMI, M. & SHIRASUGI, N. 2009. Induction of regulatory T cells and indefinite survival of fully allogeneic cardiac grafts by ursodeoxycholic acid in mice. *Transplantation*, 88, 1360-70.